

GUIDEBOOK 20

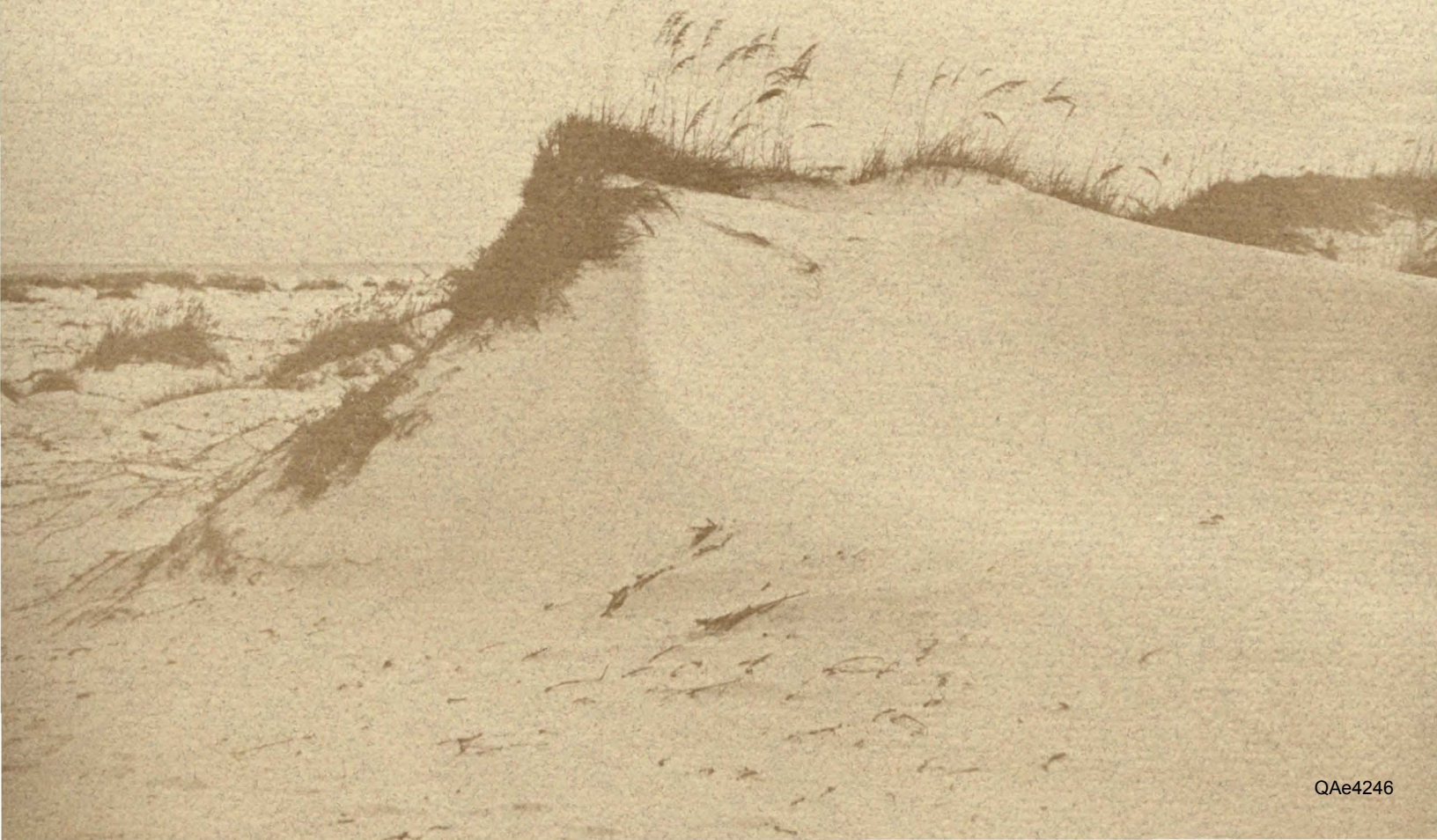
MODERN DEPOSITIONAL ENVIRONMENTS OF THE TEXAS COAST

By Robert A. Morton and J. H. McGowen

BUREAU OF ECONOMIC GEOLOGY
THE UNIVERSITY OF TEXAS AT AUSTIN
AUSTIN, TEXAS 78712
W. L. Fisher, Director



1980



Guidebook 20

MODERN DEPOSITIONAL ENVIRONMENTS
OF THE TEXAS COAST

By

Robert A. Morton and J. H. McGowen*

*Currently with Arco Oil & Gas, P. O. Box 2819,
Dallas, Texas 75221

BUREAU OF ECONOMIC GEOLOGY
THE UNIVERSITY OF TEXAS AT AUSTIN
AUSTIN, TEXAS 78712
W. L. Fisher, Director
1980

Second Printing, June 1983

CONTENTS

| | |
|---|--------|
| Summary | . xii |
| Preface | . xiii |
| Acknowledgments | . xiii |
| | |
| TEXAS COASTAL PLAIN | 1 |
| Late Quaternary history | 1 |
| Climate | 1 |
| Wind | 3 |
| Astronomical tides | 3 |
| Subsidence and relative sea-level rise | 9 |
| | |
| FLUVIAL SYSTEMS | 10 |
| Introduction | 10 |
| Classification of fluvial systems | 11 |
| Channel patterns | 11 |
| Classification of channels by sediment type | 14 |
| Fluvial models | 15 |
| Braided-stream model | 15 |
| Coarse-grained meanderbelt model | 17 |
| Fine-grained meanderbelt model | 19 |
| Brazos River | 19 |
| Brazos River floodplain | 21 |
| Blasdel point bar | 21 |
| Wallis point bar | 21 |
| Wallis point bar: June 1979 | 24 |
| Bed forms | 24 |
| Stratification types | 25 |
| Vertical succession of stratification types: Wallis point bar | 30 |
| Colorado River | 30 |
| Coarse-grained meanderbelt systems | 33 |
| Vertical succession of stratification types in coarse-grained point bars | 33 |
| Columbus point bar | 34 |

| | |
|--|----|
| Coletto Creek | 38 |
| General setting | 38 |
| Discharge | 38 |
| Stream characteristics | 39 |
| Major bed forms | 39 |
| Gross textural changes | 43 |
| Bar stratification | 43 |
| Side-attached bars | 43 |
| Point bars with chutes | 43 |
| Point bars without chutes | 44 |
| Guadalupe River | 48 |
| General setting | 48 |
| Discharge | 52 |
| Stream characteristics | 52 |
| Major bed forms | 54 |
| DELTA s | 55 |
| Introduction | 55 |
| Shallow-water delta model | 55 |
| Brazos delta | 56 |
| The Modern Brazos delta: a high-destructive wave-dominated oceanic delta | 56 |
| Colorado delta | 58 |
| History of development | 58 |
| Delta facies | 62 |
| Marsh | 64 |
| Abandoned distributary | 64 |
| Shell berms | 64 |
| Distributary-mouth bar | 64 |
| Prodelta | 64 |
| Bay | 66 |
| Guadalupe delta | 66 |
| History of development | 66 |
| Delta facies | 66 |
| Distributary channels | 66 |
| Distributary-mouth bar | 69 |

| | |
|--|--------|
| Beach ridge | 70 |
| Delta plain | 70 |
| Interdistributary bay | 70 |
| Prodelta | 70 |
| Bay | 71 |
| Gum Hollow fan delta | 71 |
| History of development | 71 |
| Depositional processes, surface features, and textural trends | 72 |
| Textural trends | 72 |
| Characteristics of depositional facies | 75 |
| TEXAS BAY SYSTEMS | 80 |
| Introduction | 80 |
| Origin of Texas bays | 80 |
| Stratigraphic sequence of bay infilling | 81 |
| Processes operating in bays | 83 |
| Astronomical tides | 89 |
| Wind | 90 |
| Rivers | 90 |
| Subsidence | 90 |
| Tropical cyclones: hurricanes and tropical storms | 93 |
| Bay circulation | 93 |
| Sediment sources and sediment distribution | 94 |
| Copano Bay | 95 |
| Origin of Copano Bay | 96 |
| Bay processes | 97 |
| Surface sediment distribution | 97 |
| Sediment characteristics | 98 |
| North Laguna Madre | 100 |
| Origin of North Padre Island and Laguna Madre | 100 |
| Barrier-island and lagoon development | 100 |
| Lagoon deposition | 101 |
| Bay processes | 102 |
| Surface sediment distribution | 102 |
| Sediment characteristics | 102 |
| South Laguna Madre | 104 |
| Origin of South Padre Island and Laguna Madre | 105 |

| | |
|--|------|
| Bay processes | .105 |
| Surface sediment distribution | .106 |
| Sediment characteristics | .106 |
| | |
| TIDAL INLETS AND DELTAS | .110 |
| Introduction | .110 |
| Major inlets | .110 |
| Aransas Pass - Harbor Island | .110 |
| Minor inlets | .116 |
| Brown Cedar Cut | .116 |
| Packery Channel area | .117 |
| Tidal-inlet facies: Corpus Christi Channel - Packery Channel area | .117 |
| Tidal-inlet and delta facies | .123 |
| Tidal channels | .123 |
| Ebb-tidal deltas | .123 |
| Flood-tidal deltas | .123 |
| | |
| BARRIER ISLANDS AND PENINSULAS | .125 |
| Introduction | .125 |
| Barrier-island facies | .126 |
| Shoreface | .127 |
| Beach | .127 |
| Fore-island dunes | .128 |
| Vegetated barrier flats | .129 |
| Active dunes | .129 |
| Washover fans | .129 |
| Wind-tidal flats | .130 |
| Accretionary barriers | .130 |
| Galveston Island | .130 |
| Morphology and history | .130 |
| Subsurface facies | .132 |
| Matagorda Island | .132 |
| Morphology and history | .132 |
| Subsurface facies | .133 |
| Padre Island | .134 |

| | |
|--|-------|
| North and central Padre Island | . 134 |
| History of development of north and central Padre Island | . 134 |
| Two-dimensional geometry of north and central Padre Island | . 137 |
| Characteristics of surface environments: north Padre Island | . 137 |
| Transgressive barriers | . 141 |
| Matagorda Peninsula | . 141 |
| Morphology and history | . 141 |
| Subsurface facies | . 141 |
| South Padre Island | . 142 |
| Holocene depositional history | . 142 |
| Two-dimensional geometry of south Padre Island and underlying Holocene Rio Grande delta | . 144 |
| Depositional facies | . 144 |
| Barrier island - strandplain facies | . 144 |
| Deltaic facies | . 144 |
| Characteristics of surface facies | . 145 |
| INNER SHELF | . 147 |
| Introduction | . 147 |
| Sediment textures | . 147 |
| Relict sediments | . 155 |
| Stratification | . 155 |
| REFERENCES | . 157 |

FIGURES

| | | |
|-----|---|----|
| 1. | Index map of major physiographic elements and geographic locations for the Texas Coastal Plain | 2 |
| 2. | Mean annual precipitation and mean annual evaporation for Texas | 8 |
| 3. | Longitudinal channel profiles for major Texas rivers | 10 |
| 4. | Flow duration curves for major Texas rivers | 12 |
| 5. | Comparison of suspension loads of Brazos and Colorado Rivers and Rio Grande | 13 |
| 6. | Depositional model of an idealized braided fluvial system | 16 |
| 7. | Depositional model of an idealized coarse-grained-meanderbelt fluvial system | 18 |
| 8. | Depositional model of an idealized fine-grained-meanderbelt fluvial system | 20 |
| 9. | Vertical succession of grain size and stratification types of the Blasdel point bar (drawn from data of Bernard and others, 1970) | 22 |
| 10. | Brazos River at bank-full stage; Wallis point bar | 23 |
| 11. | Profile of Wallis point bar with trench localities | 24 |
| 12. | Trench 1, Wallis point bar, lower and middle point bar | 26 |
| 13. | Trench 2, Wallis point bar, upper point bar | 26 |
| 14. | Trench 4, Wallis point bar, coppice bar on upper point bar | 27 |
| 15. | Trench 3, Wallis point bar, linguoid ripples on upper point bar | 28 |
| 16. | Trench 5, Wallis point bar, mud drape in swale on upper point bar | 29 |
| 17. | Trench 6, Wallis point bar, upper point bar deposits overlain by overbank mud, upper point bar | 31 |
| 18. | Generalized vertical succession of grain size and stratification types, Wallis point bar | 32 |
| 19. | Duration curve of daily flow: Amite River near Denham Springs; Colorado River near Columbus; and Atchafalaya River at Krotz Springs | 34 |
| 20. | Vertical succession of stratification types in a coarse-grained point bar, Amite River, Louisiana | 35 |
| 21. | Colorado River in flood stage; Columbus point bar | 37 |
| 22. | Bed-form distribution on Columbus point bar | 37 |
| 23. | Discharge hydrograph for Coleta Creek during September 1967 flooding associated with Hurricane Beulah | 40 |
| 24. | Location of point bars and side-attached bar, Coleta Creek | 41 |
| 25. | Locations of trenches and profiles, Coleta Creek | 41 |
| 26. | Point-bar profile, location A, Coleta Creek | 42 |

| | | |
|-----|--|----|
| 27. | Upchannel point-bar profile A, location C, Coleta Creek | 42 |
| 28. | Downchannel point-bar profile B, location C, Coleta Creek | 42 |
| 29. | Stratification types preserved in a side-attached bar, location B, Coleta Creek | 44 |
| 30. | Composite vertical sequence of stratification types from upstream point bar, location C, Coleta Creek | 45 |
| 31. | Lower point-bar stratification from trench 10, Coleta Creek | 46 |
| 32. | Upper point-bar stratification exposed in erosional face (trench 13) along bar apex | 47 |
| 33. | Internal stratification in trench 6 just upstream from avalanche face of large-scale rhomboid bed form | 49 |
| 34. | Internal stratification exposed in erosional face (trench 1) of distal point bar | 50 |
| 35. | Bed forms and internal stratification (trench 9) produced by migration of low-relief bars into side channel of convex bank | 51 |
| 36. | Isohyetal map of rainfall measured June 28 to July 1, 1936 | 53 |
| 37. | Fathometer profile extending along lower reaches of south Guadalupe River, across distributary-mouth bar, to Guadalupe Bay | 54 |
| 38. | Generalized facies diagram for Guadalupe delta | 57 |
| 39. | Surficial Pleistocene environments and interpreted shallow water fluvial- deltaic facies for the Pleistocene Nueces River system | 57 |
| 40. | Shoreline changes associated with the Brazos deltas, 1933-1971 | 58 |
| 41. | New Brazos River delta situated between Freeport Harbor Channel and the mouth of the San Bernard River | 59 |
| 42. | Locations of borings in the "new" Brazos Delta | 60 |
| 43. | Relationships between grain-size changes and SP character of the deltaic fringe deposits of the "new" Brazos delta near Freeport, Texas | 61 |
| 44. | Distribution of delta-front sediment in Egret Island | 62 |
| 45. | Core locations and bay-margin changes for southeastern lobe of the Colorado delta | 63 |
| 46. | Cores from southeastern lobe of the Colorado delta | 65 |
| 47. | Facies diagram for southern lobe of the Colorado delta | 67 |
| 48. | Location of Guadalupe delta cores | 67 |
| 49. | Cores from Guadalupe delta and Traylor Cut | 68 |
| 50. | Delta thickness and distribution of sand facies | 69 |
| 51. | Effect of sea level on deposition of Gum Hollow fan delta | 73 |
| 52. | Depositional features of Gum Hollow fan delta | 74 |
| 53. | Key to sedimentary features of Gum Hollow fan delta | 75 |
| 54. | Sedimentary features of the filled (abandoned) main braided-stream channel of the middle deltaic lobe | 76 |

| | | |
|-----|--|-----|
| 55. | Sedimentary features of filled main braided-stream channel | 77 |
| 56. | Sedimentary features of fan-plain deposits near apex of eastern (active delta lobe) | 78 |
| 57. | Sedimentary features of distal fan delta deposits near right bank of active main braided stream | 79 |
| 58. | Sedimentary features of destructional phase bar | 79 |
| 59. | Orientation of bay segments | 81 |
| 60. | Sea-level changes related to glacial and interglacial stages | 82 |
| 61. | Pleistocene erosional surface beneath Matagorda Bay system | 84 |
| 62. | Pleistocene erosional surface beneath Copano Bay | 85 |
| 63. | Simplified geologic map of Lavaca Bay area showing wash-down holes and lines of section | 86 |
| 64. | Generalized sedimentary sequence in south Lavaca Bay | 87 |
| 65. | Dip section down Lavaca River valley | 88 |
| 66. | Strike section across southern end of Lavaca Bay | 88 |
| 67. | Plan view of major bay elements | 89 |
| 68. | Bathymetric changes for Galveston Bay system for the period 1968-1977 | 91 |
| 69. | Volume of suspended-load sediment delivered to the Galveston Bay system for the period from 1936 through 1975 | 92 |
| 70. | Surface sediment distribution and core localities in Copano Bay | 96 |
| 71. | Cores taken from bay margin, tidal inlet, and adjacent to a sand spit area, Copano Bay | 99 |
| 72. | Surface sediment distribution and core localities in north Laguna Madre | 103 |
| 73. | Cores taken from lagoon margin, lagoon, and spoil areas, north Laguna Madre | 104 |
| 74. | Holocene fluvial-deltaic facies, Brownsville-Harlingen area, and surface sediment distribution, core localities, and cross section, south Laguna Madre, south Padre Island | 107 |
| 75. | Core taken in south Laguna Madre | 109 |
| 76. | Ebb-delta bathymetry and nearshore changes following modifications at Galveston Harbor | 111 |
| 77. | Migration of Aransas Pass between 1860-1866 and 1899 | 112 |
| 78. | Subenvironments of Harbor Island and adjacent areas in 1860-1866 | 113 |
| 79. | (A) Map of Harbor Island showing locations of dip section, (B) fathometer profile of ebb-oriented dunes, and (C) uppermost sequence of proximal flood-delta facies | 114 |
| 80. | Dip section showing late Pleistocene and Holocene sediments beneath Harbor Island | 115 |
| 81. | Dip section through flood-delta and underlying sediments, Brown Cedar Cut | 116 |

| | | |
|------|--|-------|
| 82. | Corpus Christi Pass - Packery Channel area with wash-down hole locations | . 118 |
| 83. | Evolution of Packery Channel area | . 119 |
| 84. | Dip section across Packery Channel area. | . 121 |
| 85. | Strike section across Packery Channel area | . 122 |
| 86. | Tidal-delta bathymetry, channels, and shoals at Brazos-Santiago Pass | . 124 |
| 87. | Generalized profiles across shoreline features associated with (A) erosional deltaic headlands, (B) peninsulas, and (C) barrier islands | . 125 |
| 88. | Generalized diagram of high- and low-profile barrier-island environments | . 126 |
| 89. | Strike section showing late Pleistocene and Holocene sediments beneath Bolivar Peninsula | . 127 |
| 90. | Generalized barrier-island (Mustang Island) profile | . 128 |
| 91. | Dip sections of Galveston Island from Eight Mile Road and near San Luis Pass | . 131 |
| 92. | Dip section from northern part of Matagorda Island. | . 133 |
| 93. | Padre Island beach profiles (January 1972) | . 135 |
| 94. | Modern barrier-island system, central Padre Island, near Land-Cut Area | . 136 |
| 95. | Profile of beach and shoreface | . 138 |
| 96. | Strike section of late Pleistocene and Holocene sediments beneath Matagorda Peninsula | . 143 |
| 97. | Cross section south Padre Island area, Texas | . 143 |
| 98. | Generalized distribution of surface sediment, track of Hurricane Carla at landfall, and location of inner shelf cores | . 148 |
| 99. | Segments of cores from the Matagorda - San José trend | . 149 |
| 100. | Maps of the Sabine - Bolivar area | . 150 |
| 101. | Maps of the Brazos - Colorado area | . 151 |
| 102. | Maps of the Matagorda - San José area | . 152 |
| 103. | Maps of the Rio Grande area | . 153 |
| 104. | Surficial features, relative abundance, and distribution of restricted mollusk species, rock fragments, and caliche nodules in each of the four trends | . 154 |

TABLES

| | | |
|----|--|-------|
| 1. | Field trip localities and descriptions | . 4 |
| 2. | Characteristics of basic types of aeolian stratification | . 140 |

SUMMARY

The Texas Coastal Plain is ideal for studying physical processes and the late Quaternary sedimentological record. Together, the diversity of depositional environments, the moderate climate, and the accessibility to most areas provide unique opportunities for (1) conducting geological investigations of modern sediments and the hydrodynamics responsible for their formation and (2) developing models suitable for interpreting ancient sediments. Within a span of about 350 mi (564 km), a broad spectrum of depositional systems is found. These systems include coarse-grained and fine-grained fluvial channels, bayhead and oceanic deltas, coastal lagoons, transgressive and regressive barriers, and a host of other nearshore deposits that are commonly preserved in ancient sedimentary basins and recognized in outcrop or by applications of subsurface methods.

Morphology and facies distribution within the Coastal Zone are responses to climatic gradients, low wave energy, and low tidal range that characterize the northwest Gulf of Mexico. Within this microtidal, storm-dominated region, sediment dispersal is controlled largely by wind forcing and river flooding. Wind forces are responsible either entirely or partly for aeolian activities, wind tides, bay circulation, wave generation, shelf circulation, and longshore currents. River discharge provides the primary mechanism for sediment transport into the Coastal Zone.

The Coastal Zone is a dynamic area, as evidenced by monitoring of physical and biological parameters during historical time. Proper analysis of extant conditions requires an appreciation for the temporal and spatial variations in processes that are attributed to both natural changes and human modifications. Human alterations are clearly responsible for some significant coastal changes. For example, progradation of the Brazos and Colorado deltas, closing of Packery Channel, and lateral infilling of Pass Cavallo attendant with spit accretion are all related to major engineering projects. Documentation of specific historical conditions, such as overbank flooding and storm washover, is invaluable for understanding sediment transport and deposition during these low-frequency, high-energy events. When placed in context, such historical documentation permits hydrodynamic reconstructions for the modern sediments, which in turn can be transferred to the ancient rock record.

Vertical successions of stratification types, textural variations, crosscutting relationships, and sand-body geometry as well as three-dimensional facies distribution are diagnostic of particular depositional systems. This is demonstrated by discussions covering the broad spectrum of Texas coastal environments from the fluvial systems to the inner shelf.

PREFACE

The Texas Coastal Plain has long been recognized as a unique area for studying modern depositional environments and coastal processes to develop facies models and to understand better the physical processes that control sediment dispersal. Classical studies of the Texas coast that are now standard references are those by W. A. Price, H. N. Fisk, F. P. Shepard, J. R. Curray, T. H. van Andel, H. A. Bernard, and R. J. LeBlanc. Most of the major coastal studies of the 1950's and early 1960's were supported directly or indirectly by the petroleum industry through their research labs and grants to other researchers. In the past decade, support for research in coastal geology has shifted to academic institutions and government agencies because of the emphasis on environmental impact of human activities. Significant contributions from this research are the incorporation of time and process variability and their effect on depositional environments. Spatial and temporal changes have been documented by historical monitoring techniques that facilitated movement from description to quantification of coastal geology.

Many of the ideas contained in this report are attributable to knowledge established by previous workers. The report also synthesizes significant research of the past decade and presents new data regarding the broad spectrum of sedimentary environments along the Texas coast. Physiographic changes caused by natural elements and human activities are combined with physical process data to improve our understanding of ancient rocks and detailed events preserved in the stratigraphic record.

ACKNOWLEDGMENTS

This report was first published as a guide for a field trip co-sponsored by the Bureau of Economic Geology and the Gulf Coast Association of Geological Societies, in conjunction with the GCAGS annual meeting, October 1979, San Antonio, Texas.

Timely collection of data and publication of this report were made possible by the willing cooperation of many people. In the field, able assistance in digging trenches and taking cores was provided by Jon Herber and Steve Wright. Larry Mack plotted some of the data. Text for the report was typed under the direction of Lucille Harrell and edited by Susie Doenges; figures were drafted under the direction of J. W. Macon. The manuscript was reviewed by R. J. Finley, W. L. Fisher, C. D. Henry, E. G. Wermund, and W. A. White of the Bureau of Economic Geology. We also thank Bruce Wilkinson (University of Michigan) and Henry Chafetz (University of Houston) for their helpful suggestions.

Appreciation is extended to those colleagues who substantially improved our knowledge of the Texas coast. Challenging discussions and memorable field experiences shared with Alan Donaldson, Al Scott, Bruce Wilkinson, Charlie Winker, Frank Brown, Bill Fisher, Ed Garner, Mary McGowen, and Joe Brewton were invaluable. Credit is due to these co-workers who, through their observations and ideas, contributed to our understanding of coastal processes and depositional environments.

1. The first part of the document discusses the importance of maintaining accurate records of all transactions and activities. It emphasizes that proper record-keeping is essential for ensuring transparency and accountability in the organization's operations. This section also outlines the various methods and tools used to collect and analyze data, highlighting the need for consistency and reliability in the information gathered.

2. The second part of the document focuses on the implementation of internal controls and risk management strategies. It details how these measures are designed to prevent fraud, minimize errors, and protect the organization's assets. The text provides a comprehensive overview of the different types of risks faced by the organization and the specific controls put in place to mitigate them. It also discusses the role of management in monitoring and evaluating the effectiveness of these controls over time.

3. The third part of the document addresses the issue of financial reporting and the preparation of financial statements. It explains the various accounting standards and principles that must be followed to ensure that the financial information presented is accurate and reliable. This section also covers the process of auditing the financial statements and the role of external auditors in providing an independent opinion on the organization's financial health.

4. The fourth part of the document discusses the importance of maintaining accurate records of all transactions and activities. It emphasizes that proper record-keeping is essential for ensuring transparency and accountability in the organization's operations. This section also outlines the various methods and tools used to collect and analyze data, highlighting the need for consistency and reliability in the information gathered.

5. The fifth part of the document focuses on the implementation of internal controls and risk management strategies. It details how these measures are designed to prevent fraud, minimize errors, and protect the organization's assets. The text provides a comprehensive overview of the different types of risks faced by the organization and the specific controls put in place to mitigate them. It also discusses the role of management in monitoring and evaluating the effectiveness of these controls over time.

6. The sixth part of the document addresses the issue of financial reporting and the preparation of financial statements. It explains the various accounting standards and principles that must be followed to ensure that the financial information presented is accurate and reliable. This section also covers the process of auditing the financial statements and the role of external auditors in providing an independent opinion on the organization's financial health.

TEXAS COASTAL PLAIN

The Texas Coastal Plain embodies all principal components of nearshore sedimentation. Fluvial-deltaic, bay-lagoon, barrier-island, and tidal-inlet systems (fig. 1; table 1) are represented by depositional settings that reflect different responses to physical processes, climatic gradient, and Recent geologic history. Each system is a composite of subenvironments that together total more than 25 sedimentary facies, most of which can be recognized in ancient nearshore deposits.

Late Quaternary History

Pleistocene fluvial-deltaic systems are the principal elements responsible for coastal plain construction. Mud-rich deltas prograded into shallow marine water during the Sangamon interglacial stage (Winker, 1979) and formed broad, low-relief surfaces that maintain much of their depositional grain. Details preserved on delta surfaces are straight distributary channels, meanderbelt sands, overbank and interdistributary muds, as well as a variety of other facies associated with coastal sedimentation. The seaward extent of delta progradation is marked by strandplains formed by reworked sands deposited on delta-plain surfaces. As sea level dropped, about 50,000 years B.P., rivers and streams eroded into underlying fluvial-deltaic deposits. A network of steep-walled valleys with dendritic drainage patterns developed as shorelines receded. Depths of buried valleys at the present shoreline range from 50 to 125 ft (15 to 40 m) below sea level (Fisk, 1959).

Approximately 18,000 years B.P., the sea began to rise rapidly and flood the entrenched valleys. Estuaries were formed along lower valley segments while upper valley segments were filled by fluvial-deltaic deposits. Relict shoreline features submerged on the shelf and wave-cut terraces buried beneath the bays mark brief pauses in sea-level rise. Otherwise, the rapid transgression persisted until about 4,500 years B.P. when sea level rose slowly and extant coastal configuration began to evolve.

Modern depositional features are closely related to comparable Pleistocene features (McGowen and Garner, 1972). Topographic highs in interdeltaic areas were depositional sites for barrier islands that were supplied by erosion of Pleistocene strandplain sand exposed on the inner continental shelf (McGowen and others, 1977); lagoons formed as areas landward of the barriers were flooded. Formerly narrow drowned valleys became broad embayments as waves eroded the inland shoreline. Only minor physiographic changes have occurred during the last few thousand years as a result of shoreline erosion and deposition and coastwide subsidence.

Climate

In a broad sense, climatic changes have been responsible for major morphological changes during the late Quaternary. Even today effects of climatic changes are reflected by shoreline retreat and dune migration in some areas.

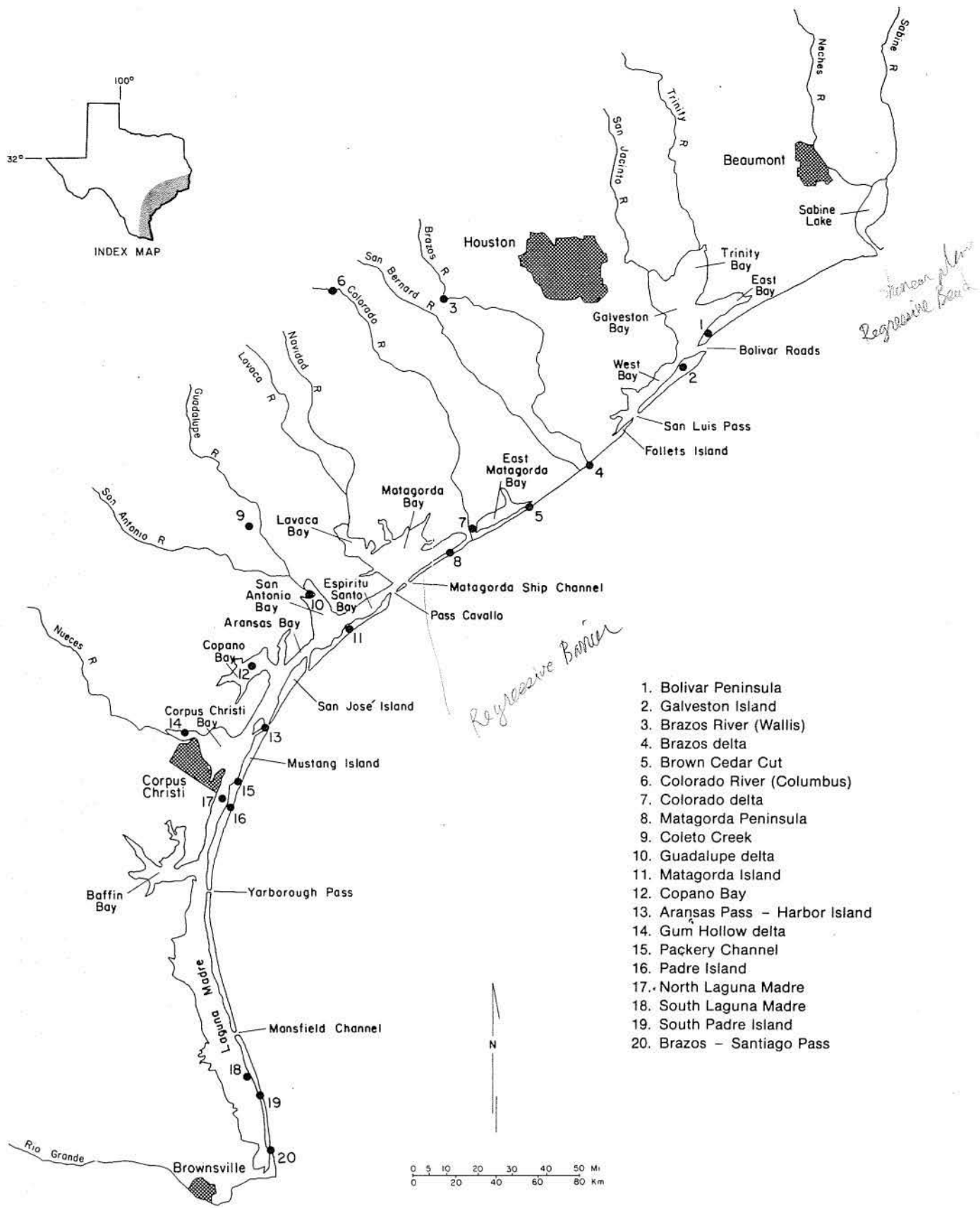


Figure 1. Index map of major physiographic elements and geographic locations for the Texas Coastal Plain. Numbers indicate areas that have been studied in detail. Localities are keyed to the official highway travel map published by the Texas Department of Highways and Public Transportation. Specific sites are keyed to USGS 7.5-minute quadrangles (see table 1).

A significant climatic gradient exists between the upper and lower coasts, as shown by mean annual precipitation and evapotranspiration (fig. 2). Rainfall decreases southwestward along the coast, whereas temperature and evapotranspiration increase. These variations have marked influences on vegetation density, water salinity, and sediment stability. In South Texas, vegetation is generally sparse, and sand dunes migrate under the influence of seasonal winds. Moreover, Baffin Bay and Laguna Madre tend to be hypersaline because fresh-water inflow and tidal exchange are minimal and evaporation exceeds precipitation.

Rainfall is seasonally distributed; highest amounts are recorded in the spring and late summer and fall (August-October) when recurring meteorological events greatly influence weather patterns. Tropical cyclones and frontal systems occur during those months, and both are capable of causing torrential rain and major floods. Throughout the year temperatures are generally mild except for short periods following outbreaks of polar continental masses.

Wind

Wind is perhaps the most important agent that influences coastal development because its effects are both direct and indirect. Winds directly accomplish geological work through aeolian processes, in particular on barriers and South Texas aeolian plains. But, more importantly, wind stresses generate currents and waves.

Circulation patterns within bays and the open gulf are influenced greatly by wind strength, duration, and direction, which change seasonally. Moderate southeast winds prevail from spring to fall (Lohse, 1955); however, during winter months, polar fronts are accompanied by strong northerly winds that abruptly alter wave characteristics and current directions. Fetch across most bays is such that northers generate higher than normal ebb velocities and inundate wind-tidal flats and other low-lying areas.

Wind properties also determine wave characteristics such as height, period, and angle of approach. Those conditions that combine to produce strong longshore currents are high, steep waves and high angle of approach. Configuration of the Gulf shoreline coupled with prevailing southeast winds and wave approach commonly produces southwesterly littoral drift along the upper and central Texas coast, whereas littoral drift is northerly along the lower coast (Lohse, 1955; Watson, 1968). Net convergence of longshore currents occurs near latitude 27°N.

Strongest winds occur during tropical storms and hurricanes that strike the Texas coast about once every 1.5 years (Hayes, 1967). High-velocity currents generated by hurricane-force winds blowing over shallow water can transport vast quantities of sediment in relatively short periods of time. These conditions, although unusual, are responsible for major geomorphic changes on subaerial barrier flats including (1) counterclockwise curvature of washover channels, (2) closely spaced striations, (3) flame-shaped fans emerging from deeply incised channels, (4) transverse bars along bay shorelines, and (5) rhomboid bed forms (Morton, 1979).

Astronomical Tides

Astronomical tides in the Gulf of Mexico are diurnal or mixed and normally range from 1.5 to 2 ft (45 to 60 cm); tidal variations are considerably lower in bays and

Table 1. Field Trip Localities and Descriptions.

| Geomorphic Feature | U.S.G.S. Quadrangle | Field Location | General Description |
|-------------------------------------|--------------------------|--|--|
| 1. Bolivar Peninsula | Flake | From Galveston take State Highway 87 and public ferry to Port Bolivar, proceed on State Highway 87 to first beach access road. | <p>Like other regressive barriers, the surficial environments of Bolivar Peninsula include marshes that fringe and cover abandoned tidal deltas and washover fans, broad vegetated barrier flats with low ridge-and-swale topography, and a narrow strip of fore-island dunes that occurs landward of broad sand beaches fronting the Gulf of Mexico. Both shell content of beach sediment and beach slope are locally high where an offshore shell trend intersects the peninsula just west of Rollover Pass.</p> <p>Shallow subsurface facies beneath Bolivar Peninsula are complex because of sea-level changes during the late Quaternary. Holocene bay and barrier sediments overlie the eroded and overcompacted Pleistocene deposits of fluvial-deltaic origin. The Holocene sediments are thin (less than 10 ft [3.0 m]) in the vicinity of High Island where Pleistocene sediments crop out; however, they thicken towards Bolivar Roads, which overlies an entrenched valley now filled with up to 100 ft (30 m) of unconsolidated sands and muds and varying amounts of shell. The dominantly sand facies that comprises the barrier ranges in thickness from 15 to 30 ft (4.6 to 9 m). The thickest sand sections appear to be related to former tidal inlets and associated tidal deltas.</p> |
| 2. Galveston Island | Galveston | From Galveston take Seawall Boulevard to West Beach and beach access areas. | <p>This compound barrier is characterized by accretion ridges and thick (30 ft [9 m]) progradational shoreface sequences along its eastern half, whereas the western half is thin (15 ft [4.6 m]) and marked by numerous washover channels and erosional beaches. The latter features are typical of the transgressive barrier segment that retreated over the Holocene Brazos delta. Although modified by residential and commercial development, the barrier embodies beaches, fore-island dunes, vegetated barrier flats, washovers, and marsh environments.</p> <p>Sedimentary features exposed in abandoned sand pits near West Beach formed the basis for the first barrier-island facies model. These pits as well as cores through the island show a coarsening-upward offlap sequence beginning with shelf deposits of bioturbated, interbedded, shelly sand and mud that grade upward into burrowed and parallel laminated shoreface sands. These sediments are overlain by structureless or root-disrupted sand of dune or barrier-flat origin.</p> |
| 7 3. Wallis point bar, Brazos River | Orchard | From Wallis take FM 1093 northeast 4 mi (6.4 km) to Brazos River, walk upstream on the west bank approximately 1 mi (1.6 km) to first point bar. | <p>River basin controls and infrequent flooding have significantly altered the surficial bed forms and internal stratification preserved in this fine-grained point bar. Because of decreased peak annual discharge, dense stands of willow and cottonwood trees occupy and modify deposition on the middle and upper point-bar surfaces. Despite these surficial changes, the upward decreases in grain size and scale of stratification have remained unaltered.</p> <p>Point-bar deposits, including overbank muds, are about 40 ft (12 m) thick. The vertical succession of internal structures includes (1) massive to trough cross-stratified gravel, (2) trough cross-stratified sand, (3) parallel-inclined laminated sand with mud drapes, (4) ripple-drift and foreset cross-stratified sand with mud drapes, (5) ripple cross-laminated sand, and (6) alternating ripple cross-laminated silt and mud drapes.</p> |
| 4. Brazos delta | Freeport and Jones Creek | From Freeport take FM 1495 to Bryan Beach State Park, drive southwest on Gulf beach to mouth of Brazos River. | <p>Sandy beach ridges with intervening swales comprising marshes and ponds characterize the surface of this wave-dominated delta. The ponds are narrow, shallow, and tidally influenced where ephemeral channels breach the Gulf beaches. The subaerial delta is asymmetrical because sediment eroded from Bryan Beach is deposited by littoral currents on the downdrift (southwest) side of the delta. At its apex, the delta is 30 ft (9 m) thick, but it pinches out landward and along the former (1929) shoreline.</p> <p>The deltaic wedge is composed dominantly of silt and fine-grained sand, which exhibit a coarsening-upward pattern that is typical of other shoreface deposits. Sandy shoreface and beach sediments are the dominant facies, whereas channel-margin and channel-fill facies and marsh and pond facies are volumetrically less important. The shoreface sequence includes prodelta deposits (4 to 5 m) of mud interbedded with sand that grade into overlying distributary-mouth bar and delta-fringe deposits (3 m) of crossbedded and contorted sand and subordinate mud. Delta-plain equivalents are thin (less than 1 m) marsh and pond deposits of organic-rich mud or clean sand of beach and dune origins.</p> |
| 5. Brown Cedar Cut | Brown Cedar Cut | From Sargent take FM 457 to Gulf beach, drive southwest on beach 6 mi (9.7 km) to inlet using four-wheel-drive vehicle. | <p>Ephemeral tidal inlets such as Brown Cedar Cut have poorly developed ebb deltas and irregularly developed, mostly subaqueous, flood deltas delineated by partially vegetated sand shoals. These shoals and their precursors form a sand wedge that attains a maximum thickness of 10 ft (3 m) adjacent to Matagorda Peninsula. This wedge merges with laterally equivalent and underlying lagoon deposits of sandy and shelly mud. This thin sequence records the marine transgression that accompanied abandonment and subsidence of the Holocene Colorado delta.</p> <p>Brown Cedar Cut aggrades and progrades primarily during storms; therefore, the associated deposits are practically indistinguishable from washover sands. Horizontal and inclined parallel stratification, trough cross-stratification, graded beds, and shell layers are the most common structures and features preserved in the flood delta deposits.</p> |

Table 1 (continued).

| Geomorphic Feature | U.S.G.S. Quadrangle | Field Location | General Description |
|---------------------------------------|--------------------------------|---|--|
| 6. Columbus point bar, Colorado River | Columbus | From Columbus take State Highway 71 to Colorado River; point bar is downstream 0.5 mi (0.8 km). | <p>Sediments deposited by coarse-grained meandering channels with flashy discharge resemble braided-stream deposits because they typically lack systematic variations in textures and sedimentary structures. At the Columbus point bar, sediments are predominantly coarse sand; however, grain sizes range from cobble gravel to clay. Coarsest deposits are associated with the thalweg of the main channel and the chute that separates the lower and upper point bars. Except for thin mud drapes, the silts and clays are restricted to overbank material.</p> <p>Natural levees and chutes as well as transverse and longitudinal bars of different morphologies give rise to a variety of sedimentary structures. A typical sequence includes (1) massive sandy granule to cobble gravel, (2) foreset and trough cross-stratified medium- to coarse-grained sand, (3) foreset and trough cross-stratified poorly sorted gravel-bearing sand, and (4) parallel laminated and wavy-bedded medium- to coarse-grained sand and gravel.</p> |
| 7. Colorado delta | Matagorda | From Matagorda take FM 2031 south 3.2 mi (5.2 km) to southeast lobe; low levee along distributary channel leads to the bay margin. | <p>Rapid progradation following human modifications led to limited development of delta subenvironments. Low marshes interspersed with brackish-water ponds, branching distributary channels with poorly developed levees, and narrow shell beaches along the bay margin account for most of the partially submerged delta plain. Thickness (less than 12 ft [3.7 m]) of this large crevasse splay is controlled by water depths in the bay. As a result, individual facies are thin except for abandoned channel fill, which includes about 9 ft (3 m) of burrowed mud. Highly fossiliferous bay muds grade upward into burrowed and color laminated, sandy prodelta muds. Overlying distributary-mouth bar deposits is parallel laminated and ripple cross-laminated sand interbedded with sandy mud that grades upward into mottled and sandy marsh muds.</p> |
| 8. Matagorda Peninsula | Palacios SE and Palacios Point | Accessible by boat from Matagorda Bay via the Colorado River and Tiger Island Channel; landowner's permission required. | <p>West of the Colorado River, Matagorda Peninsula exhibits a typical barrier-island profile with beaches, fore-island dunes, vegetated barrier flats, and marshes that fringe the washover channels and fans. This transgressive barrier was substantially altered by Hurricane Carla in 1961, when the island was eroded and breached by numerous deep washover channels that have partially been filled by littoral processes and storms of minor intensity. Steep beaches along the peninsula are attributed to shoreline erosion and high shell content in some areas.</p> <p>Entrenched valleys filled with sandy and shelly lagoon muds are buried beneath Matagorda Peninsula. These marginal marine deposits are overlain by deltaic muds of the Holocene Brazos-Colorado delta that grade upward into muddy and shelly sands of barrier-tidal inlet origin. This transgressive sequence overrides and thins toward the flank of the Holocene delta complex denoting the younger age of the barrier in an easterly direction.</p> |
| 9. Coleta Creek | Raisin | From Victoria take U.S. Highway 77 to FM 446, drive southwest 4.2 mi (6.8 km) to Coleta Creek; point bars 0.67 mi (1 km) upstream and 1.1 mi (1.75 km) downstream from bridge accessible by paths along the creek bank. | <p>Low sinuities, flashy discharge, and low suspension-load to bed-load ratio characterize this and other coarse-grained fluvial channels. Alternate side-attached bars, point bars, and chutes exhibit a variety of bed forms including ripples on dunes with sinuous crests and scour troughs. In contrast to other fluvial models, largest bed forms (rhombs) are preserved on the upper point bars, which were inundated during peak discharge associated with Hurricane Beulah in 1967.</p> <p>These sand and gravel deposits exhibiting thin mud lenses and drapes lack systematic variations in texture and stratification. Point-bar deposits are characterized by horizontal and slightly inclined parallel stratification, foresets, and trough cross-stratifications.</p> |
| 10. Guadalupe delta | Austwell | Take State Highway 35 to Guadalupe River, turn southeast on county shell road; landowner's permission required beyond locked gates; delta margins accessible by boat from Guadalupe River, Hynes Bay, or Mission Bay. | <p>Natural levees and broad subaerial plains of this shoal-water delta are well developed along the main feeder channels, whereas marshes, lakes, and interdistributary bays are prominent on the subsiding abandoned lobes. Traylor Cut, a man-made diversion opened in 1935, is actively prograding, whereas the remaining delta margins are eroding.</p> <p>Except for abandoned channels that scour into preexisting sediments, the delta is less than 12 ft (4 m) thick and overlies bay deposits of shelly and bioturbated sandy mud. Prodelta deposits, which are color laminated clay with silt laminae, grade upward into distributary-mouth bar deposits of interbedded ripple cross-laminated silty sand and mud. Overlying delta-plain deposits are typically organic-rich, alternating laminae of silt and clay (natural levee), root-mottled mud (marsh), or bioturbated mud (interdistributary bay).</p> |
| 11. Matagorda Island | Long Island | Accessible by boat from Espiritu Santo and Aransas Bays; landowner's permission required. | <p>Broad, gently sloping beaches; high, well-developed fore-island dunes; low accretion ridges; wide washover fans; and narrow fringing marshes are typical barrier environments encountered on a transect from Gulf to bay shorelines. At present, the barrier is relatively stable because it receives sand from updrift erosion. The inner shelf and nearby coastal rivers were probably more important sand sources several thousand years ago when the barrier was building seaward.</p> <p>Facies beneath Matagorda Island are as follows: (1) late Pleistocene stiff mud and strandplain sand, (2) Holocene fluvial-deltaic sands and muds, (3) bay-estuarine mud, and (4) barrier-island sands. The latter sands are 30 to 40 ft (10 to 12 m) thick and are in gradational contact with surrounding shelf and bay muds.</p> |

Table 1 (continued).

| Geomorphic Feature | U.S.G.S. Quadrangle | Field Location | General Description |
|---|------------------------|---|---|
| 12. Copano Bay | Rockport | Take State Highway 35 to Copano Bay State Park; bay sites accessible by boat. | <p>This shallow fresh- to brackish-water bay receives primarily fine-grained sediments from adjacent areas and produces considerable biogenic detritus, mainly as oystershells. Composition of near-surface sediments is controlled by water depth and proximity to the shoreline. Sands are concentrated around the bay margin where waves erode the sandy Pleistocene sediments. In contrast, sandy mud and mud are deposited in the deeper, low-energy bay areas. Mixtures of mud and shell are generally associated with nearby oyster reefs. Most bay sediments are bioturbated, although faint ripple cross-laminations are preserved in some bay-margin and tidal-channel sands.</p> <p>Copano Bay occupies a partially filled valley that formed during the Wisconsin sea-level low stand. Along its axis, valley-fill deposits range from 30 to 70 ft (9 to 21 m) thick.</p> |
| 13. Aransas Pass, Harbor Island | Port Aransas and Estes | From Aransas Pass take State Highway 361 for 6 mi (9.7 km) to Harbor Island and Aransas Pass Ferry; undeveloped areas on Harbor Island accessible by boat. | <p>This tidal inlet and associated flood-tidal delta have been modified by dredging and construction that began in the early 1860's. Prior to that time, Lydia Ann Channel was the only deep tidal channel in southern Aransas Bay. Although much of the area was submerged, narrow storm berms along the channel margins formed the highest elevations of about 3 ft (1 m) above sea level. Elsewhere, elevations of sandy wind-tidal flats and low marshes were near sea level.</p> <p>Sedimentary facies beneath Harbor Island record a brief transgression followed by a period of sea-level stability. Marsh deposits of organic-rich sand and mud are overlain by a combination of bay mud or fossiliferous sandy mud of grassflat origin. A wedge of tidal-delta and barrier sands 35 ft (11 m) thick grades laterally and landward into these bay deposits. Most of these sediments are extensively bioturbated.</p> |
| 14. Gum Hollow delta | Gregory | From Portland take FM 893 northwest 3 mi (4.8 km) to Gum Hollow channel, walk downstream 0.5 mi (0.8 km) to delta. | <p>Sand and minor mud deposited on this inactive fan delta are derived from adjacent uplands composed of Pleistocene deltaic sands and muds. The ephemeral, high-gradient, low-sinuosity channel that supplied the delta is fed primarily by a drainage system formerly activated by runoff from croplands and brine disposal. Recent aggradation and progradation of the fan resulted from floods during Hurricane Beulah in 1967.</p> <p>Textural variations across the fan are minor with the exception of mud clasts that decrease in size but increase in volume downfan. Unconfined flow across the fan produces longitudinal and transverse bars of the braided channels and fan plain. These bed forms are preserved as horizontal and slightly inclined parallel laminations as well as low-angle foresets. On the fan plain, ripple cross-stratification with mud drapes commonly forms from linguoid ripples between the bars. Delta-front and prodelta deposits are ripple cross-laminated sand interbedded with mud.</p> |
| 15. Packery Channel | Crane Islands | From Corpus Christi take JFK Causeway, turn left on Park Road 53, and drive 0.4 mi (0.6 km) to Packery Channel. | <p>This tidal inlet once separated Mustang and Padre Islands; however, the inlet closed after its tidal prism was reduced by deepening of Aransas Pass and adjacent navigation channels. The inlet is opened for brief periods by storm surge or extreme northers that drive bay water across the low barrier segment where the inlet formerly migrated.</p> <p>Inlet fill comprises much of the shallow subsurface sediment in the Packery Channel area. In basal channel-fill deposits, repetitive fining-upward cycles are controlled by the size and amount of shell, whereas upward increases in mud indicate periodic inlet abandonment. The inlet fill and laterally equivalent bay deposits of muddy sand are disconformable with the underlying Pleistocene strandplain sands, whereas they are in gradational contact with overlying washover sands. Together, the Holocene barrier and inlet-fill sequence are about 25 ft (8 m) thick.</p> |
| 16. North Padre Island | South Bird Island | From entrance to Padre Island National Seashore drive 1 mi (1.6 km), then turn left on access road to Gulf beach and nonvehicular traffic area; trenching or coring requires permission of Park Ranger. | <p>Surface environments at this locality include forebeach, backbeach, fore-island dunes, vegetated barrier flat, backisland dunes, and wind-tidal flat. The latter two environments are generally not found in barriers to the north. Active dunes partly reflect the semiarid climate, but they also show the effects of droughts and overgrazing.</p> <p>Because vehicular traffic is controlled, this area exhibits sedimentary structures typical of beaches and fore-island dunes. Forebeach deposits are sometimes burrowed, gently seaward-dipping, parallel laminated sand with various amounts of shell and minor amounts of heavy minerals accentuating the bedding surfaces. Except after storms, the backbeach is usually flat and commonly ponds water. Resulting stratification types are horizontal or gently dipping, parallel laminated sand with shallow scour and fill and ripple cross-lamination. Dune stratification is usually trough cross-stratification and wedges of parallel inclined laminae.</p> |
| 17. North Laguna Madre, South Bird Island | South Bird Island | From entrance to Padre Island National Seashore drive 2.2 mi (3.5 km) on Park Road 22, turn right and proceed to Bird Island Basin; trenching or coring requires permission of Park Ranger. | <p>North Laguna Madre is occasionally hypersaline because it is isolated from tidal inlets and riverine discharge, and evapotranspiration commonly exceeds precipitation. The dominance of surficial sand, low turbidity, and shallow depths contribute to the development of extensive stands of algae and marine grasses. High organic productivity is also shown by the numerous gastropods that inhabit these areas. Along the Gulf Intracoastal Waterway, atypical sediments such as mud-clast gravel are derived from dredged material reworked by waves.</p> <p>Active backisland dunes supply sand to Laguna Madre, especially during droughts when water levels are lower. This aeolian sand forms a shoal with avalanche face that migrates over previous grassflat deposits of massive (bioturbated) shelly sand and shell. Mud, which is generally subordinate to sand and shell, is deposited in slightly deeper water near the lagoon center.</p> |

Table 1 (continued).

| Geomorphic Feature | U.S.G.S. Quadrangle | Field Location | General Description |
|--------------------------|-------------------------|--|---|
| 18. South Laguna Madre | Three Islands | From South Padre Island take four-wheel-drive vehicle north 20 mi (32 km) along Gulf beach and proceed toward lagoon via oil field road. | Moderate temperatures, high evaporation rates, shallow water depths, and the near absence of upland runoff control the sedimentological, biological, and hydrochemical facies of this hypersaline lagoon and adjacent wind-tidal flats. In this area, lagoon deposits, including marine grassflats, are less than 1 ft (0.3 m) thick and are composed of olive-gray root-disrupted and burrowed shelly mud and sand. Wind-tidal flat deposits, which occur seaward of and beneath the lagoon sediments, are predominantly parallel laminated sand alternating with thin mud laminae or algal-bound sand. Common features also include gas-bubble structures, contorted bedding, and shell debris at sequence boundaries. The thin lagoonal facies as well as radiocarbon dates from the underlying deltaic muds document the recent formation of the lagoon in conjunction with abandonment and subsidence of the Holocene Rio Grande delta. |
| 19. South Padre Island | North of Port Isabel SW | From Port Isabel take Queen Isabella Causeway and Park Road 100 north to Andy Bowie Park and beach access road. | Southward from about Mansfield Channel, Padre Island is a transgressive barrier that is migrating landward by the combined processes of shoreline retreat and storm washover. The relatively high rates of beach erosion, dune migration, and frequent flooding by wind tides from Laguna Madre and storm surge from the Gulf make this an extremely dynamic area. Typical sedimentary structures of the barrier sands are horizontal and low-angle parallel laminations with subordinate scour and fill and rare foresets, and small-scale ripple cross-laminations. Grain-size changes within the sands are related primarily to the presence or absence of shells. The thin (less than 10 ft [3.0 m]) sand facies interfingers with and overlies lagoon muds and interbedded algal-bound sands and muds deposited on wind-tidal flats. In contrast, the underlying fluvial sands and deltaic muds of the Holocene Rio Grande delta are about 40 ft (12 m) thick. |
| 20. Brazos Santiago Pass | Port Isabel | From Port Isabel take Queen Isabella Causeway and Park Road 100 south 1 mi (1.6 km) to Isla Blanca Park. | This major tidal inlet occupies the southeastern part of Laguna Madre where Padre Island adjoins the Rio Grande delta. Prior to dredging and jetty construction in 1929, the tidal channel attained a maximum depth of about -30 ft m.s.l. (-9 m) at its narrowest point between Padre and Brazos Islands. Landward from this point, the channel shoaled and formed several drains with northwesterly alignments; the seaward terminus of the channel was abrupt but more diffuse as it merged with the broadly arcuate outer bar. These sandy shoals, that respectively represent the flood- and ebb-tidal deltas, ranged in thickness from 15 to 20 ft (5 to 6 m). They also comprise the transgressive marine sediments that unconformably overlie the delta-plain muds of the ancestral Rio Grande delta. |

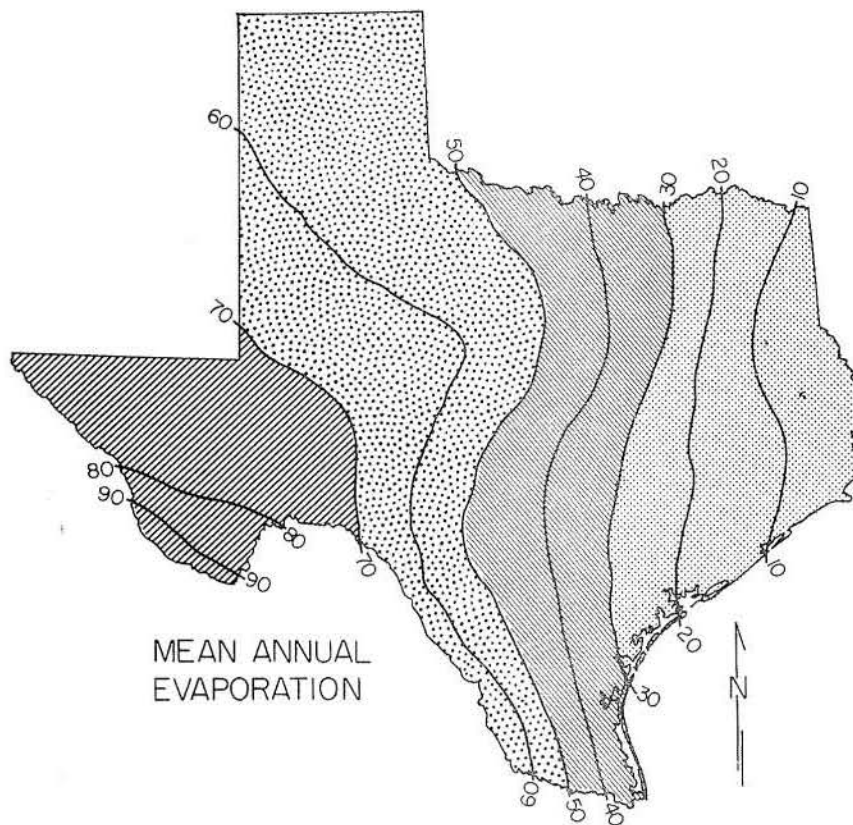
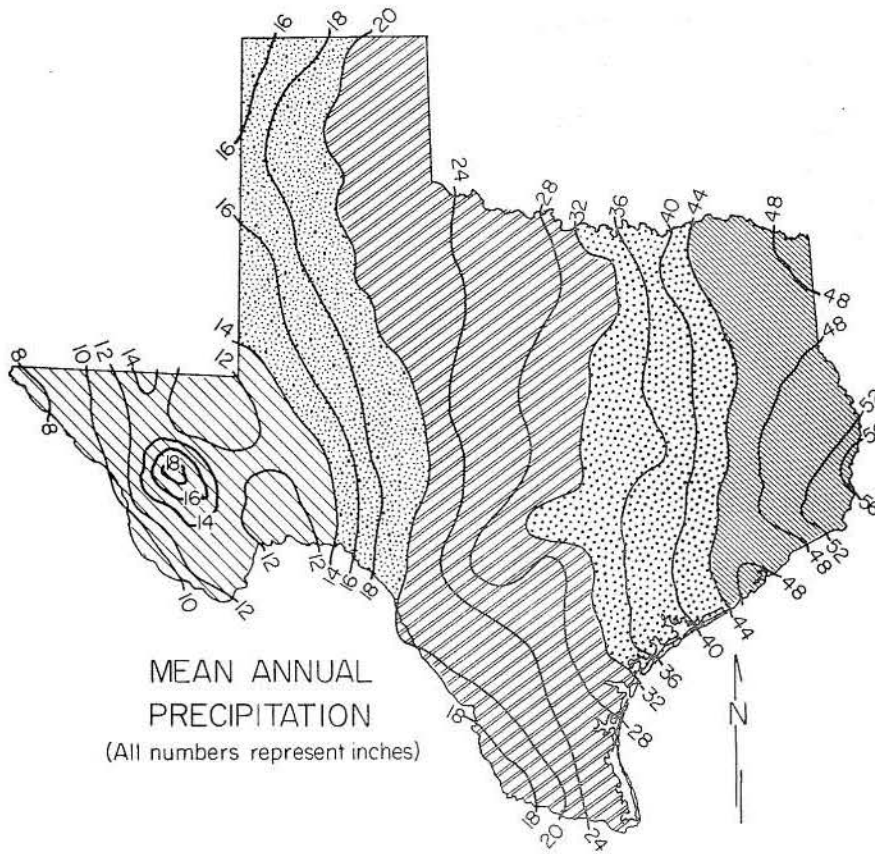


Figure 2. Mean annual precipitation and mean annual evaporation for Texas based on records for 1931-1960 and 1940-1957, respectively. From Carr (1967) and Arbingast and others (1967).

lagoons. Low current velocities attendant with this long periodicity and microtidal range (in the classification of Hayes, 1975) produce sedimentary deposits that are markedly different from those formed under mesotidal or macrotidal conditions.

Microtidal low-energy coasts are essentially synonymous with storm-dominated coasts because energy expended and geological work accomplished during storms overwhelm daily processes. Most often ebb velocities are slightly greater than flood velocities, but neither exceeds 2.5 fps (76 cm/s) on a regular basis. Strong northerly winds, return of storm surge flow, and rainfall runoff may cause high ebb velocities for brief periods, but in general, tidal velocities at most major inlets are lower now than they were a century ago because of increased (dredged) cross-sectional areas.

Subsidence and Relative Sea-Level Rise

Sea-level changes and compactional subsidence are important to land-sea relationships. Holocene sea-level changes (Shepard, 1960) are based on carbon-14 data, but relative sea-level changes during historical time are deduced by monitoring tides and developing trends based on long-term measurements (Hicks, 1972). This method, however, does not distinguish between sea-level rise and land-surface subsidence.

Compactional subsidence is important on a geological time scale, but increased subsidence from ground-water withdrawal and hydrocarbon production is important historically in some areas. Recent data support the theory of compactional subsidence along the Texas coast (Swanson and Thurlow, 1973). On a regional scale, the central Texas coast has experienced relative tectonic stability because of the San Marcos Arch, whereas adjacent areas within the Rio Grande and Houston Embayments have undergone greater subsidence during geologic time. High-resolution sparker profiles indicate that late Quaternary nearshore sedimentation was influenced by subsidence in the Rio Grande Embayment.

FLUVIAL SYSTEMS

Introduction

Modern fluvial systems have been classified by channel pattern and by their sediment loads. In general, the size of a river or stream increases in a downstream direction as discharge increases. Some streams exhibit a decrease in size downstream as the stream moves from humid to arid conditions and experiences ever-decreasing rainfall.

Texas streams increase in size from their headwaters toward the Gulf of Mexico. Some of these streams (for example, the Brazos and Colorado Rivers) head in low-rainfall areas but cross zones of high rainfall on their journey to the Gulf of Mexico. An individual stream, such as the Brazos River, may exhibit changes in channel pattern downstream, may be a bed-load stream in its upper reaches but either a mixed- or a suspended-load stream in the Coastal Zone, and it may be flashy within its headwaters but have a flood stage that may last for days along its lower reaches. The Brazos River is a flashy braided (bed-load) stream in its upper reaches (Waechter, 1972) and is a highly meandering (mixed-load) stream in the Coastal Zone (Bernard and others, 1970).

A single fluvial system undergoes changes in slope (fig. 3), discharge, channel pattern, and volume and caliber of sediment load in a downstream direction. Similar changes probably occurred in ancient fluvial systems, and these changes should be reflected in geometry, channel to overbank sediment ratio, trends in texture, and primary sedimentary structures.

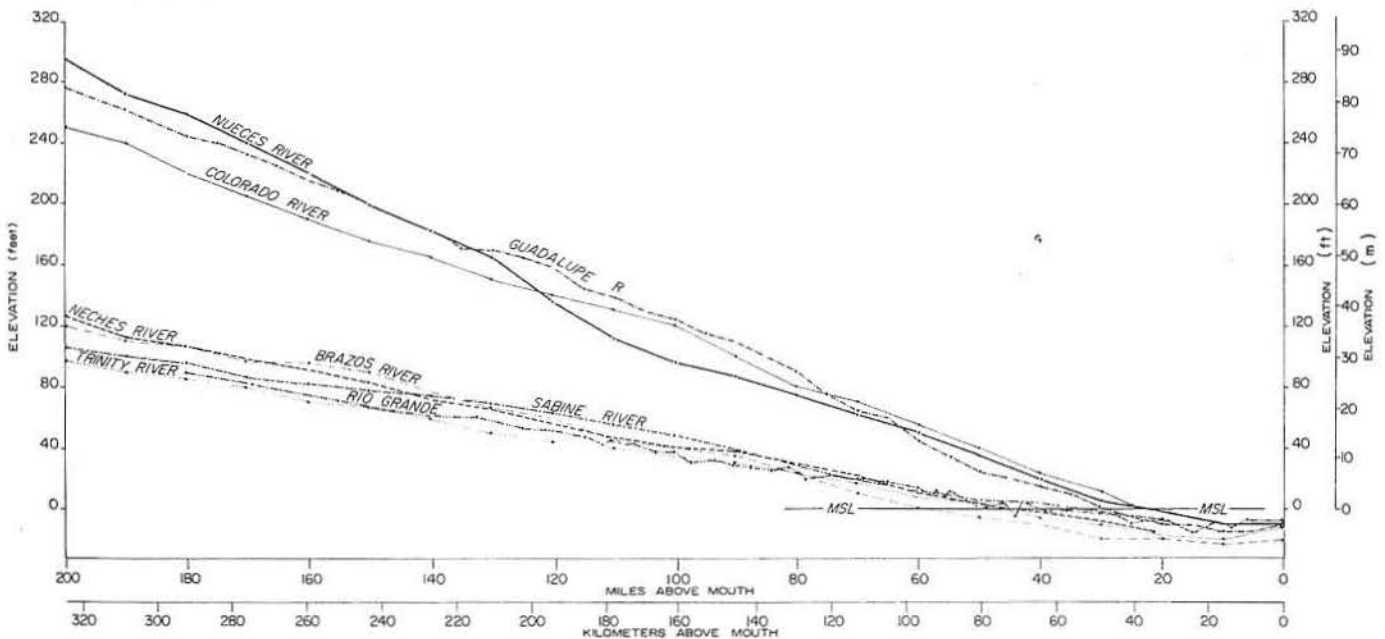


Figure 3. Longitudinal channel profiles for major Texas rivers. Drawn from river and tributary studies by the U.S. Army Corps of Engineers, Galveston and Fort Worth Districts. Profile for Rio Grande provided by the International Boundary and Water Commission (after Morton and Donaldson, 1978a).

As precipitation and temperature (fig. 2) change from northeast to southwest along the Coastal Plain, there is a corresponding change in fluvial systems. Streams along the upper coast (Sabine, Neches, Trinity, and Brazos Rivers) carry a mixed sediment load and exhibit meandering channel patterns. Upper coast streams have similar slopes and discharge characteristics (figs. 3 and 4). Central coast streams (Colorado, Guadalupe, San Antonio, and Nueces Rivers, and Coleta Creek) do not fit into a single fluvial category (although most are meandering streams) because they differ from one another in size of drainage basins (for example, Colorado River is large and Coleta Creek is small) and in bed-load/suspension-load ratio (for example, Colorado River is a bed-load stream, and Guadalupe River is a suspended-load stream). Streams at the southern part of the central coast traverse progressively more arid climatic zones toward the west; channel pattern and discharge characteristics of these streams differ somewhat from those of the other central coast streams. The Nueces River, near the southern limit of the central coast, has a relatively high gradient (fig. 3), has a flashy discharge (fig. 4), and is locally braided.

The Rio Grande at the southern limits of the lower coast is a relatively large river that has a slope similar to that of the Trinity River (fig. 3). In Texas, the Rio Grande traverses sedimentary and volcanic rocks, and along its generally westward course rainfall decreases (fig. 2) from about 25 inches (61 cm) at the coast to about 8 inches (16 cm) near El Paso. Discharge data (fig. 5) were collected for the Rio Grande near the coast at Brownsville after completion of Falcon Dam and, therefore, cannot be related to stream pattern and sediment characteristics. Prior to impoundment of water and sediment in reservoirs, the Rio Grande was a mixed-load, meandering stream along its lower reaches.

CLASSIFICATION OF FLUVIAL SYSTEMS

Modern streams have been classified by geomorphologists according to channel pattern (Leopold, Wolman, and Miller, 1964) and the type of sediment transported by the stream (Schumm, 1972). The channel patterns that have been recognized are meandering, straight, and braided. Fluvial types based on the property of sediment characteristics are bed-load, mixed-load, and suspended-load channels.

Channel Patterns

Leopold, Wolman, and Miller (1964) used the ratio of channel length to down-valley length (sinuosity) to distinguish between meandering and straight streams. Streams with a ratio greater than 1.5 are considered meandering, and those with a ratio of less than 1.5 are considered straight or sinuous. A braided channel divides into several channels that successively meet and divide again.

Straight channels are typified by a high width/depth ratio and by heterogenous bed material. Although the channel may be straight, the thalweg is sinuous. Flow within the channel is normally sinuous, but during extreme floods flow may be straight. In channels with sinuous flow, sediment accumulates and forms bars adjacent to the bank farthest from the thalweg. These bars form downstream, alternately adjacent to one bank and then the other.

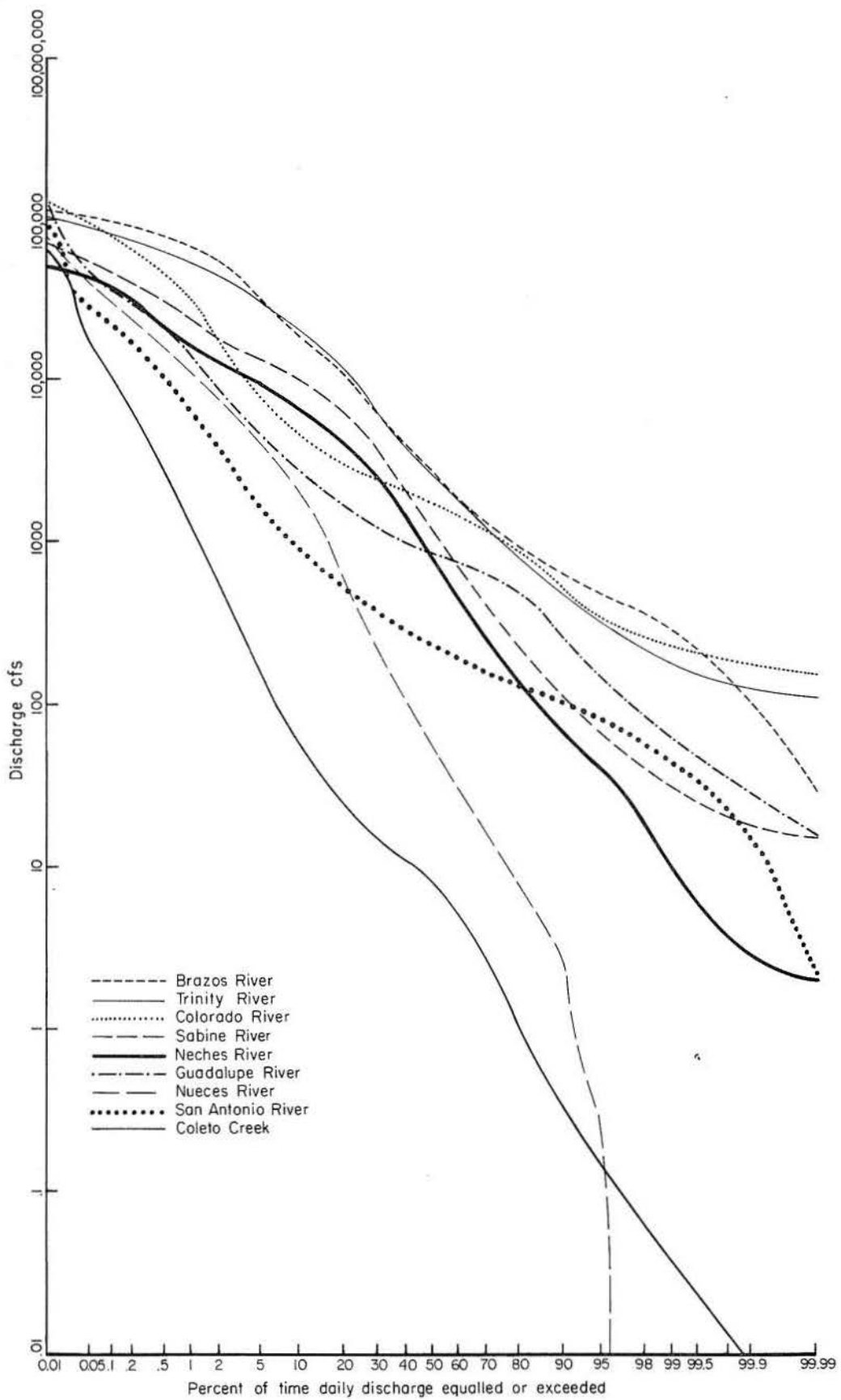


Figure 4. Flow duration curves for major Texas rivers excluding the Rio Grande. Drawn from unpublished data provided by the U.S. Geological Survey, Surface Water Branch, Austin, Texas.

Braided channels, which also have a high width/depth ratio, are separated by islands or bars that are commonly emergent at low flow but may be inundated at high flow. Braiding generally occurs where stream gradient is high, discharge is flashy, channel banks are easily eroded, and a large volume of sediment is available to the system. Not all braided streams are alike because of variations in discharge, slope, and sediment volume and caliber. But braided streams generally exhibit some common downstream trends such as a decrease in slope, grain size, discharge, and channel depth, and an increase in channel width. Accompanying these downstream changes is a predictable downstream succession of large and small bed forms (Ore, 1964; Smith, 1970; Boothroyd, 1972; and Miall, 1977). From upstream to downstream reaches the bed forms are longitudinal bars with adjacent gravel-floored channels, longitudinal bars with dunes and transverse bars in adjacent channels, transverse bars, dunes, and dunes with ripples.

Meandering streams, in addition to having a sinuous pattern, have a low-gradient, continuous flow and a pronounced flood stage, a lower sediment load relative to discharge than that of braided streams, resistive bank materials, asymmetrical channel cross sections at bends with deepest part (scour pool) adjacent to the concave bank, and shallow channel cross sections at crossovers. Meandering streams may be characterized by a dominance of bed-load material, suspended-load material, or a combination of bed-load and suspended-load material. The Brazos River is perhaps the best known meandering stream (Bernard and others, 1970); it is characterized by a small width/depth ratio, a decrease in grain size from gravel in the scour pool to mud on the upper point bar, and a decrease in scale of depositional features (bed forms) from gravel-filled troughs in the scour pool to ripples and mud drapes on the upper point bar.

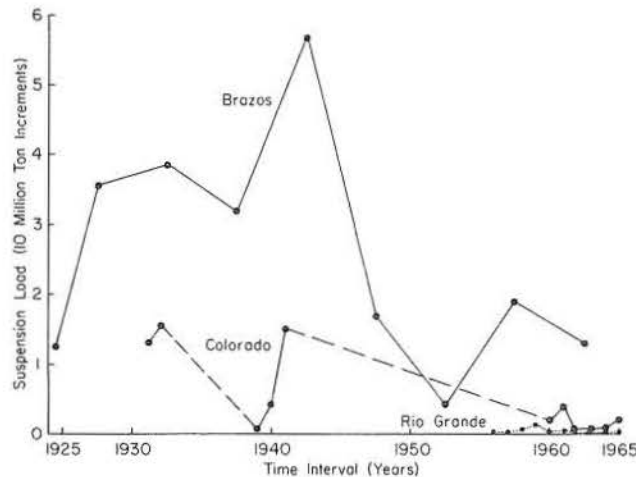


Figure 5. Comparison of suspension loads of Brazos and Colorado Rivers and Rio Grande (data from Stout and others, 1961; Adey and Cook, 1964; Cook, 1967, 1970); gaging stations on the Brazos at Richmond, on the Colorado near Eagle Lake, and on the Rio Grande at Brownsville. The Brazos clearly dominates the coastal scene. Both the Brazos and the Colorado show a decrease in suspension load. Suspension load at Brownsville was monitored only after the completion of Falcon Dam (1954) and does not, therefore, reflect the contribution of sediment to the Gulf of Mexico via the Rio Grande prior to its alteration. (After McGowen, Garner, and Wilkinson, 1977).

Classification of Channels by Sediment Type

Stream channel types are classified on the basis of sediment load as bed-load, suspended-load, and mixed-load channels (Schumm, 1968, 1972).

Bed-load streams are relatively wide, shallow, and straight, and on the average transport more than 11 percent sand-sized and larger sediment. Width/depth ratio of these channels is greater than 40; gradients are relatively steep; and sinuosity is less than 1.3. Galloway (1977, 1979) has expanded somewhat on Schumm's classification (1968, 1972) chiefly as a result of study of fluvial systems in the Tertiary of Texas. According to Galloway, the bed-load channel-fill sequence is dominated by sand. Coarse sand and gravel are commonly present but are not necessary components: the sequence could consist exclusively of fine to medium sand. A bed-load channel is characterized by a tendency to erode laterally, producing a tabular or belted sand body. Development of multilateral channel fills may produce a fluvial sheet sand. Straight channels are characterized by relatively uniform depths of scour along the base, and this may be reflected by the low relief on the base of the sand body and by preservation of laterally continuous sheet or tabular, remnant floodplain mud units. Internally, bed-load channel-fill sequences reflect the dominance of bed accretion units, such as longitudinal, transverse, lateral, and chute bars, which produce a channel fill consisting of multiple, interlensed depositional units of varying grain size and displaying complex textural sequences. Braided and coarse-grained meanderbelt models are well-documented types of bed-load channel-fill sequences.

Suspended-load channels generally transport less than 3 percent bed load; the dominant sediment transport type is a combination of suspended and dissolved load. Width/depth ratio is less than 10; sinuosity is greater than 2, and the gradient is gentle. According to Galloway (1977, 1979) suspended-load channels are narrow and confined, erosion occurs primarily at the base, and surrounding clay-rich sediments form stable, steep channel banks. Channel fill is deposited mostly along the banks and may be asymmetrical in highly sinuous channel segments or symmetrical in straight channel segments. The dominant channel-fill sediment ranges from very fine sand to silt and clay, but some very coarse sediment may be present. Sand-body geometry is highly lenticular in cross section and forms observable sinuous or anastomosing patterns. Channel-fill units are typically encased in fine-grained floodbasin deposits and tend to stack vertically. Vertical sequences may fine upward or may show little vertical variation if the range of grain sizes is limited.

The bed load of mixed-load streams ranges from 3 to 11 percent of the total load. The dominant sediment transport type is mixed suspension and bed load. Width/depth ratio is greater than 10 and less than 40. Sinuosity is greater than 1.3 but less than 2.0, and gradient is moderate. According to Schumm (1968, 1972), mixed-load streams can be braided. The fill of mixed-load channels consists of sand and minor amounts of silt and clay (Galloway, 1979). Sinuous channels with variable scour depths along the thalweg are characterized by irregular sand belts. Floodbasin deposits are lenticular and discontinuous between channel-fill sequences. A record of mixed bank- and bed-accretion (point-bar and scour-pool) deposits is preserved in the channel fill, and a repetitive fining-upward sequence typifies most vertical sections through the meanderbelt deposit. Channel meandering and consequent point-bar accretion, combined with stacking and amalgamation of successive channel fills, commonly produce a composite sand body that is much larger than the original channel. Mud-filled abandoned channels, displayed in the rock record, preserve the approximate channel dimensions. Mixed-load channel fills are typified by the fine-grained point-bar model.

FLUVIAL MODELS

Three general fluvial models have been developed from the studies of modern rivers. These models are for braided, straight, and meandering channels. Most geologists are aware that there is no sharp distinction between fluvial systems and that there is a continuous gradation from one channel type to another. A single fluvial system may therefore exhibit, from its headwaters to its mouth, braided, coarse-grained meanderbelts, fine-grained meanderbelts, and delta distributaries (Brown and others, 1973). Because of this fluvial spectrum and gradations from one fluvial type into another, it is difficult, if not impossible, to construct (for example) a single fine-grained meanderbelt model that can be applied, on a one-to-one basis, to ancient fine-grained meanderbelt deposits. A good model must be simple enough to ensure its applicability to a wide range of ancient fluvial deposits; it is not necessarily invalidated because it does not account for some minute detail observed in the rock record. The models presented in the following discussion have had rather wide use.

Braided-Stream Model

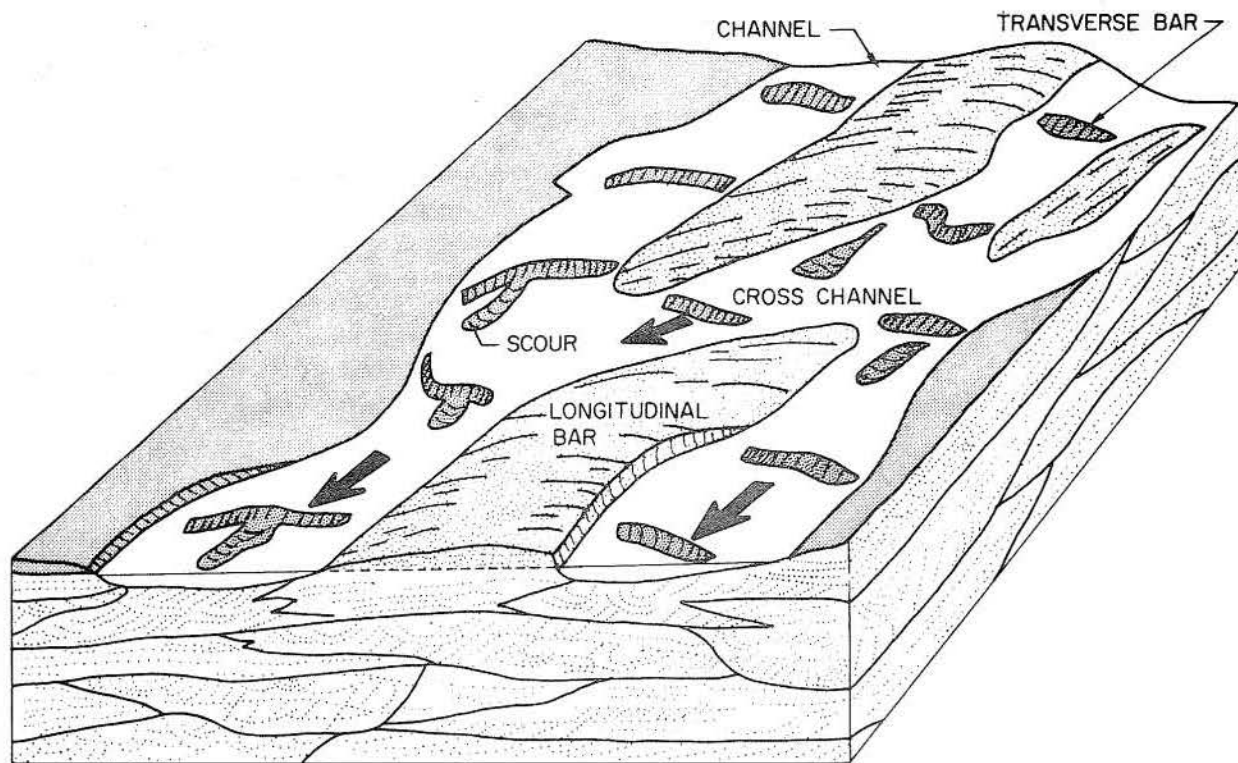
Braided streams display a pattern of stream diversion and subsequent rejoining. This pattern is apparent during low-flow conditions. Braided streams are characterized by steep gradients (normally), erodable banks, unconfined flow, flashy discharge, and a dominance of bed-load material that may range in size from silt to boulders. Sand bodies developed by braided streams are multilateral and have a high width/thickness ratio. Braided streams are commonly developed on alluvial fans, fan deltas, and sandurs, and along upper reaches of major fluvial systems (Ethridge, 1978).

Examples of braided streams (or braided-stream segments) in Texas are parts of the Brazos River, Prairie Dog Town Fork of the Red River (Waechter, 1972), South Canadian River (Kessler, 1971), and parts of the San Bernard and Nueces Rivers.

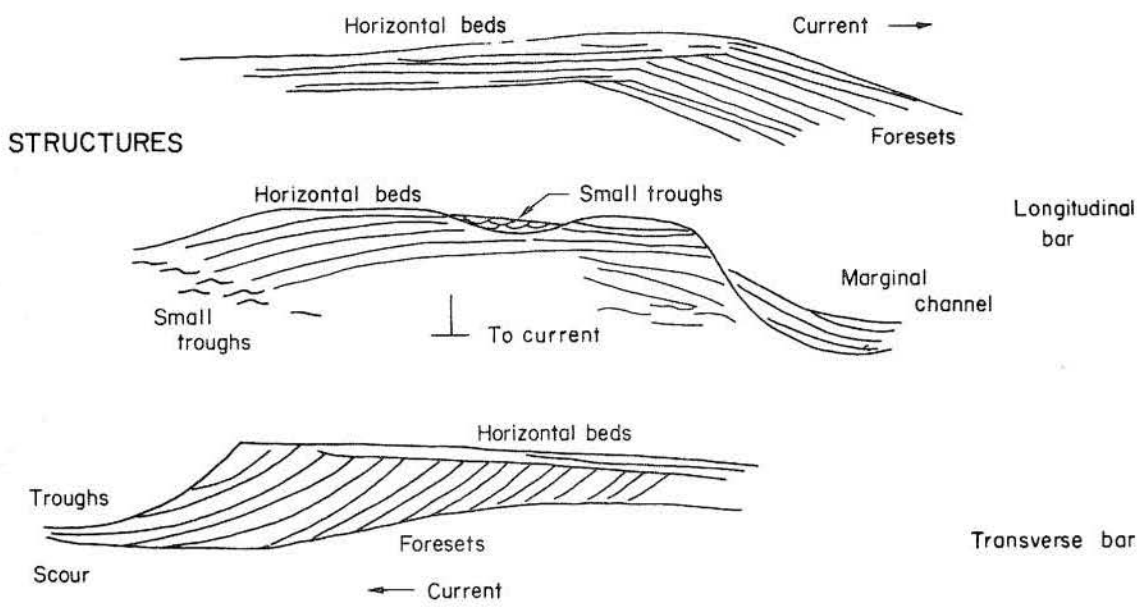
The generalized model (fig. 6) presented here is taken from Fisher and Brown (1972) and Brown and others (1973). This model, based on the work of Ore (1963, 1965) and Smith (1970), contains certain elements found in proximal and distal deposits of the South Platte River. Bed forms and resulting stratification are shown in this diagram.

Longitudinal bars are mostly confined to the more proximal parts of braided streams. They are elongate in the direction of flow and may be composed of gravel or sand, or a combination thereof, with coarsest material at the upcurrent end. Longitudinal bars may be hundreds of feet long, tens of feet wide, and about 1 to 5 ft thick. The type of stratification observed depends upon which part of the bar is exposed. At the upcurrent end the bar may be either massive or crudely horizontally bedded. Bedding becomes more distinct in a downcurrent direction where the central bar is horizontally bedded and the bar flanks and distal bar are foreset crossbedded.

Transverse bars may be developed in braided channels in the proximal stream areas, or they may form in the more distal areas. Transverse bars may be the dominant bed form, or they may occur in association with dunes. The entire channel width may be spanned by transverse bars whose slip faces are directed downcurrent. Transverse bars may be tens of feet wide and have heights from a few inches to about 3 ft (90 cm). Stratification within transverse bars is typified by foreset crossbeds that are directed downcurrent. Foreset geometry is a function of current velocity. Steep foresets with high-angle upper and lower contacts formed under low-velocity conditions, whereas sigmoidal foresets are products of high-velocity currents.



A



B

Figure 6. Depositional model of an idealized braided fluvial system. A. Block diagram showing bed forms, sedimentary structures, and multilateral-sand geometry. B. Sedimentary structures deposited by longitudinal and transverse bars. Modified from Ore (1963, 1965) and Smith (1970); described by Fisher and Brown (1972). (After Brown, Cleaves, and Erxleben, 1973).

Dunes are common bed forms in some braided-stream systems. However, the model herein (fig. 6) shows that dunes are perhaps minor bed forms in the Platte River. Dunes are discontinuous bed forms that develop and migrate downcurrent under low-flow conditions. Dunes have a wide range of shapes in plan ranging from linguoid forms to asymmetrical crescents. Spoon-shaped scours are formed and filled as dunes migrate downcurrent. Resulting stratification is trough-fill cross-strata ranging from a few feet to a few tens of feet long, generally 1 to 8 ft (30 cm to 2 m) wide, and a few inches to about 3 ft (90 cm) thick.

Distinguishing features of braided-stream systems are (1) multilateral sand-body geometry, (2) a simple suite of stratification types that exhibit no vertical trend, (3) lateral discontinuity of sedimentation units, (4) a mixture of sand and gravel with no vertical trend in grain size, and (5) rare overbank deposits.

Coarse-Grained Meanderbelt Model

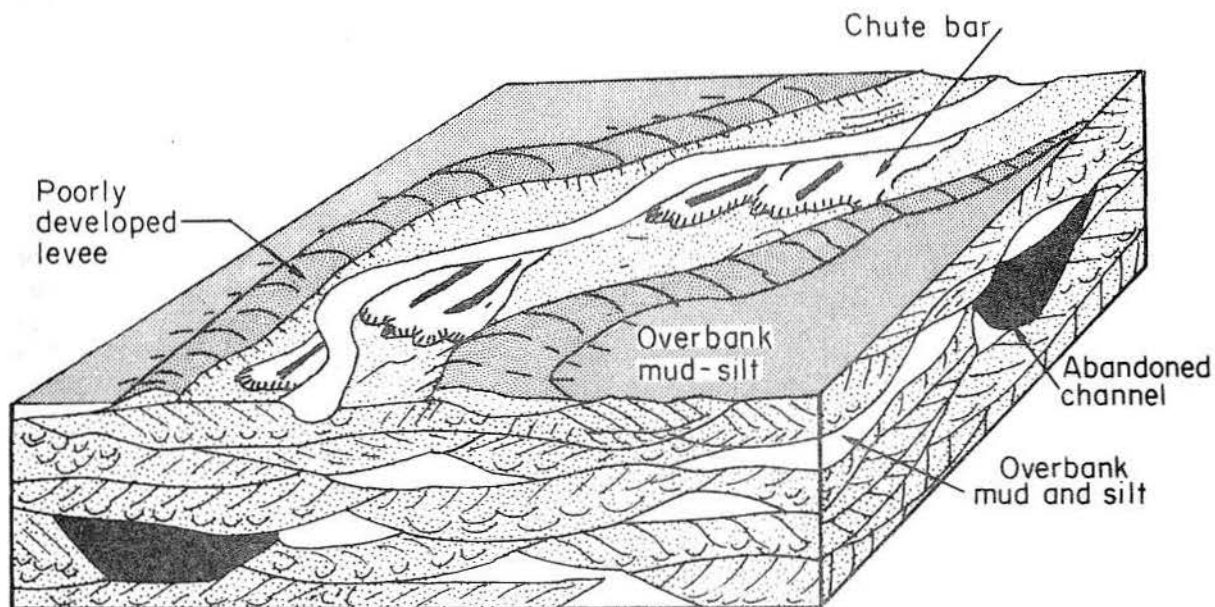
This model was developed from study of the Colorado River in Texas and the Amite River in Louisiana (McGowen and Garner, 1970). Both are bed-load streams that transport medium sand to pebble and cobble gravel. Parts of these streams probably would braid were their banks not stabilized by vegetation. Sinuosity of these streams ranges from 1.4 to 1.7. Although their courses are meandering, the streams tend to be straightened during extreme flood when flow cuts chutes across the upper point bars. Sediment, approximately as coarse grained as scour pool deposits, travels through these chutes to accumulate at about the level of flood waters as lobate features (chute bars) on the upper point bar.

Broad characteristics of coarse-grained meanderbelt systems are high gradients, alternately confined and unconfined flow, flashy discharge, high bed-load/suspension-load ratio, poorly developed levees, and multilateral sand bodies. Texas Coastal Zone streams that exhibit these properties, in addition to the Colorado River, are San Bernard River (Wenzel, 1975) and Coletto Creek (this report).

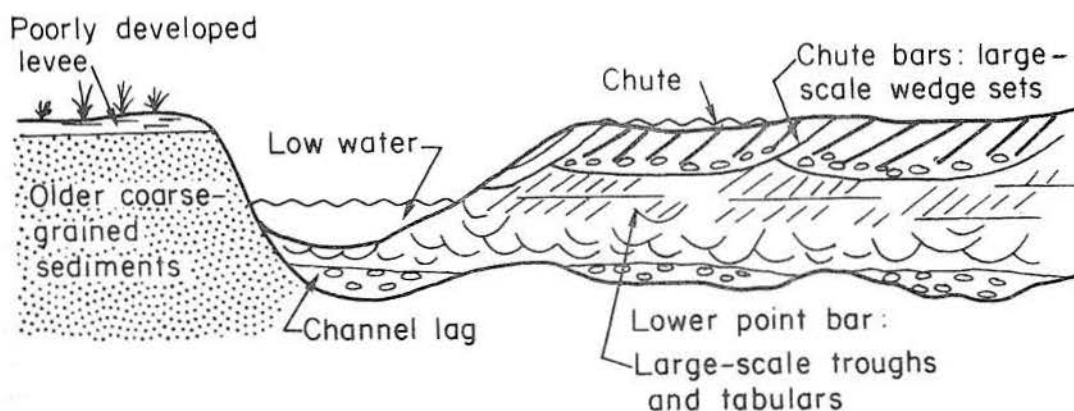
Three physiographic elements of the coarse-grained meanderbelt are the scour pool, lower point bar, and upper point bar. Depositional and erosional features of the scour pool are scour troughs 1 to 3 ft (30 to 90 cm) deep and up to 10 ft (3 m) across. Scour troughs developed around large trees that were undercut on the concave bank and are eroded into gravel deposits; scours are subsequently filled with gravel. The lower point bar has a relatively flat upper surface (slightly above low-water stage) that slopes gently toward the stream. Bed forms on the lower point bar are dunes and transverse bars; the stratification types are foreset and trough-fill cross-strata, respectively. Sediment making up the lower point bar is mostly coarse sand and gravelly coarse sand. The upper point bar (on the Amite River) ranges from about 5 to 8 ft (1.5 m to 2 m) in height above the lower point bar. Sediment from which the chute bars are constructed is coarse sand and granule to pebble gravel; chute bars have relatively flat upper surfaces and steeply sloping foresets. Stratification of chute bars consists of thin upper horizontally bedded units, and lower thick foreset crossbeds; foresets commonly are coarse at the top and fine toward the toe where rare medium sand units contain regressive ripples. Chutes are 6 to 8 ft (1.5 to 2 m) deep (Amite River), are parabolic in cross section, and are filled with fining-upward cyclic deposits (gravel at the base, followed by sand, which is capped by mud drapes). Chute-fill units conform, in general, to the channel cross section; they are thickest near the chute axis and thin toward chute flanks where ripple-drift sand units are common. Overbank

materials (Amite River) are horizontally bedded fine- to coarse-grained sands whose primary sedimentary structures have mostly been destroyed by plant roots.

A block diagram (fig. 7A) shows that coarse-grained meanderbelt systems contain only a small amount of fine-grained sediment (Brown and others, 1973). This is a high-sand system characterized by multilateral sand bodies that, for the most part, do not exhibit the classical fining-upward textural trend, or the vertical decrease in scale of sedimentation units (fig. 7B). A unique feature of coarse-grained meanderbelt sequences is a double erosional unconformity produced by the channel thalweg (at the base) and chutes (at the top) as the fluvial system migrates laterally.



A



B

Figure 7. Depositional model of an idealized coarse-grained-meanderbelt fluvial system. A. Block diagram showing bed forms, sedimentary structures, and multi-lateral-sand geometry. B. Schematic cross section of coarse-grained point-bar deposits. Modified from McGowen and Garner (1970). (After Brown, Cleaves, and Erxleben, 1973).

Fine-Grained Meanderbelt Model

Initial work by Shell Development Company (Bernard and Major, 1963; Bernard and others, 1970) on the Blasdel point bar of the Brazos River of Texas led to the development of the fine-grained point-bar model. The Brazos River is a highly meandering, mixed-load stream, that has a gradient of about 0.1 ft per mi on the outer Coastal Plain (Nienaber, 1963; fig. 3).

In general, fine-grained meanderbelts are characterized by a low-gradient, confined flow, a continuous discharge with a pronounced flood stage, high suspension-load/bed-load ratio, well-developed levees, and multistoried sand bodies (fig. 8A).

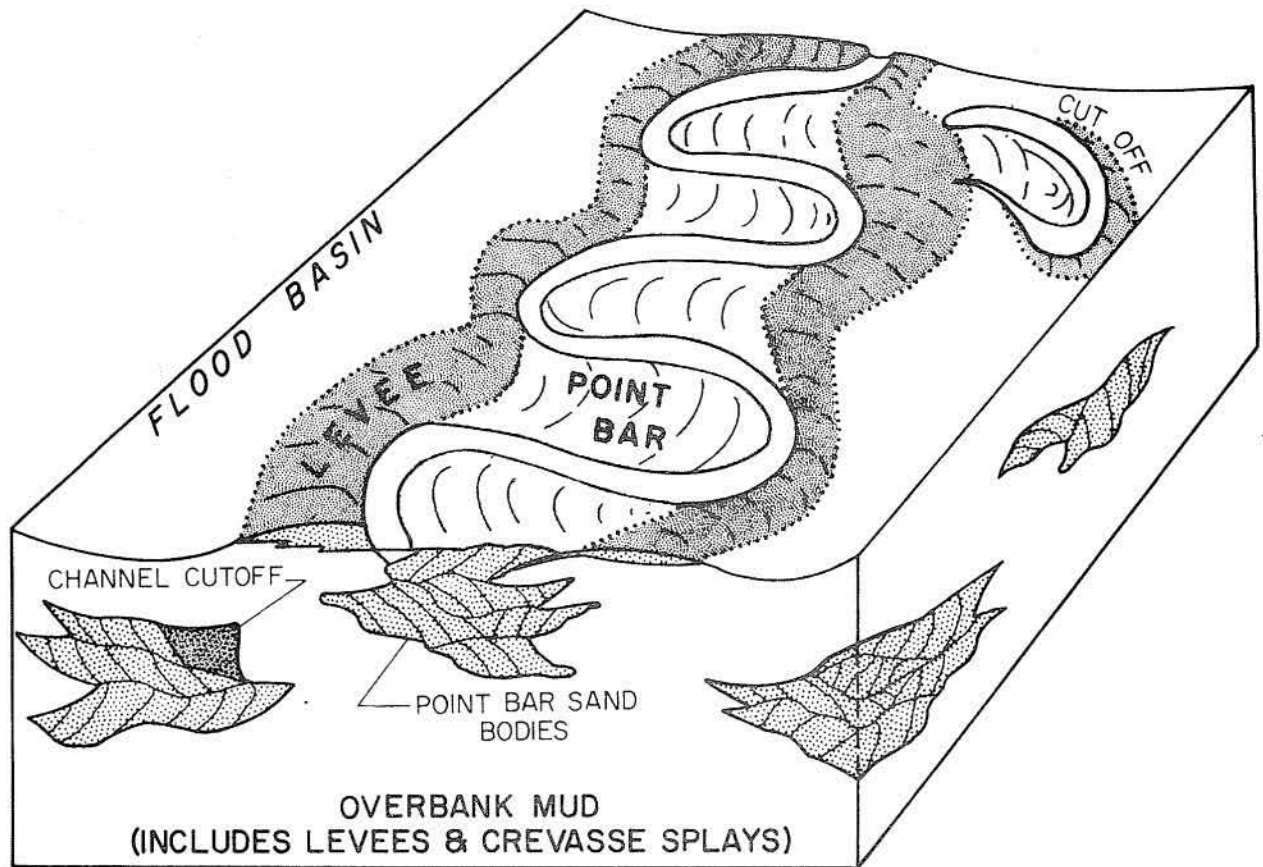
Mixed-load, fine-grained meanderbelt systems generally occupy the lower reaches of fluvial systems just upstream from deltas. These streams (such as Sabine, Trinity, and Brazos Rivers) generally have more continuous and regular runoff than do bed-load streams such as Colorado River, Coleta Creek, and Nueces River (fig. 4). Fine-grained meanderbelt systems commonly have only one channel that carries water continuously and overflows for short periods of time during extreme floods.

Physiographic elements of fine-grained meanderbelt systems are scour pool, point bar, and overbank (includes levees). Scour-pool deposits (channel lag) are commonly made up of massive gravels with poorly defined trough-fill or foreset cross-strata. Above, and gradational with, channel-lag deposits is the point-bar sequence. Perhaps the most striking features of the point bar are the meander scrolls (seen in plan) that are shown in cross section through the point bar as prominent accretionary packages (fig. 8B). The fine-grained meanderbelt sequence exhibits an upward decrease in grain size and scale of sedimentation units. From bottom to top the point-bar sequence comprises large-scale trough-fill crossbeds, foreset crossbeds, parallel laminae (these are gently inclined toward the stream), ripple cross-laminae, and ripple drift. Levees are made up of very fine grained sand, silt, and mud that are ripple cross-laminated, horizontally to wavy laminated near the river, becoming massive away from the river where roots and burrowing animals have disrupted bedding features.

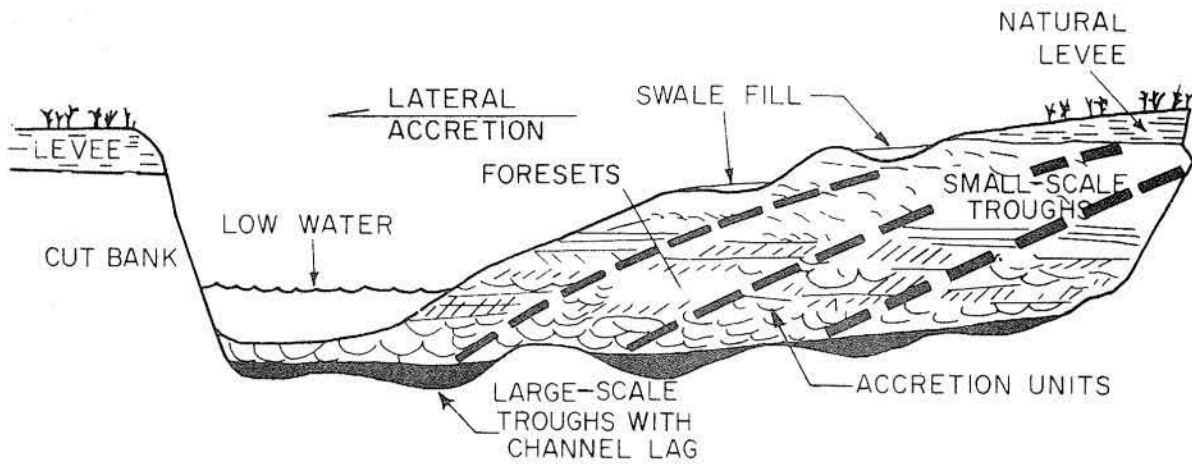
Associated features of fine-grained meanderbelt systems are abandoned channel courses and channels. The former may be several miles long; the latter forms the familiar oxbow. Abandoned courses and channels preserve in the geologic record the cross-sectional channel geometry. These features are generally filled with suspended-load materials emplaced when the river is in flood. Deposits of abandoned courses and channels commonly are dark organic muds that may contain rare ripple cross-laminated sand and/or silt lenses.

Brazos River

The drainage basin of the Brazos River (fig. 1) is 45,573 mi² (118,490 km²); 43,000 mi² (111,800 km²) of the basin is in Texas, and the rest is in New Mexico. Sedimentary rocks, ranging in age from Pennsylvanian to Pleistocene, underlie the basin. Most of the sedimentary rocks are terrigenous clastics; carbonate rocks occur in parts of the Cretaceous, Permian, and Pennsylvanian sequences.



A



B

Figure 8. Depositional model of an idealized fine-grained-meanderbelt fluvial system. A. Block diagram showing bed forms, sedimentary structures, and multistory geometry. B. Schematic cross section of fine-grained point-bar deposits. After Bernard and others (1970); described by Fisher and Brown (1972). (After Brown, Cleaves, and Erxleben, 1973).

Rainfall (fig. 2) is greatest in the Coastal Plain and decreases steadily toward the headwaters. Stream gradient is steepest in the headwaters and decreases toward the Coastal Zone (fig. 3). Flow characteristics change as rainfall increases (from headwaters to river mouth) and stream gradient decreases. The Brazos River is a flashy bed-load (braided) stream along its upper reaches, and is a continuously flowing mixed-load (fine-grained meanderbelt system) stream along its lower reaches.

Brazos River Floodplain

The floodplain of the Brazos River is 8 to 10 mi (13 to 16 km) wide west of Houston. Southward, near the coast, the Brazos and Colorado Rivers merge to form a complex alluvial plain about 28 mi (45 km) wide. Near the coastline the Brazos and Colorado fluvial systems bifurcate to form delta distributary channels; these are distributaries that were associated with older Holocene deltas that filled the common valley eroded by the Brazos and Colorado Rivers during the Pleistocene. The Modern Brazos delta is building into the Gulf of Mexico about 6 mi (10 km) west of Freeport, (fig. 1). The Modern Colorado delta was built across Matagorda Bay from 1929 to 1936; the Colorado River is now discharging directly into the Gulf of Mexico, but it is unable to construct a delta because waves and currents in the Gulf of Mexico immediately redistribute the sediment delivered to the ocean by the river (Wadsworth, 1966). The alluvial plain of the Brazos and Colorado Rivers is covered with a dense growth of trees, which obscures many of the fluvial features. Within the alluvial plain there are abandoned stream courses (Oyster Creek is the former course of the Brazos River, and Caney Creek is the former course of the Colorado River), abandoned channel segments (oxbow lakes), levees, and fresh-water lakes (McGowen and others, 1976). Prominent features of the Modern Brazos River are the meandering course, cutbank, point bar, and levees.

Blasdel Point Bar

Bernard and others (1963; 1970) defined the sedimentary parameters of fine-grained point bars in their study of the Blasdel point bar, which is on the Brazos River south of Richmond. This classic study of a fining-upward fluvial sequence provided the groundwork for subsequent research on many other types of fluvial systems. The study documented the general decrease in grain size from the scour pool, across the point bar, and onto the floodplain. Accompanying the upward decrease in grain size is a decrease in scale of primary sedimentary structures. A generalized vertical succession of grain sizes and stratification types (fig. 9) of the Blasdel point bar is (A) the zone of basal gravels; (B) the zone of giant ripple crossbedding; (C) the zone of horizontal bedding; (D) the zone of small ripple crossbedding; and (E) alternating ripple crossbedded silt to very fine grained sand, and mud drapes. Total thickness of the fine-grained point bar sequence is between 45 and 50 ft (13.5 and 15 m).

Wallis Point Bar

A study of the Wallis point bar (fig. 1), which is about 17 mi (27 km) upstream from the Blasdel point bar, was conducted by Wenzel (1975). Sinuosity of the Brazos River in the area of the Wallis point bar is 2.06, and its gradient is 1.1 ft per mi. At Wallis the Brazos River is a meandering, mixed-load stream.

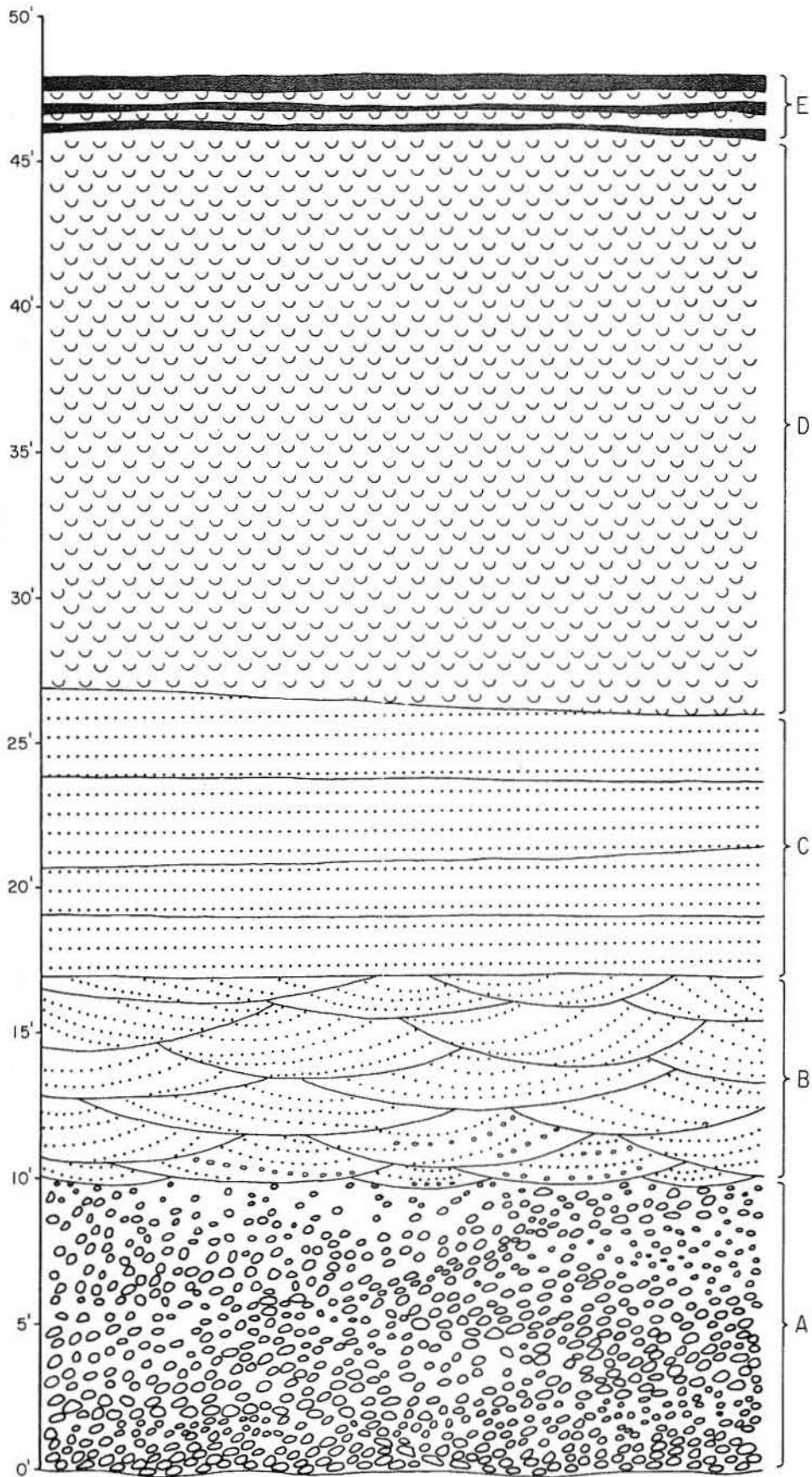


Figure 9. Vertical succession of grain size and stratification types of the Blasdel point bar (drawn from data of Bernard and others, 1970).

Average discharge of the Brazos River at Richmond is 7,254 cfs. Maximum recorded discharge (50-year record) of 123,000 cfs was on June 6, 1929 (Wenzel, 1975, p. 50). Minimum discharge for the same time period was 35 cfs on August 23, 1934.

The Brazos River can no longer be considered in pristine condition because numerous dams have been constructed across the river and its tributaries (Dowell and Petty, 1973). Possum Kingdom Lake, which has a drainage area of 22,500 mi² (58,500 km²), was completed in 1941. Whitney Lake, whose drainage area is 17,656 mi² (45,906 km²), was completed in 1951. The long-term effect of these reservoirs, which impound water and sediment, is expected to be the entrenchment of the Brazos River System and cannibalization of the existing point bars.

Wenzel (1975) concluded that impoundment of water by reservoirs had reduced flood stage to such an extent that the high parts of point bars (constructed prior to water impoundment) were no longer flooded, and that active point-bar accretion was occurring some 5 ft (1.5 m) below former flood stage. In 1972 the inactive parts of the older point bar were being reworked through gulleying.

Since Wenzel's study (1975) there have been numerous floods on the Brazos River that have been bankfull (these floods reached heights attained by the river prior to dam construction). Such an event occurred in April 1977 (fig. 10) and again in early summer 1979. Although the heights attained by recent floods are equal to those in the past, floods do not last as long because about 90 percent of the Brazos drainage has been dammed.

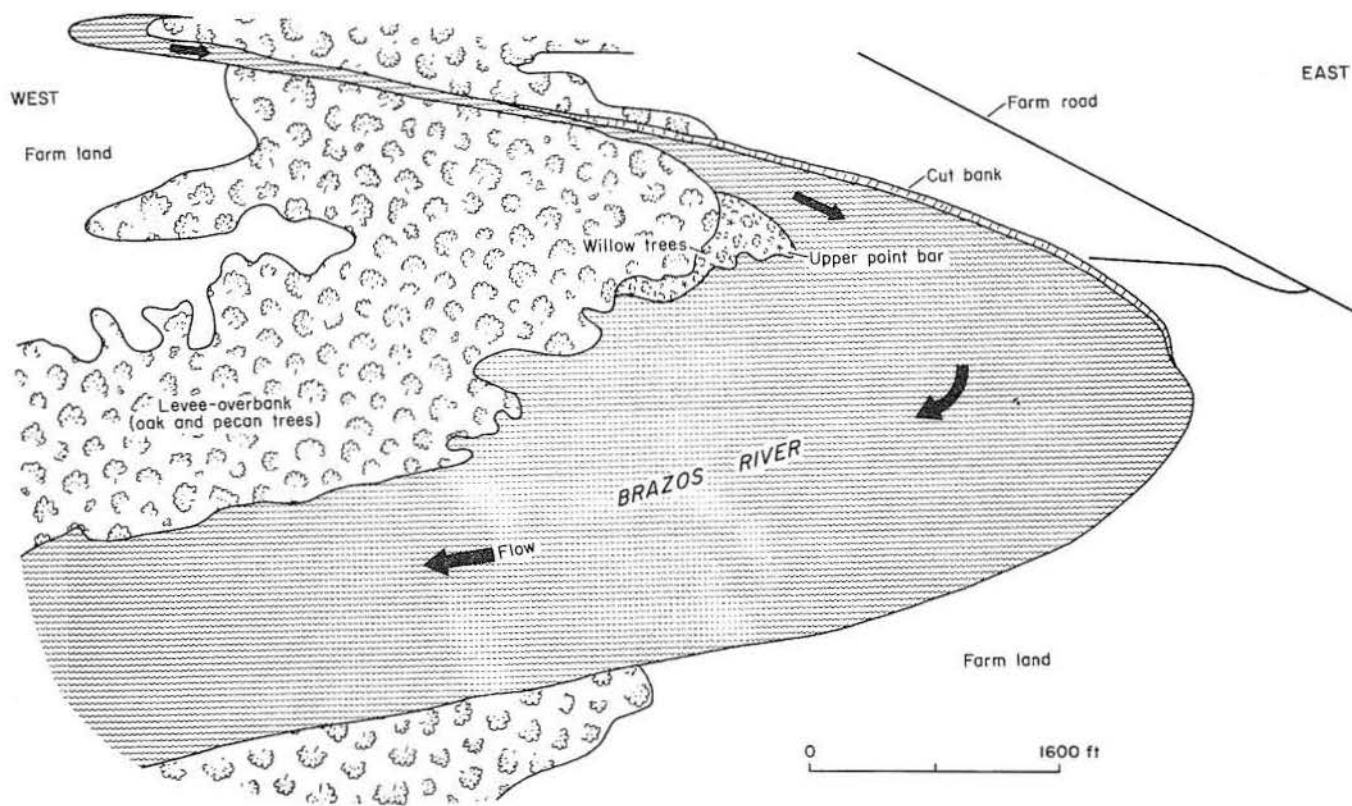


Figure 10. Brazos River at bank-full stage; Wallis point bar, drawn from a photograph. Orchard Quadrangle.

Wallis Point Bar: June 1979

In June 1979 observations were made on the Wallis point bar a few days after a major flood (fig. 11); at the time of the observations the Brazos was at low-flow stage (estimated flood height was 15 ft [4.5 m] above the low-flow stage).

Bed forms

It is assumed that the bed forms (scour and depositional features) in the scour pool were mostly dunes in June 1979. Dune bed forms with ripples were observed (in the area of trench 1) slightly above and slightly below low-flow stage; this is the lower point bar.

A rapid drop in water level was indicated for the steeply sloping middle point-bar surface between trenches 1 and 2; this is mostly an erosional surface with thin slope-wash units (low-angle wedge sets) that parallel erosional surfaces, linguoid ripples, and mud drapes.

The upper point bar surface, between trenches 2 and 6, is a broad ramp that slopes upward to the west. Bed forms in the vicinity of trench 2 are dunes with ripples; height from dune crest to trough ranges from about 0.5 ft (15 cm) to 1.5 ft (45 cm). Coppice bars (bars developed in the current shadow of small trees), which developed downcurrent from small willow and cottonwood trees, are about 3 to 6 ft (90 cm to 1.8m) wide, about 1 ft (30 cm) high, and 10 to 30 ft (3 to 9 m) long; surfaces of these bars are covered with linguoid ripples. Between trench 3 and the break-in-slope, to the east of trench 5, bed forms are linguoid ripples with a 0.5-inch (1.2 cm) to a 2.0-inch (5 cm) mud drape.

Surface sediment at trenches 5 and 6 was mud. No evidence of bed-load material was observed. A rather dense growth of small cottonwood trees occupies the upper point bar in the area defined by trenches 5 and 6.

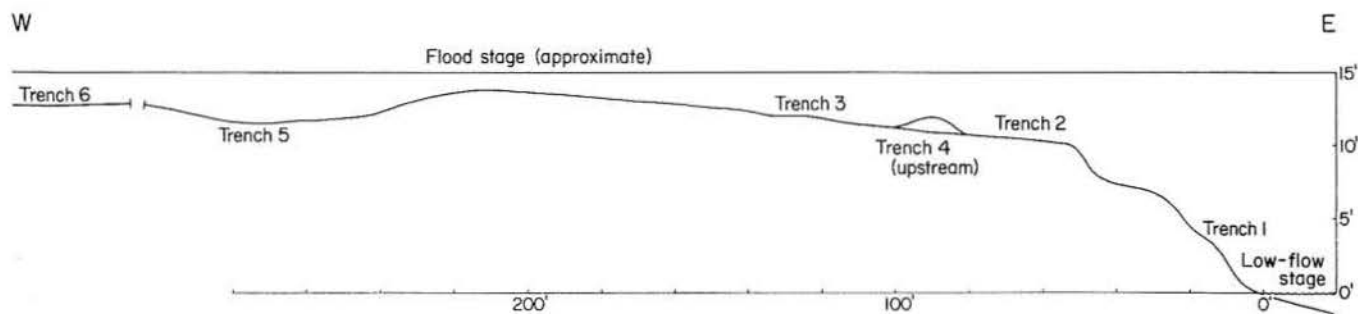


Figure 11. Profile of Wallis point bar with trench localities.

Stratification types

The lower point bar (slightly below to slightly above low-flow stage, fig. 11) was characterized by dunes with ripples, and it was assumed that the resulting stratification was trough-fill cross-strata (terminology of Harms and Fahnestock, 1965) with a downstream dip component.

The middle point bar (the steeply sloping surface between trenches 1 and 2) is made up of low-angle wedge sets (parallel inclined laminae) that are 1.0 ft to 1.5 ft (30 to 45 cm) thick (fig. 12). Wedge sets are underlain and overlain by mud and muddy sand (representing low-flow stage deposits), and grade laterally into trough-fill cross-strata of the lower point bar. Trough-fill cross-strata are inclined toward the west.

Lower and middle point bar deposits (fig. 12) consist of fine-grained terrigenous sand; stratification is accentuated by finely comminuted plant debris and sand-sized clay clasts.

Upper point bar facies are depicted by trench 2 (fig. 13), trench 4 (fig. 14, A and B), and trench 3 (fig. 15).

The lower part of trench 2 consists of about 3 inches (7.5 cm) of brown, homogeneous muddy sand, followed by up to 6 inches (15 cm) of light-brown, ripple cross-laminated fine sand. The upper part of trench 2 is made up of light-brown, trough-fill cross-stratified fine sand. Ripple cross-laminae overlie the trough-fill cross-strata, but this stratification type is not well represented in this trench because of slump. Stratification is accentuated by plant debris and sand-sized clay clasts.

Sections parallel and transverse to elongation of the coppice bars (trench 4, fig. 14, A and B) show that the dominant stratification type is ripple drift. Scale of ripple drift (and angle of inclination of false stratification) decreases upward in the section and in the direction of sediment transport; this suggests that during initial phases of bar formation a large amount of sand was transported as suspension load, and that during the latter stages of development bed-load transport became dominant. Brown, fine-grained sand composes these bars; sand is a mixture of terrigenous sand and clay clasts (percent clay clasts increases from lower point bar to upper point bar).

Stratification in upper point bar deposits at trench 3 (fig. 15) is ripple cross-laminae. Genetic sequences (underlain by muddy sand and overlain by a mud drape) are approximately 1 ft (30 cm) thick. Trench 3 is oriented transverse to transport direction; linguoid ripple bed forms are preserved by the mud drape. Sediment exposed in this trench is light-brown, fine-grained terrigenous and clay-clast sand.

A shallow swale (trench 5, fig. 16) was the site of deposition of almost 6 inches (15 cm) of mud during flooding in June 1979. This mud layer, which was partly desiccated, rests upon an irregular sand surface; the surface was disturbed by cattle walking through the area when the sediment was water saturated. The sand was emplaced by linguoid ripples during a previous flood. The sand is now burrowed and root mottled; biological activity has largely destroyed the primary sedimentary structures. Roots of small cottonwood trees have penetrated the entire thickness of the sand. The trench terminates in a homogeneous mud unit similar to that at the surface.

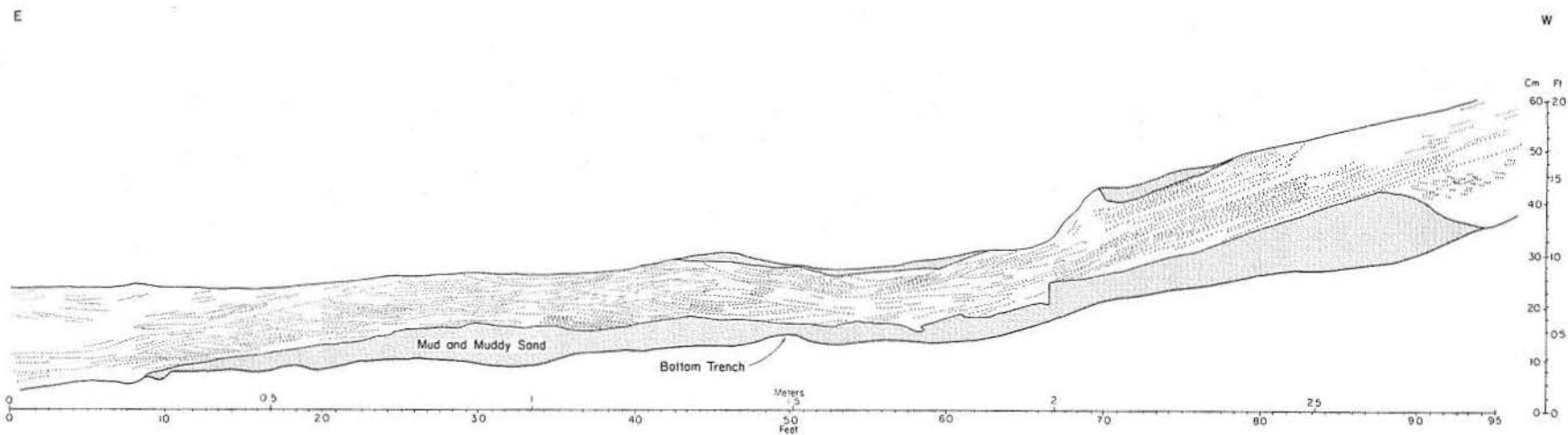


Figure 12. Trench 1, Wallis point bar, lower and middle point bar. Transverse to currents.

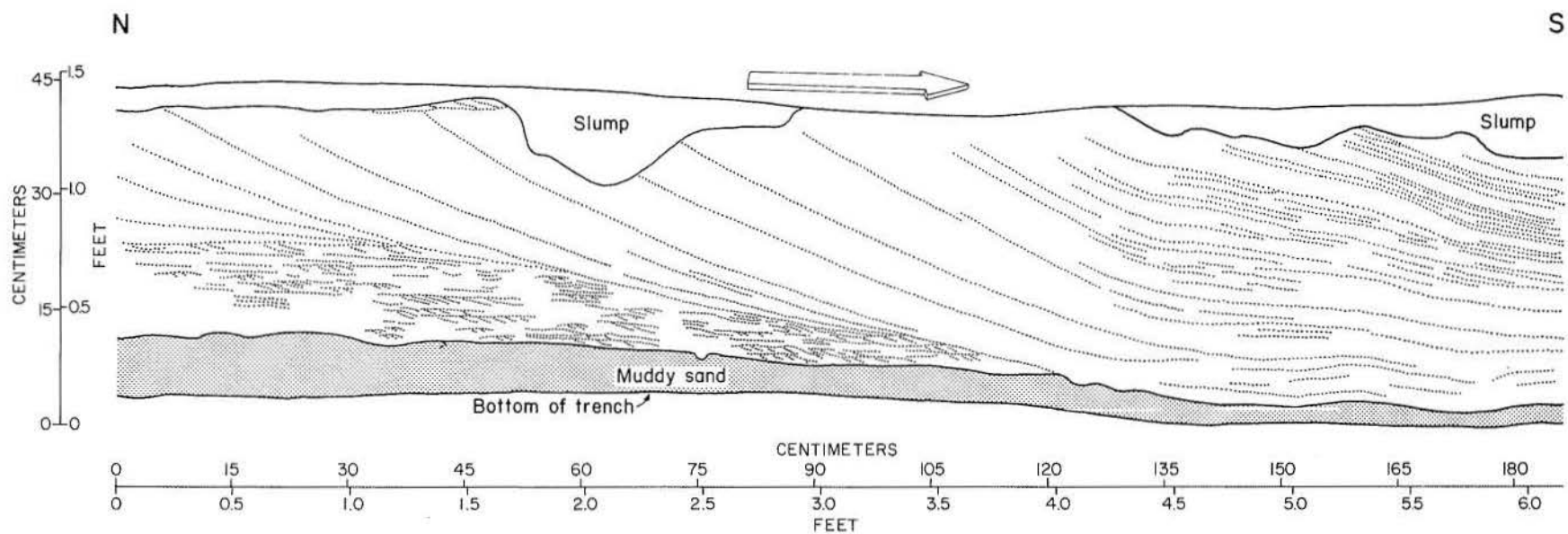


Figure 13. Trench 2, Wallis point bar, upper point bar. Parallel to currents.

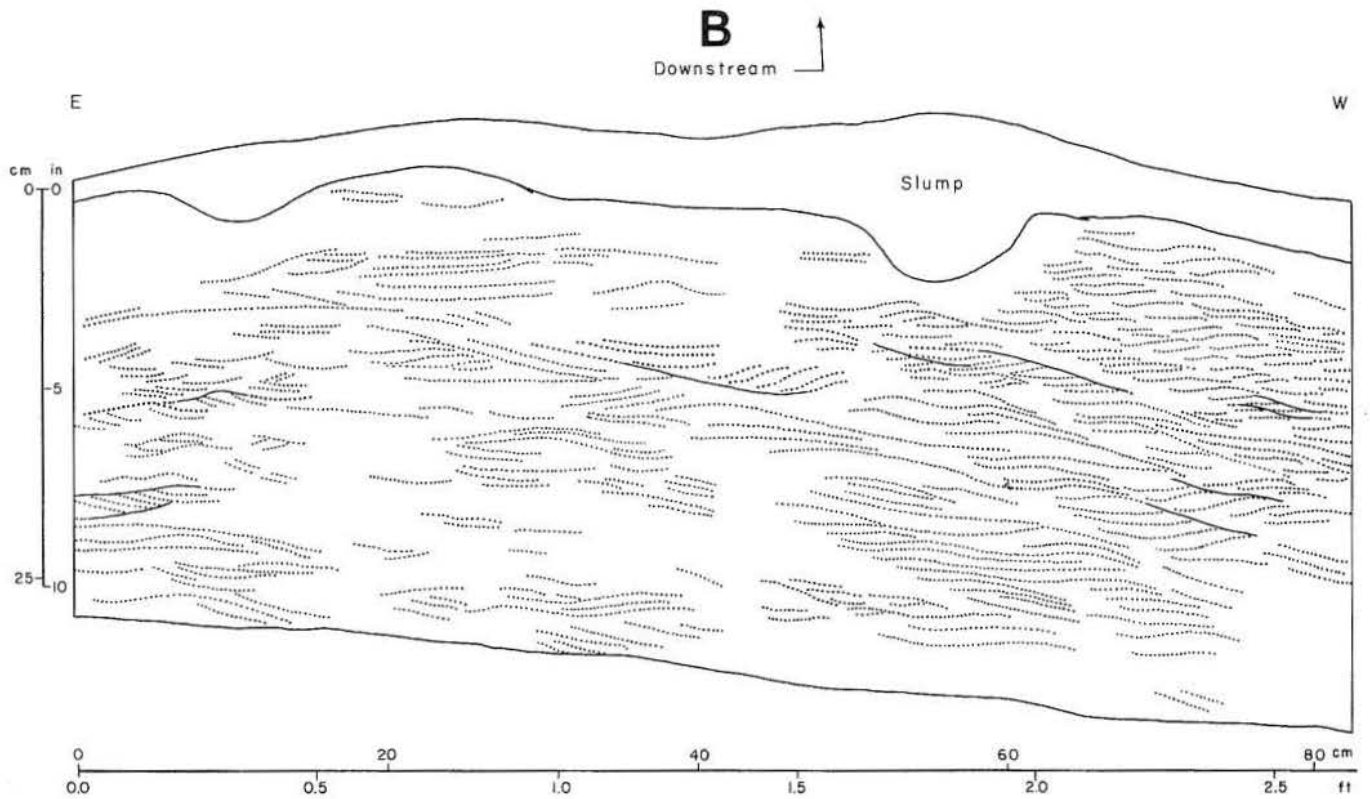
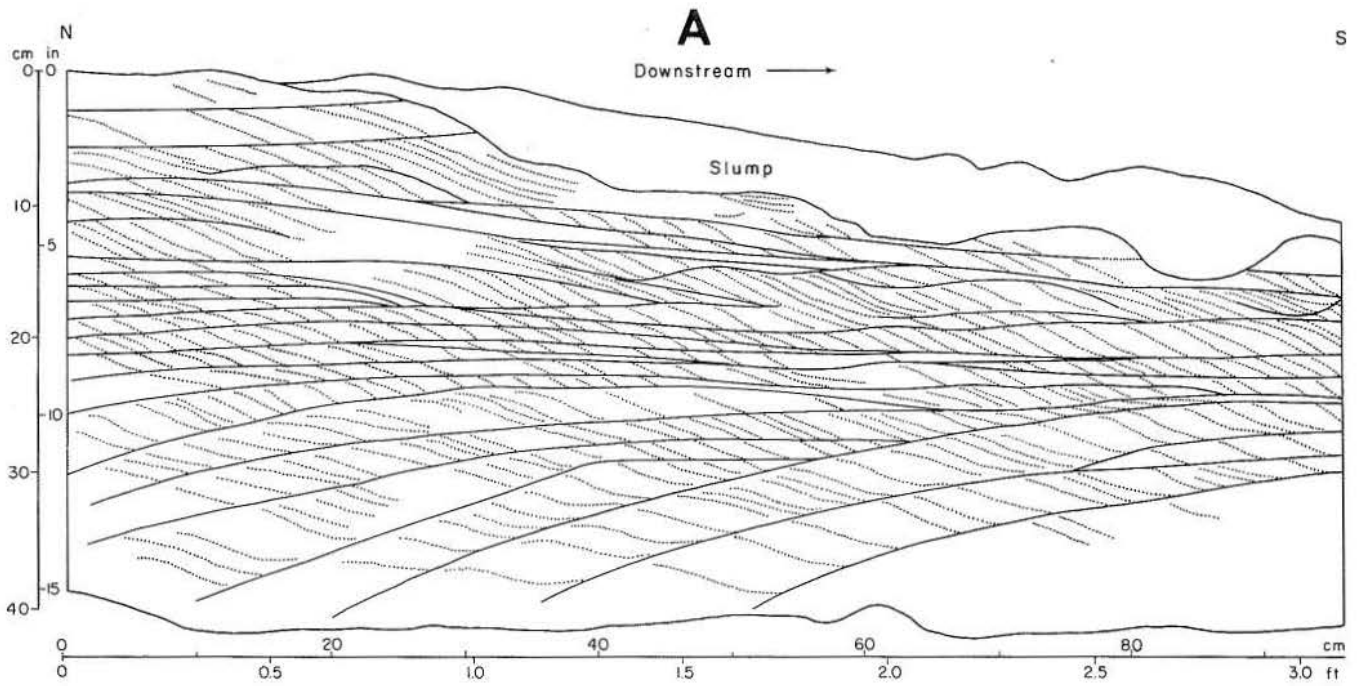


Figure 14. Trench 4, Wallis point bar, coppice bar on upper point bar. A. Parallel to currents. B. Transverse to currents.

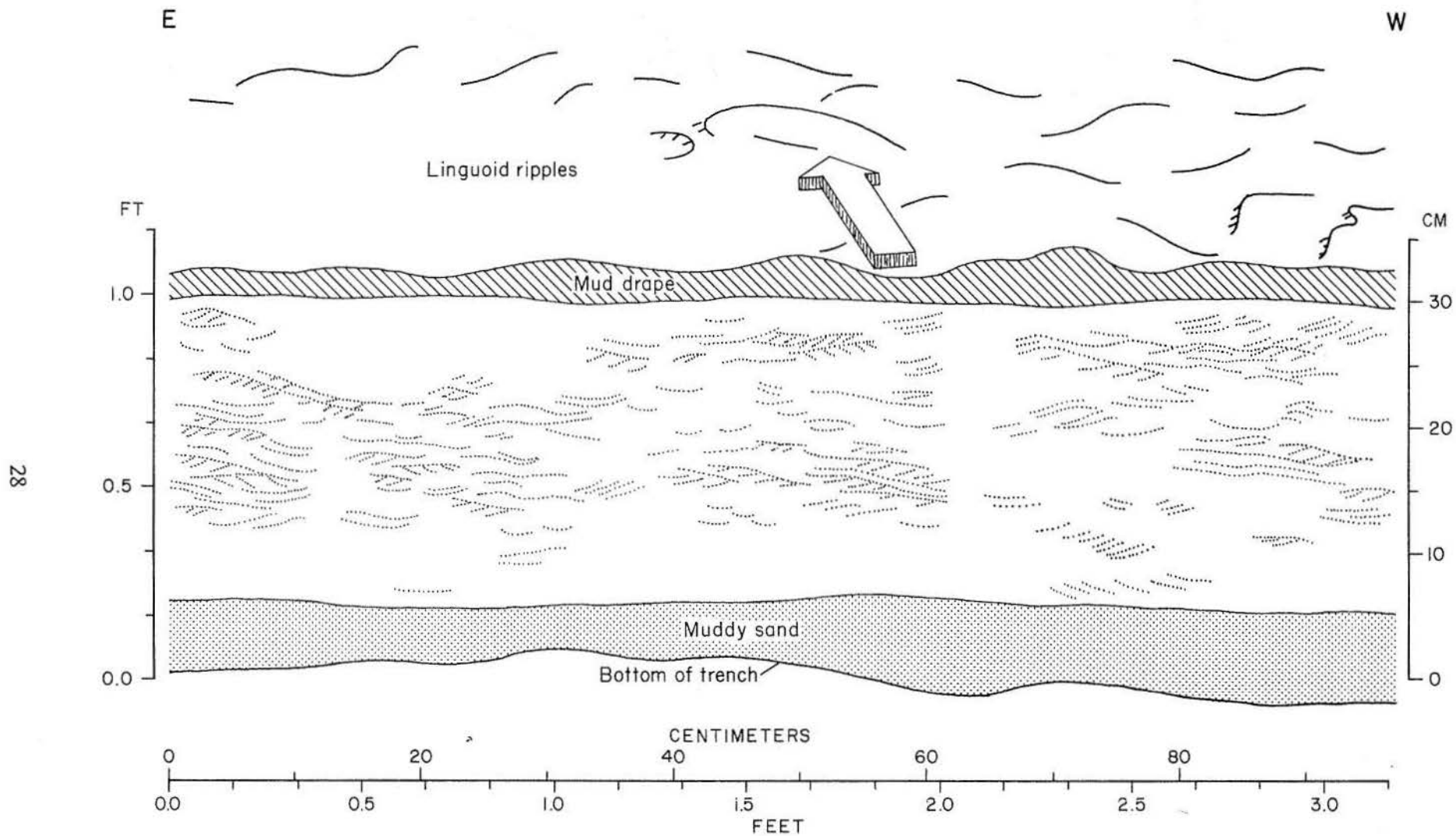


Figure 15. Trench 3, Wallis point bar, linguoid ripples on upper point bar. Transverse to currents.

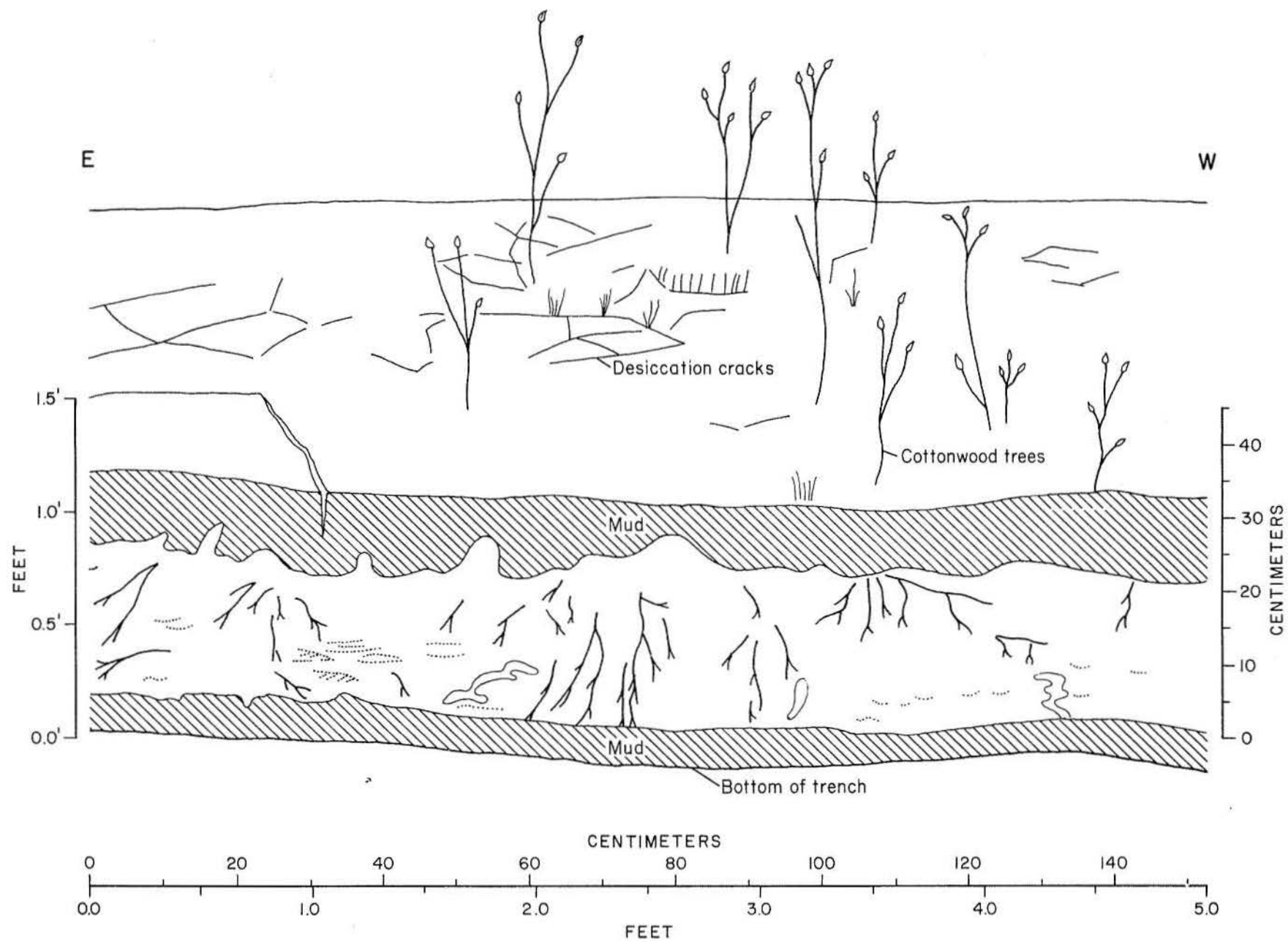


Figure 16. Trench 5, Wallis point bar, mud drape in swale on upper point bar. Transverse to currents.

Upper point bar deposits (fig. 17, units A and B) are exposed in the lower part of trench 6. Unit A has the same characteristics as the upper point bar deposits observed in trench 2, and unit B has features similar to upper point bar deposits observed in trench 3. The top of unit B is highly distorted; disruption of bedding is the result of cattle walking on the water-saturated sand. Origin of the brown muddy sand (unit C) was probably a combination of bed-load (linguoid ripples) and suspension-load (mud drape) deposits that were subsequently mixed by burrowing animals and by plant roots. The surface deposit (unit D) is a brown mud that accumulated at the same time as the mud at the surface at trench 5.

Vertical Succession of Stratification Types: Wallis Point Bar

Six distinct stratification types were observed (or inferred) at the Wallis point bar in June 1979. From these observations we have put together an idealized vertical sequence depicting sediment characteristics of the Wallis point bar (fig. 18). From bottom to top this sequence is (A) scour pool, massive to trough-fill cross-stratified gravel (basal gravels of Bernard and others, 1970, see fig. 9 this report); (B) lower point bar, trough-fill cross-stratified fine sand (giant ripple crossbedding of Bernard and others, 1970); (C) middle point bar (fine sand), parallel inclined laminated units (wedge sets), with mud drapes, that grade into trough-fill cross-strata of the lower point bar (no equivalent in the Blasdel point-bar sequence of Bernard and others, 1970); (D) upper point bar, a complex of mud drapes, homogeneous muddy fine sand, ripple cross-laminated fine sand, foreset cross-stratified fine sand, and ripple drift fine sand (no equivalent in the Blasdel point-bar sequence of Bernard and others, 1970); (E) upper point bar, ripple cross-laminated, slightly muddy very fine to fine sand (small ripple crossbedding of Bernard and others, 1970); and (F) overbank deposits, alternating ripple cross-laminated silt to very fine sand, and mud drapes.

The chief difference between the Blasdel point-bar sequence and that of the Wallis point bar is in the details of the upper point bar. Bernard and others (1970) observed horizontal bedding in this zone, whereas wedge sets, trough-fill cross-strata, and ripple drift were observed in the comparable interval in the Wallis point-bar sequence.

A plausible explanation for the observed differences in the upper point bar deposits of the Blasdel and Wallis point bars may be that in recent years the discharge characteristics of the Brazos River have changed. Flood stage may drop off more rapidly now than in the past before so much of the volume of water and bed load were impounded by dams.

Colorado River

One of the major fluvial systems of Texas is the Colorado River (fig. 1). In the Austin area the Colorado has numerous dams and reservoirs making up the well-known "highland lakes" recreational sites. Water from these lakes is released periodically for use by rice-farmers on the Coastal Plain.

The slope of the Colorado River decreases from its headwaters to the Coastal Plain (fig. 3), and precipitation decreases from the Coastal Zone toward the headwaters (fig. 2). The Colorado varies in discharge and sediment load from a flashy discharge and predominantly bed-load (braided) system in its upper reaches to a continuously flowing mixed-load (meandering) stream in the Coastal Plain.

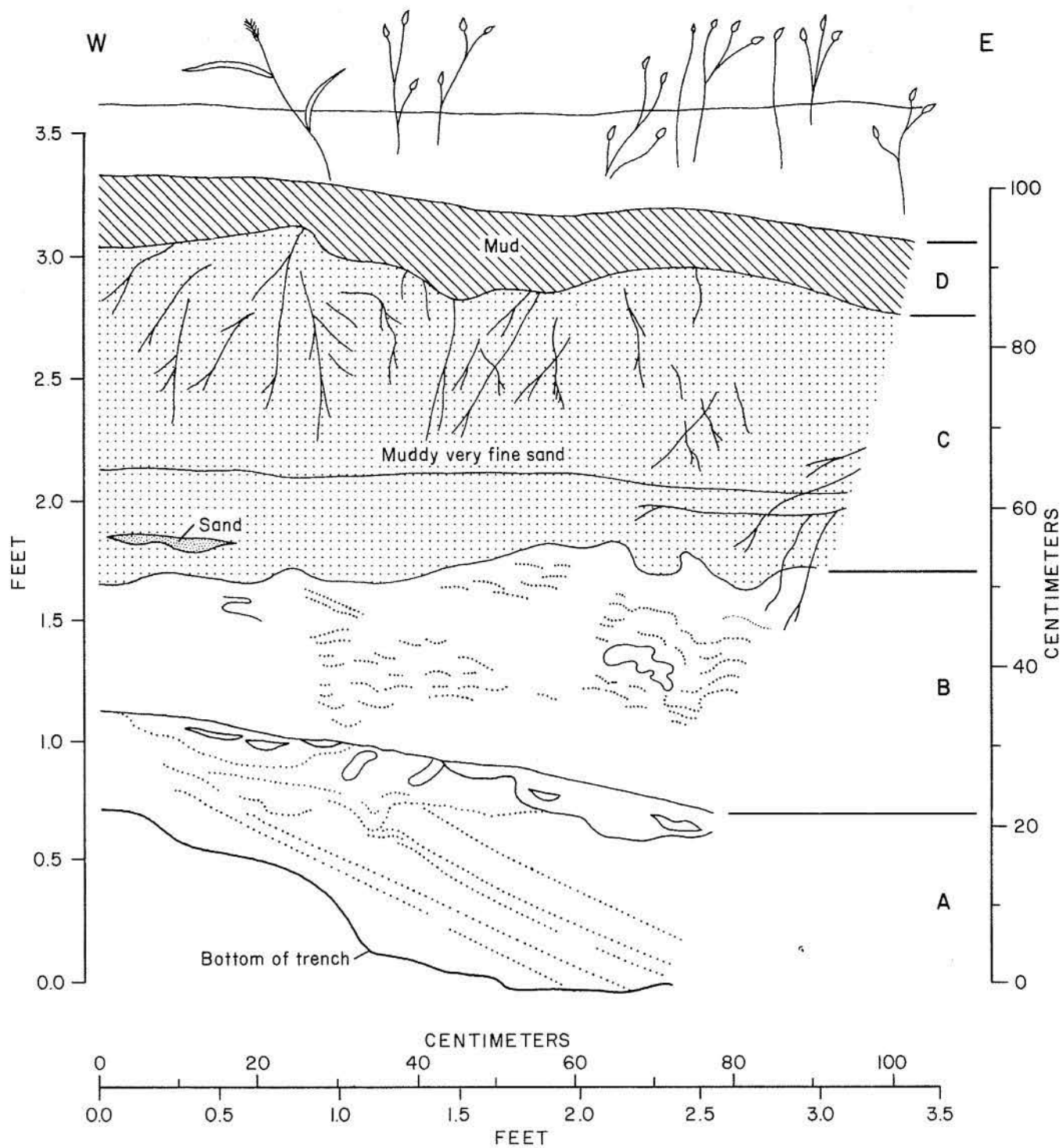


Figure 17. Trench 6, Wallis point bar, upper point bar deposits overlain by overbank mud, upper point bar. Transverse to currents.

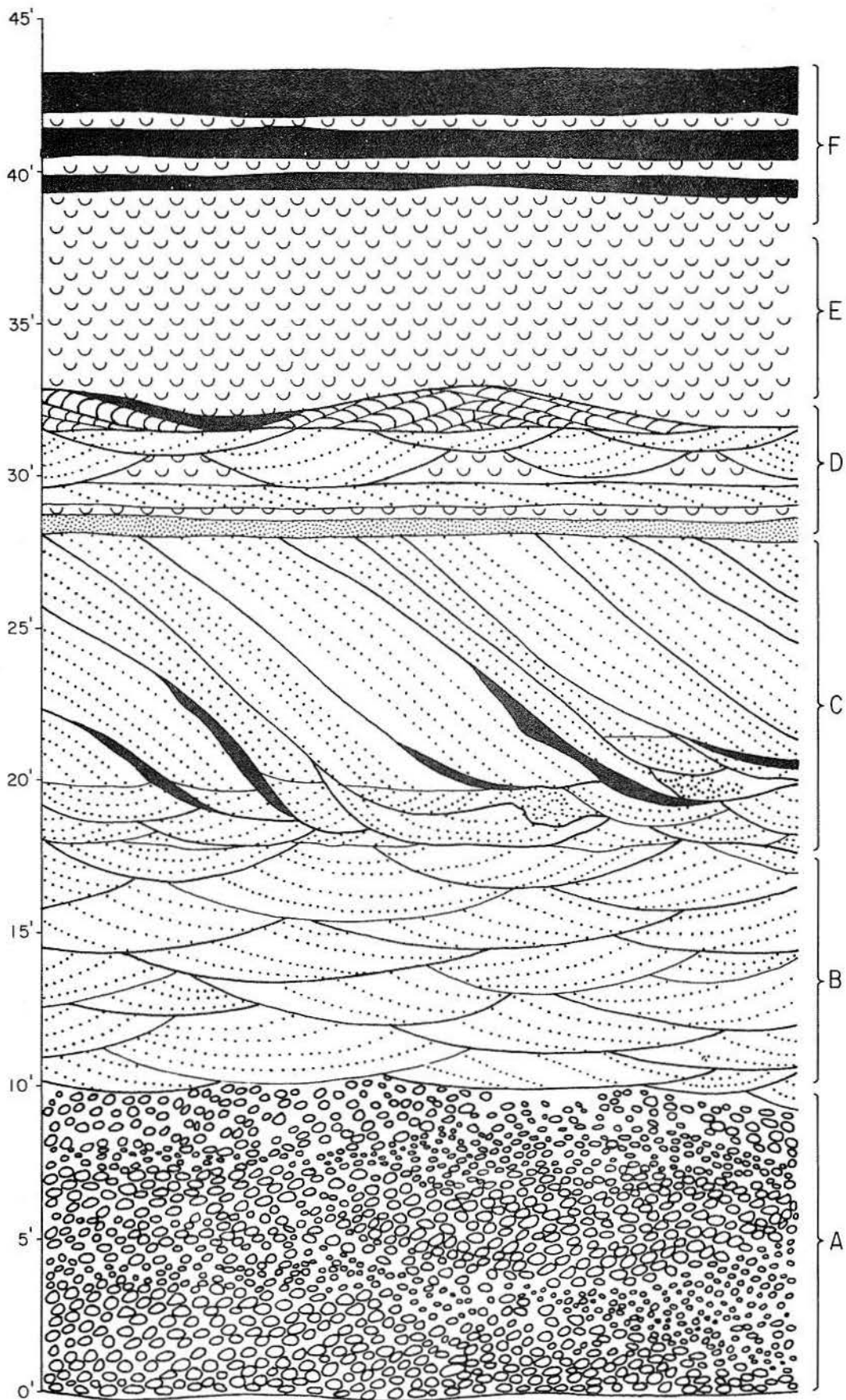


Figure 18. Generalized vertical succession of grain size and stratification types, Wallis point bar.

The drainage basin of the Colorado River, approximately 42,000 mi² in area, is underlain mostly by terrigenous clastic sedimentary rocks that range in age from Cambrian to Pleistocene. The Llano Uplift area is traversed by the Colorado River and the Llano River, a tributary of the Colorado. Coarse granular materials are contributed to the Colorado River from igneous, metamorphic, and terrigenous clastic rocks that crop out in the Llano Uplift area.

Coarse-Grained Meanderbelt Systems

McGowen and Garner (1970) described a variant of the meandering-stream depositional model involving point-bar sequences on the Amite River of Louisiana and the Colorado River of Texas. Although each of these streams (or segments thereof) falls into the meandering-stream category (sinuosity of 1.5 or more) as defined by Leopold, Wolman, and Miller (1964), they resemble the fine-grained meanderbelt systems or mixed-load streams (Schumm, 1968) only in plan. The coarse-grained meanderbelt streams differ from the fine-grained meanderbelt streams in discharge characteristics, nature of bank materials, ratio of bed load to suspension load, and characteristics of the point-bar deposits.

Discharge curves for the Amite and Colorado Rivers (fig. 19) are similar. Flow through the Amite and Colorado is less than 5,000 cfs 95 percent of the time. Peak discharge of about 50,000 cfs for the Amite and 150,000 cfs for the Colorado occurs about 5 percent of the time. These streams are "flashy" when compared with a highly meandering, mixed-load stream such as the Atchafalaya River, which has a continuous flow with a high discharge over a much longer period of time (fig. 19). The study of coarse-grained point bars indicated that the type of discharge (flashy or continuous) is a critical factor in determining channel pattern, grain-size distribution, and the distribution of bed forms (hence the vertical succession of stratification types present in the larger accretionary features).

Banks of the Amite and Colorado Rivers are resistant to erosion chiefly as a consequence of dense vegetation on the floodplain, since floodplains of coarse-grained meanderbelt systems consist, for the most part, of easily eroded sand-sized material. Resistance to erosion of banks of mixed-load streams is related to the high clay content of overbank material.

Vertical Succession of Stratification Types in Coarse-Grained Point Bars

Utilization of vertical trends in grain size and stratification types to interpret terrigenous clastic deposits is now a common practice among sedimentologists and stratigraphers. The vertical sequence of stratification types in coarse-grained point bars derives primarily from observations of the Amite River of Louisiana. Coarse-grained meanderbelt deposits are commonly thinner than fine-grained meanderbelt deposits (compare figs. 9 and 20) by as much as 15 to 20 ft (4.5 to 6 m). The coarse-grained point-bar sequence is as follows (fig. 20): (A) scour pool (channel lag), sandy, granule to cobble gravel; massive, may have scour-and-fill (current crescents) features associated with tree limbs and trunks; (B) lower point bar, gravel-bearing medium- to coarse-grained sand, foreset and trough-fill cross-stratified; (C) upper point bar, generally poorly sorted gravel-bearing medium- to coarse-grained sand and sandy granule to cobble gravel. Low- to high-angle foreset cross-strata (individual units may attain thicknesses up to 8 ft [2.4 m]); minor, scour troughs filled with medium- to coarse-grained sand, ripple cross-laminated and foreset crossbedded. Thick foresets

are representative of chute-bars; these features set coarse-grained point-bar sequences apart from fine-grained point-bar sequences; and (D) overbank (floodplain) deposits; medium- to coarse-grained sand and gravel-bearing sand, parallel laminated, foreset crossbedded, and wavy bedded (stratification may be partly destroyed by plant roots and burrowing animals).

Columbus Point Bar

The Colorado River near Columbus is a meandering (sinuosity greater than 1.5) bed-load stream with flashy discharge (fig. 19). Discharge of the Colorado River is

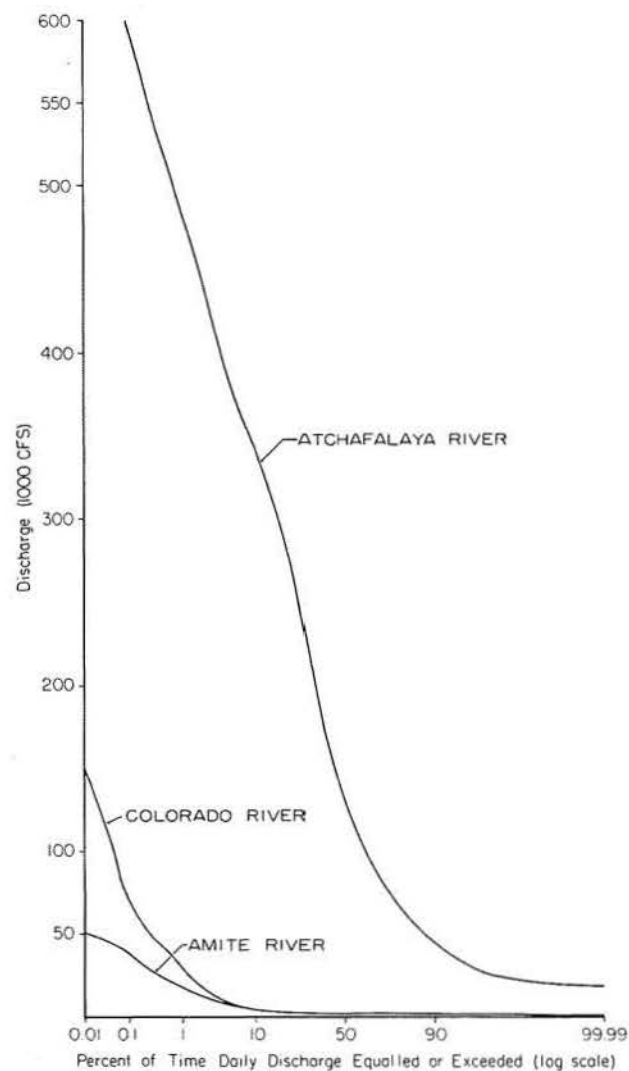


Figure 19. Duration curve of daily flow: Amite River near Denham Springs; Colorado River near Columbus; and Atchafalaya River at Krotz Springs. Data for the Amite and Atchafalaya Rivers are from M. F. Cook (1968) and for the Colorado River from unpublished records, U.S. Department of Interior, Geological Survey, Water Resources Division, Austin, Texas (from McGowen and Garner, 1970).

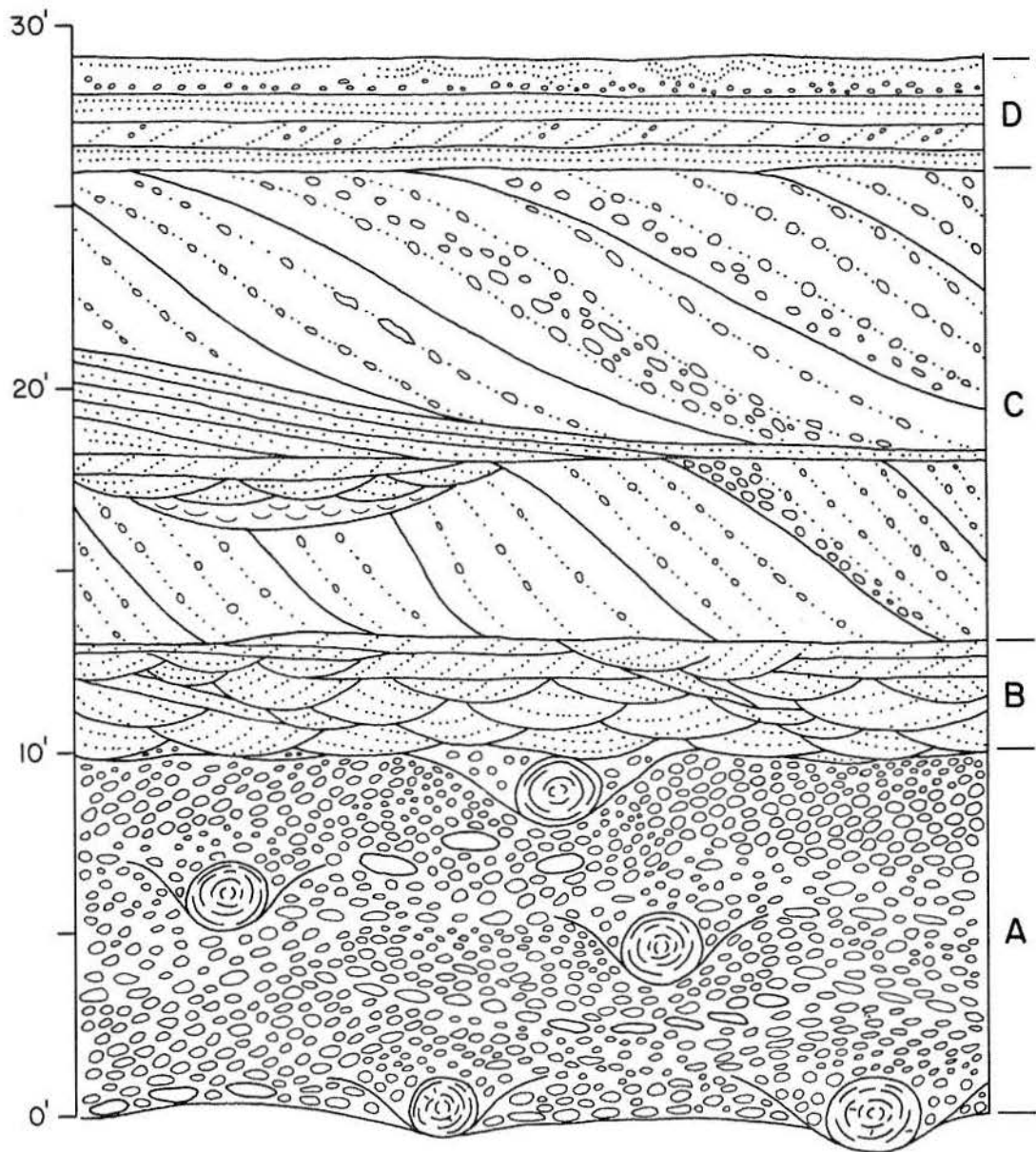


Figure 20. Vertical succession of stratification types in a coarse-grained point bar, Amite River, Louisiana.

affected by dams; the reservoir nearest the Columbus point bar is Lake Austin. This reservoir receives water and sediment from a 38,240 mi² drainage area (Dowell and Petty, 1971). Since construction of the dam at Austin in 1893, duration of peak discharge has probably decreased (the stream is probably more flashy than before 1893); low discharge is probably more continuous now than prior to 1893 since water is released periodically from the reservoir.

The Colorado River has been at bankfull flood stage several times since 1977. In April 1977 the Columbus point bar was covered by up to 5 ft (1.5 m) of water. During floods the Colorado tends to straighten its course by "chuting" across the relatively flat upper point bar (fig. 21). Part of the flow is diverted from the main channel through chutes at the upcurrent end of the point bar; flow decreases in depth (northward) as chutes widen and lose their identity. Part of the flow returns to the main channel (by breaching the vegetated levee), and part of the flow continues northward where it again returns to the main channel.

Bed forms (fig. 22) generated by shallow flow across the upper point bar are analogous to those produced by some braided streams (Doeglas, 1962; Ore, 1963, 1964, 1965; Smith, 1970; Miall, 1977). Depositional (and erosional) features of the upper point bar at Columbus are chutes, natural levees, longitudinal bars, transverse bars, coppice bars, lobate bars, dunes, current crescents, chute bars, and aeolian dunes.

Chutes are shallow channels that exhibit a downcurrent increase in width from about 50 to greater than 175 ft (15 to 53 m). The chute is floored with cobble gravel at the upcurrent end decreasing to granule gravel downcurrent; length of the gravel deposit is about 1,800 ft (540 m).

Natural levees are a maximum of about 5 ft (1.5 m) high. They are densely vegetated by willow trees and are breached here and there. Coppice bars form downcurrent from some breaches, whereas lobate bars form downcurrent from other breaches. Coppice bars are elongate in direction of sediment transport (they are approximately 10 ft [3 m] wide, 1.5 ft [35 cm] high, and 30 ft [9 m] or more in length). Coppice bars are made up of granule-bearing coarse sand; stratification within the bar consists chiefly of foreset cross-strata that dip away from the bar axis. Lobate bars are up to 1 ft (30 cm) high. They comprise coarse sand that is foreset crossbedded; strata are inclined radially away from the bar apex.

Transverse bars cover much of the bar surface between vegetated levees and longitudinal bars. The area covered by these bed forms is approximately 1,700 ft (510 m) long and 400 ft (120 m) wide. These features are sinuous-crested sand bodies that are oriented transverse to flow direction. Height of these bars is a few inches to about 2 ft (60 cm). They are made up of foreset crossbedded granule-bearing medium- to coarse-grained sand.

The only longitudinal bar present in April 1977 was an erosional-depositional feature that is elongate in the direction of flow. This feature is approximately 2,400 ft (620 m) long, 200 ft (60 m) wide, and about 3 ft (1 m) high. Bed forms along this bar during the April 1977 flood were transverse bars. Because of the position of the longitudinal bar relative to low-water stage, it is dry most of the time, and its upper surface is commonly reworked by the wind.

Current crescents are horseshoe-shaped scour features at the upcurrent ends of debris piles and/or trees. These features are up to 15 ft (4.5 m) wide, about equally long, and 2 to 2.5 ft (0.6 to 0.76 m) deep. Current crescents are filled with sand that

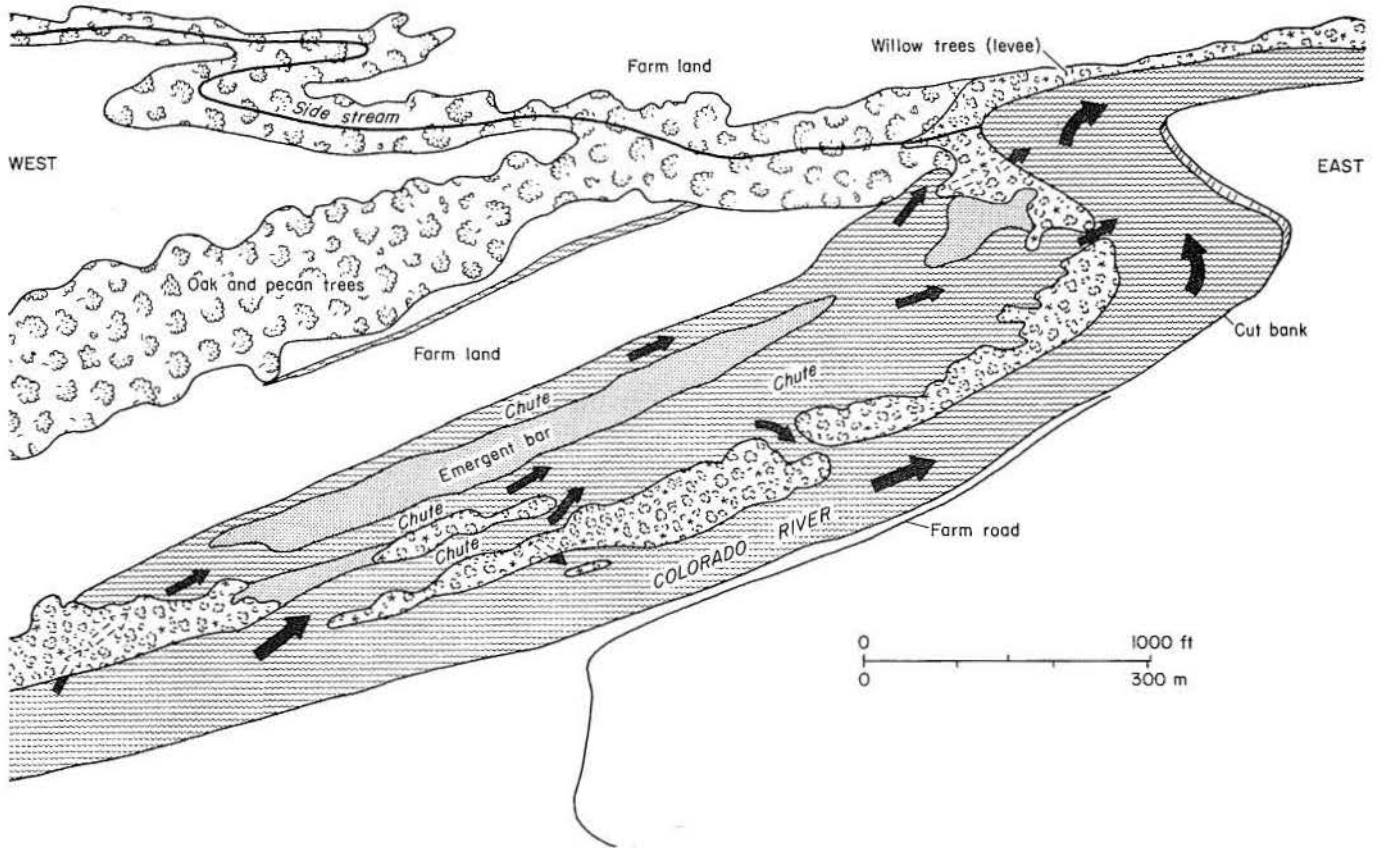


Figure 21. Colorado River in flood stage; Columbus point bar. Columbus Quadrangle.

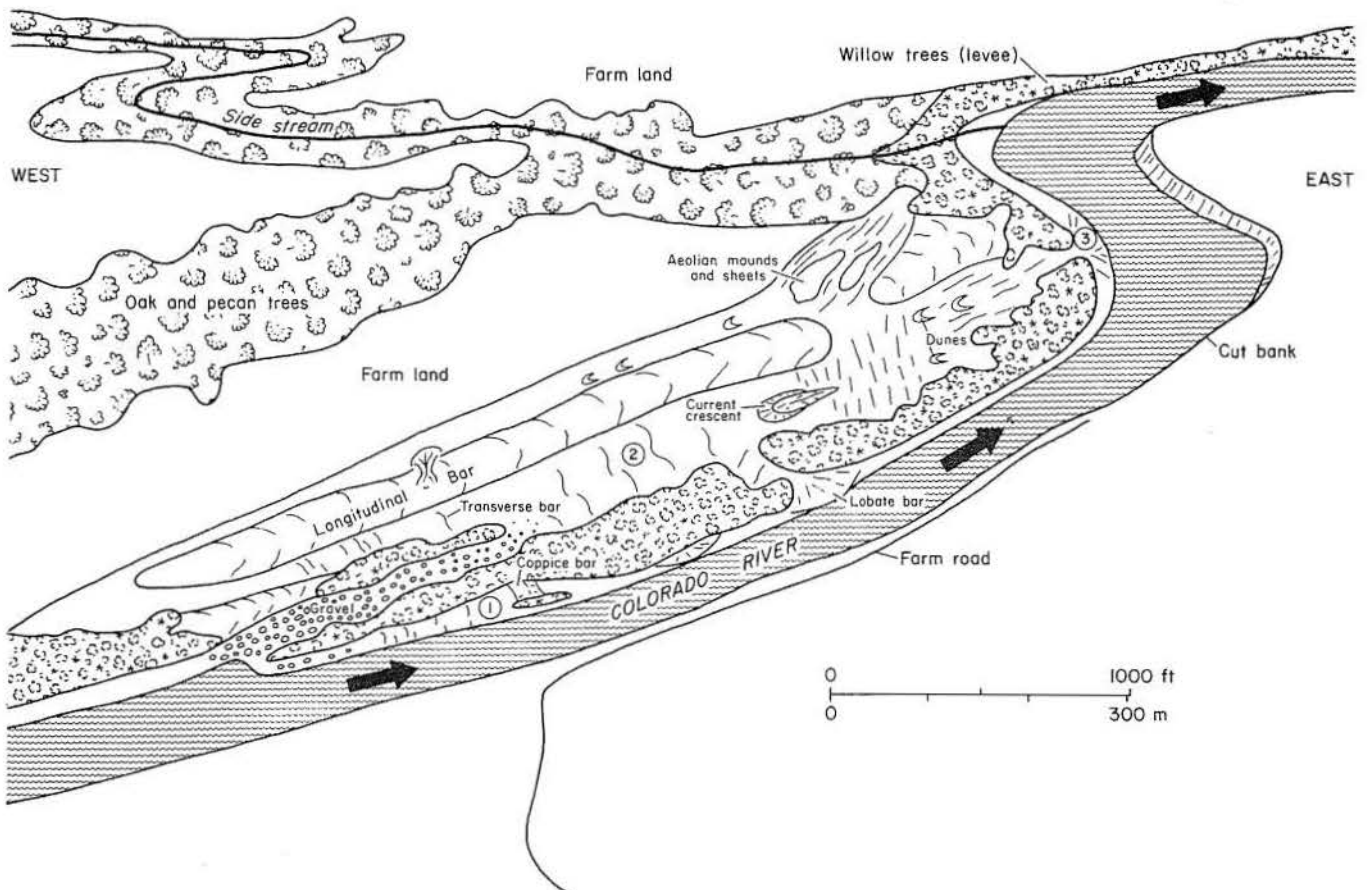


Figure 22. Bed-form distribution on Columbus point bar. Columbus Quadrangle.

avalanches into the scour from each side. Commonly, these features are not completely filled during a single flood event; residual depressions are normally floored with a mud drape and plant debris. Coppice bars occur downcurrent from the current crescents.

Isolated dune fields occur in the shallow channel north of the large longitudinal bar and in an area beginning at the downcurrent terminus of the Columbus point bar and extending upcurrent for almost 900 ft (270 m). In plan these dunes are linguoid to crescent shaped. Fine- to medium-grained sand composes the dunes; stratification produced by these bed forms is trough-fill cross-strata.

Relief on the distal part of the Columbus point bar is (depending on river stage) 6 to 8 ft (1.8 to 2.4 m) above low water level. This distal bar is similar to the chute bar on the Amite River. Sand is transported to the bar crest chiefly by migrating dune bed forms. Here sand avalanches down the bar face. Medium- to coarse-grained sand composes the distal bar, which is characterized by steep, large-scale, foreset cross-strata. The Colorado River flood stage drops rapidly, and during this drop at least two processes operate to modify the large-scale foreset cross-strata. First, when water level drops below the bar crest, sediment supply is cut off, and currents in the main channel remove parts of this distal bar. Second, the sediment composing the distal bar is water saturated, and, when water level of the Colorado River drops, the water contained within the distal bar flows toward the river; this water movement displaces some of the distal bar sands, producing convolute bedding. Faulting, with displacement measured in inches, also occurs as sediment and water move toward the river as water level drops; faults are down-to-the-river.

Following a flood, the sands on the bar surface rapidly dry out, and the wind reworks much of the upper surface into aeolian dunes and thin aeolian sheets. Most of the dunes are situated along the north and northeast parts of the Columbus point bars.

Coletto Creek

General Setting

Coletto Creek (fig. 1) is a major but ephemeral tributary of the Guadalupe River that originates in the Tertiary Catahoula and Oakville Formations. Along its lower reaches Coletto Creek is entrenched in sands and muds of Pleistocene fluvial-deltaic origin; the Pleistocene surface is about 45 ft (14 m) above the Holocene floodplain.

Total drainage area of Coletto Creek is less than 400 mi² (1,300 km²). Average rainfall in the drainage basin is 31 inches (79 cm), and the climate is dry subhumid (Thornthwaite, 1948).

Discharge

Flow of Coletto Creek is unregulated, and the drainage basin is relatively undisturbed by human activities; consequently, point bars are active sites of deposition and erosion. Bed forms and associated stratification that make up the point bars are records of specific responses to natural flow conditions, some of which can be related to historical discharge data.

The stream has extremely flashy discharge (fig. 4) with seasonal periods of low flow and occasionally no flow during droughts. Maximum recorded discharge was related to Hurricane Beulah in 1967 (U.S. Geological Survey, 1968) when instantaneous discharge exceeded 120,000 cfs (3,360 m³/s, fig. 23). Maximum flood depths were approximately 33 ft (10 m) according to debris lines at the Schroeder gaging station. There the stream is confined to a relatively deep and narrow valley where extreme flooding from Beulah was contained within the entrenched valley. Calculations using valley width (300 ft [90 m]), flood depth (33 ft [10 m]), and peak discharge (122,000 cfs [3,457 m³/s]) suggest that average velocity was about 12 fps (3.7 mps) during peak flooding. Near Victoria, about 12 mi (20 km) downstream from the gaging station, floodplains are progressively better developed and from 2,500 to 5,000 ft (0.7 to 1.4 km) wide (fig. 24). Flow depths decrease where floodplains are widest, and consequently, upstream flood elevations and average velocities do not apply downstream. Although flow depths would have been reduced, velocities would have been substantial near the channel where flow was unimpeded by dense floodplain vegetation (fig. 25). Shallow flow depths combined with high velocities would produce transition or upper flow-regime bed forms. Large-scale bed forms that developed under these conditions are preserved on point-bar surfaces at location C (fig. 24).

Stream Characteristics

Coletto Creek exhibits a relatively low sinuosity (1.37), intermediate width-depth ratio (16:1), and low gradient (2 ft/mi). These quantities fall within the mixed-load classification according to criteria of Schumm (1968), but Coletto Creek is primarily a bed-load stream. Gravel, sand, and mud are transported during extreme floods, but the proportions of gravel and mud are minor. Bed material is coarse to medium sand having a mean grain size of 0.3 mm.

Where floodplains are well developed, the stream is about 400 ft (120 m) wide and 25 ft (7.5 m) deep. However, channel widths and depths vary considerably upstream and downstream, and in particular around meander bends (figs. 26, 27, and 28).

Major Bed Forms

Major depositional features of Coletto Creek are alternate side-attached bars and point bars. These bars, which are active only at high discharge, are incised and modified by a low-stage meandering thalweg within the channel. Point bars of Coletto Creek are coarse grained. These distinct types of fluvial deposits were first reported by McGowen and Garner (1970). Characteristic features of coarse-grained point bars and their similarity to some braided-stream deposits (Miall, 1977) are now widely recognized from studies of modern (Bluck, 1971; Jackson, 1975; Levey, 1978) and ancient (Morton and Donaldson, 1978b; Nijman and Puigdefabregas, 1978) fluvial sequences. Point bars consist of lower and upper point bar deposits commonly separated by a scour trough or chute. Total bar thickness is about 20 ft (6 m).

Bar surfaces exhibit low-relief rhomboid ripples and ripples on dunes with sinuous lee faces extending transversely across the bar. Mud drapes occur as thin veneers and as local concentrations between small bed forms. Other high-discharge bed forms include flat-crested medial bars stabilized by vegetation. These bars have steep lee faces and are 6 to 7 ft (1.8 to 2.1 m) high (Morton and Donaldson, 1978a).

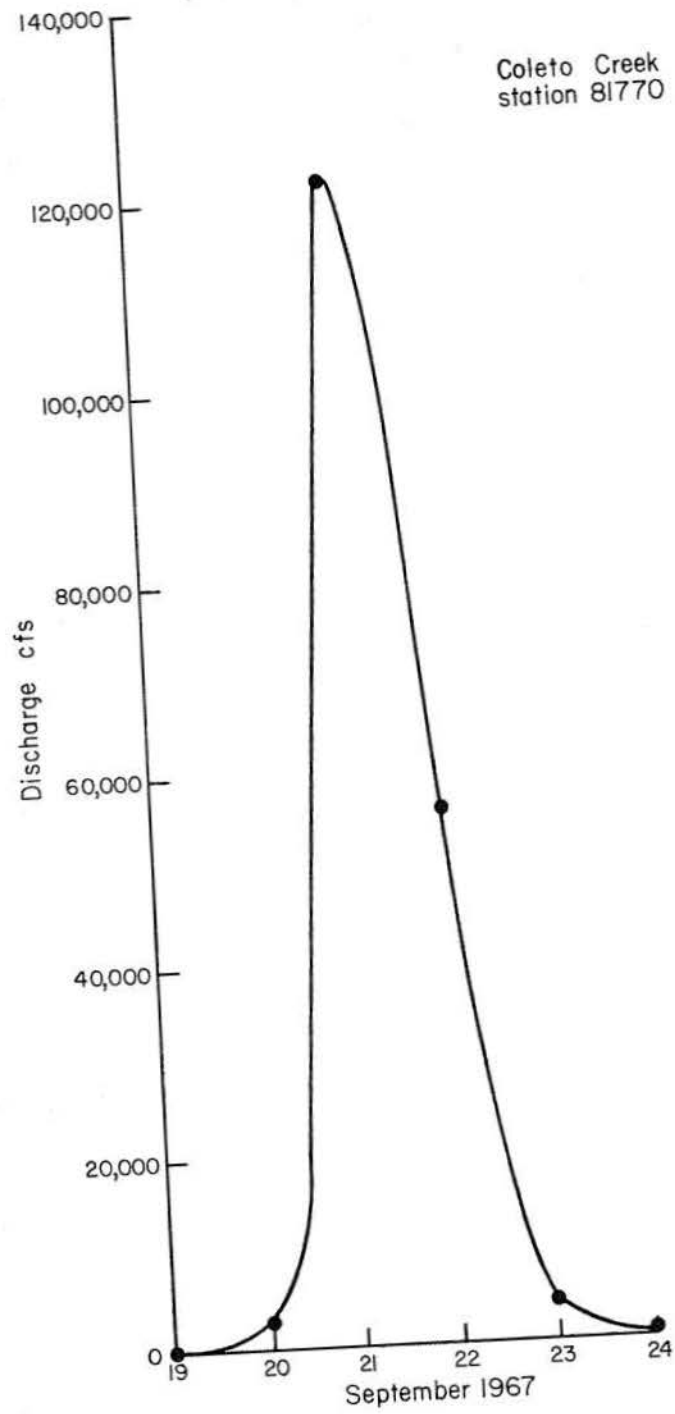


Figure 23. Discharge hydrograph for Coletto Creek during September 1967 flooding associated with Hurricane Beulah. Data from U.S. Geological Survey (1968).

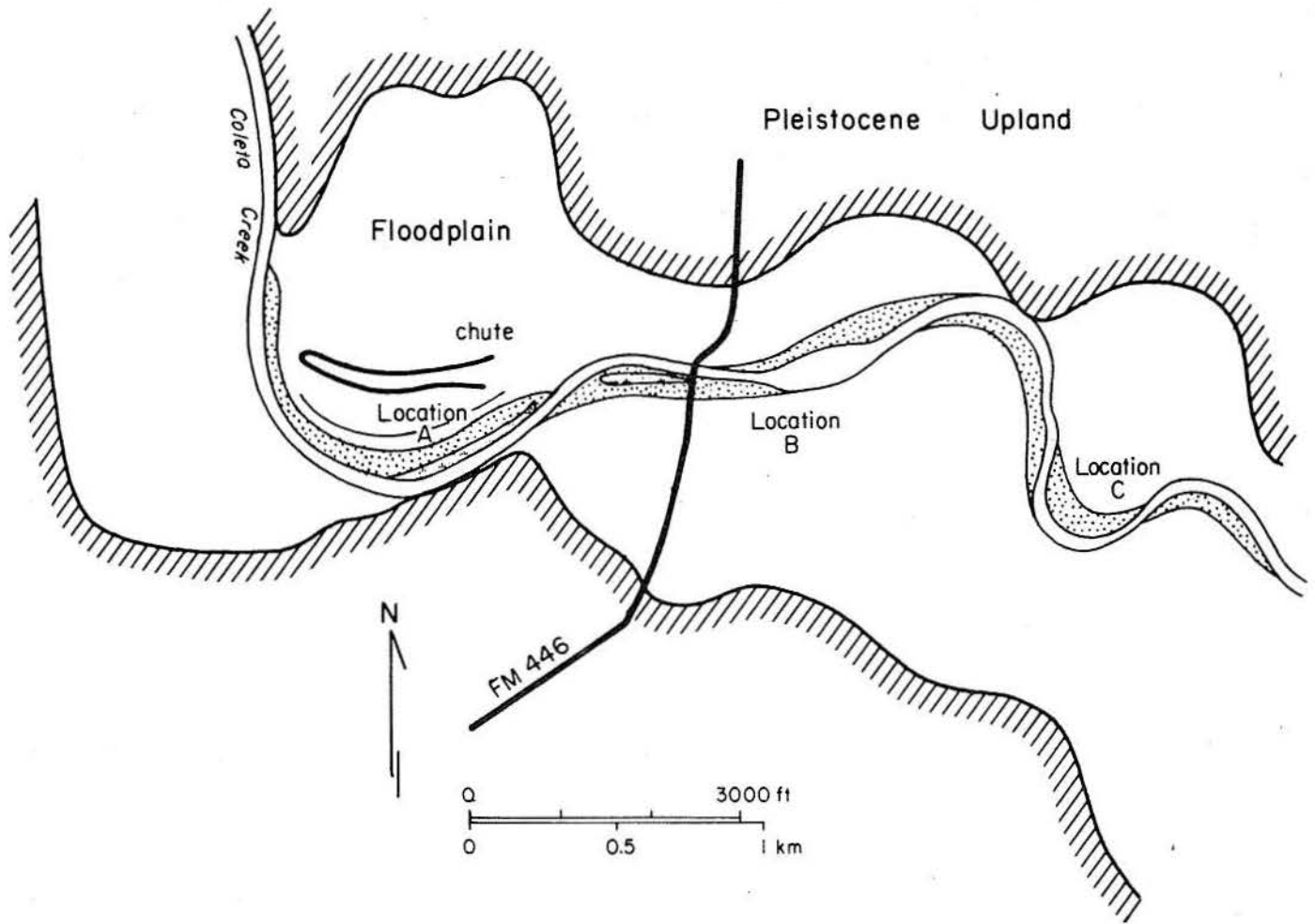


Figure 24. Location of point bars and side-attached bar, Coletto Creek. Raisin Quadrangle.

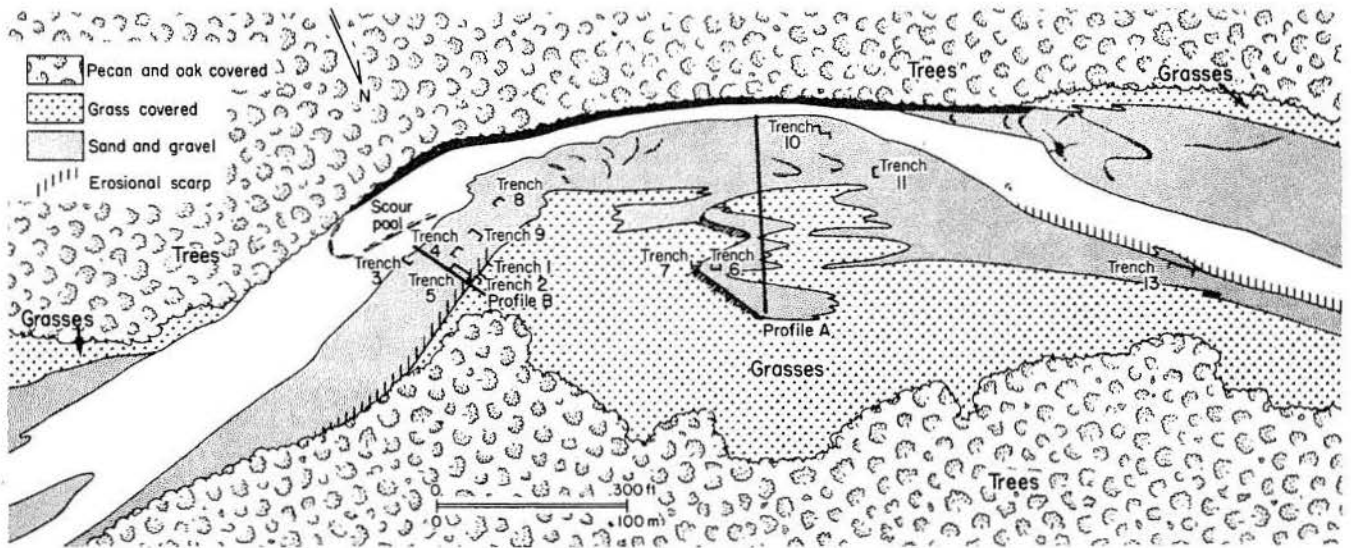


Figure 25. Locations of trenches and profiles, location C, Coletto Creek.

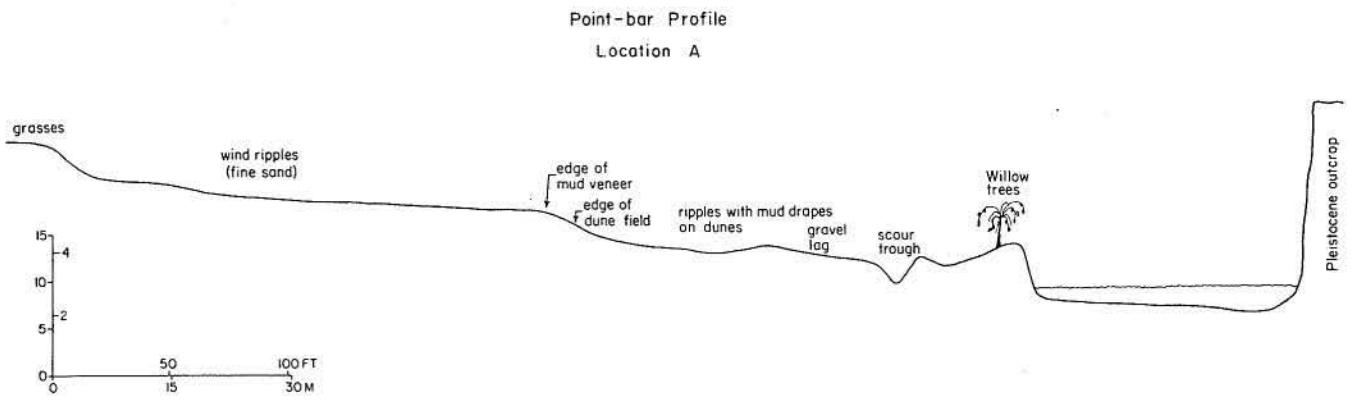


Figure 26. Point-bar profile, location A, Coledo Creek.

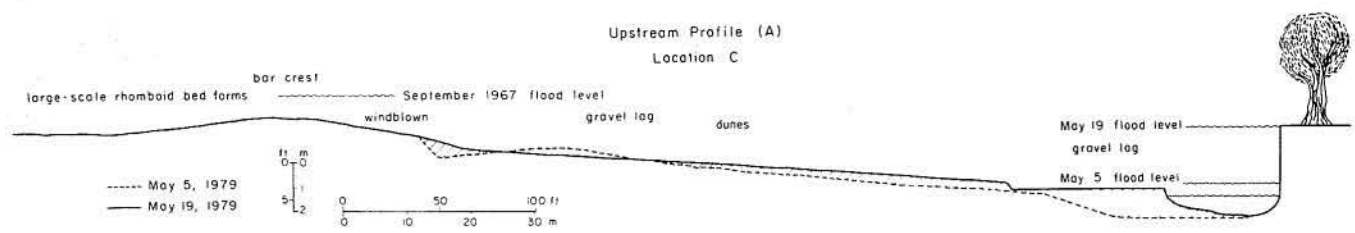


Figure 27. Upchannel point-bar profile A, location C, Coledo Creek.

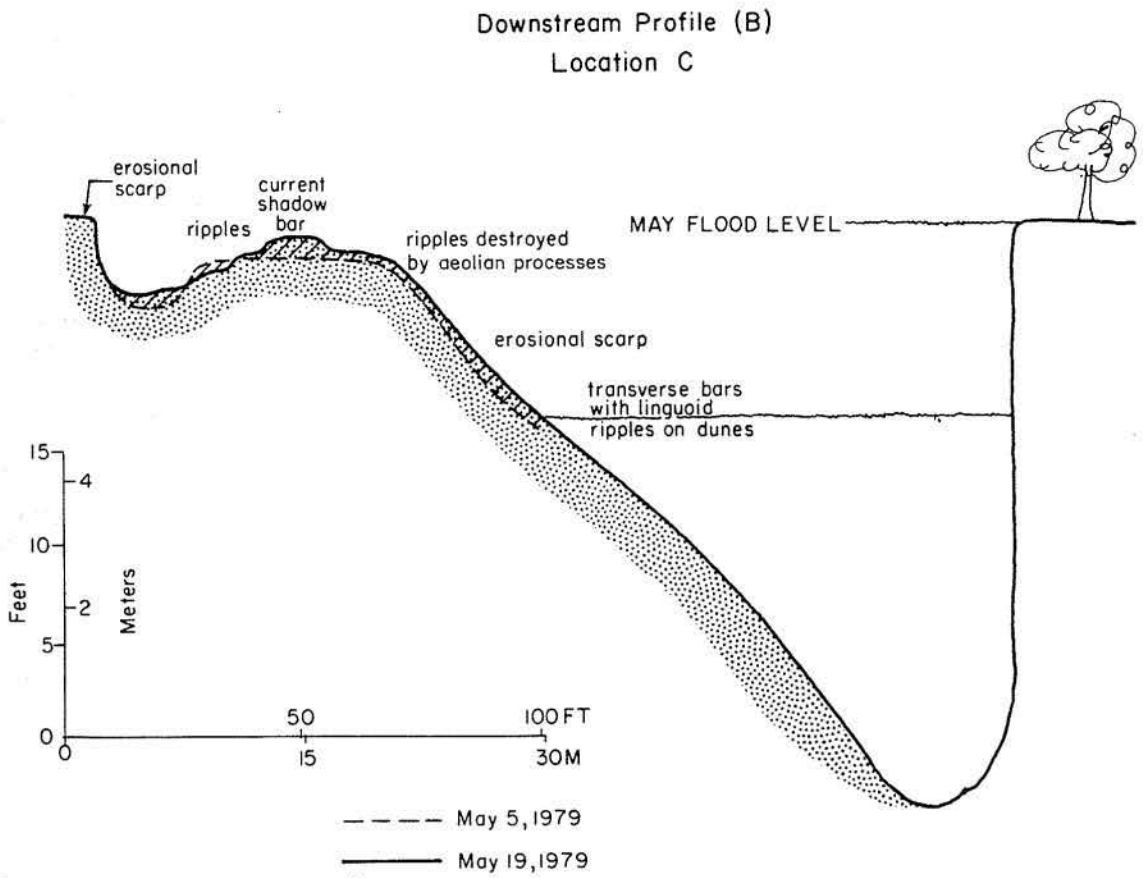


Figure 28. Downchannel point-bar profile B, location C, Coledo Creek.

Bed forms in the low-stage thalweg are primarily transverse bars with amplitudes less than 3 ft (1 m) and wave lengths of about 100 ft (30 m). Some of these transverse bars are marked by scour troughs that contain lag gravel and that form around clumps of vegetation.

Morphologies and sediment textures change most noticeably during extreme floods that carve channels and shape shoals and side-attached bars. Largest bed forms, highest rates of sedimentation, highest elevations of deposition, and greatest potential for preservation are related to these floods. However, bankfull floods of lower magnitude and higher frequency are also significant in point-bar development.

Gross Textural Changes

Textural changes and vertical sequences of sedimentary structures from Coleta Creek are markedly different from most fluvial models. In general, large-scale sedimentary structures are confined to upper point bars, and grain size does not systematically fine upward. In fact, gravel commonly occurs throughout the sediment and as a lag on bar surfaces. Furthermore, mud deposits are usually destroyed by desiccation and aeolian erosion. Rare occurrences of thick, homogeneous mud or a mixture of mud and gravel are concentrated in lenses within chutes and along channel margins. Systematic size segregation is evident, however, around each bend as shown by a slight decrease in mean sand size and rare gravel along downstream or distal portions of the bars.

Bar Stratification

Side-attached bars

Side-attached bars between point bars (fig. 24) are inundated frequently because of their low elevation above the channel floor. Despite continuous modification, side-attached bars exhibit orderly stacking of stratification types. When viewed perpendicular to flow, the complete sequence grades upward from horizontal parallel laminations to medium-scale trough cross-strata and finally to ripple-cross laminations. In places, a veneer of mud conforms to the uppermost rippled surface. Incomplete cycles consisting of horizontal stratified sand overlain by either medium-scale troughs or ripple cross-stratified sand are commonly repeated in vertical sequences (fig. 29). In sections parallel to flow, intervals comparable to trough cross-strata exhibit foresets that are slightly concave upward. These internal structures are formed by sinuous transverse bars or dunes that cover bar surfaces. Thin clay drapes deposited with the falling stage accentuate the ripples, but the drapes are usually destroyed when subaerially exposed.

Point bars with chutes

Point bars with chutes and scour troughs (figs. 24 and 26) contain a wide range of sediment sizes. Gravel lag and slackwater mud are both deposited in topographic lows, and gravel is slightly more abundant than mud. Sand, however, is volumetrically the dominant grain size throughout the bar.

Sedimentary structures associated with side-attached bars are also preserved in point bars with chutes. One exception is the predominance of foresets over troughs, especially in trenches oriented parallel to flow. Across the point-bar surface, foresets and horizontal stratification are commonly overlain by ripple cross-laminations. Stratification parallel to bar surfaces is also found on middle and upper bars in trenches perpendicular to flow. Such slope-parallel stratification would appear as foresets in the stratigraphic record. Thickest foreset units (up to 20 inches [5 cm]) are found in upper bar deposits where dunes spaced 10 ft (3 m) migrate during bankfull floods. Because of prolonged subaerial exposure and fine to medium grain sizes, upper bar surfaces are modified by wind ripples (fig. 26) except immediately after flooding.

Preserved vertical sequences in these bars would be alternating cycles of horizontal stratification, foresets, and occasionally ripple cross-laminations. In addition to horizontal and foreset stratification, upper bars also exhibit broad, low-relief undulations that may have formed by standing waves or antidunes. Scour troughs in lower bars and chutes in upper bars contain both coarse and fine sediment because of flashy discharge and rapid fluctuations in flow depths.

Point bars without chutes

Internal stratification of flat-crested point bars without chutes is exceedingly complex because of vertical and lateral variations in bed forms and textural differences that occur around each meander. Also contributing to bar complexity are erosional scarps that are less pronounced on point bars with chutes (fig. 25). By reducing the radius of maximum curvature, chutes also retard downchannel development of strong vortices that impinge on the distal bar. Cross-channel currents and counter currents are collectively responsible for erosional scarps that occur at different elevations around the bars. Large downchannel vortices associated with deep scour pools (figs. 25 and 28) are unusual on the inside of meanders because they develop counter currents that interfere with deposition. Local upstream currents

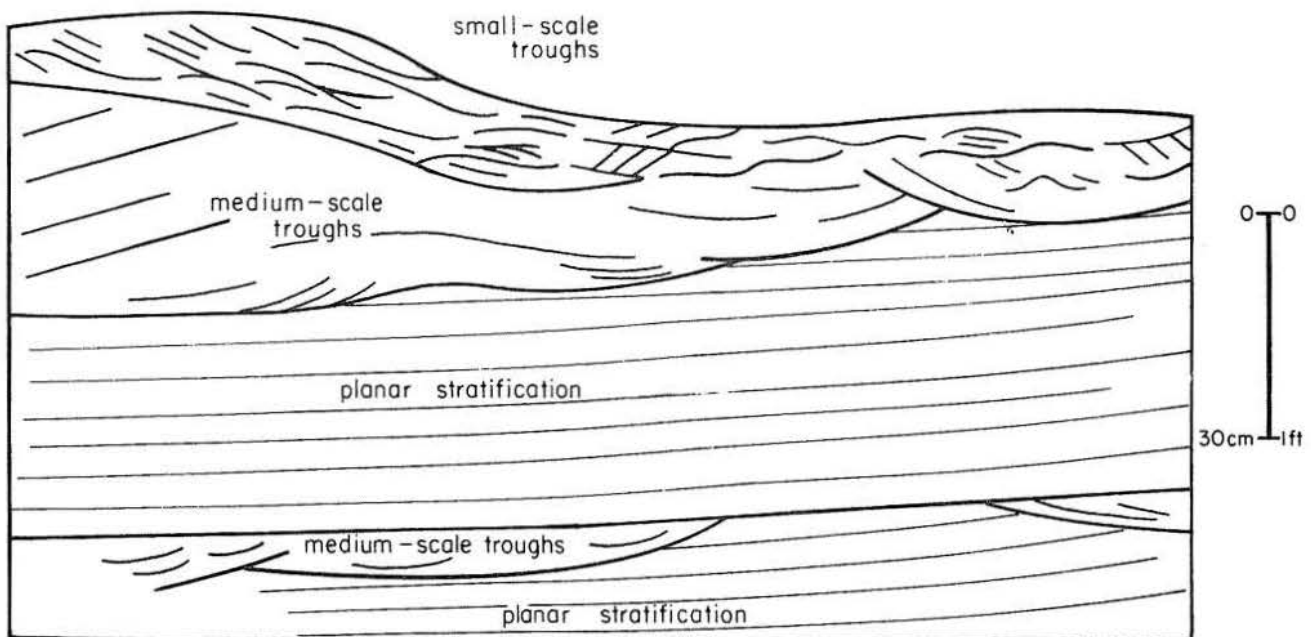


Figure 29. Stratification types preserved in a side-attached bar, location B, Coleta Creek.

associated with the vortices are responsible for erosional scarps developed adjacent to scour pools. Transverse bars migrating downstream into the scour pools merge to form steep avalanche faces that are 3 to 6 ft (1 to 2 m) high.

Composite vertical sequences for upchannel and mid-bar segments (fig. 30) show a predominance of medium-scale troughs and tabular foresets with reactivation surfaces (fig. 31). These structures are interbedded with thin and thick beds of horizontal parallel laminations that grade from coarse to medium sand. Gravel-lag deposits are scattered across upchannel and mid-bar surfaces and are concentrated along margins of scour troughs that form digitate patterns oriented downchannel.

Upchannel (apex) trenches show an upward-coarsening sequence related to larger stratification types preserved in upper point bar deposits (figs. 30 and 32). Medium- to large-scale troughs discordantly overlie horizontal parallel stratification that dips gently downstream and grades upward into low-angle foresets. The foresets are truncated by overlying large-scale troughs probably formed by three-dimensional dunes during an extreme flood. Large troughs are exposed in an erosional face oriented slightly oblique to the strike of bed-form migration. These strata were deposited during overbank flow when valley walls became channel margins (fig. 24).

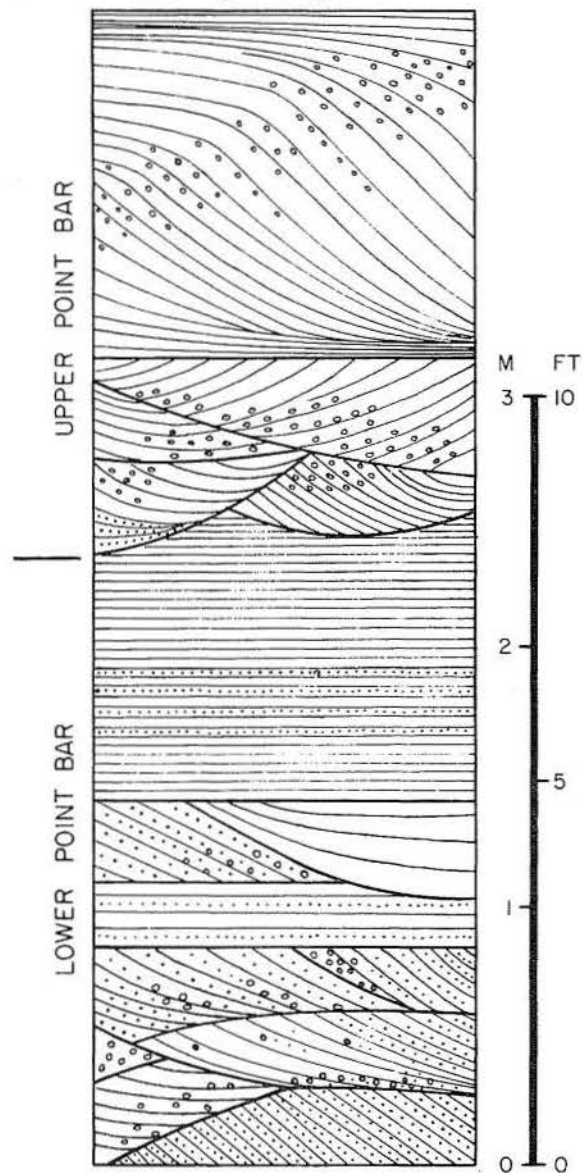


Figure 30. Composite vertical sequence of stratification types from upstream point bar, location C, Coleta Creek.

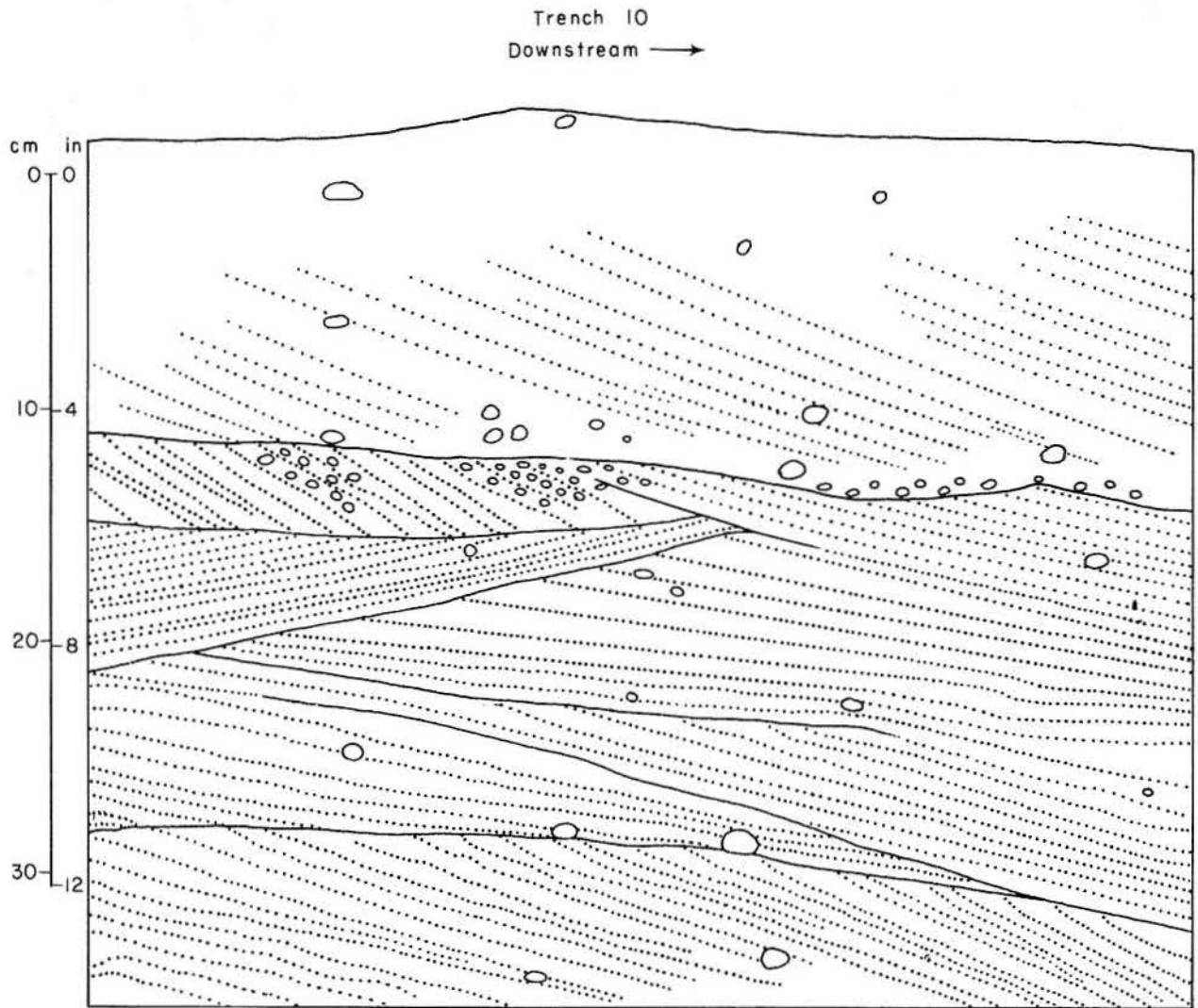


Figure 31. Lower point-bar stratification from trench 10, Coletto Creek.

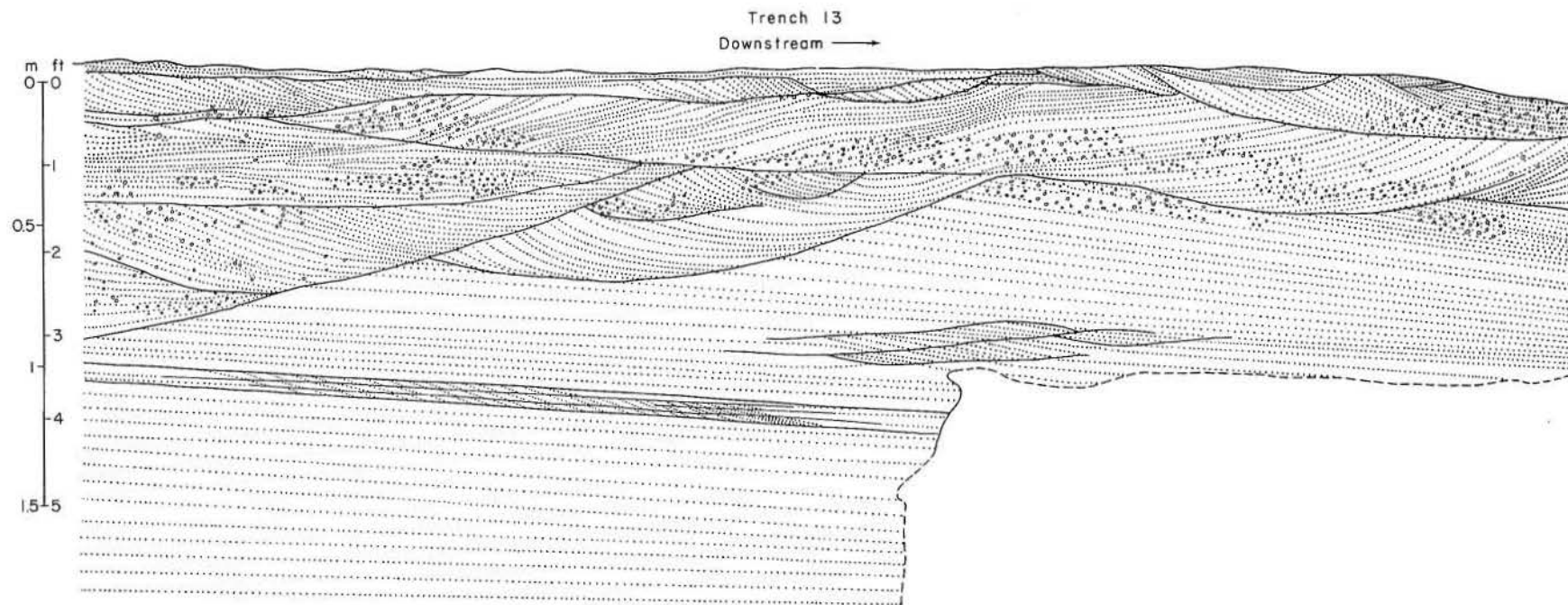


Figure 32. Upper point-bar stratification exposed in erosional face (trench 13) along bar apex. Note coarse textures and large-scale troughs deposited under extreme flood conditions.

Other large-scale features produced during overbank flooding are preserved on the point-bar crest at location B. Large-scale rhomboid bed forms and adjacent scour troughs (fig. 25) were most likely formed during the maximum flood of record in September 1967. In cross section, the rhombs display plane parallel stratification, slightly inclined downstream, and foresets (fig. 33) composed of coarse to fine sand that is poorly sorted. Coarse sand and gravel are deposited downcurrent of the brink point, whereas finer sand is deposited lower on the foreset. Poor sorting, simultaneous vertical and downstream migration of the brink point (fig. 33), and low foreset angle collectively suggest rapid deposition at relatively high velocities. Foresets steepen downstream from 15° to 29° at the terminal avalanche face indicating a decrease in flow velocities. Preserved relief on the avalanche face is 4.5 ft (1.4 m).

Uppermost distal bar deposits are characterized by low-angle, concave-upward foresets and horizontal to wavy parallel laminations that show coarse to fine alternations. Evenly laminated units are separated by troughs with a homogeneous appearance or by medium-scale trough cross-strata (fig. 34). Foresets and trough cross-strata are generally coarser than overlying horizontal parallel strata.

Distal bar sediments range in size from gravel to mud, but each is rare; medium to fine sand predominates. Also rarely present are lenses of organic detritus representing backwater deposition in topographic lows.

Stratification types preserved in distal point bars are diverse owing to complex morphologies and variations in flow direction. Some striking preserved features are erosional scarps, regressive ripples on foresets, and ripple-drift lamination (fig. 35). Despite the uncertainty of idealized sedimentary sequences, some generalizations can be made. For example, lowermost stratification types are medium-scale foresets formed by migration of transverse bars. Foreset units, up to 6 ft (2 m) thick, may be replaced downstream by small-scale sigmoidal to tabular foresets that underlie regressive ripples and that grade laterally into ripple-drift lamination. Reactivation surfaces are also common in this sequence.

Where scour channels or levee-like depositional highs are present along the distal bar (fig. 28), small-scale foresets actually dip away from the channel and toward the convex bank (fig. 35). This stratification is associated with lateral infilling of lows between lower and upper point bar deposits.

Guadalupe River

General Setting

The Guadalupe and San Antonio Rivers collectively form the Guadalupe drainage basin that encompasses about $10,000 \text{ mi}^2$ ($25,900 \text{ km}^2$) of Central and South Texas (fig. 1). These rivers originate as spring-fed streams in Cretaceous carbonates of the southern Edwards Plateau and cross the Balcones Fault Zone, a major physiographic feature that separates the carbonates from the Cretaceous and Tertiary clastics of the Coastal Plain. Coastal Plain sediments are primary sources of fine-grained clastics that are transported by the Guadalupe fluvial system and deposited either within alluvial channels or within environs of the Guadalupe delta.

Annual rainfall near the coast averages about 31 inches (79 cm), and the climate is dry subhumid (Thorntwaite, 1948), but drought periods and flood-producing storms

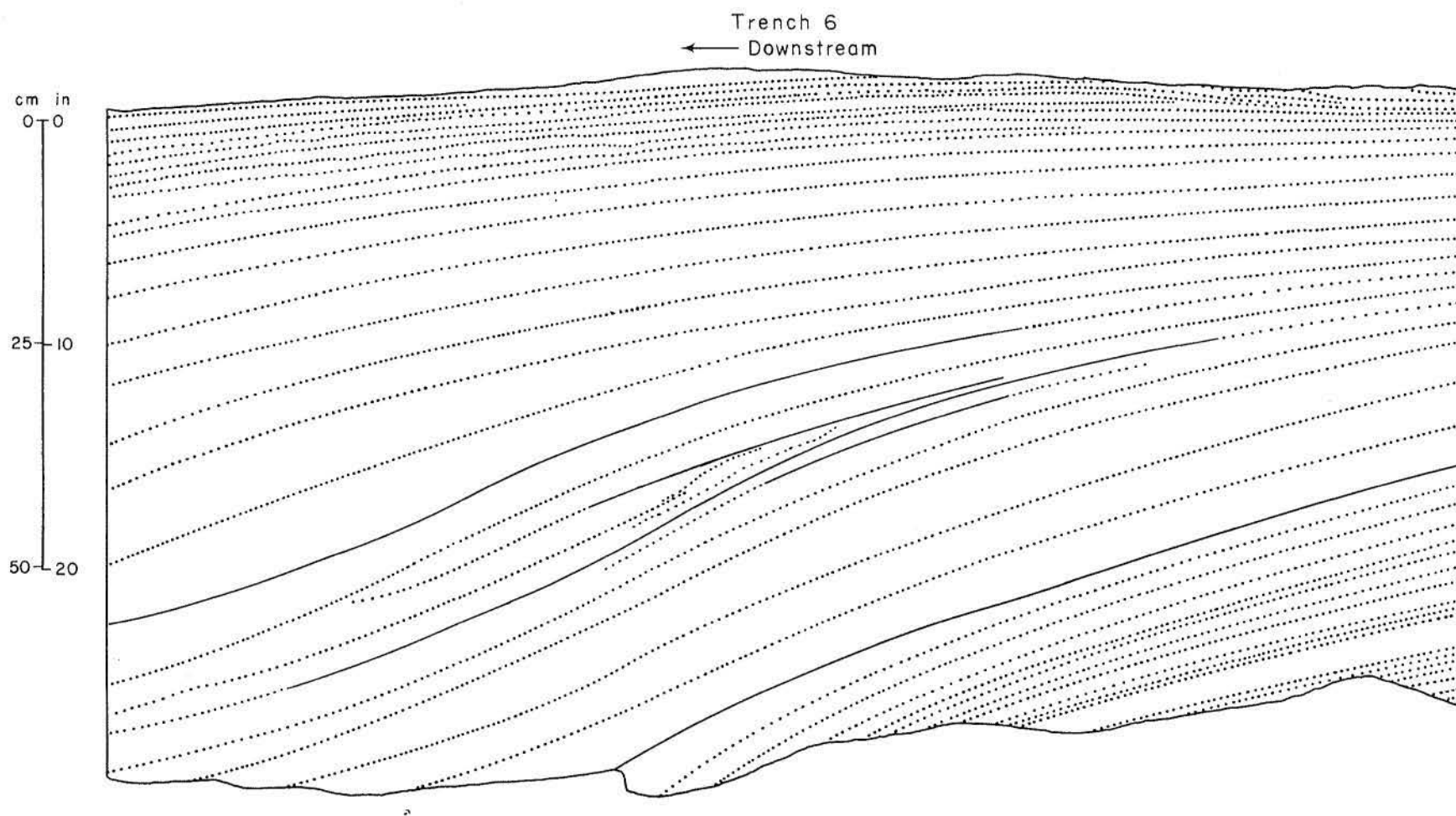


Figure 33. Internal stratification in trench 6 just upstream from avalanche face of large-scale rhomboid bed form. Bed-form and trench location shown in figure 25.

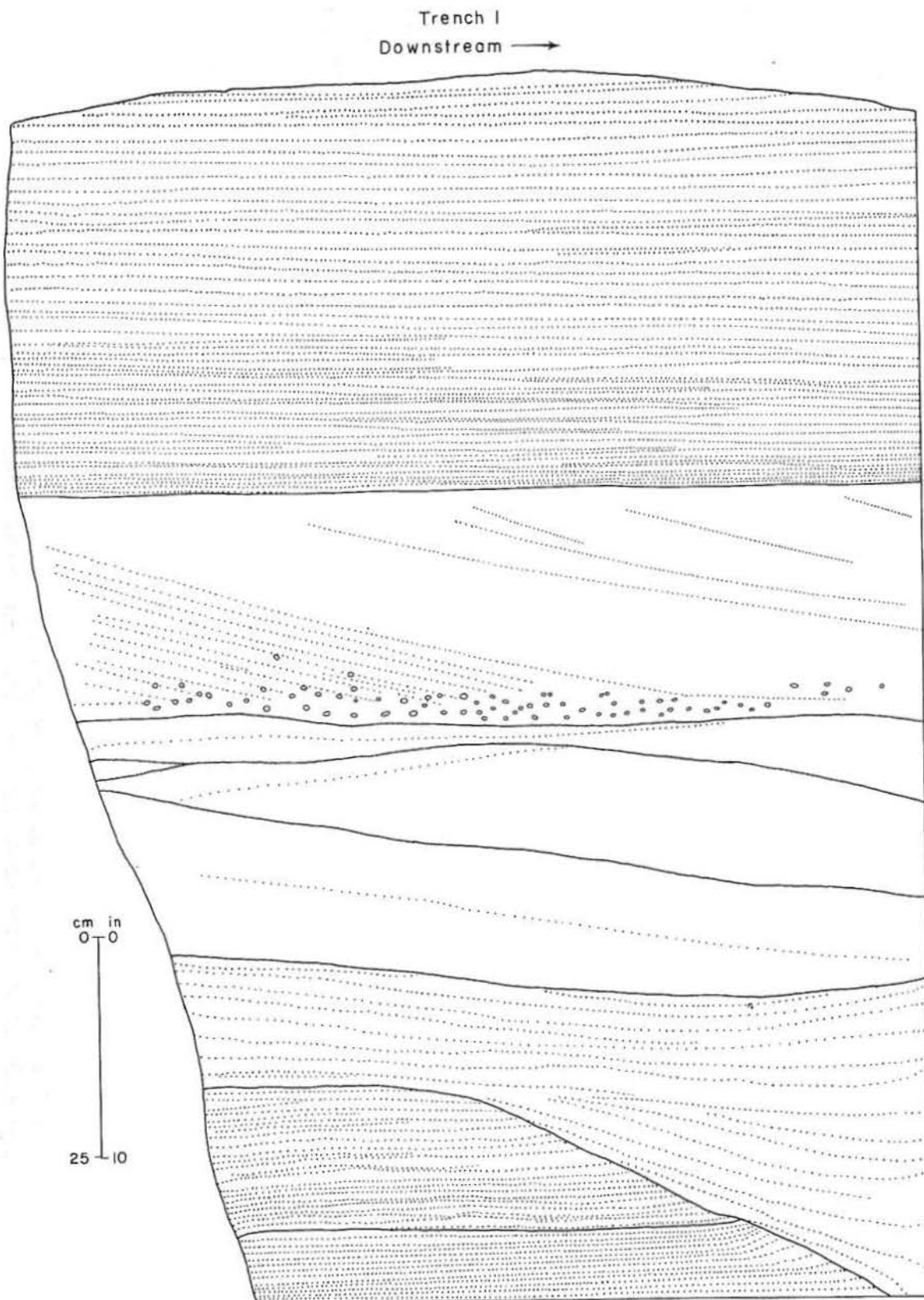


Figure 34. Internal stratification exposed in erosional face (trench I) of distal point bar.

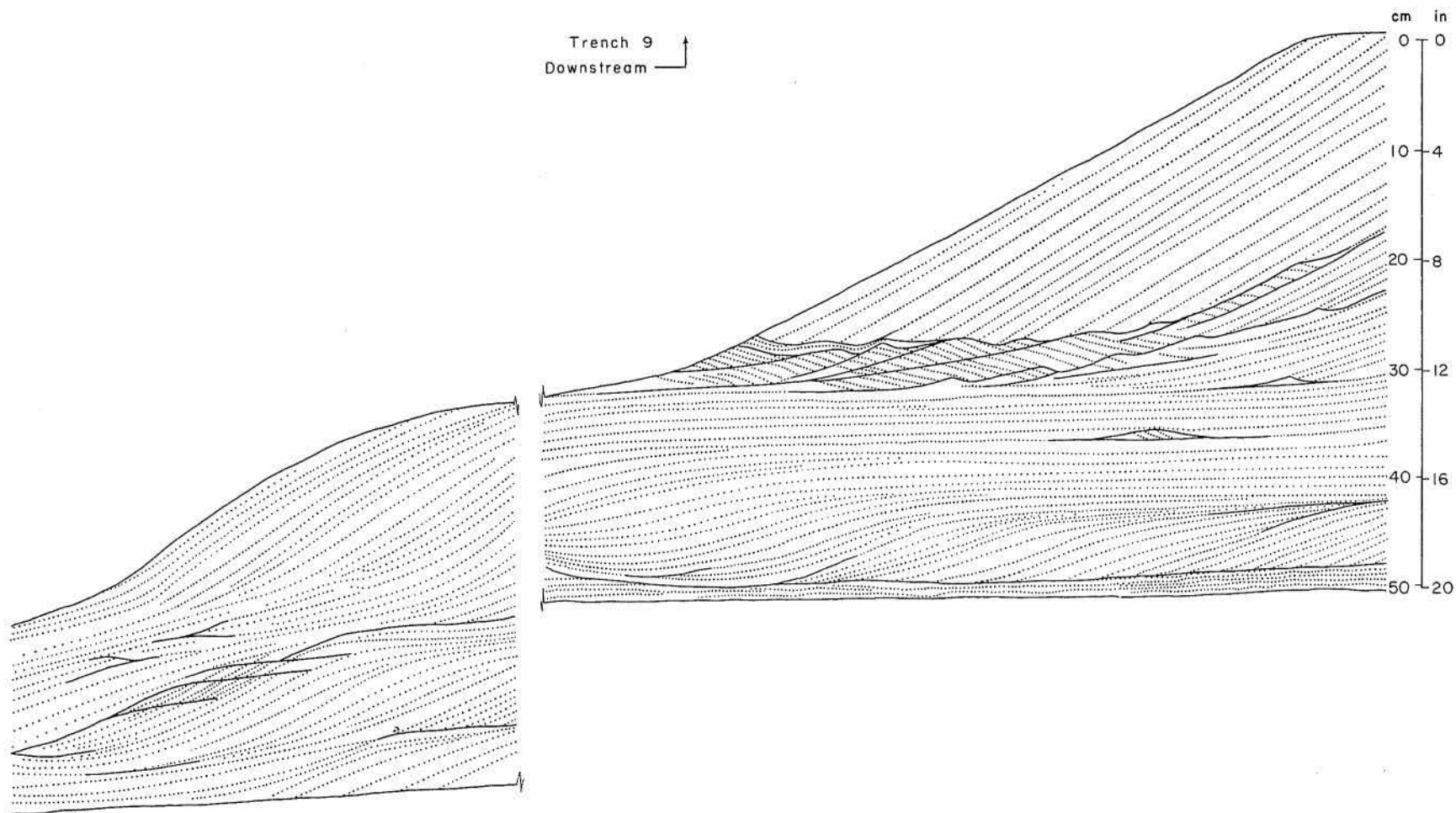


Figure 35. Bed forms and internal stratification (trench 9) produced by migration of low-relief bars into side channel of convex bank. Position of side channel shown on figure 28.

cause considerable variations in discharge. Prior to 1954, the basin was relatively unaltered by human activities. Flood-retarding structures built after 1954 only partly control flow from less than 300 mi² (800 km²).

Discharge

Like Coleta Creek and most other Texas streams, the Guadalupe and San Antonio Rivers have highly variable discharge (fig. 4). Minimum and maximum discharges are respectively associated with droughts and aftermath rainfall from tropical cyclones. Rainfall rates in excess of 1 inch (2.5 cm) per hour occur throughout the drainage basin, but they are most common along the Balcones Escarpment and near the coast (fig. 36). In these areas meteorological conditions favor prolonged rainfalls at extremely high rates that together produce widespread flooding. Cumulative rainfall from storms moving inland from the Gulf is responsible for highest rates of streamflow. Maximum recorded discharge for the Guadalupe River near Victoria (180,000 cfs) occurred during such a storm (fig. 36).

According to records from downstream gaging stations, average discharge for the lower Guadalupe River is 2,250 cfs (65 m³/s). Nearly two-thirds of the water and sediment flow into Mission Bay through Traylor Cut (Morton and Donaldson, 1978a), a man-made diversion opened in 1935.

Stream Characteristics

Sedimentological and morphological parameters of the Guadalupe River change downstream. In general, width/depth ratio, channel sinuosity, channel gradient, valley gradient, mean grain size of bed material, and percent sand in channel and bank sediment decrease downstream. Greatest changes in these parameters occur between alluvial-plain and delta-plain segments. For example, between Victoria and the river mouth, sinuosity changes from 2.24 to 1.03; width/depth ratio decreases from 8.1 to 5.8; and channel gradient decreases from 1.73 ft/mi (0.33 m/km) to near 0 along lower reaches of distributary channels. Higher-than-average upstream gradients (fig. 3) are influenced by crustal uplift over the San Marcos Arch.

According to Schumm's classification (1968), the Guadalupe and San Antonio Rivers are suspended-load streams. Low rates of sediment transport are inferred from stream measurements by Mirabal (1974). Suspended sediment carried by the San Antonio River represents 0.09 percent by weight of discharge, whereas sediment discharge in the Guadalupe River represents 0.034 percent by weight.

At Victoria, point-bar deposits consist mainly of fine to medium sand except for gravel lag in the lower 5 ft (1.5 m). Swales within the main bar that also contain gravel are 2.5 to 5 ft (0.75 to 1.5 m) deep. Farther downstream point-bar deposits consist of fine sand, but extant point-bar surfaces are inactive and lack diagnostic bed forms.

Point-bar deposits on the Guadalupe River are composed predominantly of gravel and coarse to fine sand that grade vertically into flood-basin muds. Gravel bars in the active alluvial channel and gravel beds in Holocene valley fill are reworked late Tertiary and Quaternary gravels that form an extensive cover over Coastal Plain sediments. According to surficial mapping (McGowen and others, 1976) and water-well records, alluvial valley fill averages from 4 to 6 mi (6.5 and 10 km) wide and 25 to 35 ft (7.5 to 11 m) thick.

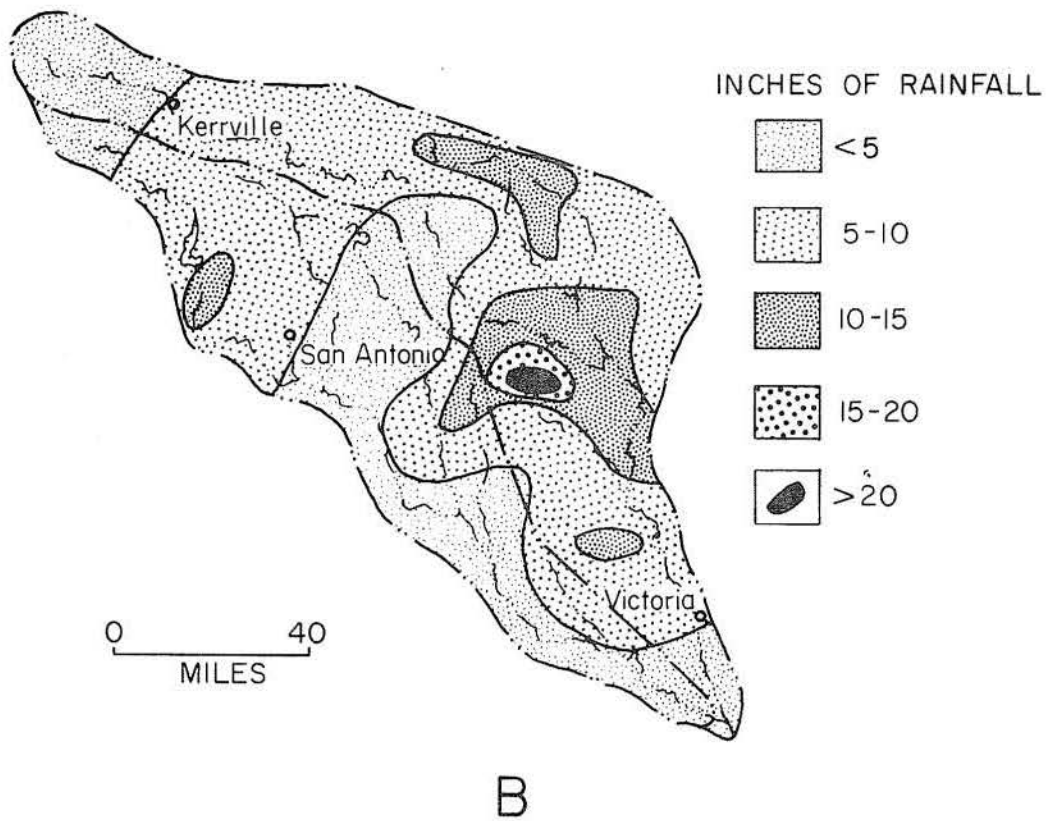
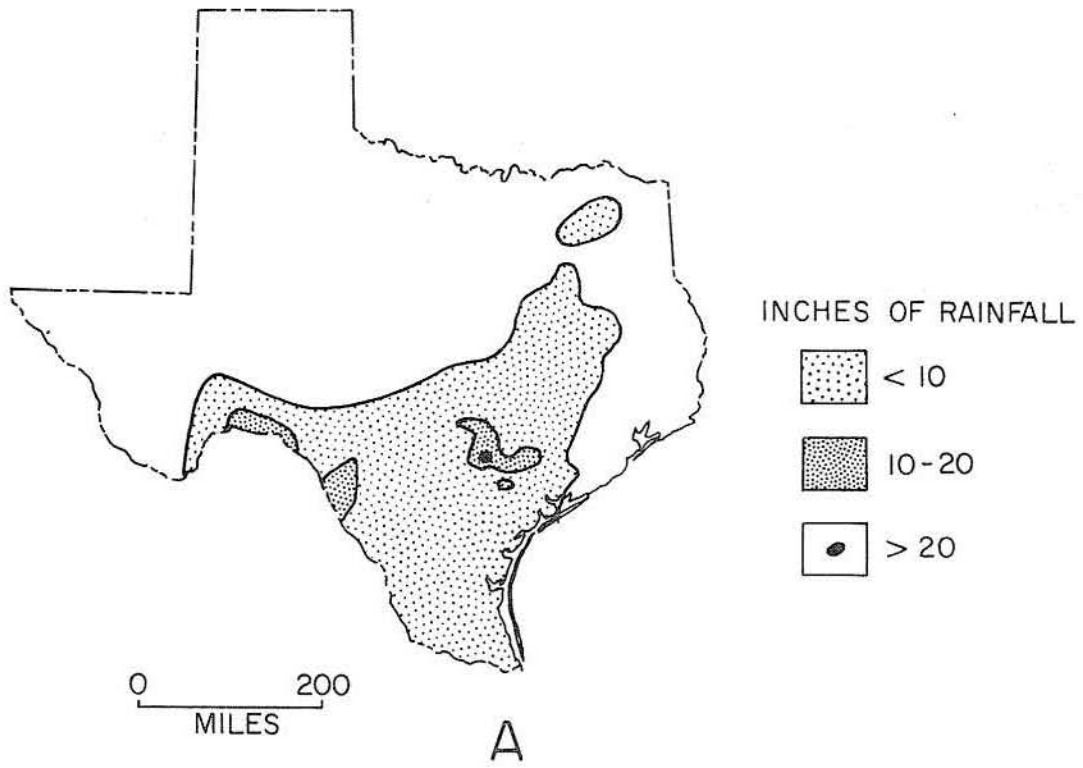


Figure 36. Isohyetal map of rainfall measured June 28 to July 1, 1936, in (A) Central and South Texas, and (B) the Guadalupe and San Antonio River basins (from Dalrymple, 1937).

Major Bed Forms

The Guadalupe River exhibits two populations of dunes with ripples commonly superimposed on these dunes. Small dunes have amplitudes from 0.5 to 1.0 ft (0.15 to 0.3 m) and wavelengths from 1 to 100 ft (3 to 30 m). Comparable ranges for large dunes are 1 to 3 ft (0.3 to 1.0 m) and 100 to 330 ft (30 to 100 m), respectively.

Large differences in channel depth occur along the alluvial plain where point bars and alternate bars are best developed. In contrast, channel depth is more uniform and bed forms are more regularly spaced along distributary channels (fig. 37). Dune size diminishes downstream, and bed forms are washed out at the river mouth.

Point bars of the Guadalupe and San Antonio Rivers typically are poorly developed, probably because of decreased discharge and subsequent increased suspended-load transport attendant with climatic changes during the past few thousand years. Much of the valley fill that serves as a resource for aggregate mining operations near Victoria is sand or gravel. Despite a coarse substratum, the surface is fine grained, commonly mud veneered, and lacks accretionary depositional features such as ridge-and-swale topography (McGowen and others, 1976).

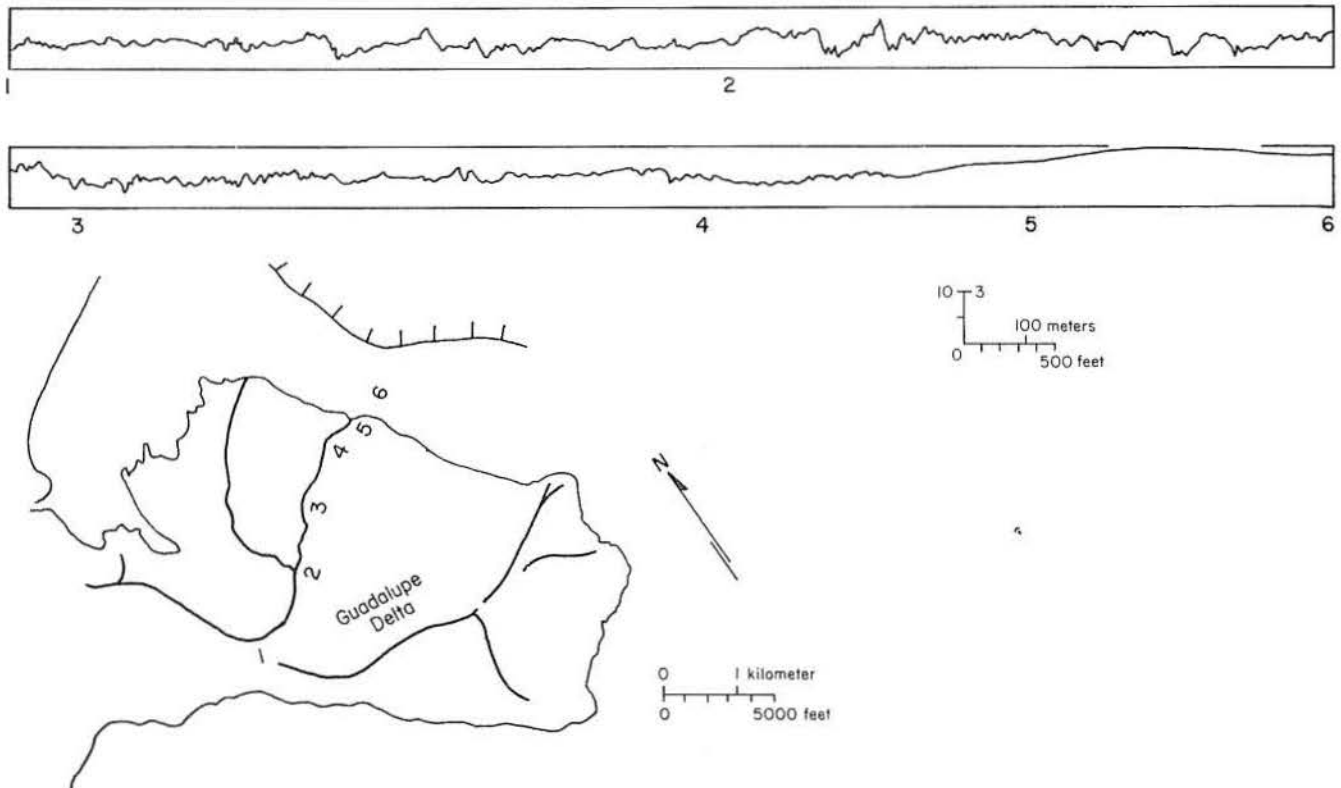


Figure 37. Fathometer profile extending along lower reaches of south Guadalupe River, across distributary-mouth bar, to Guadalupe Bay (after Morton and Donaldson, 1978a). Austwell Quadrangle.

DELTA

Introduction

Oceanic, bayhead, and fan deltas are three distinctly different types of delta represented in Holocene and Modern sediments of the Texas coast (McGowen, 1979). Apart from being much broader in areal extent, oceanic deltas of the Rio Grande and Brazos-Colorado Rivers are slightly thicker and have a more complex history than bayhead deltas. Distribution of facies in these deltas is poorly understood because of their size. Except for coring by major oil companies (Bernard and others, 1970; Pryor and others, 1975; Fulton, 1975) studies of these fluvial-deltaic systems have been limited to surficial mapping (McGowen and others, 1976; Brown and others, 1980) and geomorphic studies (Price, 1958; Lohse and Cook, 1958). These and other Holocene deltaic complexes are inactive and retreating rapidly (Morton and Pieper, 1975a, 1975b) because of natural decreases in discharge and sediment supply as well as human modifications in the drainage basins.

The new Brazos delta, which developed following river diversion in 1929, is typical of high-destructive wave-dominated deltas according to the classification of Scott and Fisher (1969). Historical data, however, indicate that its formation is due largely to human activities. Regardless of its origin, this type of delta has low preservation potential (Bernard and others, 1970). In contrast, bayhead deltas can easily be preserved in the rock record. Their small size facilitates study; several have been studied in detail. Salient features and facies characteristics of shallow-water bayhead deltas were described by McEwen (1969) for the Trinity delta, by Donaldson and others (1970) for the Guadalupe delta, and by Kanen (1970) and Manka and Steinmetz (1971) for the Colorado delta.

Gum Hollow delta, located in Nueces Bay (McGowen, 1970), serves as a model for small fan deltas. This delta is inactive except during spring thunderstorms and hurricane flooding, but sedimentary textures and structure developed when it was active are similar to, albeit on a smaller scale than, other fan deltas.

Shallow-Water Delta Model

Most shallow-water deltas are situated within stable depositional basins where fluvial processes dominate marine processes and where sediment supply is greater than compactional subsidence. This physical setting causes other distinguishing features of shallow-water fluvial-deltaic systems (Guadalupe type, fig. 38) such as relatively thin prodelta facies, relatively thick delta-plain facies, and the cannibalization of previously deposited deltaic sediments, which are replaced by active and abandoned alluvial channel and distributary channel deposits during delta progradation. Channel meandering and active point bars are restricted to the alluvial plain and upper delta plain, whereas delta distributaries are single, straight symmetrical channels. These fluvial facies represent the greatest total sand preserved in the stratigraphic record.

Shallow-water deltas have played an important role in filling the Gulf of Mexico during Tertiary and Quaternary Periods. Late Pleistocene deltas that form the lower Coastal Plain are extensive but only 30 to 50 ft (9 to 15 m) thick (fig. 39). Descriptions from subsurface borings indicate that much of the mud was deposited on delta plains or in interdistributary bays, whereas sands are related to crevasse splays and distributary channels.

Brazos Delta

The Holocene Brazos delta (fig. 1) has occupied at least four positions (two of these in historic times). From oldest to youngest, and from east to west the Holocene Brazos delta was constructed (1) in the San Luis Pass area (some 20 mi [32 km] east of the present mouth of the Brazos River), (2) at the mouth of Oyster Creek (about 8 mi [13 km] east of the mouth of the Brazos River), (3) at Surfside in the area of the Freeport Harbor Channel (about 6 mi [10 km] east of the present river mouth), and (4) at the present mouth of the Brazos River (Bernard and others, 1970; McGowen and others, 1976). The Modern Brazos delta is about 50 years old; deltation began at the present site in 1929 when the U.S. Army Corps of Engineers dredged a diversion channel from Velasco to the Gulf of Mexico. At the time of diversion there was a delta at Surfside comparable in size to the Modern Brazos delta; the Surfside delta, as well as the Oyster Creek delta and the delta in the San Luis Pass area, has been destroyed.

Local areas near the river mouth have had the highest rate of shoreline advance on the Texas coast (Seelig and Sorensen, 1973). Although the Brazos River continues to discharge a relatively large sediment load into the Gulf of Mexico, parts of the delta have eroded (fig. 40). The delta continues to prograde the shoreline, but the site of rapid accretion has shifted to the west away from the river mouth.

The Modern Brazos Delta: A High-Destructive Wave-Dominated Oceanic Delta

The Brazos River meanders almost to the Gulf shoreline; along the last 5.25 mi (8 km) it has a straight artificial channel (Bernard and others, 1970; McGowen and others, 1976). The Brazos delta has no distributaries, and the delta plain is characterized by levees, salt marshes, beaches, beach ridges, interridge areas, and shallow bays and ponds (fig. 41). The subaerial part of the delta exhibits a cusped form resulting from almost immediate reworking of materials (once they are delivered to the Gulf by the Brazos River) by waves and currents; marine processes dominate fluvial processes in molding the delta. This type of delta has been termed a high-destructive wave-dominated delta (Scott and Fisher, 1969).

Beaches, beach ridges, and interridge deposits consist chiefly of well-sorted fine-grained sand and shell. Marshes and ponds are represented by mud and muddy sand deposits. Subaqueous delta deposits (fig. 41) cover a significantly larger area than the subaerial segment. The Brazos delta-front area includes several environments including bar channel, distributary-mouth bar, and delta fringe (Bernard and others, 1970). The Brazos delta front comprises an area greater than 30 mi² (48 km²), extends from shoreline into water depths of about 4 fathoms, and is made up of sand, silt, and mud. Prodelta muds accumulated in water more than 4 fathoms deep.

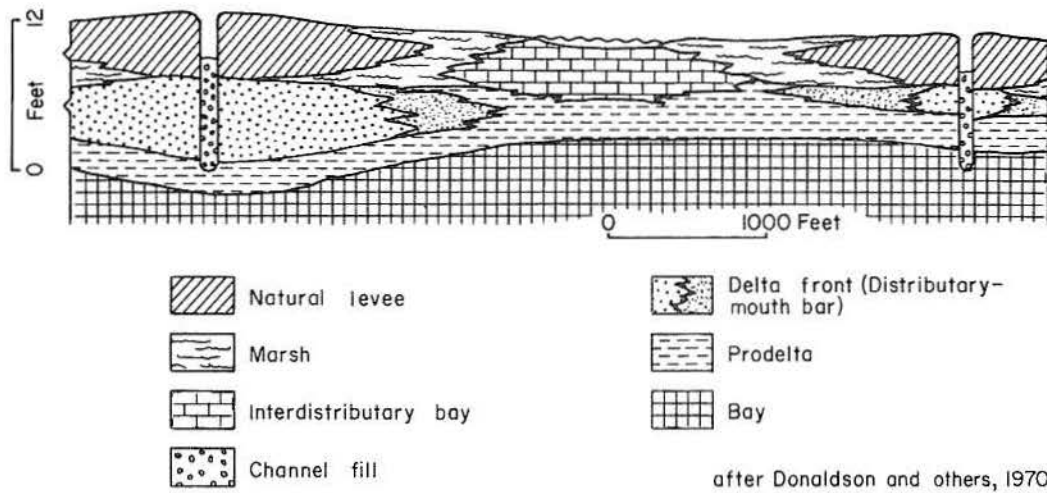


Figure 38. Generalized facies diagram for Guadalupe delta. Austwell Quadrangle.

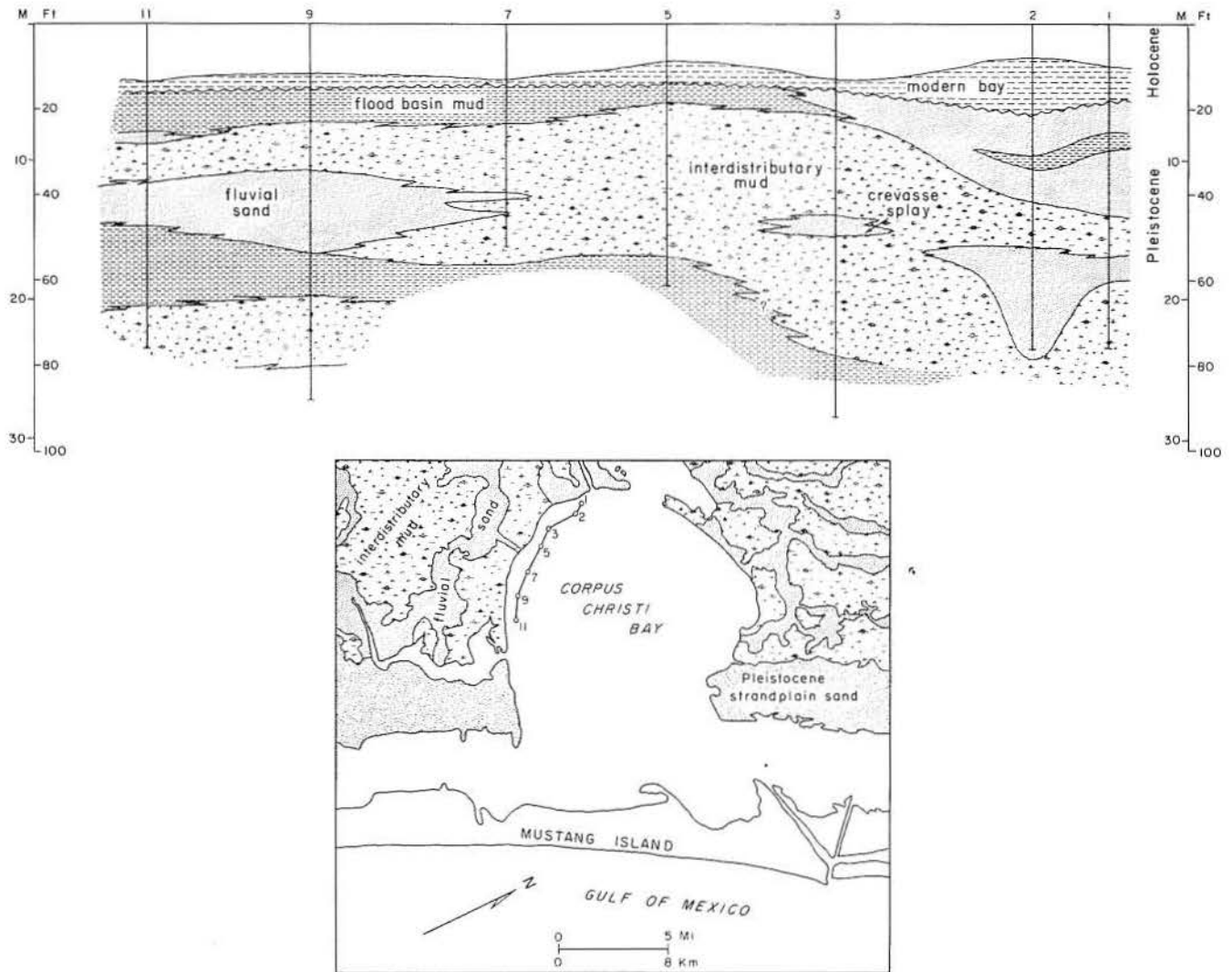


Figure 39. Surficial Pleistocene environments (from Brown and others, 1976) and interpreted shallow water fluvial-deltaic facies for the Pleistocene Nueces River system. Corpus Christi Quadrangle.

Coring by Bernard and others (1970) indicates that the Brazos delta, like progradational sequences of high-constructive lobate deltas (Fisher, 1969) and Galveston Island (Bernard and others, 1970), is characterized by a coarsening-upward textural trend (figs. 42 and 43). Immediate reworking of silt- and sand-sized sediment by marine processes produces similarities between the subaqueous Brazos delta and the shoreface of barrier islands. Observations made (by divers) in the fall of 1973 indicate that sand is transported at least 2 mi (3.1 km) offshore from the deltaic shoreline; this sand, occurring in water more than 4 fathoms deep, was firmly packed (McGowen, 1979).

Colorado Delta

History of Development

Unlike most other Modern deltas, the Colorado delta (fig. 1) prograded rapidly and developed as a result of human modifications. Large volumes of sediment formerly trapped by a log jam were released and transported downstream after the jam was removed in 1929. A major flood in June 1929 initiated rapid growth of the delta, which traversed Matagorda Bay by 1935. After a channel was dredged through the delta and Matagorda Peninsula in 1936, the Colorado River deposited much of its sediment load directly into the Gulf of Mexico. A minor active lobe of the delta is building into West Matagorda Bay through Tiger Island Cut. More detailed descriptions of delta advance and retreat were presented by Wadsworth (1966), Kanes (1970), and Manka and Steinmetz (1971).

The Colorado delta has been cored and studied more than any other Modern delta on the Texas coast. Previous sedimentological studies were conducted by Shepard and

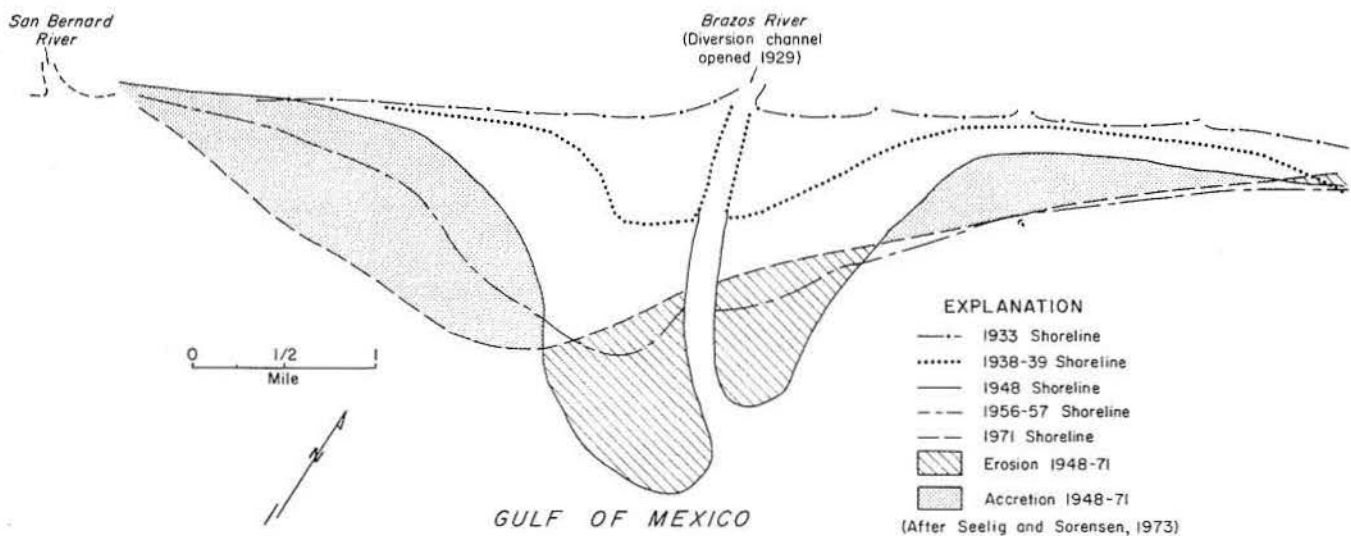


Figure 40. Shoreline changes associated with the Brazos deltas, 1933-1971 (modified from Seelig and Sorensen, 1973). Freeport and Jones Creek Quadrangles.

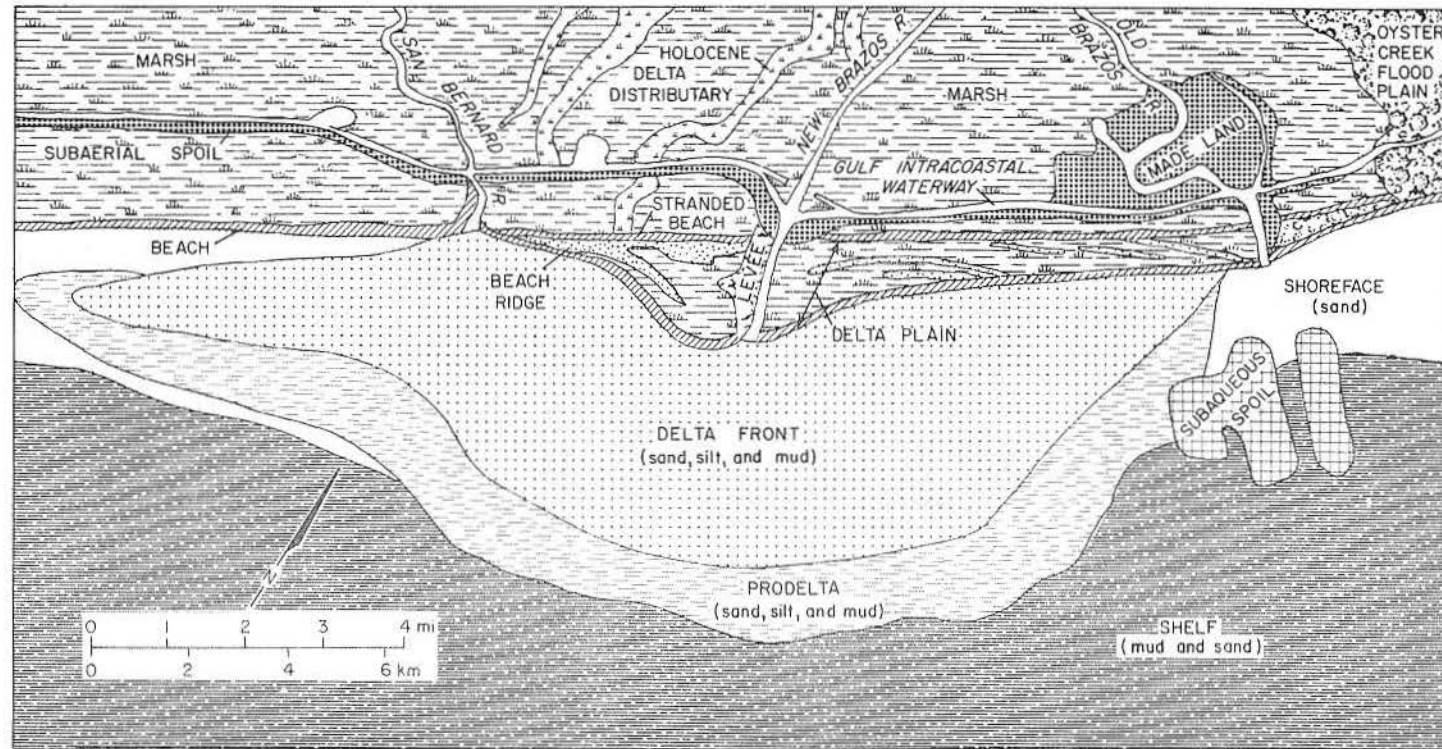


Figure 41. New Brazos River delta situated between Freeport Harbor Channel and the mouth of the San Bernard River. This delta is a high-destructive, wave-dominated delta with a characteristic cusped form. There are associated with this delta numerous subaerial and subaqueous environments (from McGowen and others, 1976).

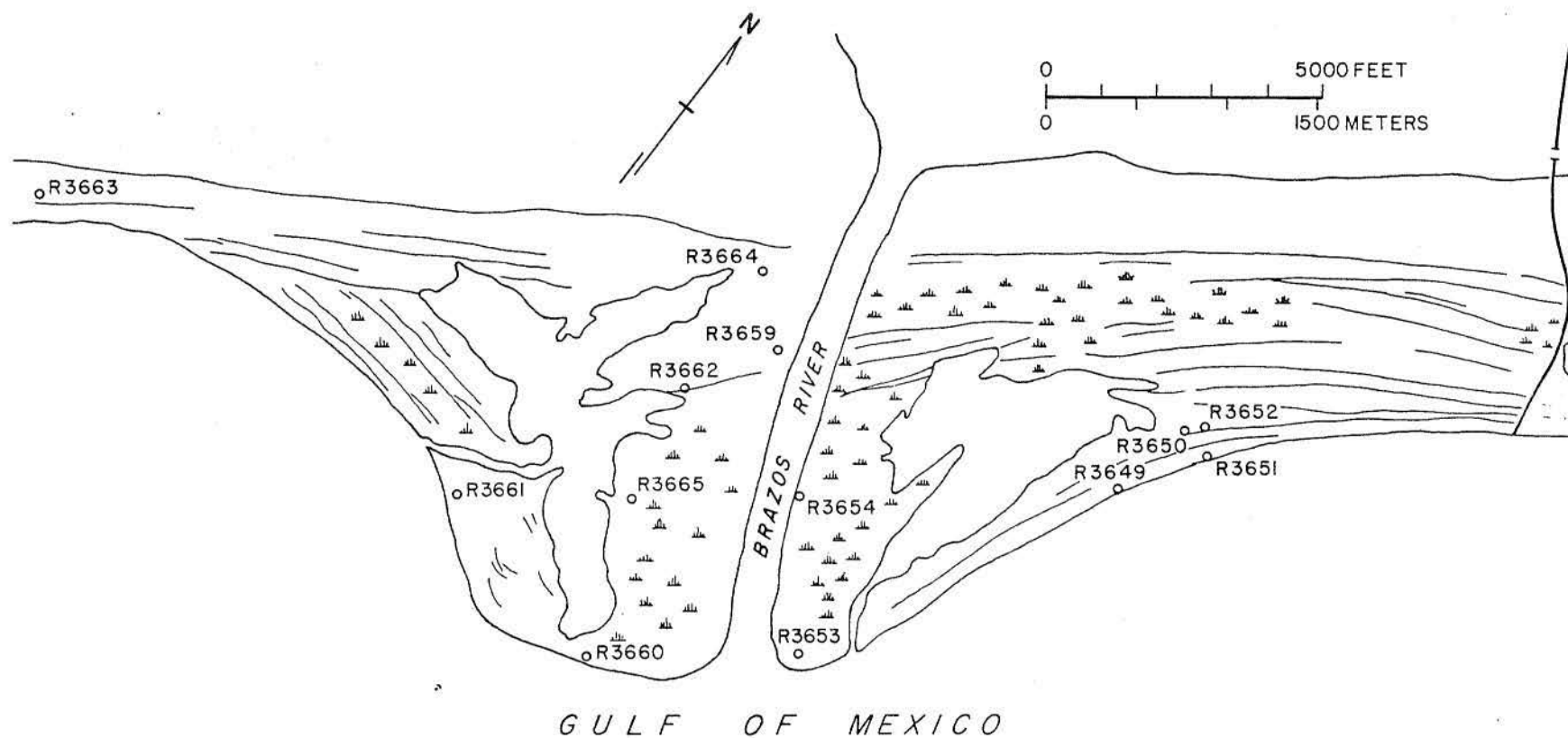


Figure 42. Locations of borings in the "new" Brazos delta (after Bernard and others, 1970). Freeport and Jones Creek Quadrangles.

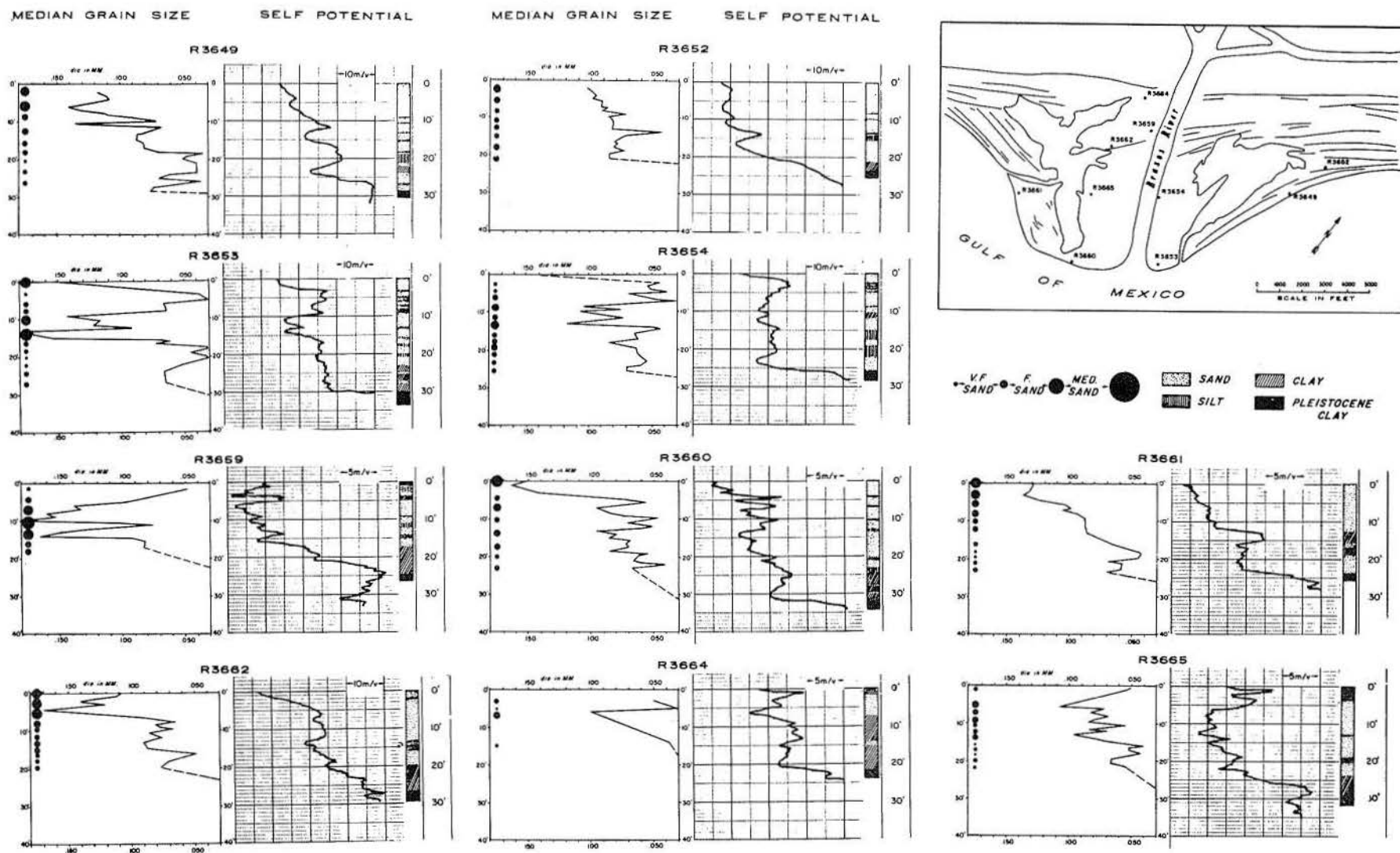


Figure 43. Relationships between grain-size changes and SP character of the deltaic fringe deposits of the "new" Brazos delta near Freeport, Texas. The serrate funnel-shaped character predominates. See figure 42 for bore-hole locations (after Bernard and others, 1970).

Moore (1960), Wadsworth (1966), Bouma and Bryant (1969), Kanes (1970), and Manka and Steinmetz (1971). Because its rapid development was related to historical flooding, the Colorado delta is analogous, in many respects, to crevasse systems of larger deltas.

Delta Facies

The Colorado delta plain is predominantly marsh. Levees along distributary channels are poorly developed. Moreover, individual lobes are fan shaped, and distributaries are closely spaced, especially on Egret Island (figs. 44 and 45).

Other common environments include interdistributary bays, beaches, prodelta, and distributary-mouth bars. Boundaries between various environments are vague because differences in surface elevations are less than 1.5 ft (0.5 m).

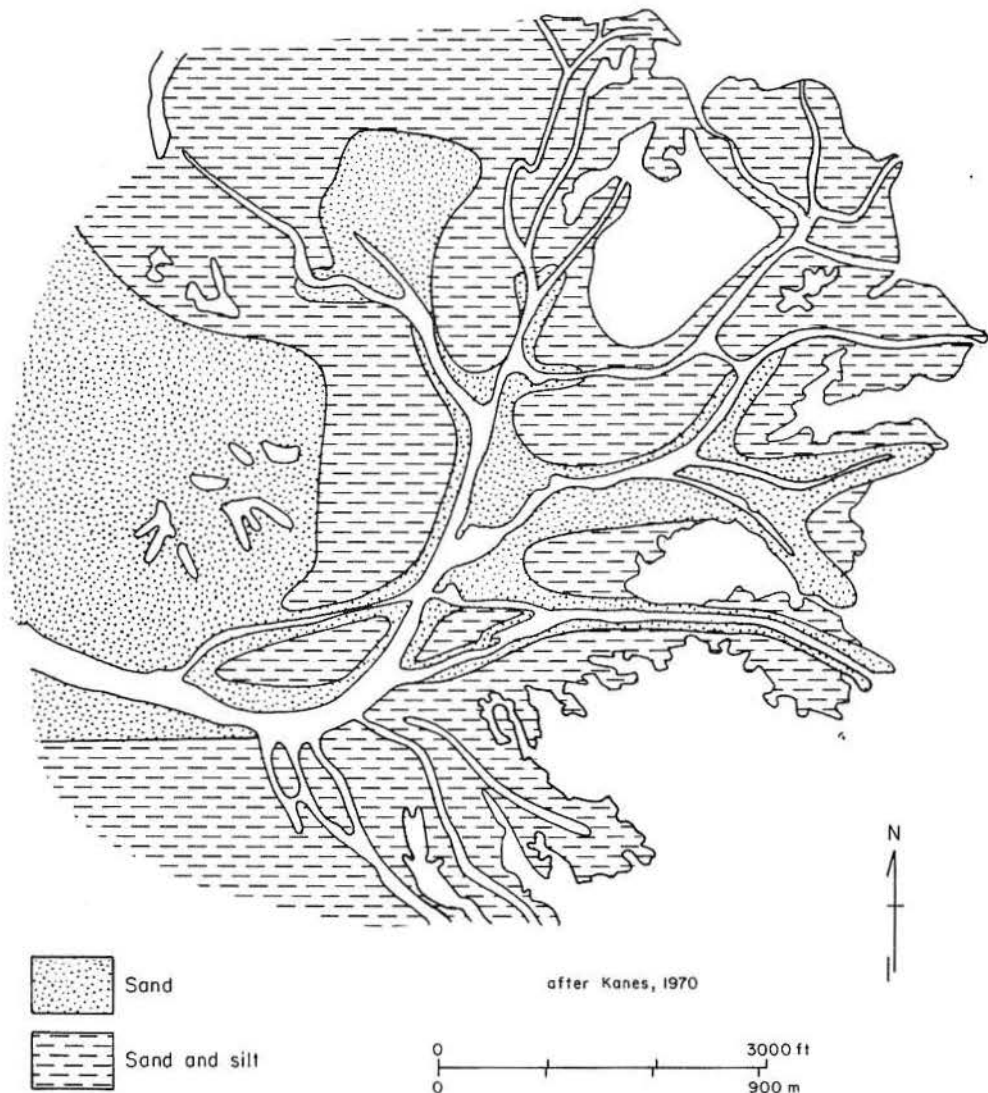


Figure 44. Distribution of delta-front sediment on Egret Island (location on fig. 45) lobe of the Colorado delta (after Kanes, 1970).

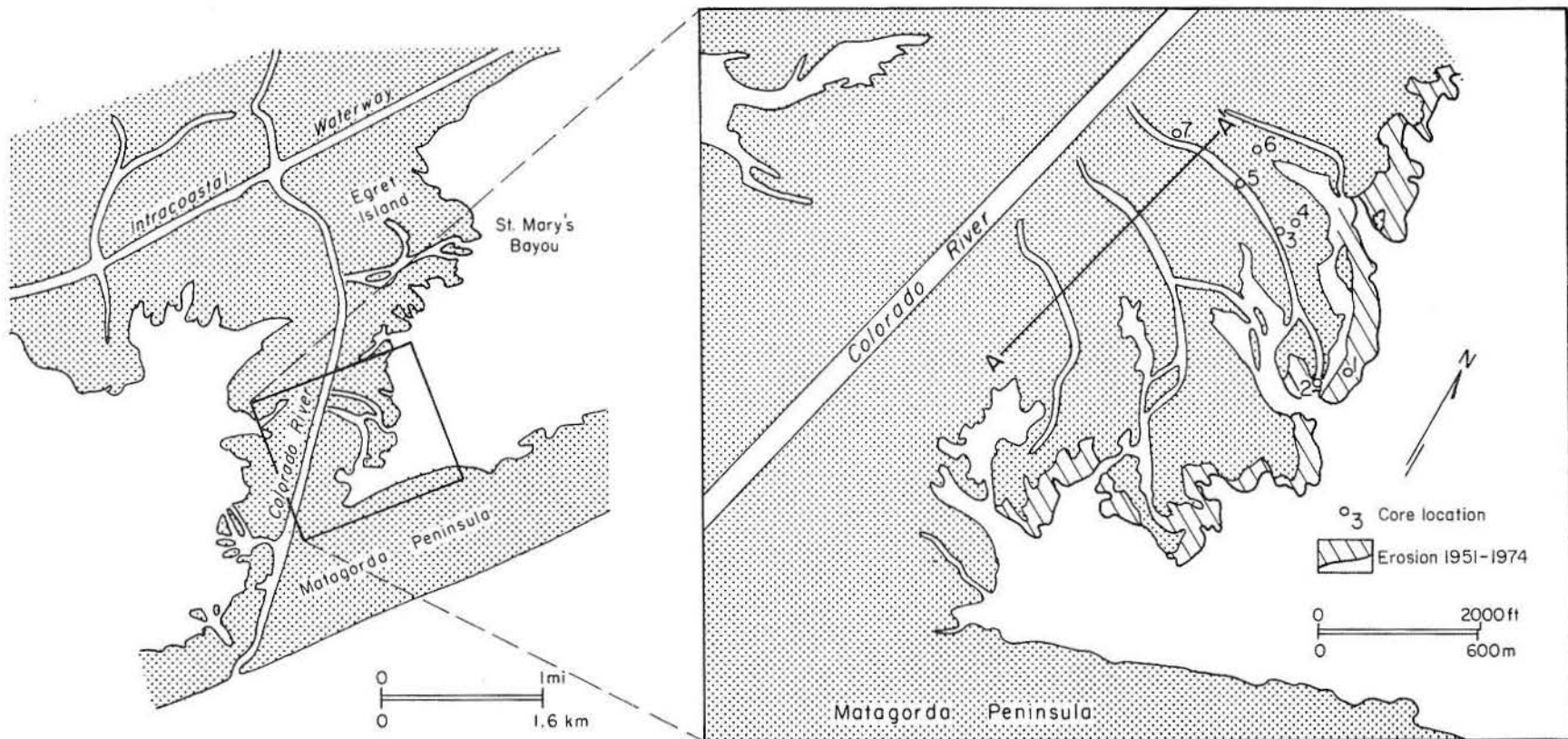


Figure 45. Core locations and bay-margin changes for southeastern lobe of the Colorado delta. Shoreline erosion based on shoreline position on topographic map and aerial photographs. Matagorda Quadrangle.

Marsh

Marshes between distributary channels are characterized by gray-brown -yellow-brown - red-brown mottled muddy very fine sand and fine sandy mud with abundant roots and iron-stain patches throughout (fig. 46). As described by Kanes (1970), coarser textures are found in higher marsh areas, whereas finer textures are representative of lower interdistributary marshes that are frequently submerged. Faint-color laminations as well as sand-sized shell fragments are commonly preserved in lower marsh sediments. Kanes (1970) reported that shell fragments were absent in high-marsh sediments.

Abandoned distributary

Channel fill (fig. 46) is about 8 to 9 ft (2.4 to 2.7 m) thick and composed predominantly of homogeneous mud. Muds are burrow mottled, light brown - dark gray - reddish brown with sand-filled burrows about 1/2 inch (1 cm) in diameter. Plant debris and shell fragments are rare but occur throughout the channel fill.

Kanes (1970) reported that cores from Egret Island showed distributary channels in sharp contact with underlying deposits and floored by sand containing abundant clay clasts. A similar sequence was described by Manka and Steinmetz (1971) for the southeastern lobe (fig. 47); however, cores from this area (fig. 46) have gradational lower contacts and lack significant amounts of sand.

Shell berms

Shell berms, which are areally restricted to the east shore of the Colorado delta, represent delta destruction and deposition of reworked bay and deltaic deposits. The berms are composed of whole shell and shell fragments (mostly *Crassostrea virginica*) from sand to pebble size and generally overlie marsh or interdistributary-bay sediments.

Distributary-mouth bar

Parallel laminated and ripple cross-laminated fine to very fine sands interbedded with faintly laminated sandy mud (fig. 46) are typical distributary-mouth deposits. Shell fragments and plant debris represent only a minor portion of the sediment, but they are commonly associated with the sand fraction. As in the Guadalupe and other deltas, sands closely parallel the distributary pattern (fig. 44).

Prodelta

Delta-front sands are underlain by and in gradational contact with color laminated muddy very fine sand and sandy mud. Sand-filled burrows 1/4 to 1/2 inch (0.5 to 1 cm) in diameter, plant debris, and shell fragments are common; shell content tends to increase and plant debris tends to decrease downward in each progradational sequence.

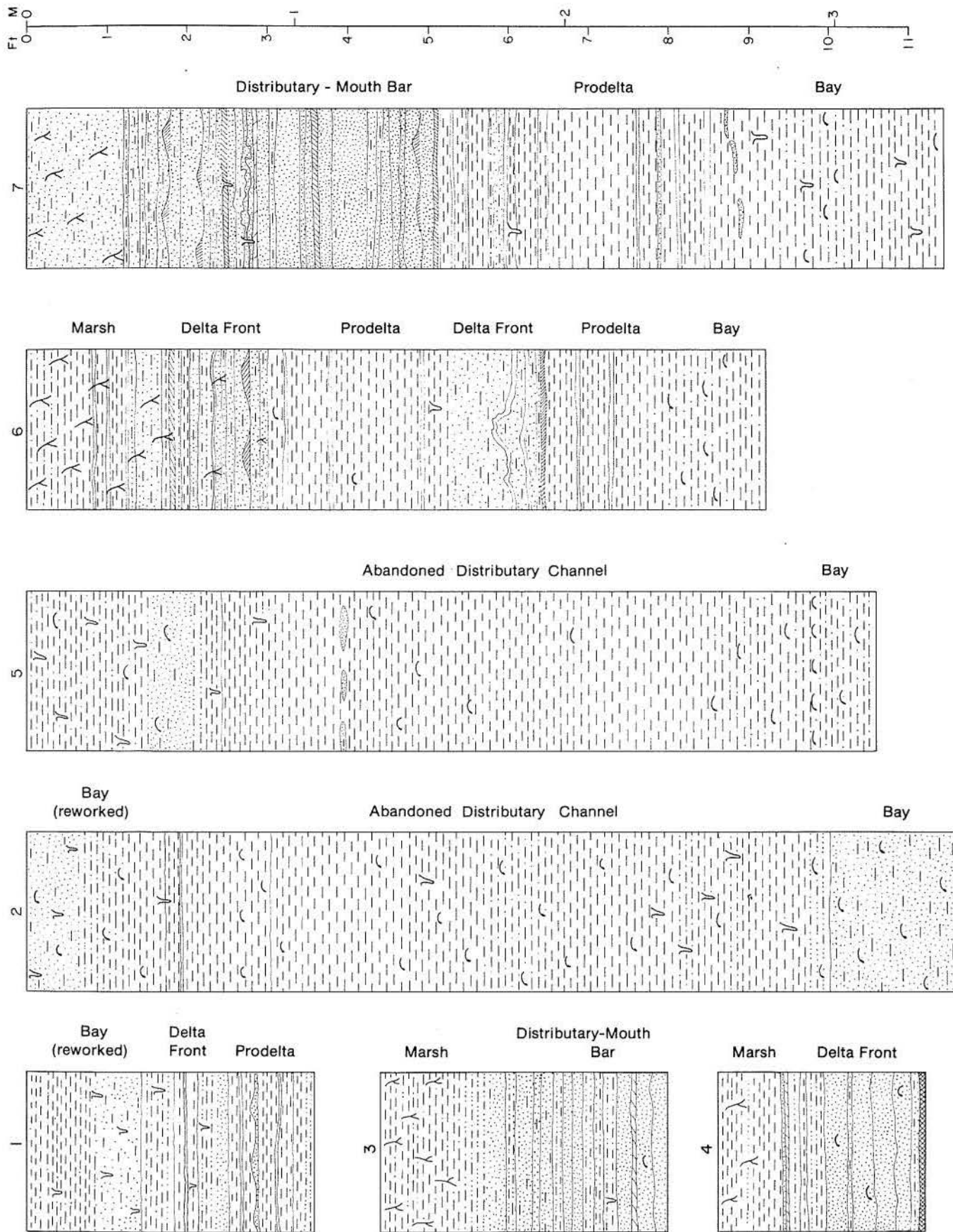


Figure 46. Cores from southeastern lobe of the Colorado delta. Locations shown on figure 45.

Bay

Bay deposits are greenish-medium-gray muddy shelly very fine sand and sandy mud. Sediments are burrow mottled and commonly contain abundant high-spined gastropods and pelecypod fragments. Uppermost bay deposits are gradational with overlying burrowed and laminated prodelta muds.

Guadalupe Delta

History of Development

The history of progradation of the Guadalupe delta (figs. 1 and 48) within the entrenched valley and into San Antonio Bay can be documented by examining older lobes and sediment bypass areas (Green Lake, Mission Lake) near the confluence of the Guadalupe and San Antonio Rivers. Youngest lobes, which are about 2,000 years old (Shepard and Moore, 1960), were further subdivided by Donaldson and others (1970) on the basis of surface and subsurface data. Initial progradation down the valley axis was followed by delta building in a counterclockwise pattern attendant with river avulsion. Active progradation is now limited to Traylor Cut (fig. 48) even though 1 million tons of sediment (Mirabal, 1974) are transported annually through the delta. In fact, comparison of recent aerial photographs with topographic maps surveyed in 1859 shows relatively minor changes in delta size and morphology during historical time. Most noticeable changes are shoreline erosion shown by map comparisons, wave-cut banks, and serrated outlines of the delta margin. Vertical stacking of thin progradational sequences is preserved in the Traylor Cut lobe (fig. 49).

Delta Facies

Lithofacies of the Guadalupe delta are either dominantly mud or sand or a mixture of sand, mud, and shell. Sand facies include active distributary channel, distributary-mouth bar, and beach-ridge environments, whereas mud facies include delta-plain and prodelta environments. Mixtures of sand, mud, and shell are typical of bay deposits. Detailed descriptions of these environments were presented by Donaldson and others (1970).

Distributary channels

Channel fill in abandoned distributaries of the Guadalupe delta consists of fine sand and silty sand that grades upward into clay and silty clay (fig. 49), denoting the change from active to abandoned conditions (Donaldson and others, 1970). The sands and silty sands exhibit medium-scale troughs and ripple cross-laminations; logs and plant fragments are abundant, but fauna is rare. An erosional contact separates these sediments from underlying deposits.

Distributary channels are limited in width to several hundred feet, suggesting lateral stability both spatially and temporally. Maximum cored thickness of distributary channel fill was 20 ft (6 m); however, most channel-fill deposits are between 10 and 15 ft (3 and 4.5 m) thick.

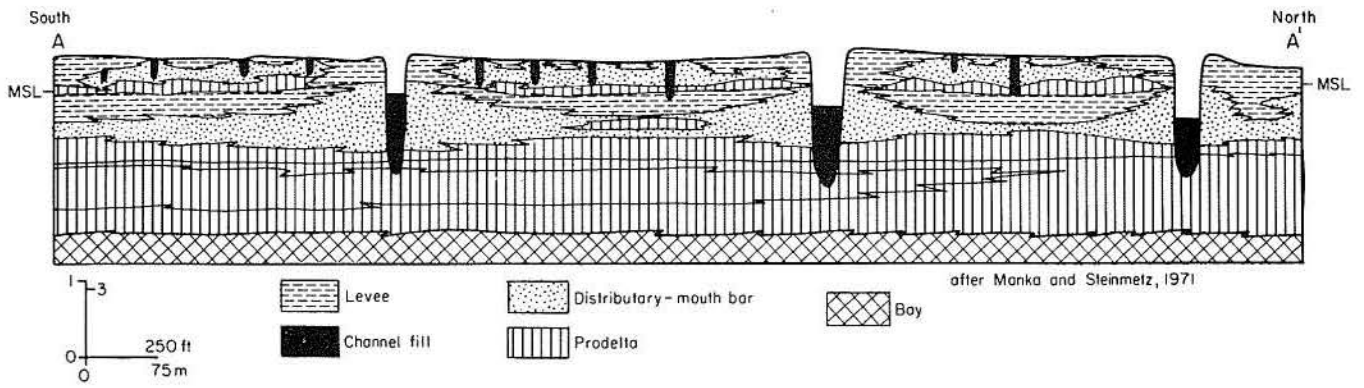


Figure 47. Facies diagram for southern lobe of the Colorado delta (after Manka and Steinmetz, 1971). Line of section shown on figure 45.

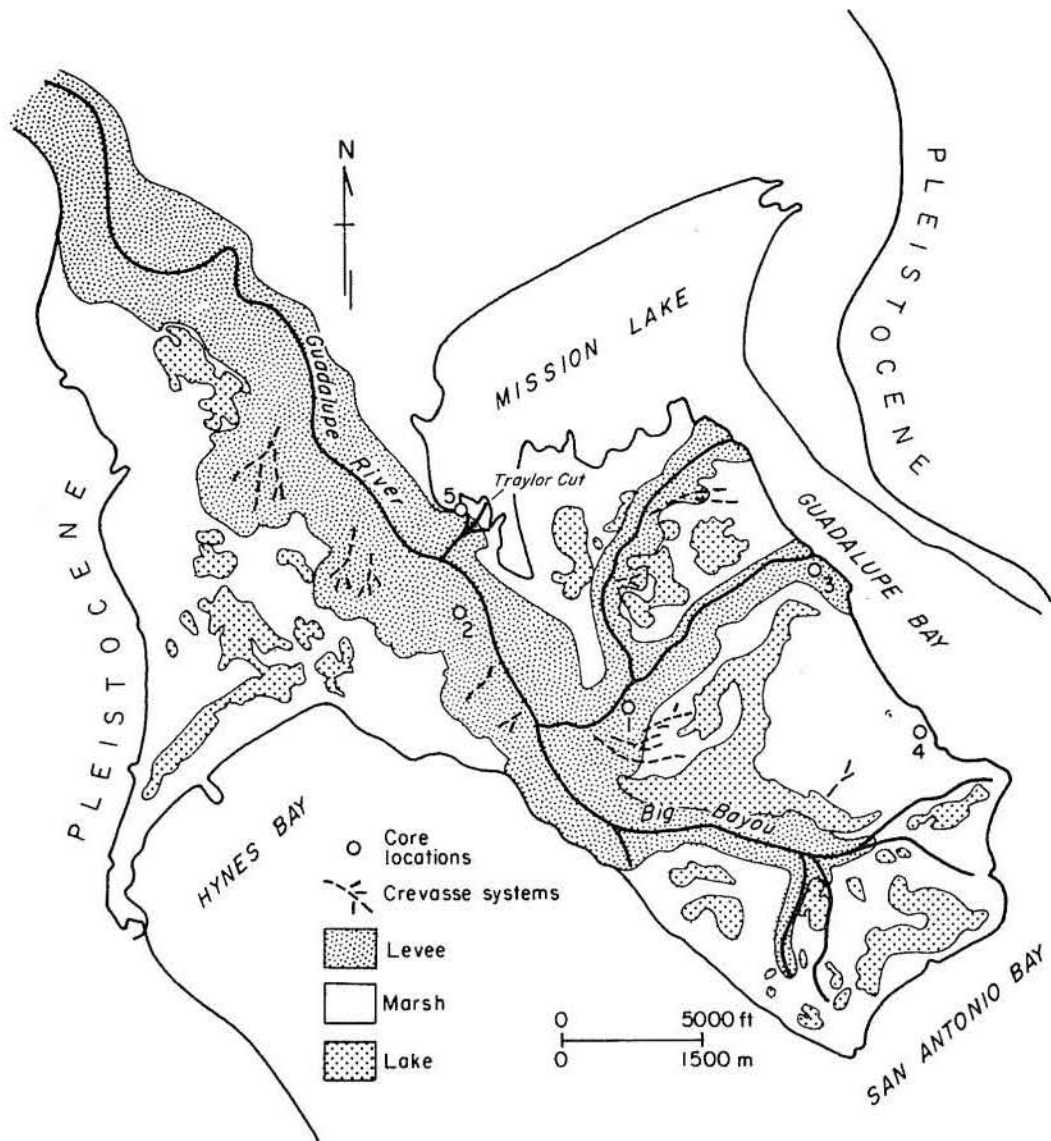


Figure 48. Location of Guadalupe delta cores. Delta-plain environments from Donaldson and others (1970). Austwell Quadrangle.

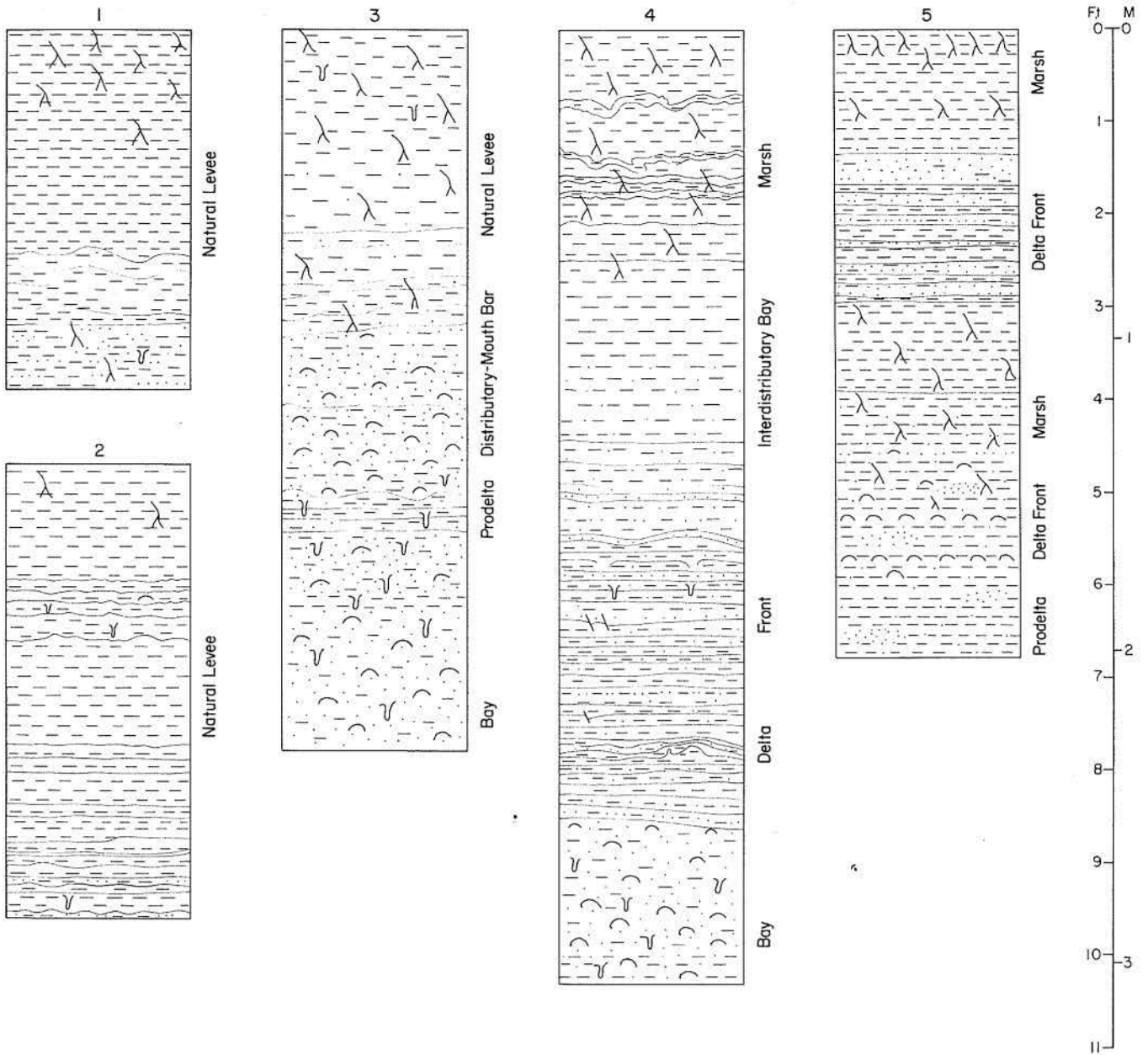


Figure 49. Cores from Guadalupe delta and Traylor Cut. Locations shown on figure 48.

Distributary-mouth bar

Distributary-mouth bar deposits are light-brown to gray fine sand, silty sand, and sandy silt, interbedded with thick beds and laminae of silty clay (fig. 49). Rounded mud clasts and shells may or may not be present depending on the rate of sedimentation. Sedimentary structures are primarily ripple cross-laminations that grade into starved ripples and burrow-mottled structures from the bar crest toward the distal limits of the bar (Donaldson and others, 1970).

Distributary-mouth bars extend laterally from 0.75 to 1 mi (1.2 to 1.8 km), and thicknesses range from 3 to 6 ft (1 to 2 m) and average about 4 ft (1.2 m); however, local sand accumulations up to 8 ft (2.4 m) thick in alternate positions along the Guadalupe River suggest frequent abandonment of distributaries contemporaneously with delta growth. Distribution of distributary and delta-front sands is proximal and parallel to the channel pattern (fig. 50). These elongate sand bodies are similar to bar-finger sands described by Fisk (1961).

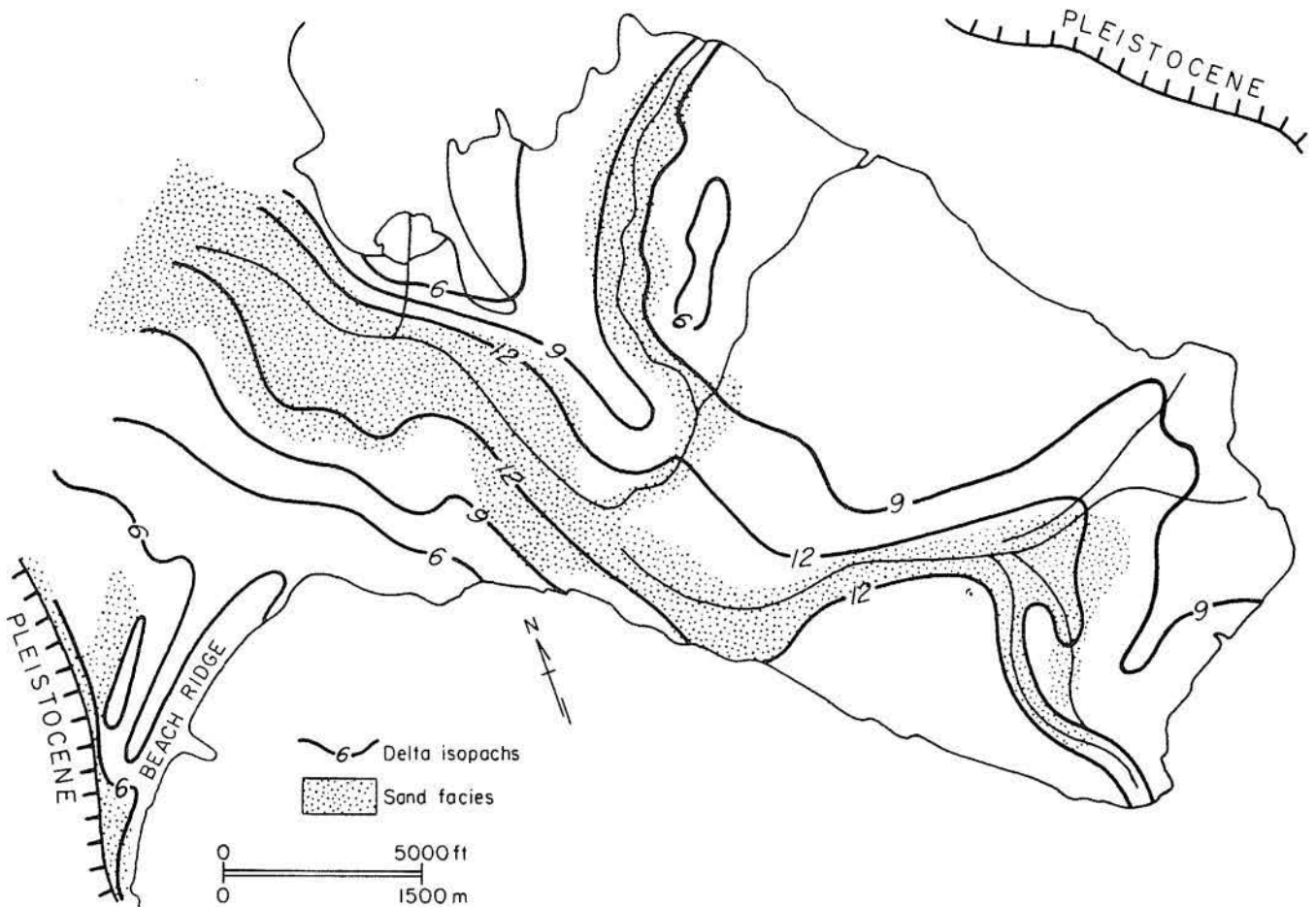


Figure 50. Delta thickness and distribution of sand facies (after Donaldson and others, 1970).

Beach ridge

The strandplain (fig. 50) incorporates reworked sediment locally derived from the bay and nearby Pleistocene escarpment. The abandoned beach ridge, the most prominent feature on the plain, is dominantly sand but contains gravel of caliche nodules, and shell fragments. Grain size increases upward in the vertical sequence, and the coarsest material is concentrated at the surface as a storm-lag deposit. The caliche nodules and much of the sand are reworked from Pleistocene sediments. The beach ridge ranges in thickness from 2 to 8.5 ft (0.6 to 2.6 m) and extends laterally about 1 mi (1.6 km). Primary sedimentary structures are not commonly preserved within beach-ridge deposits because of extensive bioturbation.

Delta plain

Delta-plain deposits, which represent the great volume of sediment in shallow-water deltas, decrease in thickness outward from the distributary channel. Levee, marsh, and lake deposits directly overlie but have gradational contacts with delta-front sands and silts or interdistributary-bay mud or prodelta mud (fig. 49).

Natural levee and crevasse splay sediments consist of root-mottled, olive-gray - medium-gray - yellow-gray mud; alternating silt and clay laminae accentuate the stratification. Small calcium carbonate nodules (caliche) are common in the vadose zone. Other chemical alterations include the fixation of iron shown by limonitic concentrations along plant rootlets. Marsh sediments are also root-mottled brown to medium-gray mud. The abundance of root traces and organic detritus either in thin beds or distributed throughout the fine-grained sediments distinguishes the marsh from other environments in which mud is deposited.

Interdistributary bay

Medium-gray to olive-gray clay and mud are characteristic of interdistributary-bay sediments; laminations are commonly destroyed by extensive bioturbation. These sediments are distinguished from overlying mud (marsh) by their burrow-mottled texture and by lack of root traces. Interdistributary-bay sediments have a greater abundance of ostracod carapaces and fewer mollusks than do bay deposits (Donaldson and others, 1970). Fauna, in general, is slightly less diverse but more abundant than fauna found in either delta-front or prodelta deposits.

Prodelta

Prodelta deposits are characteristically alternating beds of dark- and light-gray to olive-gray laminated mud that commonly contain transported wood fragments and other plant debris. Shells in the prodelta facies, predominantly mollusks, are less common than in underlying bay facies. Stratification types include faint laminations, rare starved ripples, inverted graded beds, and graded beds represented by thin beds of silt alternating with thick silty clay beds.

Variation in thickness of prodelta sediments is attributed more to rates of sedimentation or progradation than to compaction. Prodelta sediments are consistently thinner where delta-front facies are burrow mottled. Slow progradation permits organisms to churn originally laminated prodelta clays, converting them into burrow-mottled bay sediments.

Bay

Bay sediments consist of extensively bioturbated light-gray to olive-gray sand, silt, and clay and abundant whole shell and shell fragments (fig. 49) that represent 5 to 15 percent of the sediment. Faunal assemblages indicate low to intermediate salinities characteristic of river-influenced deposits (Parker, 1959). Higher salinity assemblages are found seaward from the delta. Burrows are vertical and range from 1/8 to 1/2 inch (3 to 10 mm) in diameter. A few burrows are open, but most are filled with sand. The greater abundance of shells, the burrowing structures, the mixture of sand, silt, and clay, and the lighter color distinguish bay sediments from overlying prodelta, delta-front, and interdistributary-bay deposits.

Gum Hollow Fan Delta

Gum Hollow fan delta (fig. 1) lies at the base of a 35- to 40-ft (10.5 to 12 m) erosional escarpment along the north shore of Nueces Bay. The delta is a young feature dating from the construction of an artificial drainage network, about 17 mi² (27 km²) in area, that comprises the fluvial feeder system.

Conditions requisite for formation of a fan delta, which is an alluvial fan that progrades into a standing body of water (Holmes, 1965), are that a highland and a lowland be juxtaposed; these conditions are met in the Nueces Bay area by the Pleistocene erosional escarpment (the highland) and the adjacent shallow Nueces Bay (the lowland).

History of Development

Prior to 1939, there existed at the foot of the Pleistocene erosional escarpment along the north shore of Nueces Bay a small (less than 5 acres) marsh-covered salient feature that had been constructed by terrigenous sand and mud transported to the bay margin through a small headwardly eroding stream known as Gum Hollow. After the construction of the drainage system for the farmlands to the north of Nueces Bay, Gum Hollow fan delta began to grow rapidly (McGowen, 1970). Accelerated growth resulted from increased drainage network for Gum Hollow, which made available considerable sediment from the surrounding Pleistocene Nueces fluvial-deltaic sediments (Brown and others, 1976). Between 1939 and 1962 two fan-delta lobes were constructed. In 1962, the mouth of Gum Hollow was artificially diverted a few hundred yards to the east, and a third delta lobe was constructed. Since that time the two western lobes have undergone erosion largely through waves approaching from the southeast. The eastern (active lobe) now extends approximately 1,500 ft (450 m) into Nueces Bay.

Gum Hollow fan delta is lens shaped in cross section (both across the fan and from apex to toe). Its maximum thickness is about 8 ft (2.4 m); it is convex downward, and the fan-delta surface is slightly convex upward from east to west and slightly concave upward from apex to toe. Slopes of the fan surface, from apex to toe (in 1966-1968) were in the range of 0.003 to 0.004.

Depositional Processes, Surface Features, and Textural Trends

Many factors interacted to produce Gum Hollow fan delta. Of primary importance are (1) the relatively small drainage system; (2) the relatively steep gradient of the fluvial system (up to 8 ft per mi in the natural system); (3) the availability of a limited size range of sediment for construction of the delta (coarsest terrigenous clastics are very fine grained to fine-grained sand); (4) a shallow receiving basin that is virtually tideless (with respect to astronomical tides), but is affected by wind waves and wind setup; and (5) hurricanes.

Gum Hollow fan delta is the product of (1) progradation and slight vertical accretion resulting from local thunderstorms in the spring and summer when water level in Nueces Bay is normal (fig. 51A), (2) limited progradation during northers when bay level is below its normal position (fig. 51B), and (3) maximum vertical accretion during hurricanes when the level of Nueces Bay may be more than 5 ft (1.5 m) above its normal position (fig. 51C, Scott and others, 1969; McGowen, 1970; McGowen and Scott, 1975).

In the spring and summer, when thunderstorms drop more than 2 inches (5 cm) of rain per storm on the Gum Hollow drainage system, sediment is transported and deposited by braided streams that traverse the delta. These streams construct longitudinal bars on the fan plain (fig. 52). These bars have nuclei of oystershell (derived from shell middens) or plant debris. Braid-channels adjacent to longitudinal bars generally are less than 1 ft (30 cm) deep and are several tens of feet wide. Downfan the longitudinal bars decrease in scale; sheet flow occurs where longitudinal bars are absent and the fan plain grades into a virtually featureless distal fan. Fan plain and distal fan are products of unconfined flow during floods. As flood water subsides, one braid-channel becomes dominant (all remaining flow moves through this channel) and is scoured a few inches to about 3 ft below the fan surface; this main channel is also braided.

During the winter months numerous polar fronts are accompanied by strong winds (and sometimes by rainfall) that lower the water level along the north shore of Nueces Bay. At this time, the main channel is entrenched and sediment is transported well beyond the channel mouth position during normal bay level; this sediment progrades the fan delta in a rather narrow zone in the immediate vicinity of the new channel-mouth position (fig. 51A). When north winds subside, water level rises again to its normal position, and waves approaching from the southeast rework the sand that was deposited when water level was low.

Hurricanes raise the water level in Nueces Bay several feet above normal and commonly drop as much as 2 ft (60 cm) of rainfall on the Pleistocene uplands. At this time the fan delta aggrades because of high sediment input and a higher base level (fig. 51C). Aftermath rains associated with Hurricane Beulah, September 1967 (Scott and others, 1969), caused extreme flooding and runoff in the Gum Hollow drainage basin. At this time approximately 40,000 yd³ of sand accumulated on Gum Hollow fan delta. The surface of the fan delta was drastically altered through massive sediment accumulation; the depositional feature is, in effect, a small Gilbert delta perched atop the braided-stream deposits of the older fan plain.

Textural trends

Textural trends are not as pronounced on Gum Hollow fan delta as are trends on the coarse-grained alluvial fans and sandurs (Bull, 1972; Boothroyd, 1972) because of

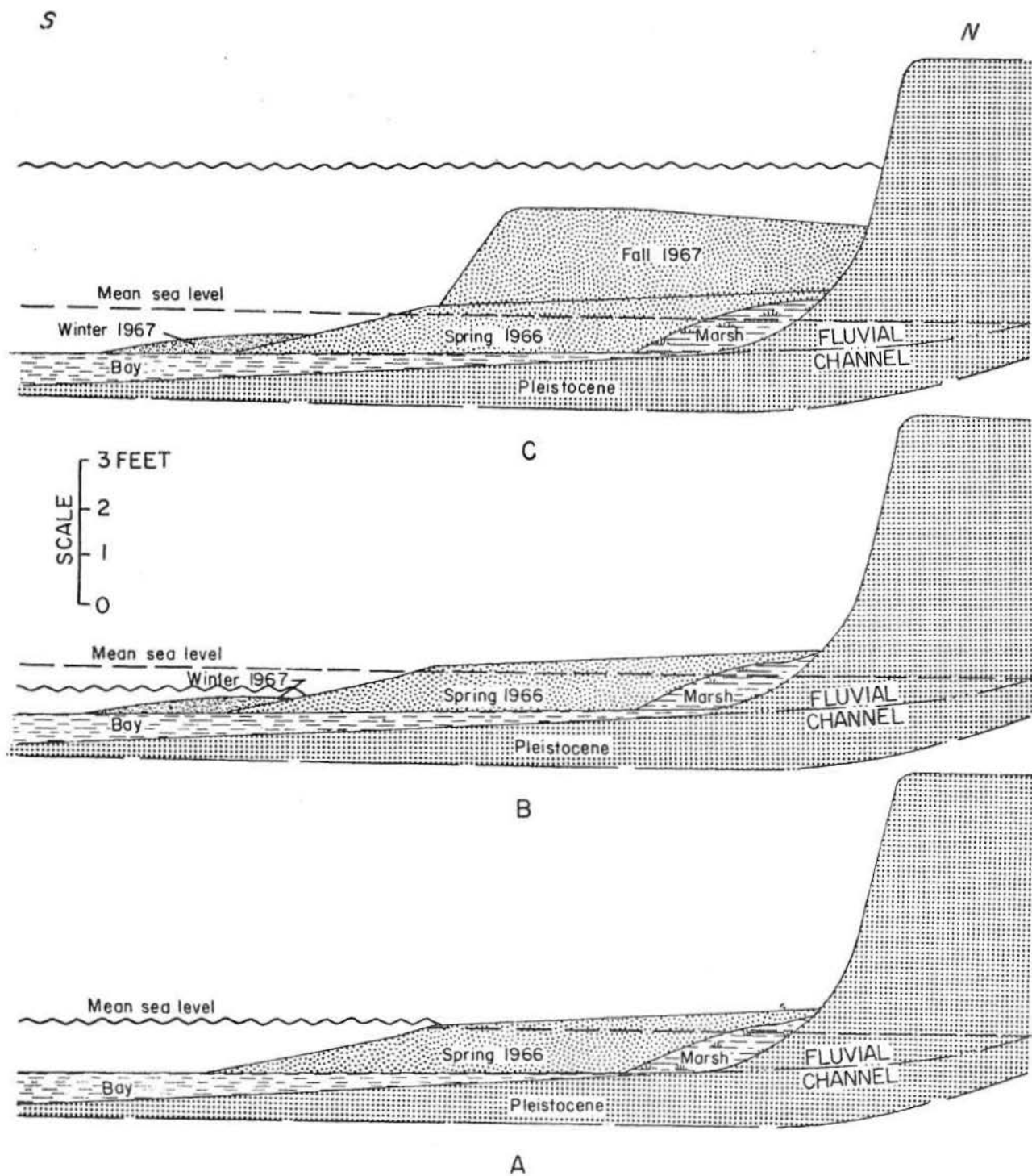


Figure 51. Effect of sea level on deposition of Gum Hollow fan delta. Progradation under normal (A) and lowered (B) sea-level conditions. Aggradation (C) when sea level is above normal. (After McGowen, 1970). Gregory Quadrangle.

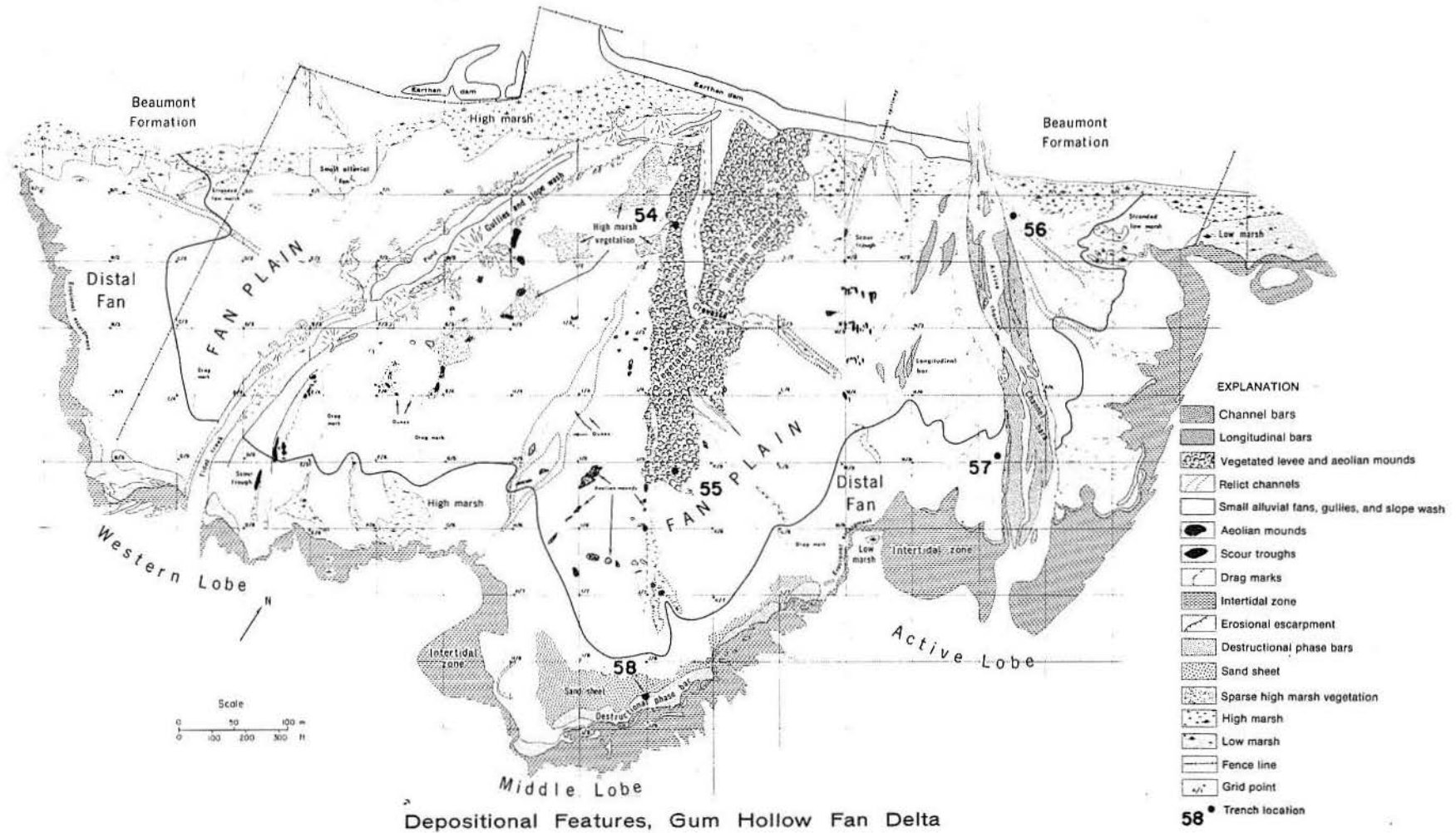


Figure 52. Depositional features of Gum Hollow fan delta (after McGowen, 1970). Gregory Quadrangle.

the limited range of sizes available to the Gum Hollow fluvial system. With the exception of oyster shell gravel, which is distributed no more than 600 ft (180 m) bayward from the apex of the fan delta, most of the subaerial fan is made up of very fine grained to fine-grained terrigenous sand with varying amounts of granule- and sand-sized mud clasts; mud clasts are derived from the Pleistocene uplands. Size of terrigenous sand remains the same from apex to distal parts of fan delta; however, size and amount of mud clasts exhibit some downfan changes. Largest (granule-sized) clasts accumulate near the apex; mud-clast size decreases downfan, but volume of mud clasts increases.

Characteristics of Depositional Facies

Facies of Gum Hollow fan delta fall into three categories. These facies are genetically related and were developed under (1) a braided-stream regime whose activity is triggered by spring and summer thunderstorms, (2) the penetration of polar fronts into the Coastal Zone, and (3) hurricane activity. Depositional environments recognized as part of the fan delta system are main braided streams, fan plain, distal fan with destructional phase bars, and the delta front. Main braided-stream deposits are most conveniently studied in areas where these channels have been abandoned and filled (fig. 52). Near the right channel bank (figs. 53 and 54), evidence of repeated flooding and inactivity are recorded in mud drapes. When the channel was actively

GRAVEL SIZE TERRIGENOUS MATERIAL

| | |
|---|--|
| Mud clasts | |
| Caliche and calcareous mudstone fragments | |

STRATIFICATION TYPES IN SAND DEPOSITS

| | |
|----------------------------------|-------|
| Quartz sand | |
| Sand - sized clay pellets | +++++ |
| Heavy mineral laminae | ----- |
| Climbing ripples laminae | |
| Small trough sets | |
| Trough-fill cross-stratification | |
| Parallel laminae | |
| Foreset cross-stratification | |
| Animal tracks | |
| Homogeneous sand | |

MUD AND ASSOCIATED FEATURES

| | |
|----------------------------------|--|
| Mud drapes | |
| Desiccation cracks | |
| Thoroughly desiccated mud | |
| Mud with wood fragments | |
| Mud with incomplete sand ripples | |

ORGANIC CONSTITUENTS

| | |
|-------------------------------|--|
| Oyster shell debris | |
| Undifferentiated shell debris | |
| <i>Uca</i> burrows | |
| Mottles | |
| Logs and tree limbs | |
| Plants in growth position | |
| Plant debris | |

Figure 53. Key to sedimentary features of Gum Hollow fan delta (after McGowen, 1970).

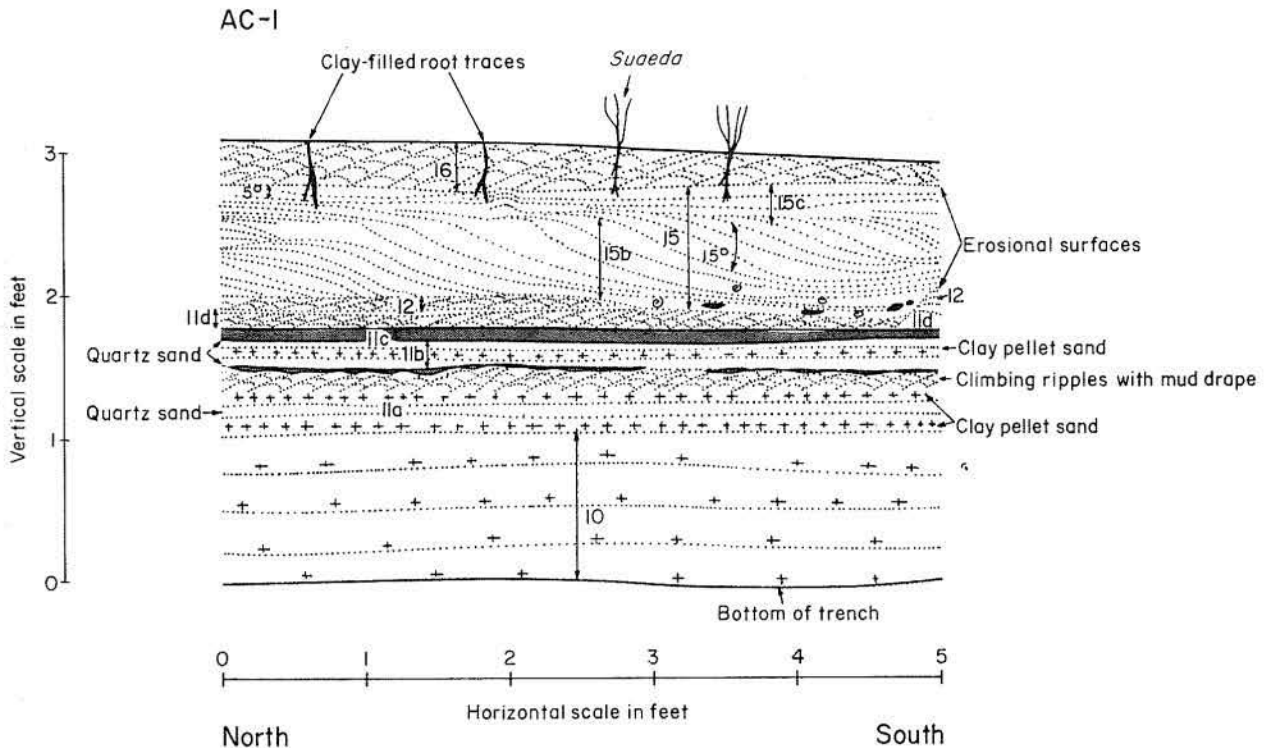
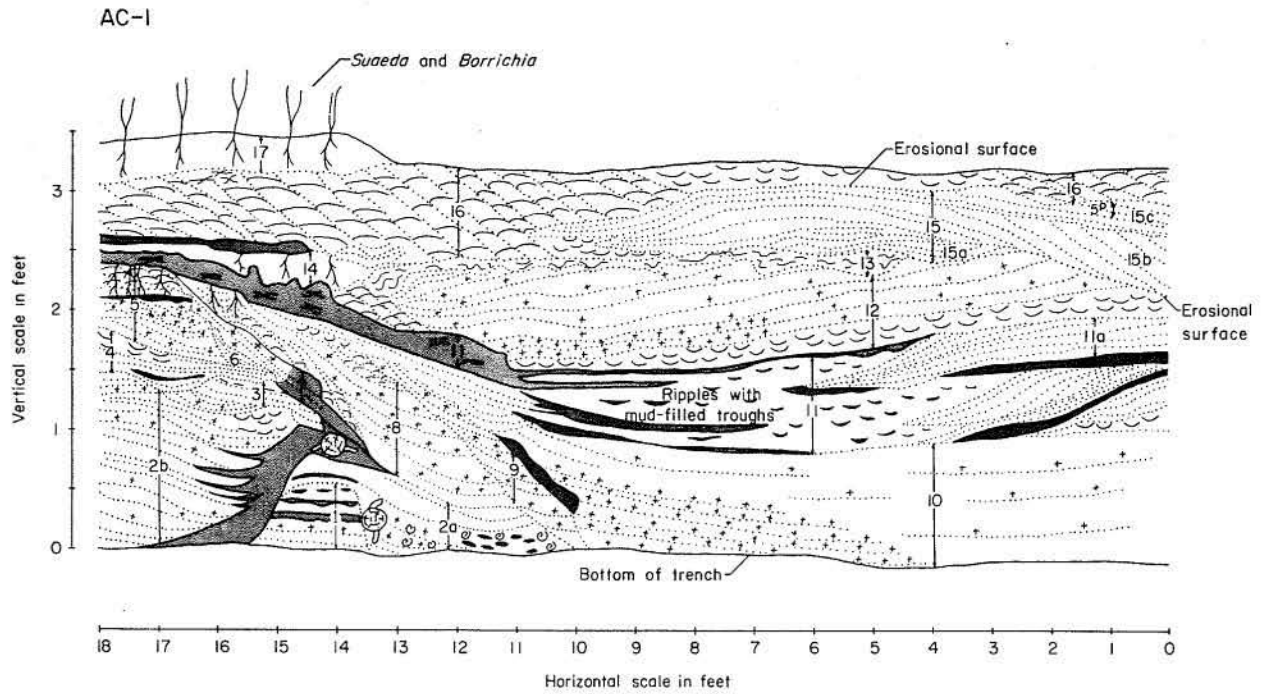


Figure 54. Sedimentary features of the filled (abandoned) main braided-stream channel of the middle deltaic lobe; east-west trench section is near right channel bank; oriented perpendicular to flow; north-south trench section (ties to east end of east-west trench) is oriented parallel to flow (see fig. 52 for location) (after McGowen, 1970).

transporting sand, the bed forms were longitudinal bars (parallel laminae and low-angle foresets); during low-flow conditions bed forms were mostly linguoid ripples (ripple cross-laminae). Ripple drift records rising water-level conditions with abundant sand-sized material falling out of suspension. Near the center of the main braided-stream environment bed forms were predominantly longitudinal bars; stratification consists of parallel laminae, parallel inclined laminae, and low-angle foreset cross-strata (fig. 55).

The fan-plain nucleus of the eastern (active) lobe consists of a gravel bed (fig. 56) about 1 ft (30 cm) thick near the apex and thins irregularly downfan where it pinches out at a distance of some 600 ft (180 m) from the apex; the nucleus is massive, whole oyster shell and caliche pebbles and cobbles. Fine sand composes the upper part of the fan plain; longitudinal bars were the dominant bed forms, transverse bars were present but not volumetrically significant. Stratification of longitudinal bars was parallel inclined laminae. Stratification of transverse bars was low-angle foreset cross-strata. Residual channels lying between longitudinal or transverse bars were floored with linguoid ripples (ripple cross-laminae) that were locally draped with mud when parts of the channels were ponded.

Distal fan lies from sea level to just a few inches above sea level, and its deposits bear the imprint of both fluvial and wind-tide processes. Sediment of the distal fan consists of quartz and mud-clast sand with mud drapes. The fluvial process is mostly sheet flow that generates linguoid ripples and low-relief bars. Stratification (fig. 57) types are ripple cross-laminae, parallel laminae, parallel inclined laminae, and ripple drift. When the distal fan is inundated by wind tides, sand ribbons, ladder-back ripples, incomplete sand ripples, and mud drapes are laid down.

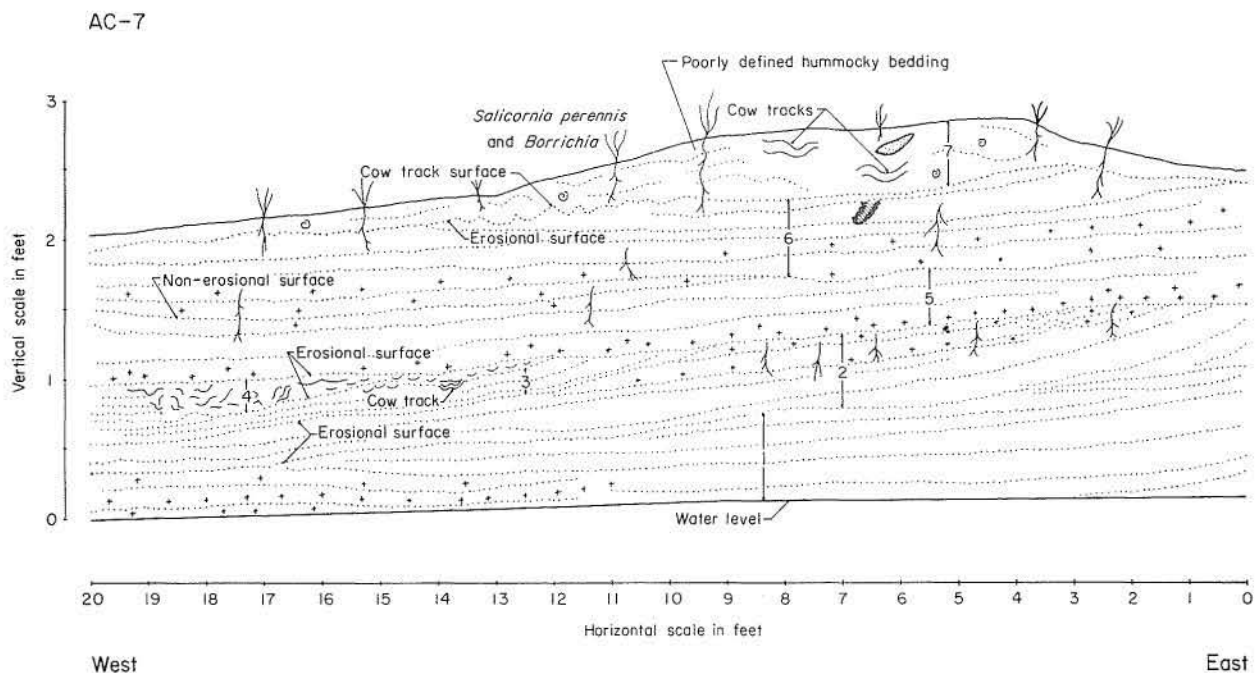


Figure 55. Sedimentary features of filled main braided-stream channel; trench is near the center of the channel and is oriented transverse to flow (see fig. 52 for location) (after McGowen, 1970).

Distal parts of fan deltas are reworked between depositional events by waves and longshore currents when segments of the fan delta become inactive. Sand is reworked from the distal fan and deposited as a berm (or destructional phase bar). Bed forms produced by the swash resulting from breaking waves are linguoid and sinuous crested ripples. Stratification (fig. 58) is ripple cross-laminae and ripple drift. A forebeach (generally less than 1 ft [30 cm] high) is produced by swash and backwash.

Gum Hollow delta is prograding into Nueces Bay whose maximum depth is about 3 ft (1 m); the bay-margin area where most of the delta-front deposition occurs is generally less than 1.5 ft (45 cm) deep. Delta-front deposits consist of alternating 1- to 2-inch (2.5- to 5-cm) ripple cross-laminated sand beds and mud drapes of comparable thickness.

Sand is laid down at the mouth of the main braided channel when northers pass through the area. Water level is lowered, and the strand line is displaced some 200 ft (60 m) southward of its normal position. As a consequence of this temporary lowering of base level, the channel floor is scoured and the sand is deposited at the new channel-mouth position as a rippled sand bar. The bar is a few inches thick and about 100 ft (30 m) wide parallel to shoreline; its dimension parallel to stream flow is about 50 ft (15 m). Stratification is ripple cross-laminae. With a return of water level to the normal position, the upper surface of the bar is planed off.

Hurricanes (such as Hurricane Beulah, 1967) raise the water level in Nueces Bay by as much as 5 ft (1.5 m) above normal and trigger heavy rainfall (as much as 24 inches [60 cm] in 24 hours). The result of heavy rainfall, coupled with higher-than-normal water level, was deposition of about 40,000 yds³ of sand upon the previously constructed fan plain (McGowen, 1970; McGowen and Scott, 1975). These deposits have an almost planar upper surface, broken here and there by large crescent scours, each of which has a debris pile at its upcurrent end. These deposits (small Gilbert deltas) terminate distally with steep avalanche faces as much as 2 ft (60 cm) high.

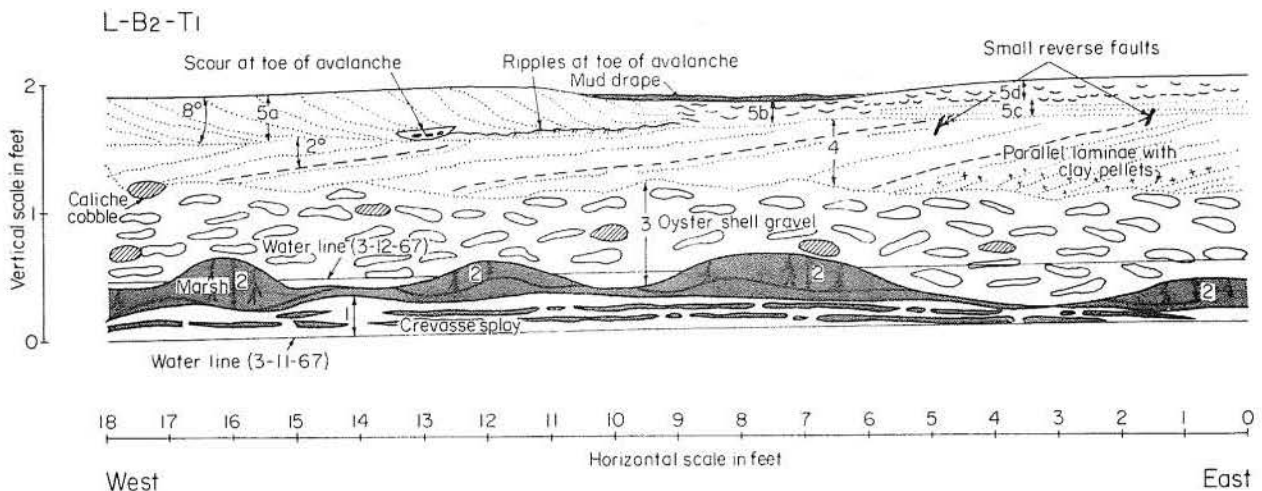


Figure 56. Sedimentary features of fan-plain deposits near apex of eastern (active delta lobe); trench is oriented approximately transverse to flow (see fig. 52 for location) (after McGowen, 1970).

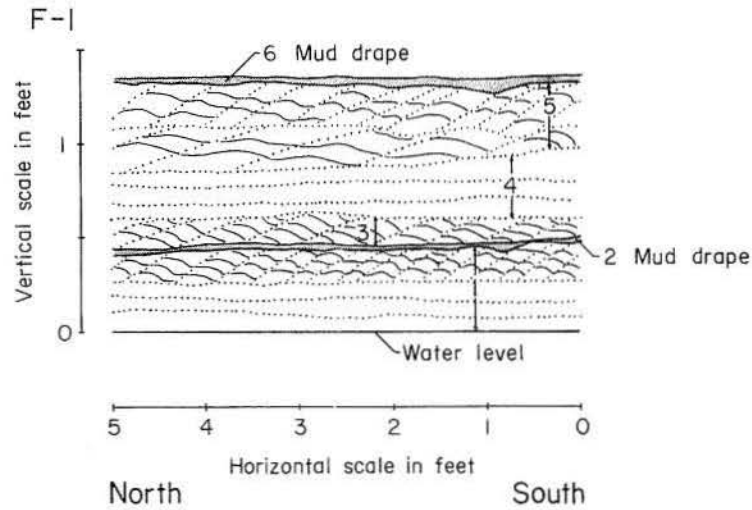
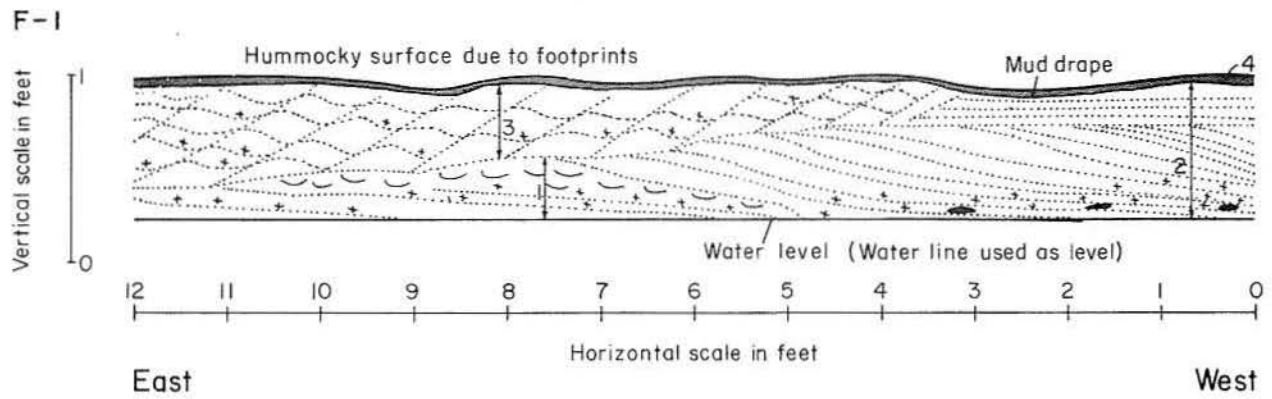


Figure 57. Sedimentary features of distal fan delta deposits near right bank of active main braided stream; east-west trench and north-south trenches are both oblique to flow direction (see fig. 52 for location) (after McGowen, 1970).

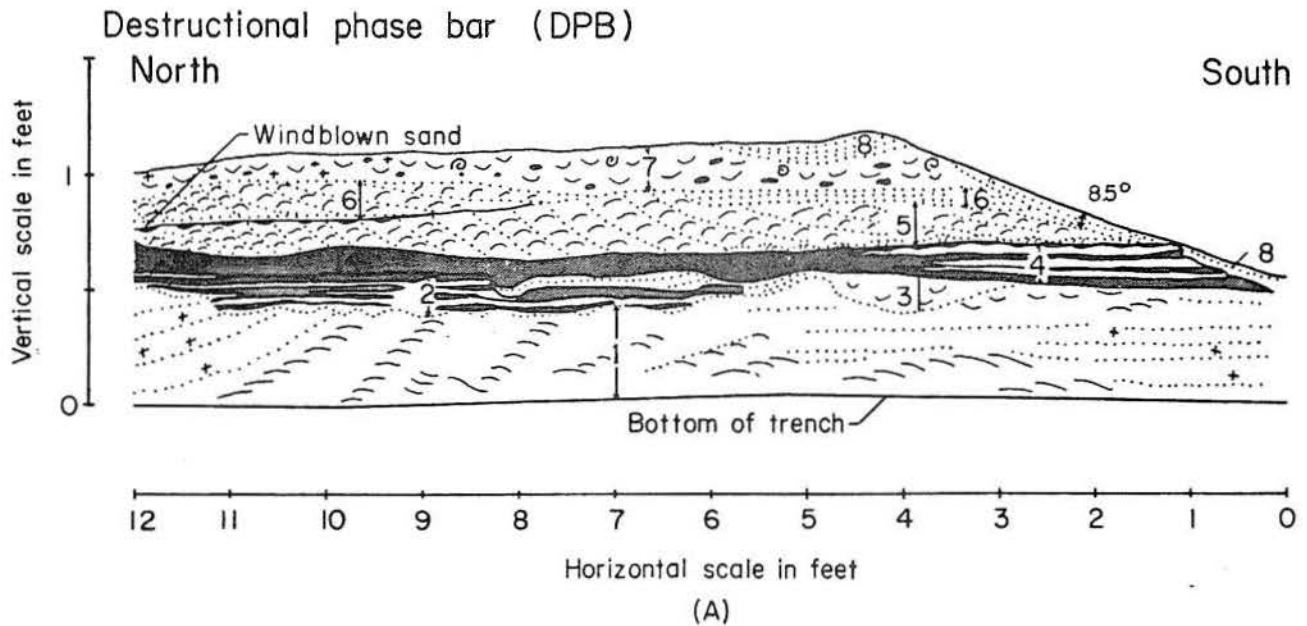


Figure 58. Sedimentary features of destructional phase bar; north-south trench is oriented perpendicular to trend of the bar (see fig. 52 for location) (after McGowen, 1970).

TEXAS BAY SYSTEMS

Introduction

Much of the Texas Coastal Zone is characterized by inland water bodies (variously termed bays, estuaries, and lagoons) that lie between barrier islands and peninsulas and the mainland (fig. 1). These water bodies do not exhibit the features of the classical estuary, which has unrestricted tidal exchange with the open ocean. Because water exchange is restricted by relatively small inlets between barrier islands and the Gulf of Mexico, and some have little or no fresh-water influx, these Texas water bodies are more properly labeled coastal lagoons.

Texas coastal lagoons exhibit two orientation patterns. Part of the system is perpendicular to the Gulf shoreline, and part is parallel to the Gulf shoreline (as shown by San Antonio and Espiritu Santo Bays, fig. 59). Many of the Texas bays occupy drowned river valleys, hence the orientation perpendicular to shoreline. Some bays and segments of bays are aligned parallel to the barrier-island trend; these bays are positioned over divides between Pleistocene river valleys, or they overlie abandoned Holocene deltas.

Texas bays generally decrease in size and depth from the upper to the lower coast. Bay size was largely predetermined by the size of the Pleistocene rivers. Depth to the Pleistocene beneath the bays decreases from upper coast (about 160 ft [50 m] beneath the southwest tip of Bolivar Peninsula) to the lower coast (about 60 ft [18 m] beneath Baffin Bay). Climatic zones during the Pleistocene were similar to present zones--a decrease in rainfall and an increase in temperature from upper to lower coast. Major tidal inlets of the Modern coast coincide with Pleistocene valley axes, or they are displaced down longshore drift from valley axes; all major inlets were initiated over the Pleistocene valleys.

Origin of Texas Bays

During the Pleistocene, the continental shelves of the world were repeatedly exposed and inundated as continental ice caps alternately increased and decreased in size. As glaciers increased in size and sea level dropped, base level was lowered and streams were incised several tens of feet below present sea level (fig. 60).

The Wisconsin glacial stage was accompanied by 390 to 450 ft (120 to 137m) of sea-level lowering (Curry, 1960; Le Blanc and Hodgson, 1959). At this time the major fluvial systems in Texas were deeply incised. With the last (Holocene) rise in sea level these river valleys were flooded. Initially, only the valleys were flooded, and the resulting "estuarine" system was oriented perpendicular to shoreline. Barrier islands and peninsulas developed later, forming the shallower water bodies that are elongate parallel to the barrier-island trend.

Since sea level reached its present approximate position, the configuration and depth of the bays have changed through (1) shoreline erosion, (2) construction of bayhead deltas, (3) transgression of barrier islands over parts of bays, (4) decrease in depth through sediment accumulation, and (5) recently an increase in depth as a result of subsidence (due to ground-water withdrawal, Brown and others, 1974; Kreitler, 1976) and a decrease in rate of sedimentation (due to damming of major streams).

Stratigraphic Sequence of Bay Infilling

The deepest parts of the bay systems were initially occupied by fluvial systems (fluvial gravel containing shells of the Cretaceous pelecypod *Exogyra arietina* were encountered by the U.S. Army Corps of Engineers in the Trinity - San Jacinto river valley beneath Bolivar Peninsula). A fluvial network has been documented beneath

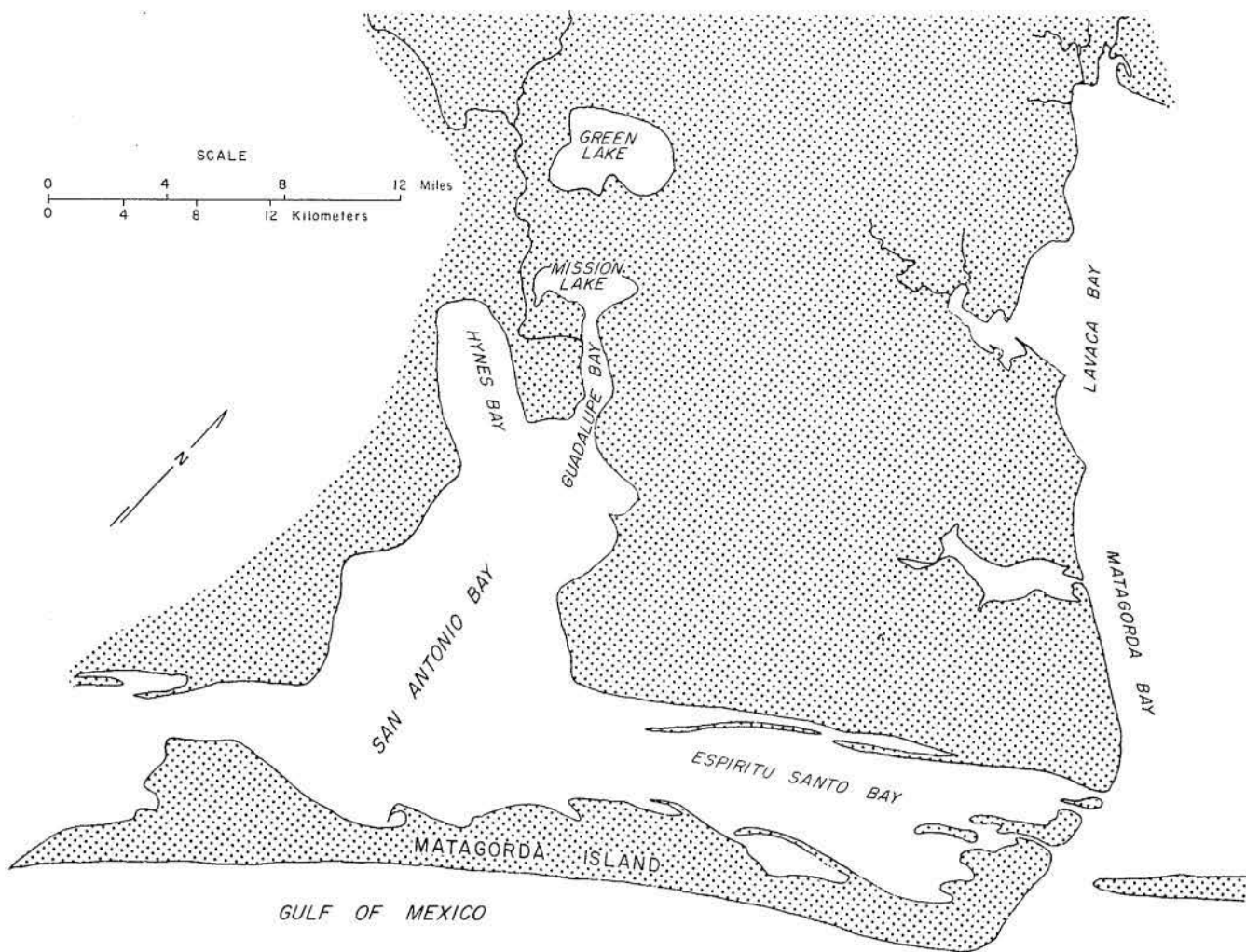
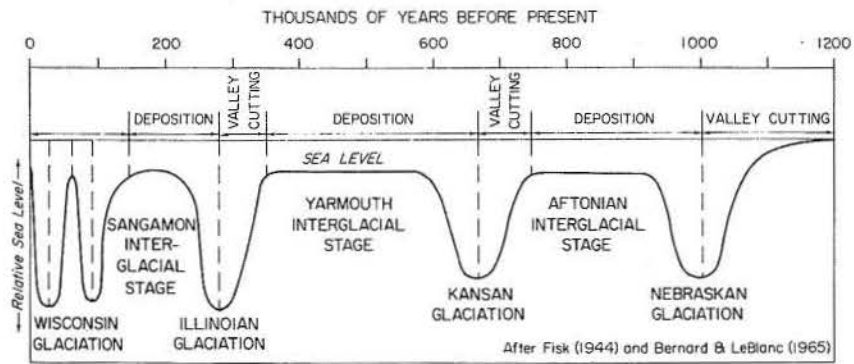
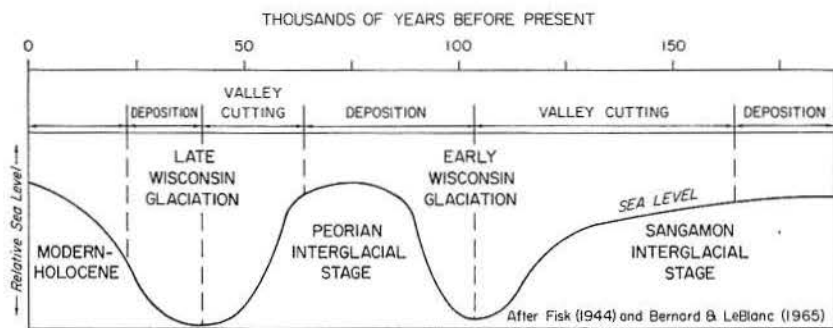


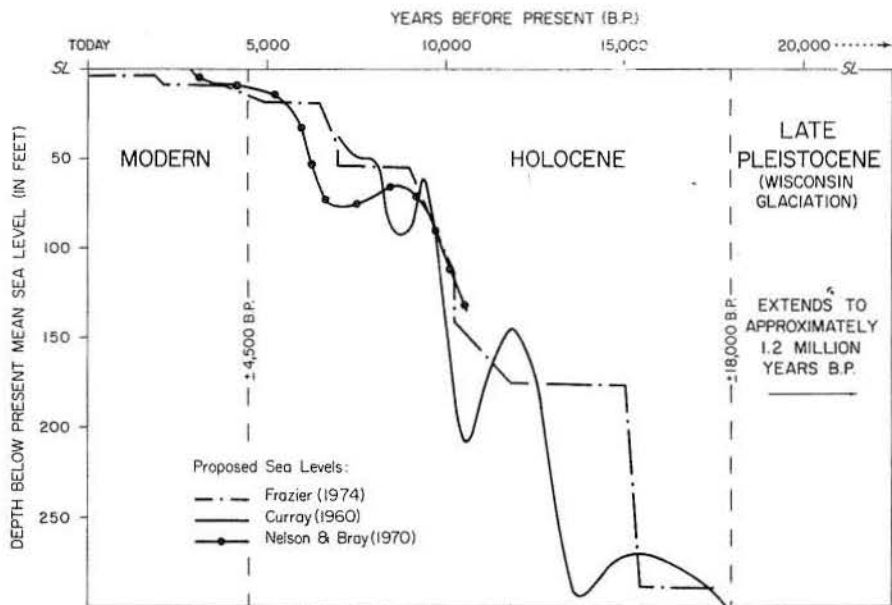
Figure 59. Orientation of bay segments: San Antonio Bay, oriented perpendicular to Gulf shoreline, is situated over a drowned river valley; Espiritu Santo Bay, oriented parallel to Gulf shoreline, is situated over a Pleistocene drainage divide.



A



B



C

Figure 60. Sea-level changes related to glacial and interglacial stages. A. Generalized Pleistocene sea-level variations and associated erosional and depositional episodes. B. Generalized sea-level changes during Late Wisconsin glaciation. C. Proposed sea-level changes during the last 20,000 years.

most of the Texas bays (Fagg, 1957; Byrne, 1975; Wilkinson and Byrne, 1977). Documentation has been achieved by drilling and coring and by acoustical methods (figs. 61 and 62).

Sedimentation was initially confined to the river valleys and later spread laterally across interfluvial divides as sea level continued to rise and barrier islands developed.

Upper and central coastal bayfill has similar geometries and similar histories. The fill of Lavaca Bay (Byrne, 1975; Wilkinson and Byrne, 1977) is an example of the geometry of bay sediment chiefly confined to the Pleistocene Lavaca River valley (figs. 63, 64, 65, and 66). During the Pleistocene the Lavaca River scoured a valley floor that is more than 100 ft (30m) below present sea level.

The age of the fill of Lavaca Bay ranges from about 10,000 years B.P. to the present. Much of this sediment accumulated as a transgressive fluvial-deltaic-estuarine sequence as sea level continued to rise. Sedimentation rates were initially high because the cross-sectional area of the valley was relatively small; sedimentation rates declined as larger volumes of sediment were required to fill an increasingly larger valley cross section. Since stillstand (some 3,000 years B.P.) the Lavaca fluvial-deltaic system has filled the lower reaches of the valley and has constructed a small delta at the head of Lavaca Bay.

The vertical succession (about 115 ft [34.5 m] thick, fig. 65) can be divided into three sequences. A lower transgressive unit consists of a lower fluvial system and an upper deltaic system (this sequence is not what one would normally expect). A middle sequence is made up of "lacustrine" and bay muds. The uppermost deposits consist of fluvial and deltaic sands and bay muds, a regressive sequence, related to the Modern Lavaca River.

Geometry of the fill of larger bays, for example, Galveston and Matagorda Bays, is characterized by a linear thick zone (the valley fill) paralleled by thin zones (areas of fluvial divides).

Processes Operating In Bays

Bays are a transition zone between continental and marine environments. At times they are dominated by their associated fluvial systems. Marine elements may become dominant during prolonged dry periods. Bays are also subjected to the effects of large waves and excessive tides for short periods of time when hurricanes cross the Texas Coastal Zone.

Bays are affected by climatic regime, tides, relative sea-level change, tropical cyclone frequency, volume of sediment delivered to the system by rivers, and rate of sediment dispersal by waves and currents. Processes operating within the bays can be divided into two categories, those that are active each day throughout the year, and those that are seasonal and of short duration and high intensity. The normal daily processes are astronomical tides, winds, waves, longshore currents, river processes, and subsidence.

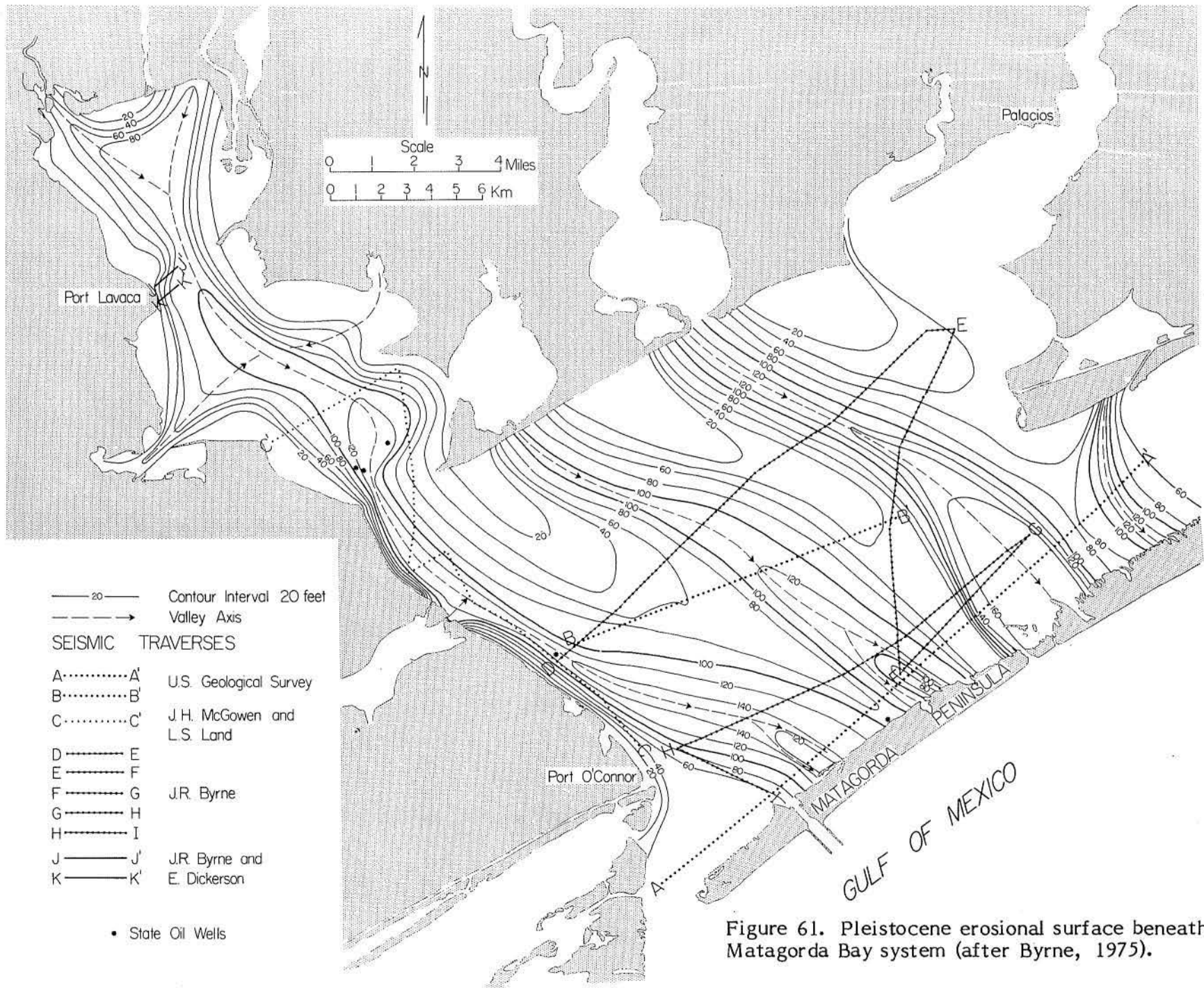


Figure 61. Pleistocene erosional surface beneath Matagorda Bay system (after Byrne, 1975).

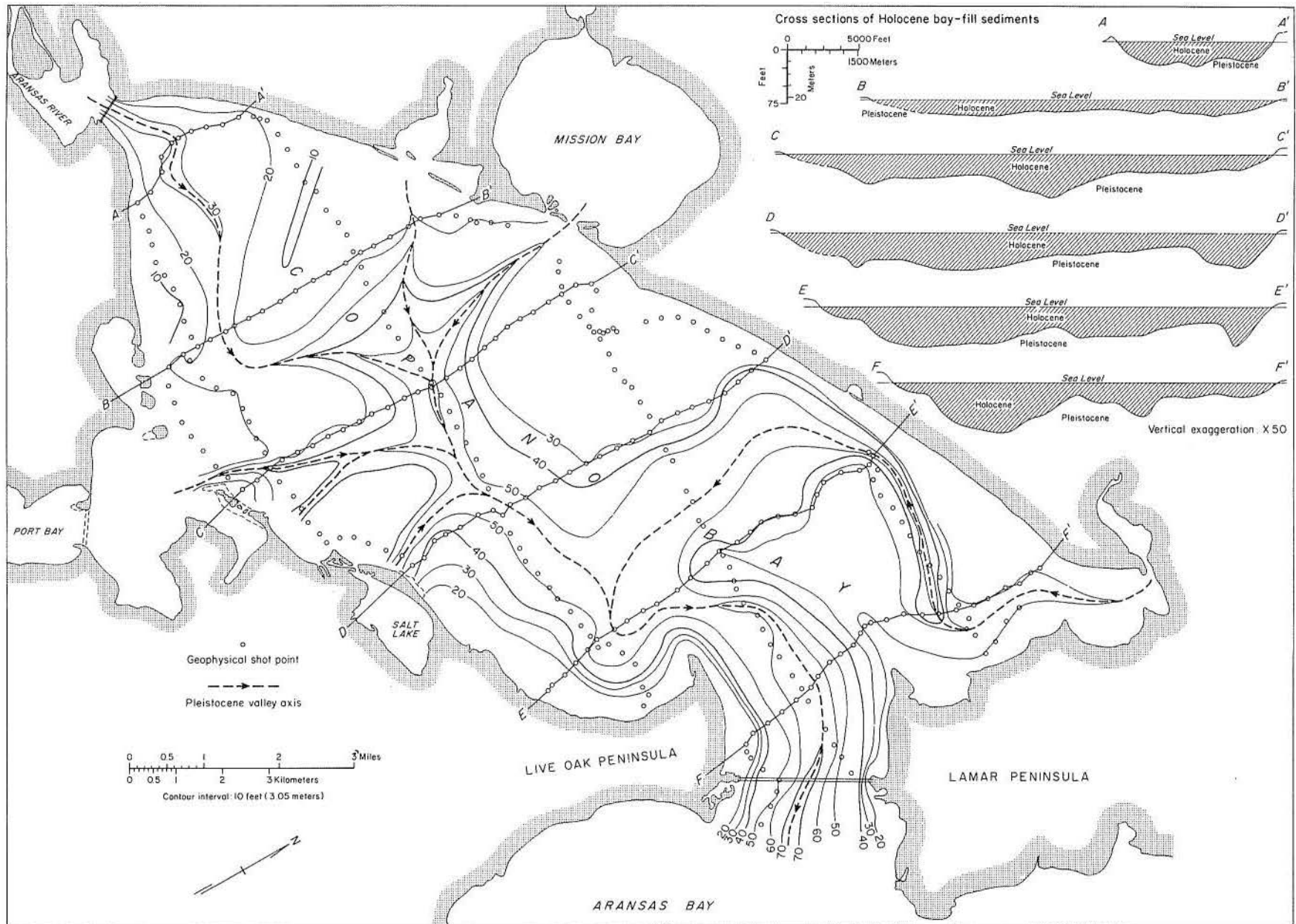


Figure 62. Pleistocene erosional surface beneath Copano Bay (mapping by Stephen S. Wright).

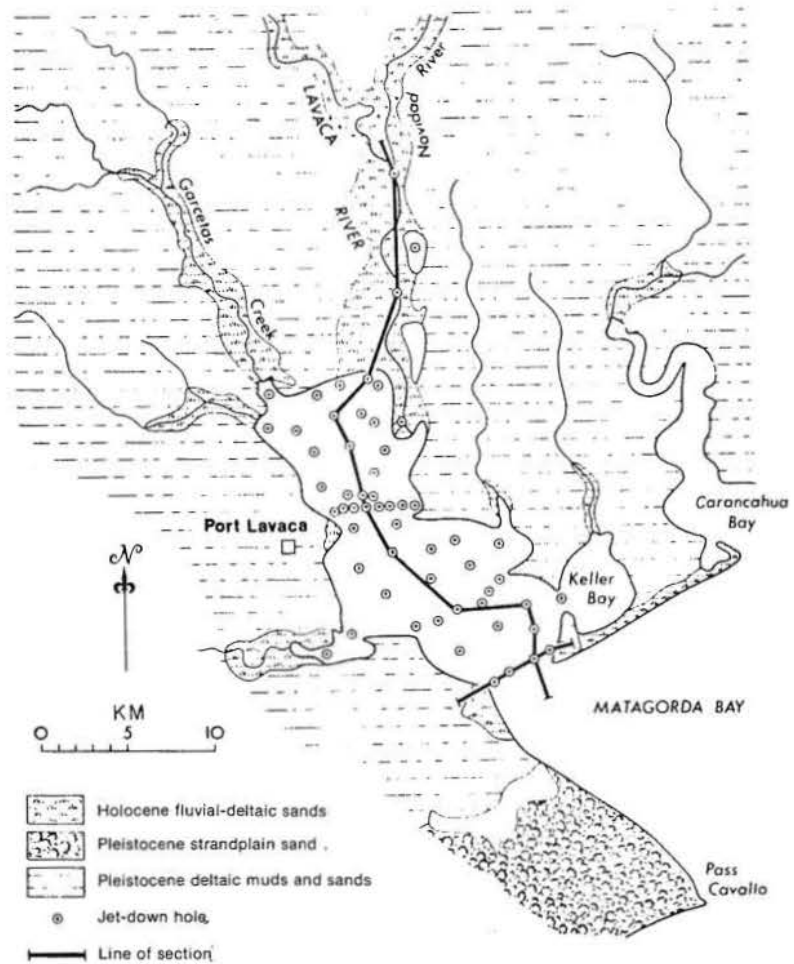


Figure 63. Simplified geologic map of Lavaca Bay area showing wash-down holes and lines of section (after Wilkinson and Byrne, 1977).

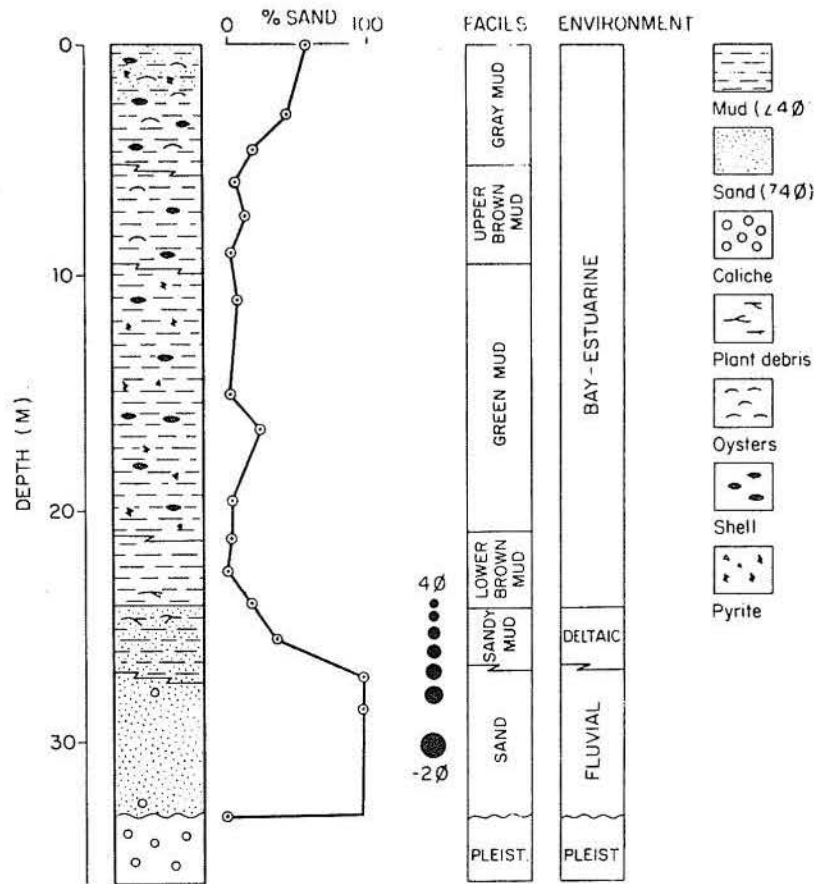


Figure 64. Generalized sedimentary sequence in south Lavaca Bay (after Wilkinson and Byrne, 1977).

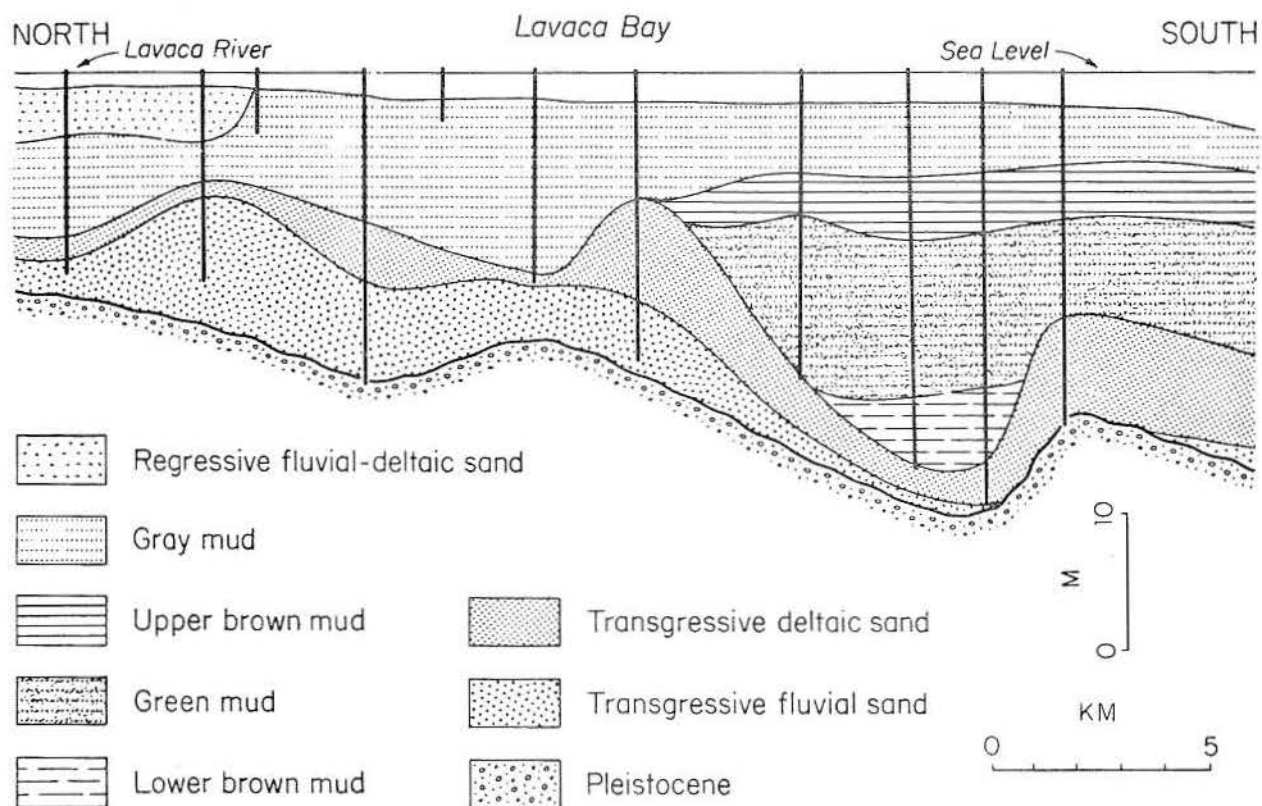


Figure 65. Dip section down Lavaca River valley. There is apparent relief in Holocene fluvial-deltaic units and Pleistocene surface because line of section does not follow valley axis exactly (see fig. 63 for section location) (after Wilkinson and Byrne, 1977).

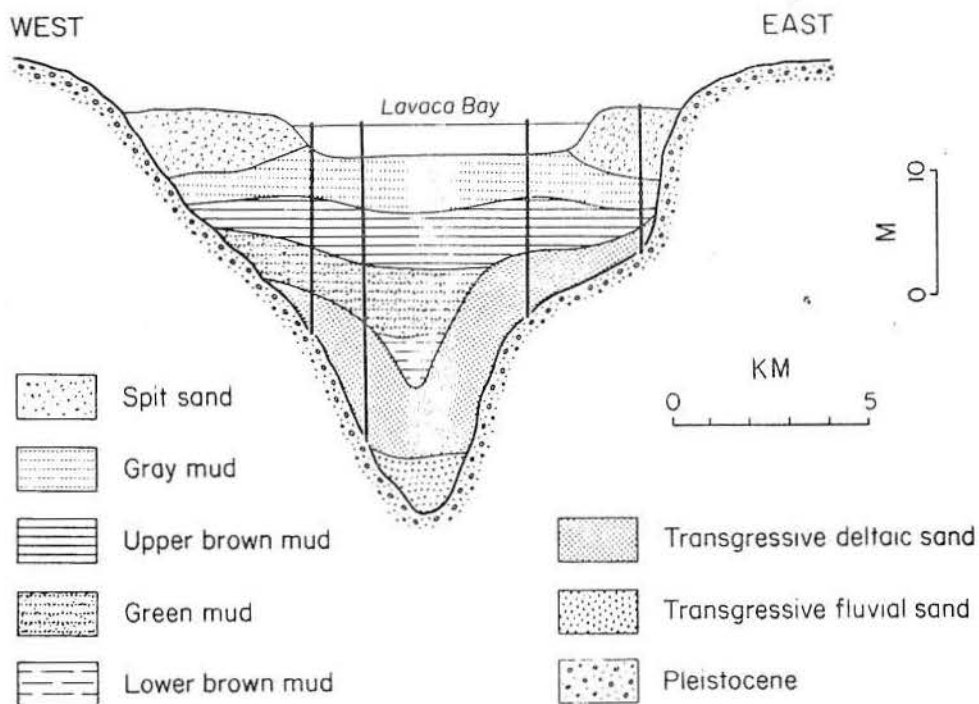


Figure 66. Strike section across southern end of Lavaca Bay (see fig. 63 for section location) (after Wilkinson and Byrne, 1977).

Astronomical Tides

Tides in the Gulf of Mexico are dominantly diurnal, with a mean tidal range along the Gulf Coast of about 1.5 to 2.0 ft (45 to 60 cm). Astronomical tides are low within the bays, particularly toward bayheads, where the range may be less than 0.5 ft (15 cm). Astronomical tides exert their greatest influence on the bay systems at the tidal inlet (fig. 67). Tides move coarse material (sand and shell) from the Gulf of Mexico into the bays where some of this material accumulates as flood-tidal deltas; the rest is returned to the Gulf of Mexico to be picked up by the longshore-drift system. Ebb-tidal currents transport suspension-load material from the bays through the inlet to the Gulf of Mexico. Astronomical tides exert very little influence on sediment transport within the bays.

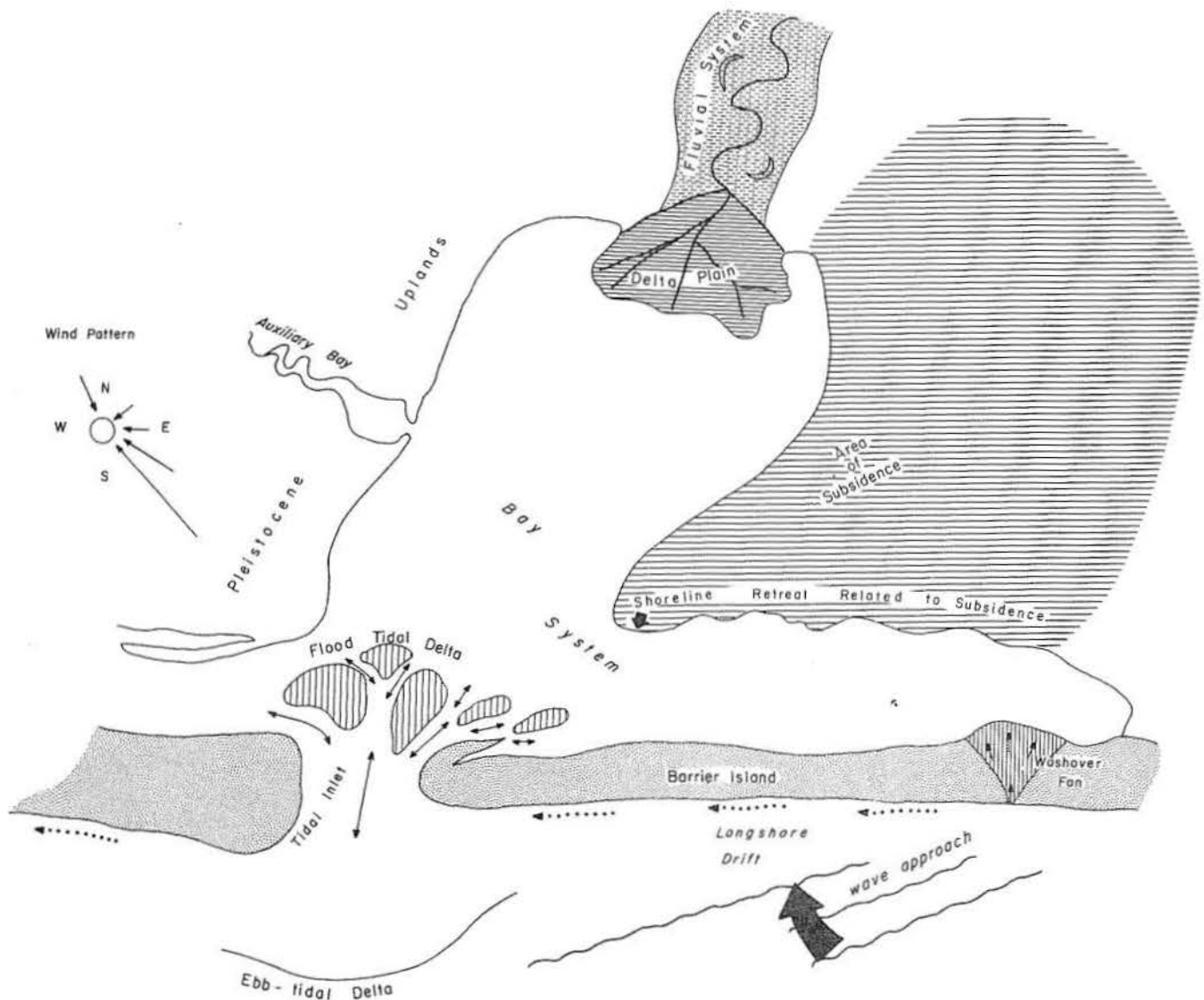


Figure 67. Plan view of major bay elements. Sketch shows fluvial, deltaic, tidal-inlet, bay, and barrier-island associations.

Wind

Wind direction is onshore approximately 10 months of the year. Wind is perhaps the single most important geologic agent affecting the bay systems. Wind stress along the water surface creates waves and causes a rise in the water surface (called wind tide) in the downwind direction. Wind tides inundate areas not normally affected by astronomical tide. Superimposed upon the wind tide are waves that may strike the shoreline at an angle, thereby setting up longshore drift. (South winds set up west- and north-flowing longshore currents; north winds set up east- and south-flowing longshore currents--this is the flow direction for fig. 67).

Waves, wind tides, and longshore currents generated by south winds tend to move sediment northward or westward (this is the direction for fig. 67). North winds generate waves, wind tides, and longshore currents that tend to move sediment southward.

Rivers

Rivers contribute fresh water and sediment to the bay systems. In the past, the flow from rivers was not impeded (impounded by man-made structures), and they exerted a much greater influence on the bay system than at present. In general, rivers along the upper coast contribute much more sediment and water to the bays than do rivers of the lower coast (fig. 5).

The most obvious effect of rivers on the bay system is to prograde the shoreline through the process of delatation. Five bays are characterized by deltas. These are Trinity Bay (Trinity delta), Matagorda Bay (Colorado delta), Lavaca Bay (Lavaca delta), San Antonio Bay (Guadalupe delta), and Nueces Bay (Nueces delta and Gum Hollow delta). The Brazos River and Rio Grande have filled their respective bays and now discharge into the Gulf of Mexico. In simple terms, a river discharges both bed load and suspended load into the bay where bed load (sand) accumulates as channel-mouth bars and delta-front sand, and part of the suspension load (silt and clay) accumulates beyond the sand as prodelta mud. Some of the suspended load is transported beyond the influence of the river where part of it settles to the bay bottom and part of it moves within the fresher surface water that passes through inlets into the Gulf of Mexico.

Subsidence

Subsidence is a natural geologic process throughout the Texas Coastal Zone. Natural subsidence results from compaction of muddy sediments and from tectonism. The effect of subsidence is a relative rise in sea level (transgression of bay waters over low-lying shorelines) as bay waters increase in depth. Ground-water withdrawal creates additional subsidence in the Houston and Texas City areas. The Galveston Bay system (fig. 68) has undergone bathymetric changes (deepening) as a consequence of ground-water withdrawal in the Houston and Texas City areas, dewatering of muds that underlie the bay system, and decreases in volume of sediment delivered to the bay system by the San Jacinto and Trinity Rivers (fig. 69). All of these processes increase the area and depth of the bay system.

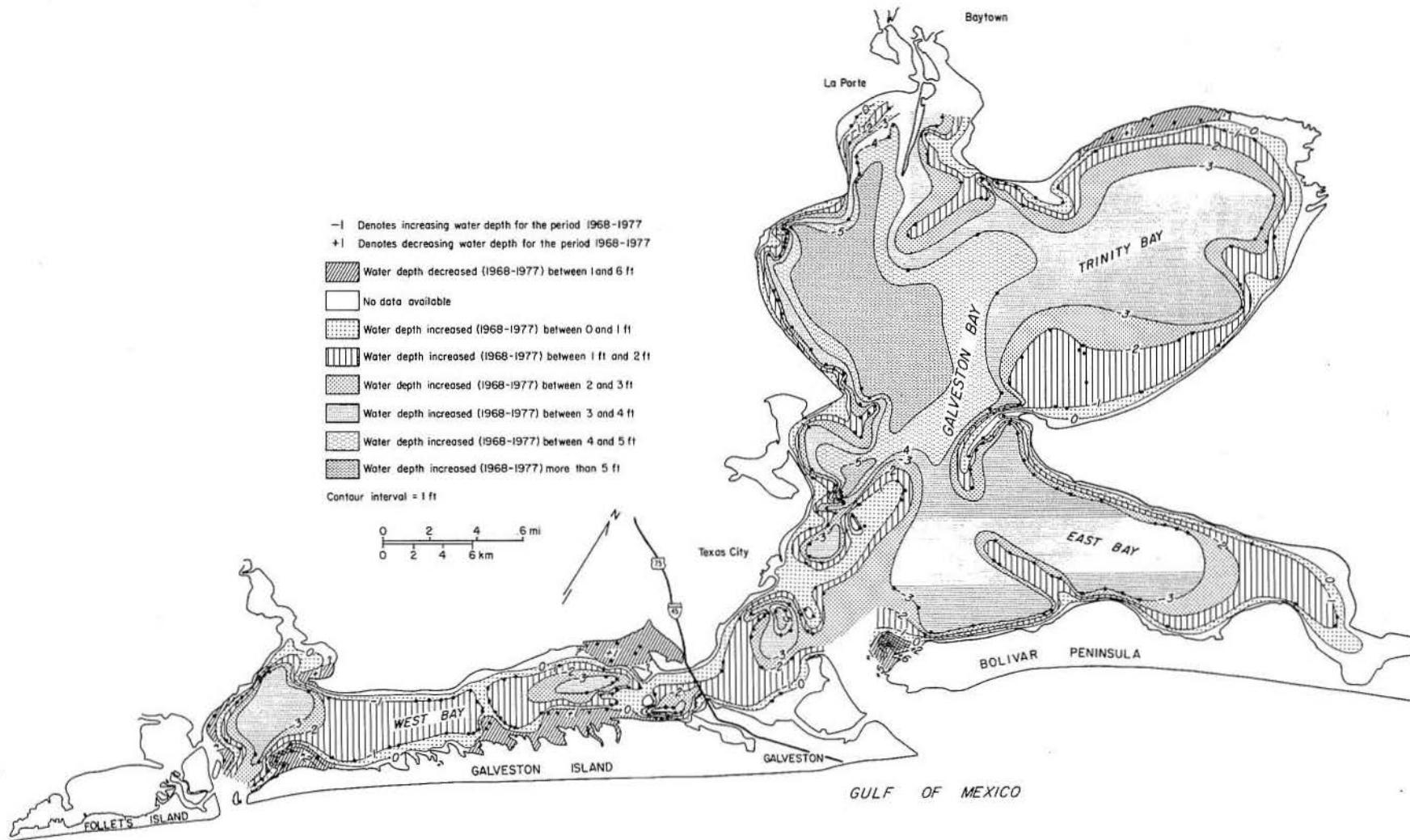


Figure 68. Bathymetric changes for Galveston Bay system for the period 1968-1977. Bathymetry for 1968 is from published navigation charts. Bathymetry for 1977 is based on soundings taken at sampling stations, on 1-mi centers, in the fall and winter 1977. Sounding data were not adjusted to m.s.l., therefore, the numbers shown on this map (fig. 68) must not be taken as absolute values; the map depicts direction of change.

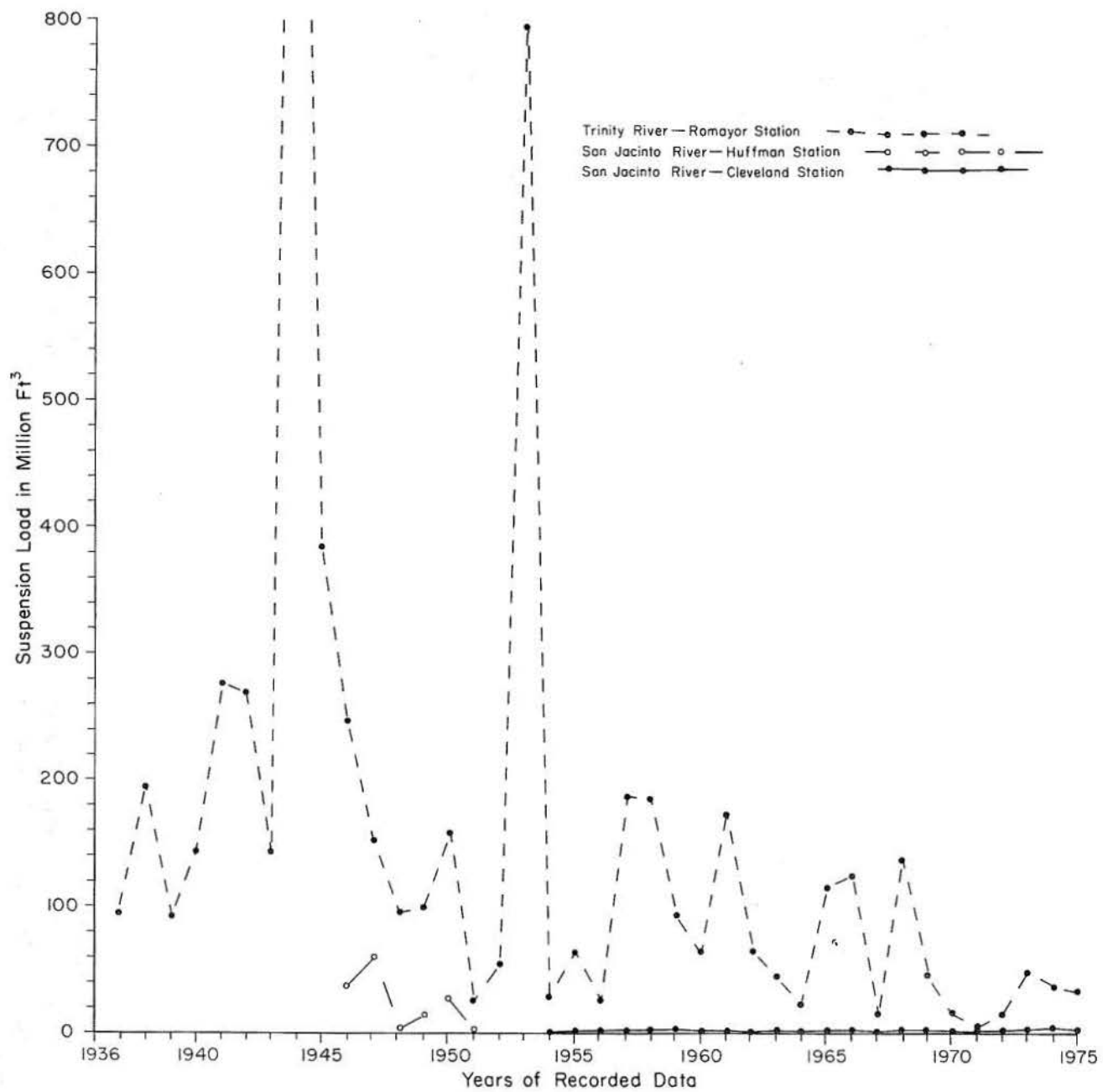


Figure 69. Volume of suspended-load sediment delivered to the Galveston Bay system for the period from 1936 through 1975. Construction of dams on the Trinity and San Jacinto Rivers has reduced the volume of sediment delivered to the bay system.

Tropical Cyclones: Hurricanes and Tropical Storms

The Texas coast is hit by tropical storms and hurricanes on an average of once every 1.5 years (Hayes, 1965, 1967). Hurricanes and tropical storms are characterized by counterclockwise winds hundreds of miles in diameter. These storms possess high-velocity winds, a calm area (the eye) at the center of the storm, low barometric pressure, torrential rainfall, and tornadoes (McGowen, 1970; Brown, 1974).

Hurricanes breach low-lying barrier islands and peninsulas and transport sand and shell through these cuts and deposit it along the bay margin. Hurricanes create a storm surge that may attain a height of 20 ft (6 m) above mean sea level at the heads of bays. This surge is accompanied by large waves that stir up bottom sediment and erode bay shorelines. As the hurricane moves inland, wind direction changes, the surge is directed toward the Gulf of Mexico, and sediment suspended from the bay bottom then exits the bay system through tidal inlets and storm channels. Heavy rainfall commonly accompanies hurricanes and tropical storms. Rivers flood at this time, and deltas prograde, bay bottoms aggrade, and some suspension-load moves through the system with the surface fresh-water layer into the Gulf of Mexico.

Bay Circulation

Numerous papers have been written on estuarine circulation, classification of estuaries, and origin of estuaries (Schubel, Hayes, and Pritchard, 1971). According to Pritchard (1967), estuaries are semi-enclosed coastal bodies of sea water, diluted with fresh water from land drainage, that have free connection with the open sea. Texas bays do not fall into this classification because they do not have a free connection with the open sea, and some of them are not measurably diluted with fresh water. Texas bays were formed partly by drowning of river valleys, and partly by construction of barrier islands and peninsulas that greatly restrict tidal exchange between the Gulf of Mexico and bays. Pritchard (1967) preferred to call the Texas bays bar-built estuaries; a better term is coastal lagoon since this avoids the use of the term estuary.

Circulation within the Texas bays (coastal lagoons) is influenced by astronomical tides, wind, fresh-water inflow, and bathymetry. Since inlets are relatively small, the effect of astronomical tides is restricted to the immediate area of tidal inlets and tidal deltas. Most of the Texas bays are shallow; depth generally decreases from the upper Texas coast (Galveston Bay -- about 10 ft [3 m]) to the lower Texas coast (south Laguna Madre -- 2 to 3 ft [60 to 90 cm]) (McGowen and Morton, 1979).

As a result of the shallow depth of bays and relatively small tidal prism, wind exerts a much greater influence on bay circulation than do astronomical tides. Wind generates wind tides and waves that are effective in mixing salt water and fresh water.

Temperature and rainfall (fig. 2) also affect bay circulation. In general, salinity is least in bays of the upper coast and greatest in bays of the lower coast. This is a function of high river discharge and low evaporation in bays of the upper coast; the opposite is true for the lower coast. During high river discharge (spring and fall) a fresh-water head occurs at the bayhead, slope of fresh-water surface decreases toward the Gulf of Mexico, surface fresh water flows toward the Gulf, and surface currents may be strong at ebb tide.

River influence decreases southward along the coast as rainfall decreases and as evaporation exceeds fresh-water inflow. Laguna Madre and Baffin Bay normally have very little fresh-water inflow. Astronomical tidal exchange is limited because Laguna Madre is a long water body (approximately 110 mi [176 km]) with tidal inlets near its southern limits (Brazos Santiago Pass and Port Mansfield Ship Channel, fig. 1). North Laguna Madre is connected to Corpus Christi Bay, which receives marine waters through Aransas Pass and Corpus Christi Water Exchange Pass (fig. 1). Unlike the other Texas bays, Laguna Madre and Baffin Bay are commonly hypersaline; salinity decreases toward the tidal inlets. The force that drives water circulation within this system is wind tides, which may attain heights of more than 3 ft (1 m) above mean sea level (Fisk, 1959). North and south winds blow down the axis of north and south Laguna Madre. Wind tides increase in the direction of air movement. North winds move water from north to south with highest tides on the north side of the Land-Cut Area (fig. 1). South winds move water from south to north, and highest tides are on the south side of the Land-Cut Area.

Sediment Sources and Sediment Distribution

Sediment that accumulates in the Texas bay systems is derived from rivers that discharge at the heads of bays, from the Gulf of Mexico through tidal inlets and storm channels, from materials eroded from Pleistocene deposits that form bay shorelines, from plants and animals living within and adjacent to bays, and from calcium carbonate generated within warm hypersaline water bodies.

Sediment type delivered to the Coastal Zone by Texas streams is chiefly a function of climate (fig. 2). Identifiable sediment delivered to bays, estuaries, and lagoons from the Gulf of Mexico is chiefly sand, shell, and rock fragments that are eroded from the inner shelf, shoreface, and beaches by tropical storms and hurricanes.

Climatic gradients (fig. 2) are reflected in (1) the vegetation cover (dense in the east and sparse in the west), (2) the type of fluvial systems that traverse the Coastal Plain (continuously flowing sinuous streams to the east, and straight to sinuous flashy streams to the west), and (3) the type of sediment delivered to the bays (streams in the east are characterized by a high suspension-load/bed-load ratio, whereas streams in the west have a high bed-load/suspension-load ratio).

Texture of bay sediment is generally (1) coarsest at river mouths, along bay margins where erosion of Pleistocene deposits is prevalent, near tidal inlets, and adjacent to barrier islands and peninsulas, and (2) finest in the deeper bay-center areas. The relative proportion of mud (fine-grained sediment) to sand (coarse-grained sediment) is greatest in the bays of the upper Texas coast and least in the bays of the lower coast; this is a reflection of decreasing rainfall across the state from east to west.

Nonterrigenous sediment composes an insignificant volume of the fill when all of the Texas bays are considered. Nonterrigenous deposits are found in (1) shell beaches, spits, and berms situated along bay margins, (2) oyster and serpulid reefs, and (3) oolite and coated-grain shoals. Oyster reefs are prolific in the area defined by the Trinity - Galveston Bay system to the northeast and Copano Bay to the southwest (fig. 1). Bays in this area are typified by salinities that range from that of almost fresh water to that of the Gulf of Mexico.

Serpulid reefs, now dead, are well developed in Baffin Bay and in parts of Laguna Madre adjacent to the mouth of Baffin Bay. These reefs probably flourished in Baffin Bay prior to closing of the tidal inlet through Padre Island opposite to the mouth of Baffin Bay (Andrews, 1964). As a consequence of the closing of the tidal inlet, Baffin Bay is no longer directly linked to the Gulf of Mexico. During tropical storms and hurricanes, aftermath rainfall and runoff from adjacent uplands convert Baffin Bay into a temporarily fresh-water body (Behrens, 1969). On the other hand, prolonged dry climatic conditions, accompanied by excessive evaporation, render Baffin Bay hypersaline. It has been suggested that the serpulids in Baffin Bay could not tolerate hypersaline conditions (Andrews, 1964).

Some bay-margin deposits are characterized by high shell content. These deposits represent reworking of oyster reefs and shell-bearing bay sediment by wave and current activity, slow sediment accumulation rates, and/or high rates of biological productivity. Oyster reefs are commonly flanked by shell debris. Oystershell spits develop downcurrent from some reefs and headlands.

Oolites and coated grains are mostly confined to Baffin Bay, where input of terrigenous clastics is low. Shoals, underlain by these carbonate sands, are situated along the north shore of Baffin Bay, which is affected by waves and currents generated by the prevailing south-southeast winds.

Laguna Madre, the shallowest of the large coastal water bodies, is being filled principally with sand that is transported from the beaches across Padre Island by wind and storm activity (McGowen and Morton, 1979).

Copano Bay

Copano Bay is located in the central coastal zone where it is a subsidiary bay of the more extensive Corpus Christi - Aransas Bay system (fig. 1). The bay is approximately rectangular with its long axis oriented northeast-southwest. The bay is approximately 14 mi (22 km) long and 5 mi (8 km) wide, and, excluding Mission Bay, covers an area of about 70 mi² (110 km²). The bay ranges in depth from about 2 ft (60 cm) along the margin to a maximum of about 10 ft (3 m) at the bay center and within the channel connecting Copano and Aransas Bays. Copano Bay is bounded mostly by Pleistocene deltaic deposits. Parts of the eastern and southern shorelines are bounded by the Pleistocene Ingleside barrier-strandplain sand (these areas are identified in fig. 70 as Lamar Peninsula and Live Oak Peninsula).

Climate in the Corpus Christi - Copano Bay area is dry subhumid (Hayes, 1965). Average annual rainfall for the area is between 34 and 36 inches (85 and 87 cm); average temperature is between 71° and 72°F (fig. 2). Evaporation exceeds precipitation by about 12 inches (30 cm) per year.

Copano Bay receives fresh water and sediment from several streams, such as Mission River, Mullen Bayou, and Aransas River. Salinity of Copano Bay may be as low as about 6 ‰ immediately after large rains associated with hurricanes or as high as about 26 ‰ during unusually dry years (Brown and others, 1976). Salinity changes result from fresh-water runoff and tidal exchange via Lydia Ann Channel and Aransas Bay; salinity is lowest toward the western part of the bay where fresh water is discharged into the system. During hurricanes and tropical storms, heavy rains (as much as 30 inches [75 cm] recorded during the passage of Hurricane Beulah in 1967)

cause excessive runoff, and at these times Copano Bay may be almost fresh. Under normal conditions salinity is considerably less than that of sea water.

The large volumes of fresh water and fine sediment that are discharged into the bay are reflected in the dominance of mud over sand in the bay fill and the proliferation of *Crassostrea virginica* reefs (fig. 70).

Origin of Copano Bay

Copano Bay now occupies a valley (fig. 62) that was eroded by Mission and Aransas Rivers during the Wisconsin Glacial Stage when sea level was 390 to 450 ft (119 to 137 m) lower than at present (see introductory section on bays). Maximum depth of scour was about 70 ft (21 m) below m.s.l. Melting of polar ice caps caused the sea to rise again, marking the beginning of the Holocene transgression. Copano Bay was not affected by sea-level rise until about 7,000 years B.P. when sea level was between -70 and -50 ft (-21 and -15 m) m.s.l. Copano Bay became a coastal lagoon after the accretionary barrier islands had developed (see Wilkinson, 1975; Byrne, 1975; Wilkinson and Byrne, 1977). Since about 7,000 years B.P. Copano Bay has been almost

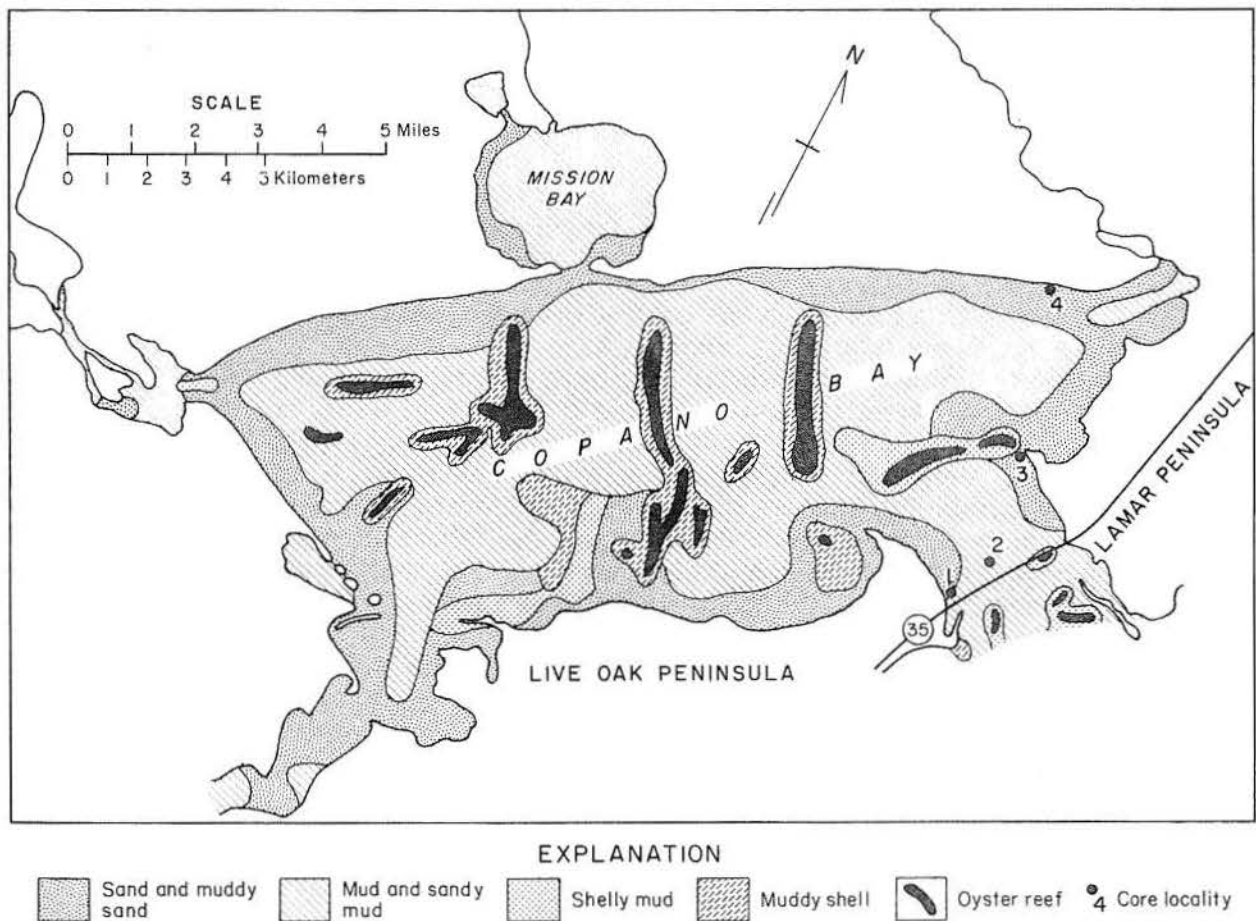


Figure 70. Surface sediment distribution and core localities in Copano Bay (modified from McGowen and Morton, 1979). Rockport Quadrangle.

completely filled (there is now a maximum of 10 ft [3 m] of water in the bay) with terrigenous clastic deposits. Mud is the dominant textural type. Oyster reefs and minor amounts of shell from other mollusks have also contributed to the bay fill. Average sedimentation rate over the 7,000-year period was approximately 0.8 ft (0.24 m) per 100 years.

Bay Processes

Water movement and sediment distribution in Copano Bay are affected by astronomical tides, wind regime, fresh-water runoff, temperature and rainfall, and hurricanes. (For further discussion, see the introductory section on bays.) The dominant processes are fluvial runoff, prevailing southeast winds, strong north winds associated with polar fronts, hurricanes, and astronomical tides. Copano Bay has been compartmentalized, to a certain degree, by oyster reefs; these reefs are elongate transverse to the bay axis and elongate approximately parallel to prevailing southeast winds (Brown and others, 1976, fig. 8, p. 28). Reefs serve to impede currents and sediment, which move in a direction parallel to the long axis of the bay.

Surface Sediment Distribution

Distribution of surface sediment was mapped using field descriptions of grab-samples taken on 1-mi (1.6-km) centers (McGowen and Morton, 1979). Figure 70 is a simplified version of the sediment map of McGowen and Morton (1979).

Sediment contained in Copano Bay is derived from fluvial systems (chiefly Mission and Aransas Rivers), from erosion of Pleistocene fluvial, deltaic, and barrier-strandplain deposits that form the bay shoreline, and from production of shell material within the bay.

Sand and muddy sand occur along the shallow bay-margin areas. Sand is derived chiefly from erosion of Pleistocene deposits exposed in bluffs that surround the bay. Waves that are generated by the prevailing southeast winds erode the north shore, and longshore currents generated by these waves move sediment generally toward the west. An abundant sand source is available to waves generated by northers; Lamar Peninsula and Live Oak Peninsula, both composed of Pleistocene Ingleside barrier-strandplain sand, face into the north wind.

Mud and sandy mud generally accumulate in the deeper central bay area. An exception to the general distribution of mud is that mud and sandy mud have accumulated in the tidal pass (connecting Copano and Aransas Bays) between Lamar and Live Oak Peninsulas. Mud is derived chiefly from modern fluvial systems; some mud is supplied to the bay via erosion of Pleistocene deposits exposed in adjacent bluffs. Most of the sandy mud areas lie just offshore from parts of Lamar and Live Oak Peninsulas.

Shelly mud occurs adjacent to oyster reefs (in these areas shelly mud is the reef-flank deposit) and in less than 1 ft (30 cm) to about 4 ft (1.2 m) of water just offshore from sand and shell spits.

Muddy shell is mostly associated with oyster reefs; this sediment type is also representative of reef flank deposits. In other areas, muddy shell is displaced some

distance downcurrent (to the west) of reefs and represents reworking of reef and reef flank deposits.

Most of the oyster reefs are aligned with wind-generated currents (northwest-southeast orientation). Other reefs are aligned transverse to wind-generated and tidal currents (for example, the reef near core locality 3, fig. 70).

Sediment Characteristics

Four short, fixed-piston cores (figs. 70 and 71) were taken along a transect of the eastern part of Copano Bay. The cores represent bay-margin (cores 1, 3, and 4) and inlet facies (core 2). Core 1 was taken in an area that is relatively protected from waves generated by southeasterly winds, whereas cores 3 and 4 were taken offshore from a spit (core 3), and offshore from a straight shoreline segment affected by waves approaching from the southeast (core 4). Core 2 was taken along the inlet axis in 12 ft (3.5 m) of water.

Bay-margin facies of the relatively protected south shore of Copano Bay (fig. 71) consists of burrowed, gray, muddy fine sand with about 1 percent shell fragments throughout. The lower 0.3 ft (9.0 cm) of the core is made up of about 25 percent oystershell fragments. Burrows are of two types: (1) 0.062- to 0.12-inch (1.5- to 3.0-mm) diameter, open burrows in the upper 3.25 ft (1.0 m); and (2) 0.25- to 0.5-inch (6.0- to 12-mm) diameter, sand-filled burrows.

Sediment that accumulated within the tidal channel between Copano and Aransas Bays is mostly gray sandy mud with thin (about 0.25 inch [6.0 mm]) muddy sand units that are faintly parallel laminated, ripple cross-laminated, and massive with preserved rippled bed forms. This facies is also burrowed and contains approximately 1 percent shell fragments throughout. Small (0.12- to 0.25-inch [3.0- to 6.0-mm] diameter) open burrows occur throughout the core interval. Evidence of scour was observed approximately 3.6 ft (1.0 m) from the top of the core; relief on the scour surface is approximately 0.5 inch (12 mm). Directly above the scour surface the shell fragment content is approximately 5 percent. Gray fine sandy mud containing approximately 2 percent plant debris underlies the erosional surface.

The high physical energy bay-margin facies (cores 3 and 4) are similar in the two areas investigated. This facies is typified by yellowish-light-brown, well-sorted, predominantly massive fine sand. Sand exhibits few primary sedimentary structures although ripple bed forms were observed on the bay bottom at both localities. Primary sedimentary structures have been destroyed by burrowing animals--in particular by mud shrimp. Some differences in subsurface facies exist between core localities 3 and 4. Sand at locality 3 accumulated in a bay-margin environment void of the sediment-trapping, substrate-stabilizing effect of marine grasses. The upper 0.8 ft (0.24 m) of sand at core locality 4 accumulated in an environment similar to that existing at core locality 3. From 0.8 to 1.9 ft (0.24 to 0.58 m), the sediment in core 4 accumulated in a bay-margin grassflat environment. Grassflat deposits are yellowish light gray with gray mottles, muddy fine sand, and well-sorted fine sand. This facies is characteristically burrowed, contains 1 to 2 percent coarse sand to granule-sized shell fragments, and has roots and stems of marine grasses. Pleistocene deposits make up the lower 0.5 ft (15 cm) of the core. The Pleistocene deposits are compact, green, homogeneous, sandy mud with caliche nodules throughout. Bay organisms burrowed into the Pleistocene, and these burrows have been filled with sand from the overlying grassflat facies.

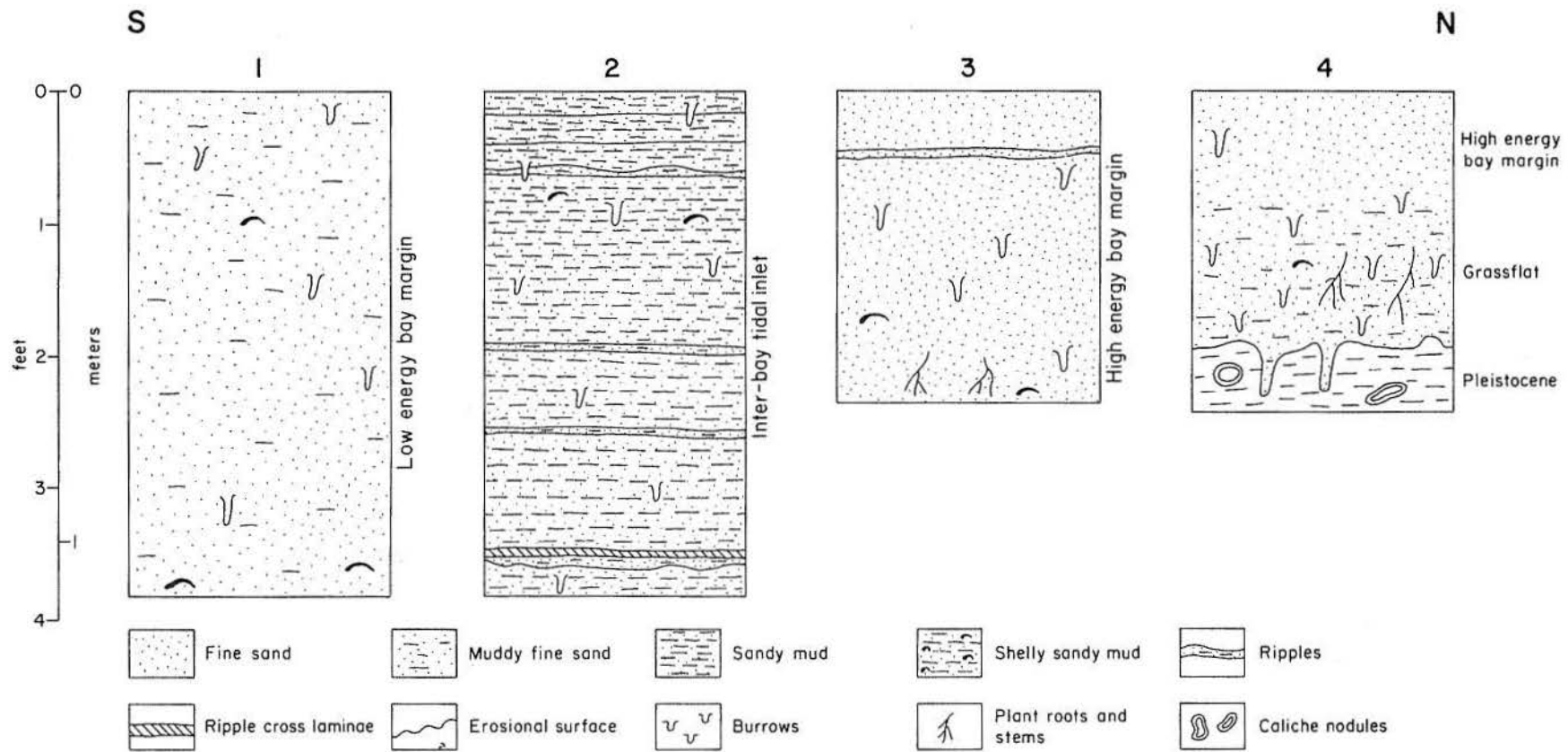


Figure 71. Cores taken from bay margin (cores 1 and 4), tidal inlet (core 2) and adjacent to a sand spit area (core 3), Copano Bay (see fig. 70 for core locations).

North Laguna Madre

North Laguna Madre (fig. 1) extends southward approximately 52 mi (83 km) from its juncture with Corpus Christi Bay to its ill-defined limit adjacent to the Land-Cut Area. North Laguna Madre is shallow; it ranges in depth from about 2 to 8 ft (60 cm to 2.5 m). It is bounded on the mainland side by the Pleistocene Ingleside barrier-strandplain system (Brown and others, 1976) and on the east by Padre Island.

The climate of the area is semiarid (Hayes, 1965). Average annual rainfall for the area is between 28 and 30 inches (70 and 75 cm), and average annual temperature is between 72° and 73°F (22° and 23°C). Evapotranspiration exceeds precipitation by about 16 to 24 inches (40 to 60 cm) (fig. 2).

No major streams discharge into north Laguna Madre. Fresh water is contributed to the system from runoff from the adjacent uplands. North Laguna Madre joins Corpus Christi Bay to the north, and Baffin Bay joins north Laguna Madre some 20 mi (32 km) north of its southern limit. Fresh water is also contributed to north Laguna Madre via Corpus Christi and Baffin Bays. Rainfall associated with certain types of hurricanes is excessive; for example Hurricane Beulah, 1967, dropped about 20 inches (50 cm) of rain in the Baffin Bay - north Laguna Madre area (Behrens, 1969). This heavy rainfall caused the salinity in Baffin Bay to change from about 67 ‰ to about 6 ‰, and salinity in north Laguna Madre, from about 55 ‰ to about 12 ‰.

The result of the shallow lagoon, restricted nature of the system, small fresh-water volume discharged into the system under normal weather conditions, and excess of evapotranspiration over precipitation is that north Laguna Madre is commonly hypersaline. Normally, salinity increases from the mouth of north Laguna Madre southward toward Baffin Bay and the Land-Cut Area.

Origin of North Padre Island and Laguna Madre

As final glacial episodes diminished about 18,000 years B.P. and meltwater began to reach the oceans, sea level began its last rise. As sea level rose between 18,000 and about 4,500 years B. P., the deeply incised lower reaches of the fluvial system (now occupied by Baffin Bay) filled slowly with brackish to marine water. The resulting estuarine system occupied a broad, submerged valley now buried beneath the shelf, Padre Island, and Laguna Madre. That part of the river system now occupied by Baffin Bay remains only partly filled; wave erosion has widened the original valley. Sea level rose at varying rates and with several pauses and minor reversals. Baffin Bay, the principal bay in the area, was later isolated from the open Gulf by development of Modern Padre Island.

Barrier-Island and Lagoon Development

At about the time that sea level reached its Modern position (4,500 years B.P.), sands eroded from submerged Pleistocene sediments on the adjacent shelf were concentrated in shoals from 3 to 8 mi (4.8 to 13 km) offshore by waves breaking on the gently sloping inner shelf (Fisk, 1959; Brown and others, 1977). The shoals became a series of emergent, low, discontinuous sandy islands aligned parallel to the mainland shoreline. Wind-driven waves approaching the emerging islands generated longshore currents. Sandy sediments were moved by longshore drift along the gulfward side of

the islands and were deposited as shallow spits at the downcurrent end of each island. Spit accretion continued as more sediment from the inner shelf, as well as from local erosional headlands along the mainland, became entrained within the longshore drift system. The islands within the discontinuous chain coalesced to form Padre Island.

As the various islands and shoals joined to form Padre Island, a broad lagoon (Laguna Madre) formed landward of the offshore island. Baffin Bay was gradually cut off from the open Gulf as spits closed its tidal inlet. Final closing of the lagoon probably occurred early in the 19th century.

Carbon-14 dates (Fisk, 1959) indicate that Padre Island and Laguna Madre began to form about 5,000 years B.P. and that Padre Island became a barrier at least 3,700 years B.P. In the Land-Cut Area, cores drilled across Padre Island (Fisk, 1959) indicate that the island is about 35 to 40 ft (10.5 to 12 m) thick and that perhaps the island has accreted at least 0.75 mi (1.2 km) during approximately the past 4,000 years. During the past several decades, Gulf shorelines of Padre Island have exhibited slight erosion, equilibrium, and some accretion.

During the past several thousand years, hurricanes and tropical storms in conjunction with aeolian processes have transported sediment from the island landward into Laguna Madre. These washover and aeolian sands built as much as 2 or 3 mi (3.2 to 4.8 km) into Laguna Madre, although they were repeatedly covered by lagoonal waters.

Although Padre Island accreted moderately gulfward and extensively landward, it has remained a low island near sea level. Locally, fore-island dunes have become elevated to 35 or 40 ft (10.5 to 12 m) above sea level. The island is in delicate balance with regard to sediment supply, wind, aridity, and vegetation. It is breached by hurricane storm tides, and beach sand is blown landward to produce extensive back-island dune fields.

Lagoon Deposition

Entrenched stream valleys, such as Baffin Bay, were flooded by rising Holocene sea level between 5,000 and 10,000 years B.P. Later, lagoonal sediments were deposited landward of Padre Island within relatively open lagoons or bays with direct connection with the Gulf of Mexico (Fisk, 1959). About 3,700 years B.P., sedimentation in Baffin Bay and Laguna Madre became increasingly restricted as the Padre Island chain coalesced into a continuous barrier island with a few tidal inlets between the Gulf and the lagoon system. Sediments and fauna reflect this shift to a closed lagoonal system (Fisk, 1959).

The deeper, open lagoonal system evolved into a shallow, closed, hypersaline system. Sand that was transported across the island by hurricanes and prevailing southeast winds accumulated in Laguna Madre, thereby decreasing the width of the water body. Finer grained sediment accumulated in the lagoon center.

Fisk (1959) estimated that central Laguna Madre was filled about 170 years ago with sand derived from Padre Island. The fill (represented by the Land-Cut Area) divided Laguna Madre into northern and southern segments. North Laguna Madre will eventually be filled from the Land-Cut Area northward to Baffin Bay.

Bay Processes

Factors that affect water movement and sediment distribution are the same in north Laguna Madre as in south Laguna Madre.

Surface Sediment Distribution

Laguna Madre differs from the bays to its north and east in (1) having very limited water exchange with the Gulf of Mexico, (2) having no perennial streams discharging into it, (3) being extremely shallow, and (4) lying in a semiarid climatic belt (McGowen and Morton, 1979). Together these factors have produced a water body with higher than normal salinity. The system is relatively unaffected by daily fluctuations of astronomical tide. The water level in Laguna Madre fluctuates with wind direction, intensity, and duration. Because of its hydrologic regime and the rate and kind of sediment delivered to it, Laguna Madre contains considerably less mud than do bays to the north and east.

Ten sediment types have been mapped in the northern part of Laguna Madre. For the sake of brevity some of these types were grouped together (fig. 72) into six classes of sediment: sand and muddy sand, mud and sandy mud, shelly mud and sandy shelly mud, shelly sand and muddy shelly sand, shell and rock fragment gravel, and sandy shell.

Sand and muddy sand form a band next to mainland and barrier-island shorelines; near the southern part of the map (fig. 72) sand is displaced toward the center of the lagoon (sand is reworked from some of the spoil areas). Most of the area mapped as mud and sandy mud is underlain predominantly by sandy mud; mud is rare in north Laguna Madre. Most of the other sediment types appear to be related to human activities within the lagoon. Exceptions are shelly sand (and muddy shelly sand) and sandy shell, which are situated adjacent to the mainland shoreline downwind from prevailing southeast wind.

Sand within Laguna Madre is derived from Padre Island and from the Pleistocene Ingleside barrier-strandplain system. Active back-island dunes on Padre Island migrate into Laguna Madre. Waves and currents rework much of this sand into a lagoon-margin sand shoal that is partly stabilized by marine grasses and algae; however, there is depositional relief on this lagoon-margin shoal of about 3 ft (90 cm). Water depth above the shoal is generally less than 1 ft (30 cm); depth in the adjacent grassflat is about 3 ft (90 cm). Sand is eroded from the Ingleside barrier-strandplain system and redistributed along the lagoon margin by waves and longshore currents. Muddy sediment, derived principally from Corpus Christi Bay, accumulates in the somewhat lower physical energy environment of the slightly deeper lagoon center.

Shell is generated within the lagoon and has been mixed with terrigenous clastic sediment chiefly through the activity of burrowing organisms. Some shell, rock fragments, and terrigenous clastic materials have been mechanically mixed through dredging operations.

Sediment Characteristics

The sediment distribution map, which is based upon field descriptions of grab samples, does not coincide precisely with descriptions made in the laboratory of fixed-

piston cores (figs. 72 and 73). This discrepancy is most noticeable at core locality 1 where surface sediment is well-sorted fine sand but appears on the map as shelly mud and sandy shelly mud.

Characteristics of sediment at the bottom and shallow sub-bottom of north Laguna Madre are depicted on fig. 73. The lower 1.2 ft (43 cm) of core 1 and all of cores 2, 3, and 4 represent lagoonal deposition; these cores exhibit similar sedimentary features. The upper 2 ft (60 cm) of core 1 is light-brown to medium-gray, homogeneous, very well sorted fine sand containing about 1 percent shell fragments. This sand was emplaced by migrating back-island dunes and has the same textural parameters as dune sand; the core was taken in about 1 ft (30 cm) of water. The sand surface was barren of vegetation; it was covered mostly with sinuous crested ripples.

Core 5 was taken to the west of the Gulf Intracoastal Waterway in about 1.5 ft (45 cm) of water; the sediment was covered by a dense growth of green and brown algae, and marine grasses. This core was taken near a spoil mound. Sediment parameters of this core are distinctly different from lagoonal sediment (cores 2, 3,

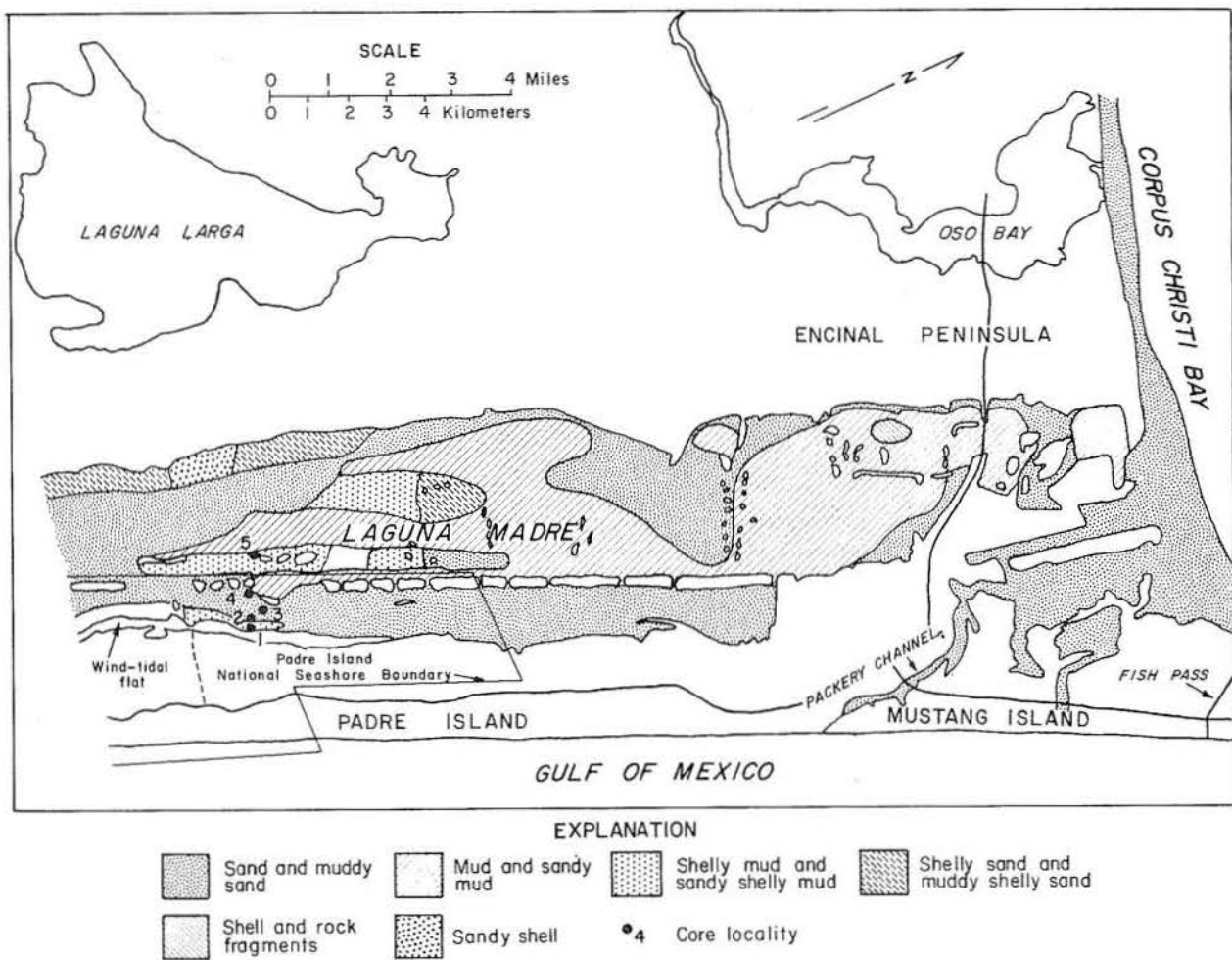


Figure 72. Surface sediment distribution and core localities in north Laguna Madre (modified from McGowen and Morton, 1979). South Bird Island Quadrangle.

and 4) and lagoon-margin deposits (upper part of core 1). The lower 5 inches (12.5 cm) of the core consists of green, gray, and brown, massive, angular to well-rounded, granule to pebble mud-clast gravel with slightly shelly sand filling interstices. This unit was emplaced by dredging equipment. Finer grained materials make up the upper 3 ft (1 m) or so of the core; sediment in the upper core represents reworking of dredge spoil by waves and currents operating within Laguna Madre. Reworked spoil consists of light-gray to medium-gray, fine sand, shelly fine sand, and sandy shell; green, gray, and brown mud-clast sand; and medium-gray mud drapes. Some inclined bedding is present in shelly sand, and ripple bed forms preserved by a mud-drape cap occur at the top of some sedimentation units.

Lagoonal deposits (recorded in the lower part of core 1 and through the entire thickness of cores 2, 3, and 4) are similar along the core transect. Lagoonal sediment consists of light-gray to medium-gray muddy shelly fine sand, fine sand, shelly fine sand, fine sandy shell, and light- to medium-gray, massive mud-sandy mud. The lagoon floor is densely covered with marine grasses in the area of cores 2, 3, and 4 (this is a grassflat). Marine grasses occur throughout the entire thickness of most of the lagoonal deposits represented by these cores. Most of the deposits are massive because of intense bioturbation; distinct burrows were observed only in cores 2 and 4. In general, shell content of the sediment tends to increase toward the lagoon center, and mud content tends to increase toward Padre Island.

South Laguna Madre

South Laguna Madre (fig. 1) extends southward from the Land-Cut Area just south of Baffin Bay to within about 7 mi (11 km) of the Rio Grande (a distance of about 54 mi [86 km]). South Laguna Madre, a shallow coastal lagoon ranging in depth from about 2 to 8 ft (0.6 to 2.4 m), is bounded on the mainland by the Holocene Rio Grande delta and the Holocene-Pleistocene aeolian sand sheet, and is cut off from the Gulf of Mexico by south Padre Island. South Laguna Madre is the southernmost of the Texas coastal lagoons.

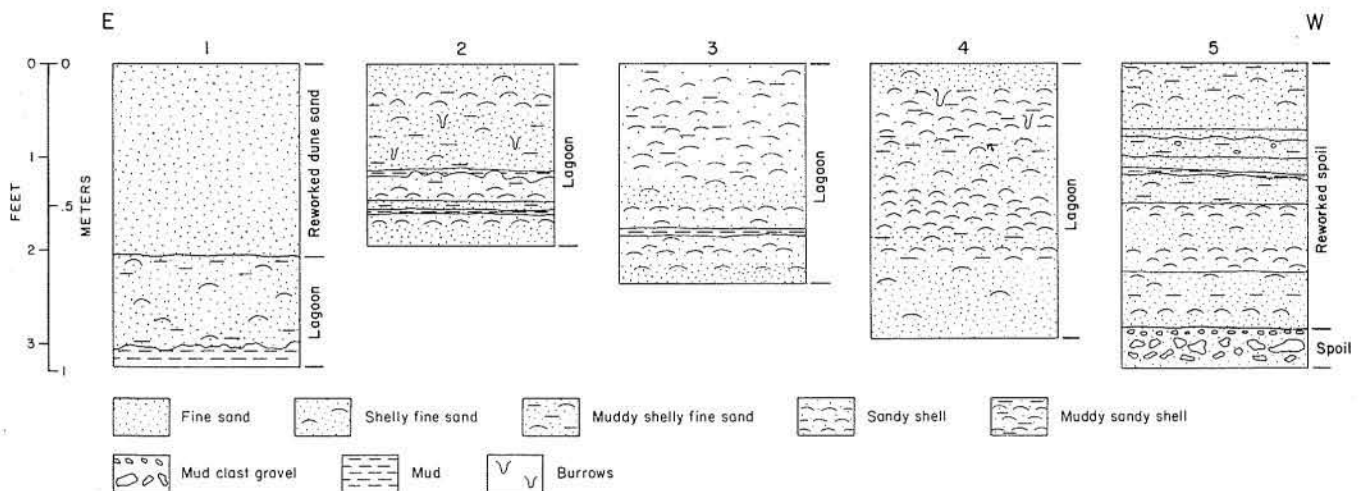


Figure 73. Cores taken from lagoon margin (upper part of core 1 is reworked dune sand), lagoon (lower part of core 1, and cores 2, 3, and 4), and spoil areas (core 5), north Laguna Madre (see fig. 74 for core locations).

The climate of South Texas is semiarid. This area receives about 26 inches (65 cm) of rainfall per year (fig. 2); the average annual temperature is about 74°F (23°C). Evaporation exceeds precipitation by about 24 inches (60 cm) per year. No major stream discharges into south Laguna Madre; fresh water is contributed intermittently through man-made drainage systems, Arroyo Colorado and Cayo Atascosa (Breuer, 1962). The combination of the shallow lagoon, the minor stream discharge into south Laguna Madre, and a rainfall deficit creates a normal hypersaline lagoon. Salinity generally increases from Brazos Santiago Pass and Port Mansfield Ship Channel across the lagoon toward the mainland. This gradient is opposite of that of the bays of the upper Texas coast. Water bodies exhibiting this reversal in salinity gradient have been termed negative estuaries by Pritchard (1967).

Origin of South Padre Island and Laguna Madre

Sediment data gathered from trenches, cores, and washdown holes on south Padre Island and south Laguna Madre indicate that the areas are underlain by a lobe of the Holocene Rio Grande delta (Fulton, 1975; Pryor and others, 1975). Deposits of south Padre Island and south Laguna Madre that overlie the delta are thin. Foundering of the Holocene Rio Grande delta, in conjunction with reworking of the deltaic deposits into beaches and dunes that formed south Padre Island, is the prime factor responsible for development of the lagoon. Compactional subsidence is continuing in the south Padre Island - south Laguna Madre area (Swanson and Thurlow, 1973). Cores taken in south Laguna Madre record this vertical succession of facies: (1) Holocene Rio Grande delta plain, (2) wind-tidal flat, and (3) lagoon.

Bay Processes

Factors that affect water movement and sediment distribution are astronomical tides, wind, temperature, rainfall, and hurricanes.

Astronomical tides are low in south Laguna Madre (Fisk, 1959). Mean annual tidal range near the northern limit of the lagoon is about 0.35 ft (12.5 cm); the tidal range at Port Isabel, near Brazos Santiago Pass, is about 1.24 ft (31 cm).

Wind data presented herein are from the Raymondville Weather Station, where the wind is from the southeast 52 percent of the time, south-southeast 28 percent, northwest 7 percent, north-northwest 7 percent, east-southeast, 3 percent, and east and south 1.5 percent (Breuer, 1962). Calculation of wind dominance (Price, 1933) shows that most of the geologic work is done by southeast and south-southeast winds. Winds generate waves that suspend lagoon sediment, and currents resulting from these waves tend to transport sediment northward or southward, depending upon wind direction. Since south Laguna Madre is oriented at low angles to prevailing southerly winds and the short-duration high-velocity northerly winds, wind-tides are at times rather high (for example, in the northern part of south Laguna Madre a wind-tide range of 3.55 ft [1 m] has been recorded; Fisk, 1959).

Rainfall has not in historic time exerted a significant influence on hydrography or on lagoonal sedimentation. Some fine-grained sediment has been contributed to the lagoon from upland drainage. Of more importance, relative to water movement within the lagoon, is the excess of evaporation over precipitation. This means that there is a more-or-less continuous movement of water from the Gulf into the lagoon; movement within the lagoon is away from inlets toward the more remote areas.

Abrupt changes in the coastal environment result from tropical storms and hurricanes (Hayes, 1967; Behrens, 1969; Scott and others, 1969; McGowen and others, 1970; Brown and others, 1974; McGowen and Scott, 1975). South Padre Island is readily breached by tropical storms and hurricanes. A rapid rise in water level may result as water from the Gulf is pumped across south Padre Island into the lagoon. As the storm makes landfall and moves inland, water is returned to the Gulf through storm channels cut into south Padre Island. Large waves created by hurricane-force winds suspend some of the lagoonal sediment; part of this sediment may be returned to the Gulf of Mexico through storm channels.

Surface Sediment Distribution

Distribution of surface sediment in south Laguna Madre differs from that of the central and upper Texas bays that are fed by fairly large fluvial systems. Central and upper Texas bays contain mostly mud derived from streams.

Much of the sediment in south Laguna Madre is derived from the beaches and dunes of south Padre Island. This source is reflected rather dramatically in the area adjacent to the expansive wind-tidal flats of south Padre Island.

Five sediment groups are shown on the map (fig. 74, modified from McGowen and Morton, 1979). Terrigenous clastics (sand and mud) are the dominant sediment type, and these deposits generally exhibit a decrease in grain size away from south Padre Island. Terrigenous clastics with a shell admixture are the next most abundant sediment type; these deposits are generally concentrated along the north-south axis of the lagoon. The third, and volumetrically least important, sediment type is shell with a mud admixture; this sediment type displays no obvious trend.

Sand is generally confined to shallow water adjacent to south Padre Island where it has been emplaced by tropical storms and hurricanes. Sand in the central part of the lagoon was emplaced by the same mechanism; subsidence in the lagoon has isolated this sand area. Coated grains are common in the sands adjacent to south Padre Island, and micrite is being generated in the adjacent wind-tidal flats.

Mud is concentrated in the deeper, central part of the lagoon where physical processes are less intense. Mud is derived from the Gulf of Mexico and from the adjacent uplands. During tropical storms and hurricanes mud is washed across south Padre Island into the lagoon where a part of it is deposited. Runoff from the mainland also contributes mud to the lagoon.

Shell is generated within the lagoon where it is mixed with sand and mud by burrowing organisms. Much of the substrate of south Laguna Madre is stabilized by marine grasses and by a variety of blue-green, green, and brown algae. South Bay, the southernmost arm of south Laguna Madre, is a mud sump that is mostly less than 2 ft (60 cm) deep; Crassostrea virginica is locally abundant in South Bay.

Sediment Characteristics

Current research on the sediment fill of south Laguna Madre (Herber, in progress) indicates that lagoonal deposits are thin; in most places lagoonal deposits are less than 1 ft (30 cm) thick. This veneer of sediment substantiates the young age of this coastal water body. The ongoing study has documented that south Laguna Madre

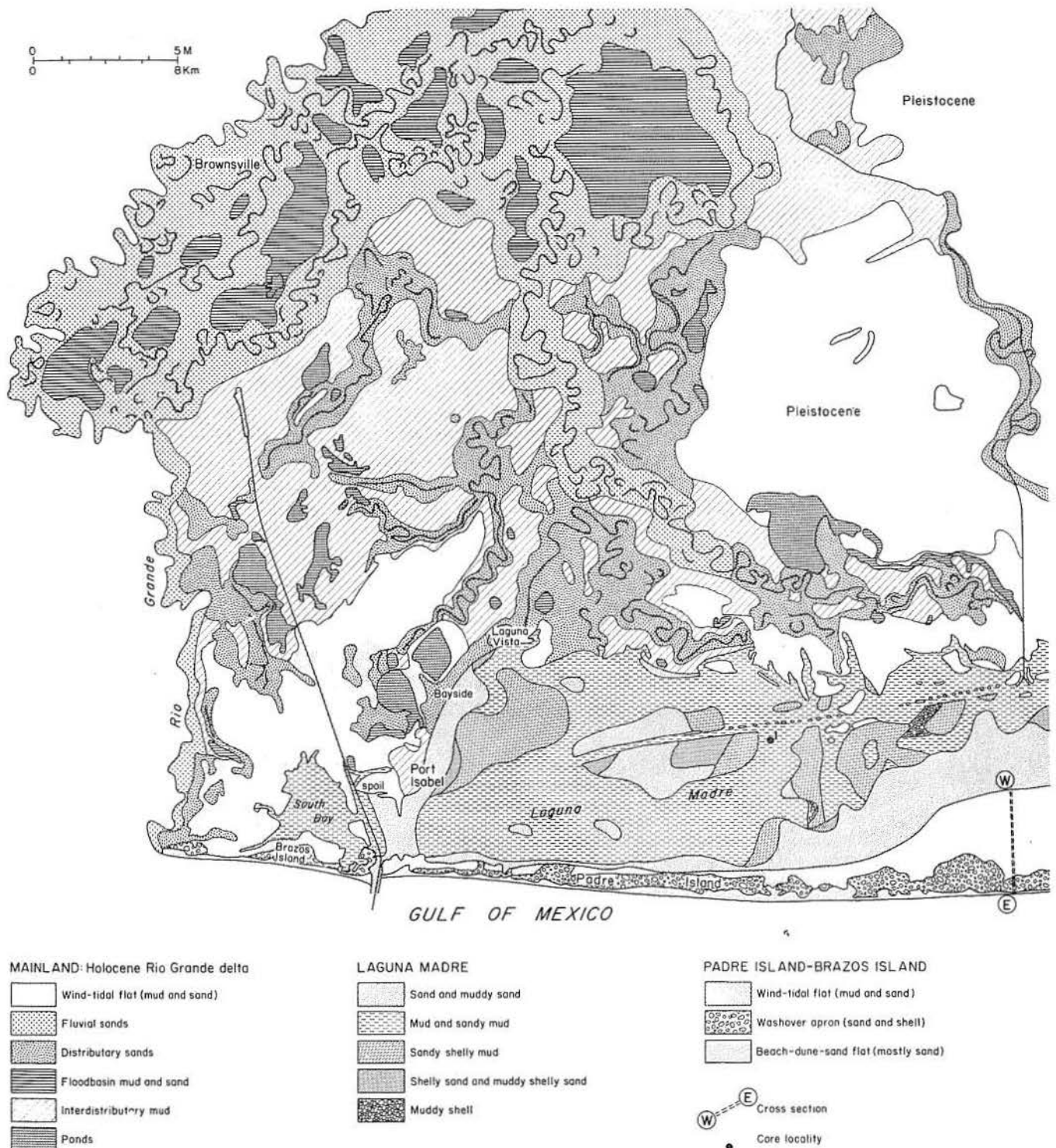


Figure 74. Holocene fluvial-deltaic facies, Brownsville-Harlingen area (after Brown and others, 1980), and surface sediment distribution (after McGowen and Morton, 1979), core localities (after Herber, in progress), and cross section (after Brown and others, 1980) south Laguna Madre, south Padre Island. Three Islands and Green Island Quadrangle.

occurs in an area once occupied by a lobe of the Holocene Rio Grande delta. As the delta foundered, wind tides inundated the area, laying down more than 4 ft (120 cm) of wind-tidal flat deposits (fig. 75). Continued subsidence exceeded sedimentation rates, and the area was flooded by lagoonal waters in which about 1 ft (30 cm) of sediment has accumulated (fig. 75, unit 1).

Vertical succession of facies from deltaic, through wind-tidal flat, to lagoonal is depicted in figure 75 (left side), and details of wind-tidal flat deposits are also depicted in figure 75 (right side).

Deltaic deposits (fig. 75, from 4.25 to 5.5 ft [1.3 to 1.7 m]) are predominantly yellowish-brown massive mud with rare silt and sand laminae. At the contact between delta-plain and wind-tidal flat facies there is an irregular bed of sugar gypsum (less than 1 inch [2.4 cm] thick at 4.25 ft [1.3 m]).

Details of wind-tidal flat facies are shown in figure 75, units 3, 4, and 6. The lower part of the wind-tidal flat facies consists of greenish-gray and light-olive-gray terrigenous mud and some impure lime mud. Algal laminae are the dominant primary sedimentary structures. Laminae are wavy and have been disrupted by desiccation cracks and deformed by gas heave. Unit 4 comprises medium-dark-gray terrigenous mud and light-olive-gray impure lime mud. Algal laminae are the dominant primary sedimentary structures. This unit is thoroughly desiccated; there are rare gypsum crystals in the lower part of the unit. The upper part of the wind-tidal flat records the longer periods of inundation (unit 3) when burrowing animals began to disrupt the bedding; this part of the wind-tidal flat sequence also received sand from south Padre Island. Unit 6 accumulated in very shallow lagoonal waters (light-olive-gray burrowed terrigenous mud and muddy sand) and on wind-tidal flats (desiccated and burrowed algal laminated terrigenous mud).

Lagoonal facies at this core locality is about 0.5 ft (15 cm) thick, comprising olive-gray, bioturbated, slightly shelly, muddy, very fine sand.

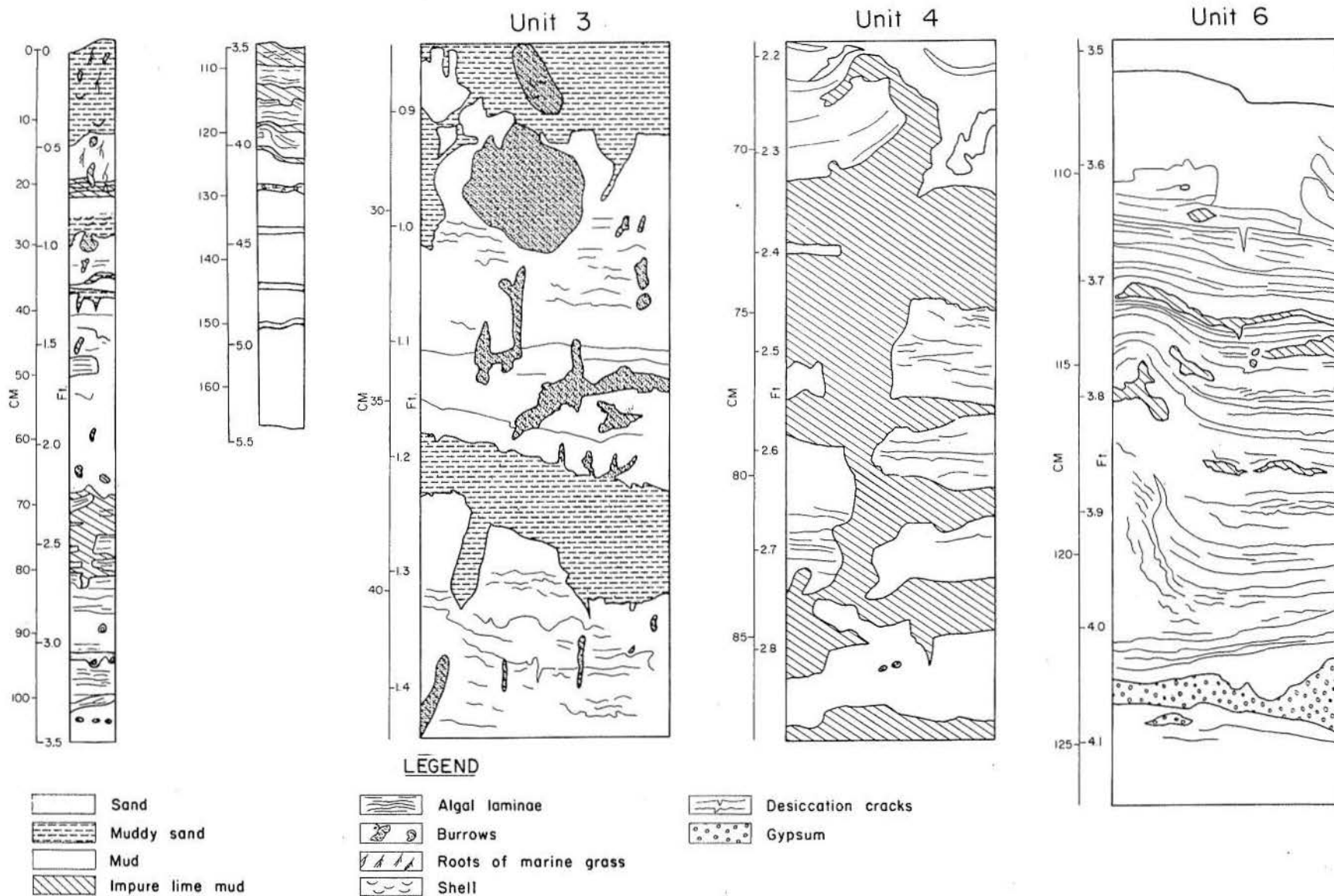


Figure 75. Core taken in south Laguna Madre (Herber, in progress). Overall facies (core on left side of fig. 75) from top to bottom are: 0.5 ft lagoonal muddy sand, 4.0 ft wind-tidal flat (sand, muddy sand, mud, and impure lime mud), and 1.25 ft dark yellowish-brown delta-plain mud with some sand laminae. Details of wind-tidal flat deposits are shown by unit 3 (from 0.9 ft to 1.4 ft), unit 4 (from 2.2 to 2.9 ft), and unit 6 (from 3.5 to 4.1 ft); depths for units 3, 4, and 6 from bottom of Laguna Madre are the same as for the core on left side of fig. 75 (see fig. 74 for core and cross-section locations).

TIDAL INLETS AND DELTAS

Introduction

Tidal inlets and associated tidal-delta deposits are controlled by such factors as tidal range and prism, bay-lagoon morphology, channel stability, substrate conditions, and inlet size. Along the Texas coast both major and minor inlets are present; some are stable, and others tend to migrate in response to littoral currents. Tidal inlets provide for the exchange of excess water caused by astronomical tides, wind-driven currents, river discharge, and storm-surge flooding. Of these factors astronomical tides have the least effect on significant changes in water level. In this microtidal environment, secondary biological structures are preserved as readily as primary stratification. Because tidal range determines thickness and extent of tidal-flat deposits, they are volumetrically least important in microtidal environments.

Major Inlets

Under natural conditions, each bay or lagoon system has a major inlet in the southwestern part of the embayment. Location and orientation of inlets are controlled primarily by longshore currents and northerly winds (Price, 1952). Inlet locations may also coincide with buried valleys that were eroded during Wisconsin glaciation.

Bolivar Roads, a major inlet, has been stable historically but modified considerably by dredging and jetty construction. Prior to modification, the ebb-tidal delta was extensive (fig. 76) and consisted of wave-sorted sand and shelly sand deposited as bars on a broad shoal 40 ft (12 m) thick. Following inlet alteration the ebb delta was destroyed. Sand eroded from the outer bar was most likely transported landward where it contributed substantially to shoreline accretion adjacent to the jetties (Morton, 1977b).

Aransas Pass - Harbor Island

Aransas Pass (fig. 1), another major inlet, was modified considerably to stop inlet migration (fig. 77) and to provide a deeper and more direct navigation route than existed naturally (fig. 78). As at Galveston, the ebb delta at Aransas Pass was destroyed, and subsequent construction and dredging have significantly altered Harbor Island (fig. 79), the flood-tidal delta. Hoover (1968) mapped surficial sediments, flora, and fauna on Harbor Island and related the facies to physical and biological processes. Subsurface lithofacies and biofacies in the vicinity of Harbor Island were reported by Munson (1975), who used these data to interpret stratigraphy and depositional events related to the Holocene rise in sea level. Vertical arrangement of bay and tidal-deltaic facies preserved in the subsurface (fig. 80) is similar to stratigraphic sequences that would be expected from brief transgressive-regressive cycles. In this sequence, the onset of transgression is marked by marsh deposits that give way to a combination of bay, tidal-flat, and tidal-delta deposits. As sea level stabilized, fine-grained

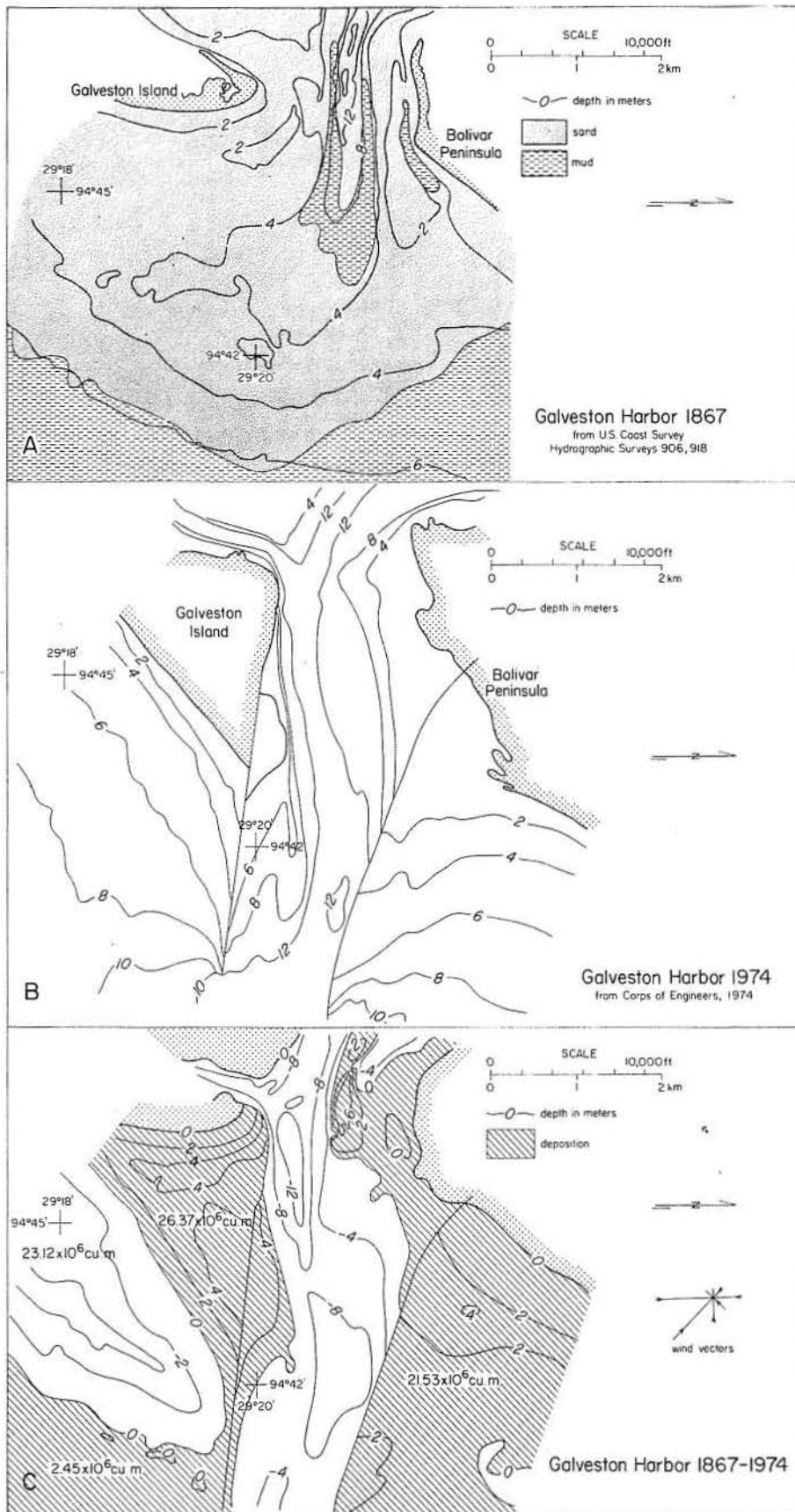


Figure 76. Ebb-delta bathymetry (in meters) and nearshore changes following modifications at Galveston Harbor (after Morton, 1977b). Galveston and Flake Quadrangles.

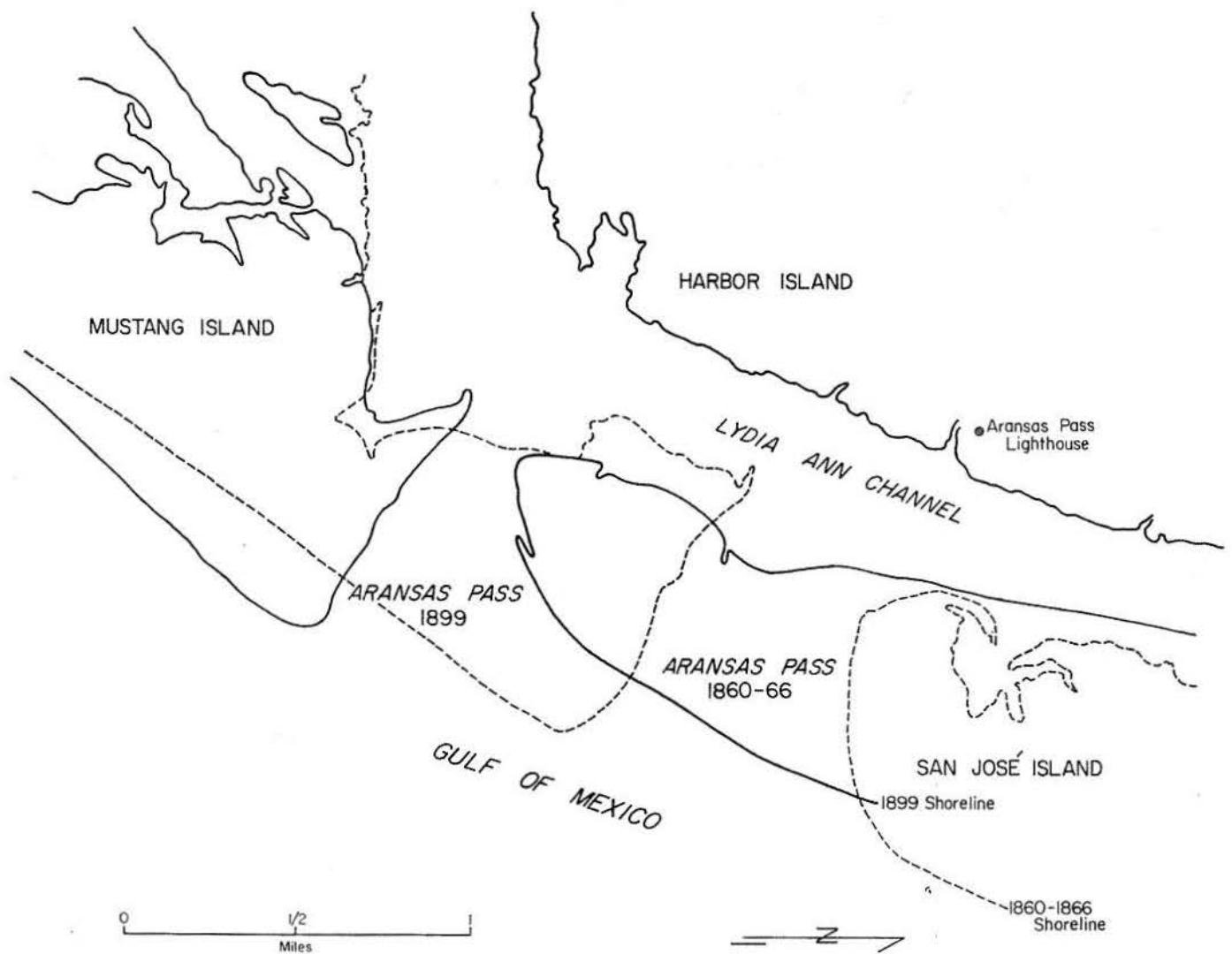


Figure 77. Migration of Aransas Pass between 1860-1866 and 1899, from U.S. Coast Survey topographic smooth sheets 823 (1860-1866) and 2354 (1899) (after Morton and Pieper, 1976).

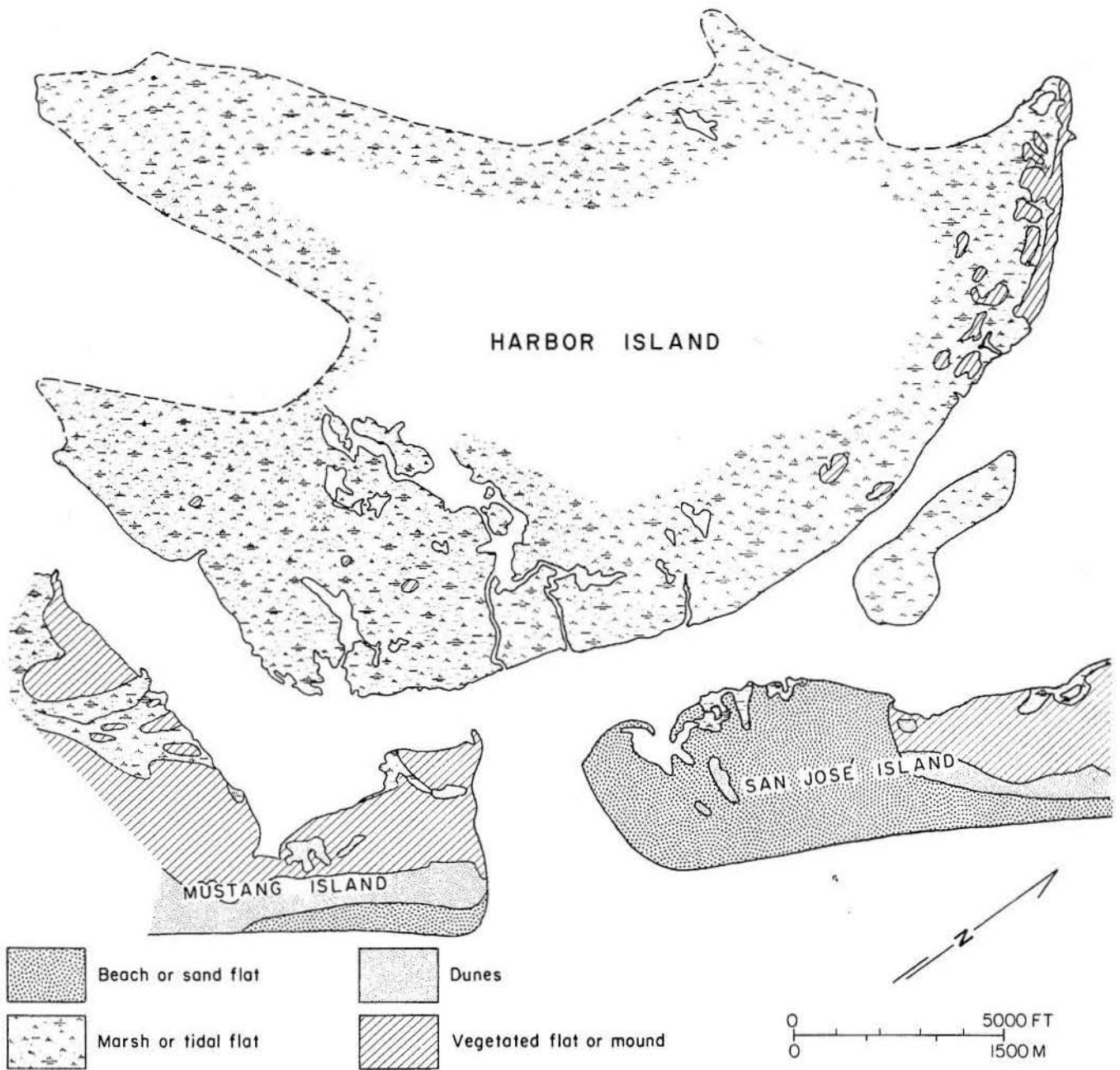


Figure 78. Subenvironments of Harbor Island and adjacent areas in 1860-1866 interpreted from U.S. Coast Survey topographic smooth sheets 823 (1860-1866) and 2354 (1899).

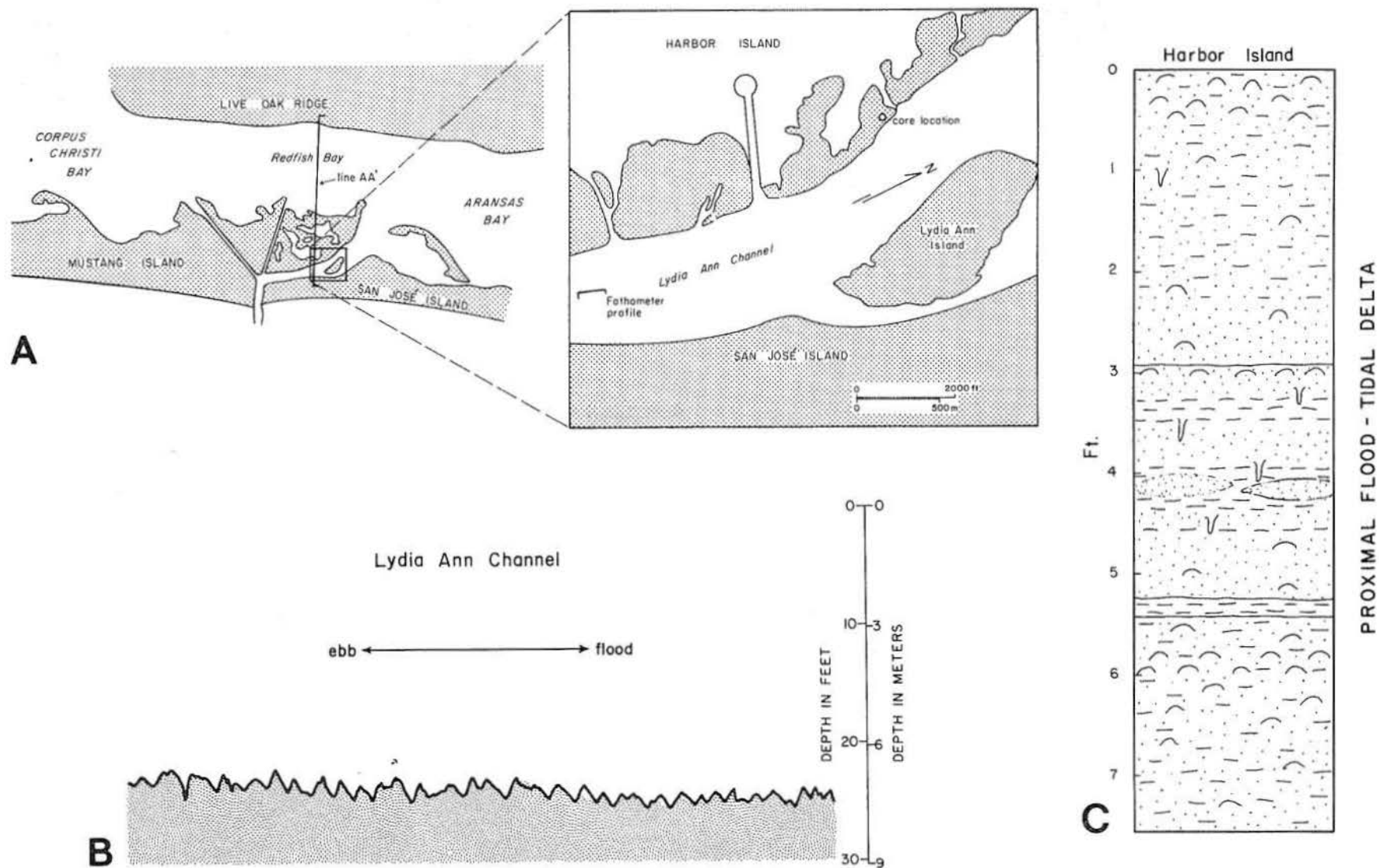


Figure 79. A. Map of Harbor Island showing locations of dip-section (after Munson, 1975), B. fathometer profile of ebb-oriented dunes, and C. uppermost sequence of proximal flood-delta facies. Port Aransas and Estes Quadrangles.

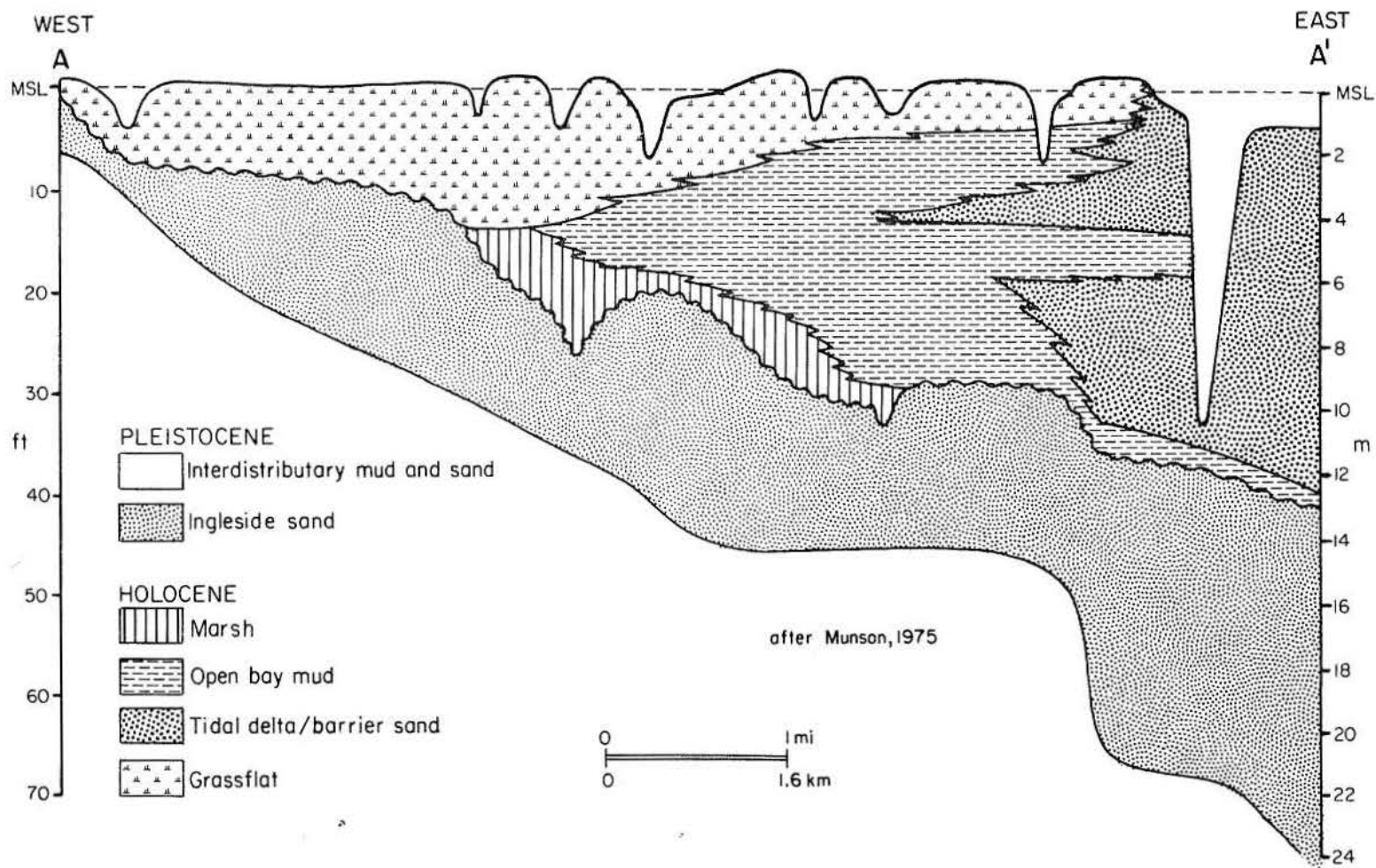


Figure 80. Dip section showing late Pleistocene and Holocene sediments beneath Harbor Island (after Munson, 1975). Line of section shown on figure 79.

sediments of marsh or similar origin were deposited. Marshes and tidal creeks that form and drain the periphery of Harbor Island are also stable as shown by comparison of older topographic surveys (fig. 78) and more recent aerial photographs.

Minor Inlets

Minor inlets such as Brown Cedar Cut (fig. 1) and Green's Bayou on Matagorda Peninsula are ephemeral. They are opened by storm washover and remain active for a few years or longer depending on subsequent meteorological events. Frequent storms tend to keep these inlets open, whereas prolonged non-storm or drought periods contribute to inlet closing. Wave energy precludes development of extensive ebb deposits, but bay deposits associated with minor inlets are transitional mid-point features in the spectrum from washover fans to flood-tidal deltas.

Brown Cedar Cut

Formation and growth of Brown Cedar Cut was documented in detail by Mason and Sorensen (1971) and Piety (1972), who used numerous nautical charts and aerial photographs to trace the development and migration of a minor inlet and flood delta. Matagorda Peninsula was breached by Brown Cedar Cut about 50 years ago; consequently, tidal-delta facies are thin (fig. 81) and lack some characteristics of mature flood-tidal deltas. In this regard, Brown Cedar Cut is typical of intermediate stages of tidal-delta evolution when shoals become subaerial and channels are partly stabilized by vegetation and fine-grained sediments (Morton and Donaldson, 1973).

A thin transgressive sequence (fig. 81) records submergence of the Holocene Colorado delta followed by deposition of bay muds and later progradation of a washover-flood delta system. Rates of shoreline retreat and depths of scour for Matagorda Peninsula suggest that preservation of these thin flood-delta deposits is unlikely; however, preservation of flood-deltas associated with marine transgressions would be enhanced if tidal range and inlet size were greater.

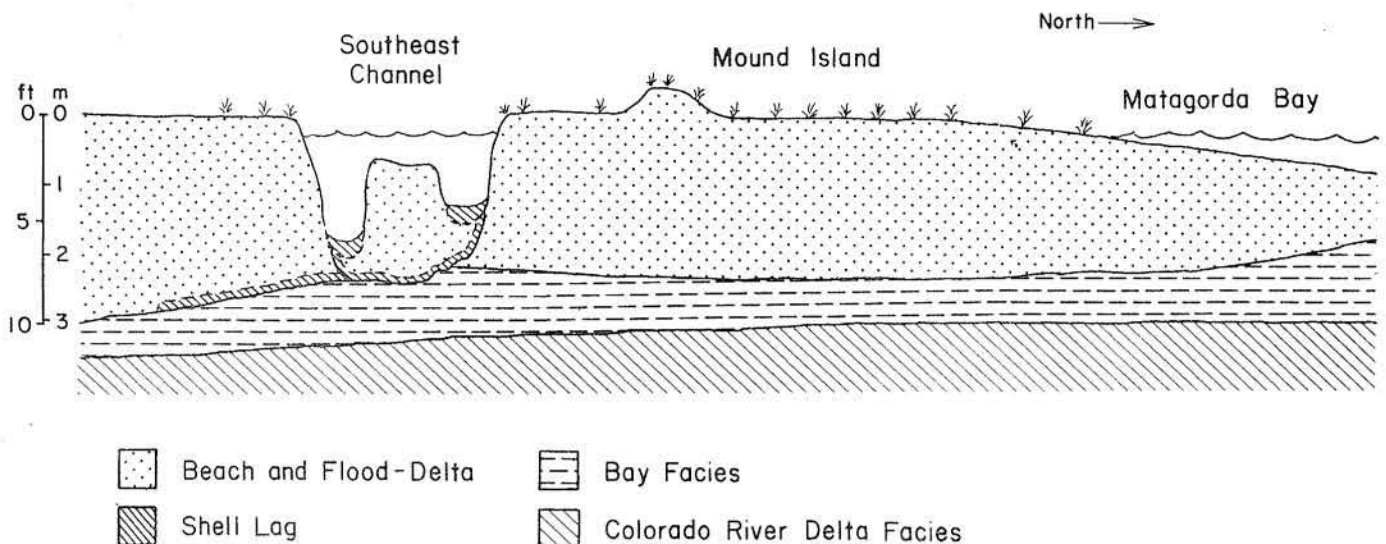


Figure 81. Dip section through flood-delta and underlying sediments, Brown Cedar Cut (after Piety, 1972). Brown Cedar Cut Quadrangle.

Packery Channel Area

The tidal inlet between Mustang Island and northern Padre Island (fig. 1) was closed in 1929 as a consequence of human activities in north Laguna Madre and Corpus Christi Bay (Price, 1952). Numerous maps and surveys indicate that the natural pass (shown as Corpus Christi Pass, fig. 82) was very long, narrow, and inefficient. The pass would have been closed, because of its configuration, had it not migrated to the southeastern part of Corpus Christi Bay (Price, 1952). This was the stable position for Corpus Christi Pass as strong currents were funneled through the inlet by strong north winds.

Although the position and alignment of Corpus Christi Pass (fig. 82) represent the stable configuration, the southern tip of Mustang Island was repeatedly breached by storm surges associated with hurricanes (Packery Channel, shown on fig. 82, is a storm surge channel). The southern tip of Mustang Island was easily breached by storms because of the low profile at the accretionary end of the island (McGowen and Scott, 1975). Storm-surge channels were scoured the shortest distance across Mustang Island as this position maximized water exchange between the Gulf of Mexico and north Laguna Madre - Corpus Christi Bay.

The flood-tidal delta associated with Corpus Christi Pass was initiated as several small islands within Laguna Madre near the point where the tidal pass bifurcated (fig. 83). Through time the islands coalesced to form a large flood delta. Eventually the flood-tidal delta became asymmetrical and was attached to the upcurrent, lagoonward end of north Padre Island; this sequence of events transpired because south-flowing longshore currents elongated the tidal channel (the mouth of the inlet was displaced southward about 4 mi [6.4 km] south of its presumed point of origin).

Tidal-inlet facies: Corpus Christi Pass - Packery Channel area

Hayes and Kana (1976, p. 1-58) state that there are three principal sand units associated with inlets: ebb-tidal deltas, flood-tidal deltas, and recurved spit-inlet fill sediment associated with inlet migration. Because of the low tidal range and dominance of wave activity along the Texas Gulf Coast, ebb deltas are not well developed and the potential for them to be preserved in the geologic record is negligible. Ancient flood-delta deposits and inlet-fill facies have been recognized in the Wilcox Indio Lagoonal System (Fisher and McGowen, 1969).

A vertical sequence of stratification types is shown by Hayes and Kana (1976, p. 1-66, fig. 74) for tidal channel, flood-tidal delta, and mud flat. Channel facies include ebb channel fill (about 10 ft [3 m] thick) consisting of ebb-oriented planar cross-bedding and some bidirectional trough crossbeds (bed forms were sand waves and dunes), and flood channel (about 6 ft [1.8 m] thick) consisting of flood-oriented planar crossbedding (bed forms were sand waves). Flood-tidal delta facies overlie the inlet channel facies. Flood-tidal delta facies consist of about 16 ft (5 m) of bidirectional trough crossbeds and flood-oriented planar crossbeds (bed forms were dunes and sand waves). Parts of tidal-flat and salt-marsh facies cap the sequence. In general, the trend is an upward decrease in scale of sedimentation units; only two stratification types are reported. Although textural trends were not reported, it is assumed that grain size decreases upward.

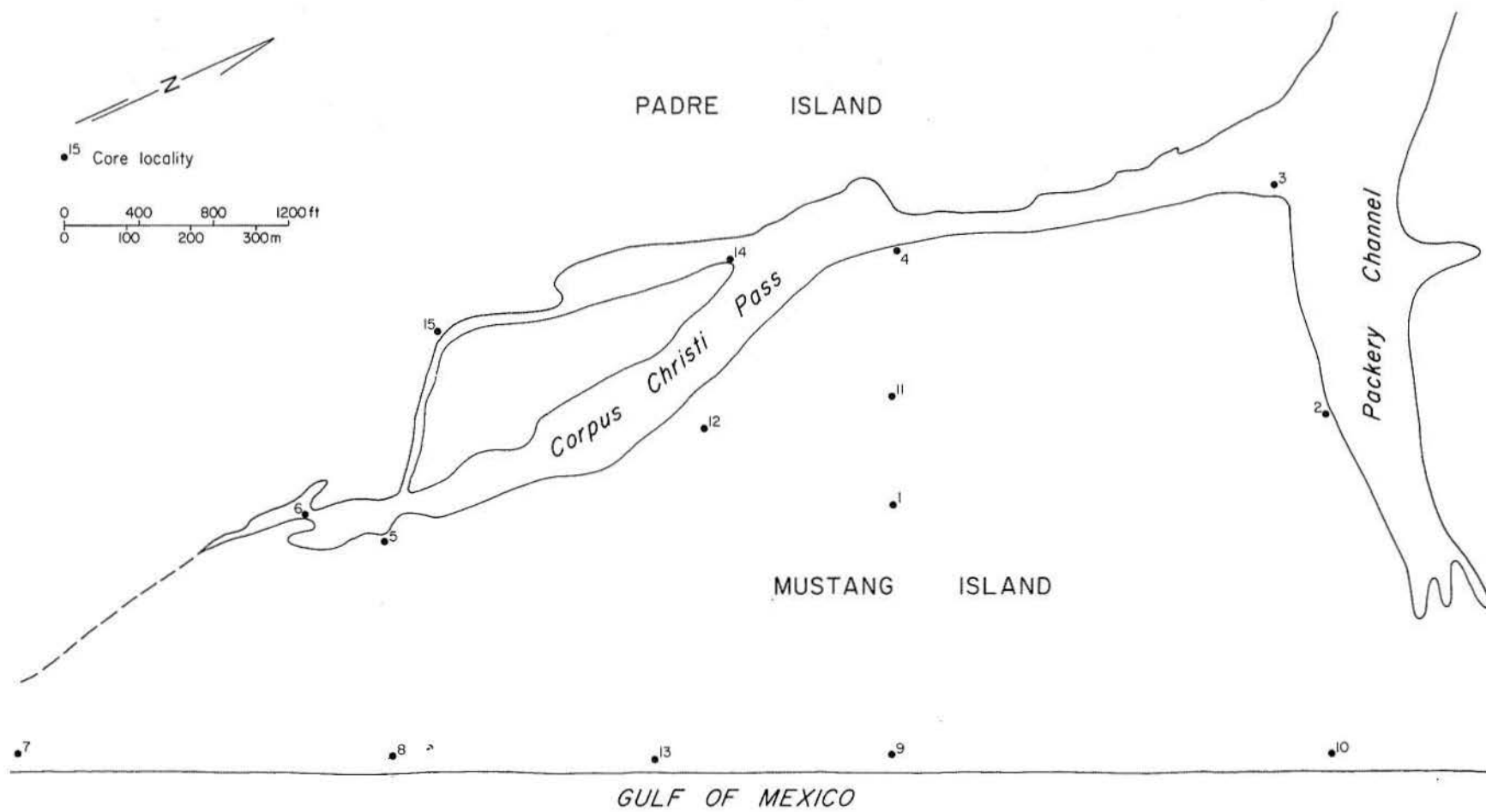


Figure 82. Corpus Christi Pass - Packery Channel area with wash-down hole locations. Crane Islands Quadrangle.

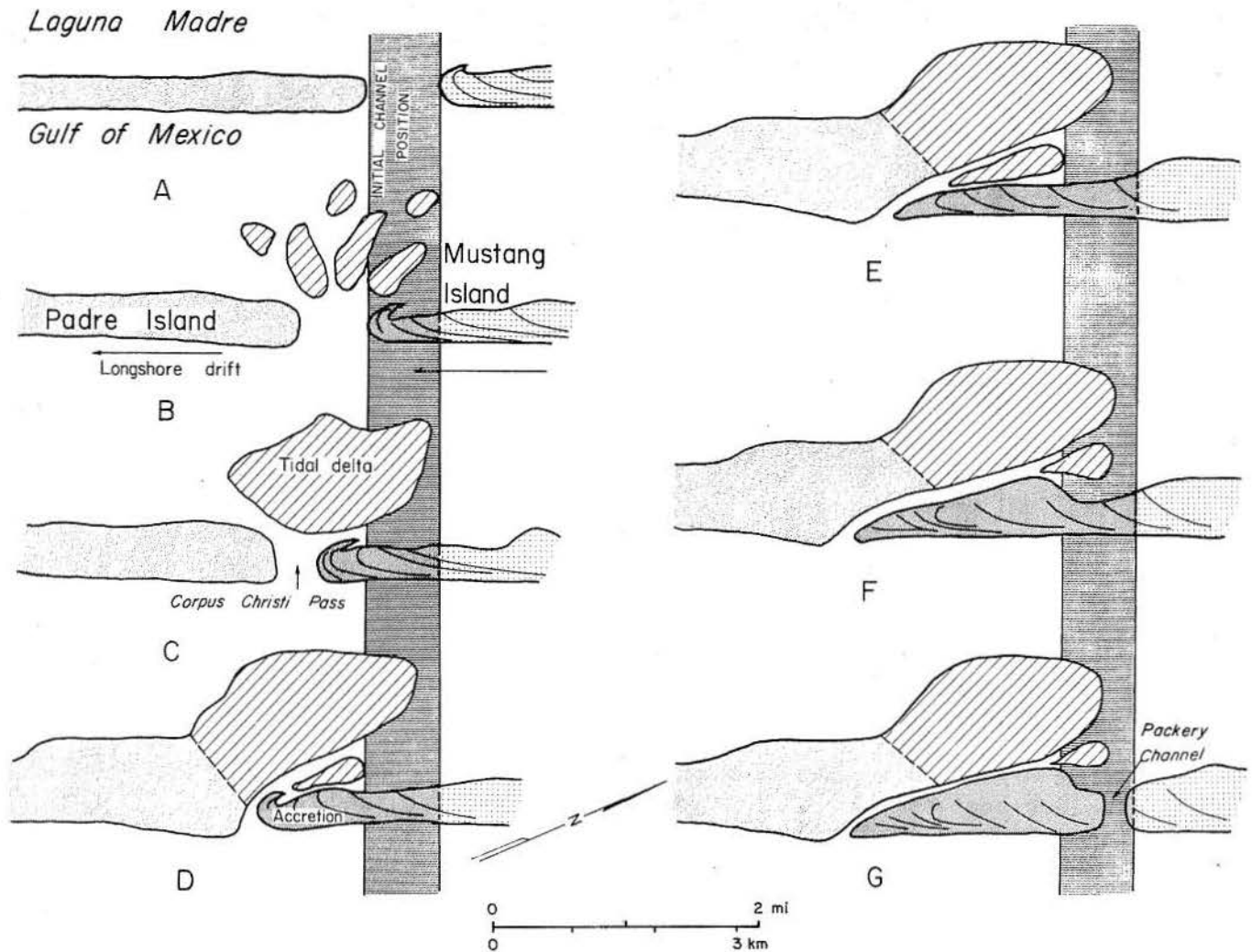


Figure 83. Evolution of Packery Channel area: northern Padre Island - southern Mustang Island, Corpus Christi Pass, a tidal inlet closed in 1929 as a consequence of altering circulation pattern in northern Laguna Madre by dredging. Location of Corpus Christi Pass is shown in stages A through G. Stage A represents initial inlet location shortly after stillstand. Stages B through F illustrate southward migration of Corpus Christi Pass with spit accretion on south Mustang Island and erosion of north Padre Island. Ebb tidal delta develops and becomes attached to north Padre Island at stage D. Corpus Christi Pass lengthened, became inefficient, and southern tip of Mustang Island was breached by storm channel, Packery Channel, at stage G (after McGowen and Scott, 1975).

Corpus Christi Pass - Packery Channel represents (1) filled tidal inlet, (2) filled storm-surge channels (these are periodically reopened), (3) flood-tidal delta, and (4) lagoonal facies. Because of frequent breaching of the southern tip of Mustang Island by storm surge channels which then became the tidal inlet that migrated rapidly southward (driven by longshore currents), some features have been observed here that were not reported by Hayes and Kana (1976). Nevertheless, the general vertical decreases in grain size and scale of sedimentation units also characterize the Corpus Christi Pass - Packery Channel tidal-inlet deposits.

One dip and one strike cross section (figs. 84 and 85) illustrate facies associations and sediment characteristics of the filled Corpus Christi Pass. Data from which these cross sections were constructed were derived from 15 washdown holes that penetrated the Holocene section, the Pleistocene Ingleside barrier island - strandplain sand, and, in a few holes, a few feet of the Pleistocene Nueces delta system. In addition to the 15 washdown holes, 8 continuous cores were taken through the Holocene section and the Pleistocene barrier island - strandplain sand.

The area investigated (fig. 82) did not include the flood-tidal delta. The sands that overlie the inlet facies are shoreface, beach, vegetated barrier flat, washover fans, and dune sands. Corpus Christi Pass was scoured to a depth of about 22 ft (6.6 m) below m.s.l. Facies through which it cut (in the area studied) are mostly bay and lagoonal.

Near the Gulf shoreline inlet channel fill consists of as many as five fining-upward sequences beginning with a shell-gravel lag grading upward into fine sand and slightly shelly fine sand. As the channel migrated southward it became elongate and less efficient. In these channel segments finer grained sediment accumulated (fig. 84, core localities 1 and 11). Mud and muddy sand are interbedded with clean sand and shelly sand. Generally, as the inlet channel fill becomes muddier, bay molluscan species become dominant.

The strike section (fig. 85) depicts a filled channel (locality 3), an inactive but water-filled inlet channel (between localities 4 and 14), a sand-filled inlet channel sequence (between localities 14 and 15), and the older bay-lagoon deposits capped by wind-tidal flat and washover fan deposits (between localities 3 and 4). The inlet channel fill between localities 14 and 15 indicates a channel that was alternately active (shelly sand with Gulf species) and inactive (burrowed muddy sand with bay species).

Bay-lagoonal facies (between localities 3 and 4) accumulated mostly under hypersaline conditions as indicated from faunal evidence. Bay-lagoonal deposits are predominantly sand and muddy sand with varying amounts of shell material. At least three episodes of grassflat development are recorded in the bay-lagoonal deposits.

Radiocarbon ages were obtained from the lagoonal deposits (fig. 85, locality 4) at a depth of 15 to 17 ft (4.5 to 5.1 m) below ground level. An age of 4,580 to 4,360 years B.P. is indicated for these deposits. Radiocarbon ages were also obtained from wood in the inlet channel fill (fig. 85, locality 3) at depths of 6 to 11 ft (1.8 to 3.3 m) below ground level; an age of about 1,160 to 640 years B.P. is indicated for these deposits.

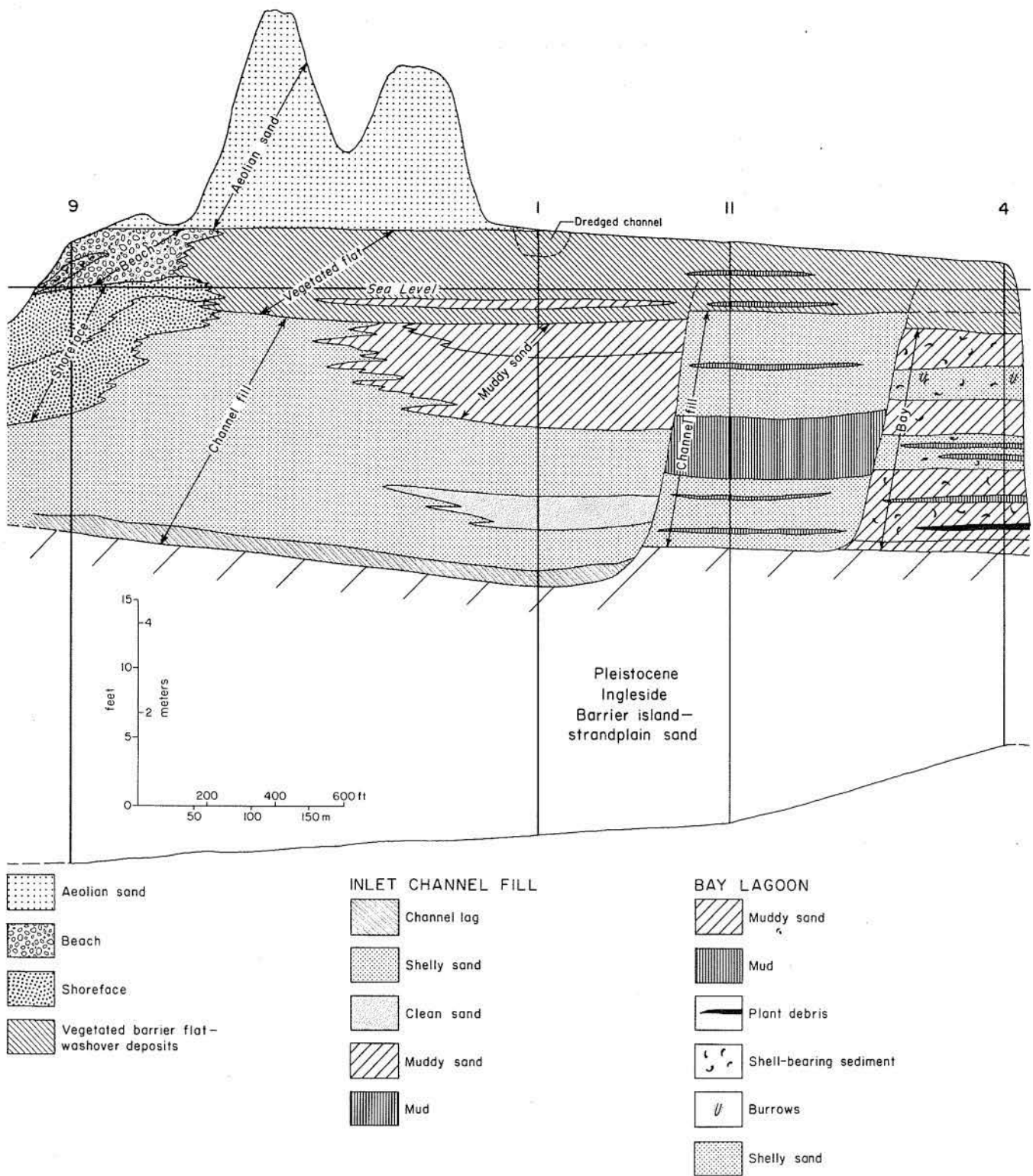


Figure 84. Dip section across Packery Channel area.

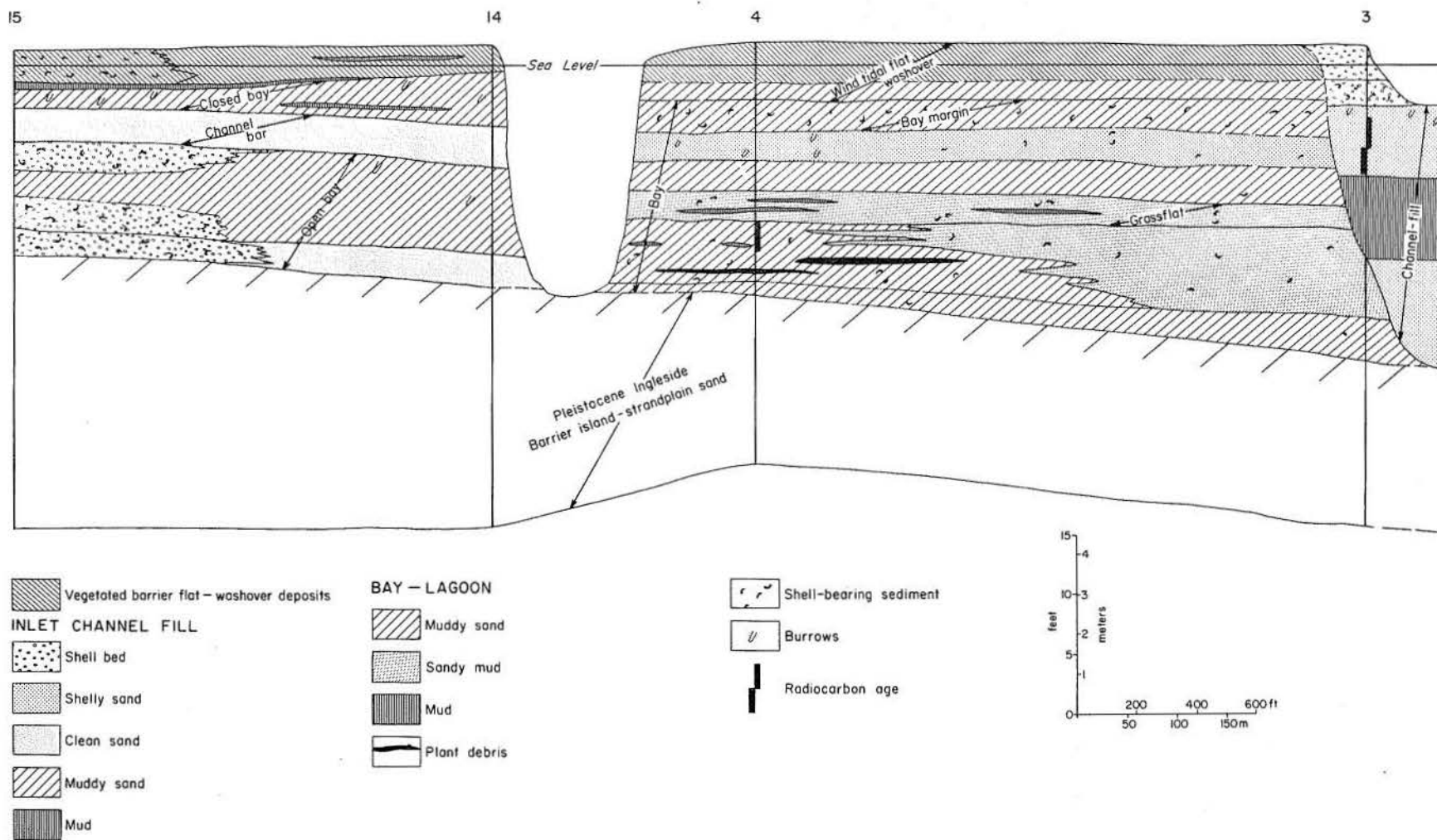


Figure 85. Strike section across Packery Channel area.

Tidal-Inlet and Delta Facies

Tidal-inlet and flood-tidal delta deposits are similar to their riverine counterparts. For example, both deltas coarsen upward to a sand facies that is overlain by finer grained sediments. Tidal and fluvial channels have erosional basal contacts with gravel lag overlain by fining-upward sequences. Low tidal velocities and concomitant low rates of sedimentation in conjunction with high biological activity contribute to extensive bioturbation of tidal deposits.

Tidal Channels

Major inlets in microtidal environments scour to depths of 30 to 35 ft (9 to 10 m) (fig. 76 and 86). Therefore, sediments deposited during inlet migration should be of comparable thickness. Because of the complex processes and existing sediment sizes, vertical textural variations may not be systematic. Littoral sands are fine grained and well sorted; thus, major textural differences are attributed to variations in shell and mud content. Mud is less likely to be preserved than shell in tidal channels although shifting shoals can create slack water areas in which mud is deposited (fig. 76). Mud is also deposited by weak currents where tidal channels merge with the lagoonal floor. Bed forms in tidal channels are nearly symmetrical or ebb oriented owing to slightly higher ebb velocities. Bed forms are not present in fine-grained sediments (sandy mud and mud), but dunes may develop in sand-floored channels (fig. 79). A core in tidal channel fill from San Luis Pass (Bernard and others, 1970) shows normally graded sequences of shell and sand, homogeneous sand, faint horizontal laminations, and burrow-mottled sand. Gravel-sized shell and overlying sand and muddy sand indicate that the vertical sequence fines upward. Piety (1972) observed trough cross-stratification interbedded with muddy fine sand in tidal-channel deposits.

Ebb-Tidal Deltas

In microtidal environments, wave energy is sufficiently greater than tidal currents so that ebb deltas are simple in plan, subaqueous, and of limited areal extent (figs. 76 and 86). Ebb deltas are composed almost entirely of sand and shell. Sand thickness depends on water depths, chiefly a function of shoreface slope, and depositional history. Ebb-delta deposits at minor inlets, or associated with transgressive barriers (figs. 81 and 86) are apt to be thin (20 ft [6 m]) and in abrupt contact with underlying bay-lagoon or deltaic mud. Ebb deltas connected with accretionary barriers tend to be thick (up to 40 ft [12 m]) and have gradational contacts with underlying shoreface deposits. Regardless of thickness, ebb deltas have low preservation potential.

Flood-Tidal Deltas

In sand facies of flood-tidal deltas, trough crossbedding, graded beds, and shell layers are typical structures. The graded beds and shell layers represent storm

deposits. In addition to these features, burrow-mottled sands and shelly sands are also common. On Harbor Island (fig. 79), the upper 7.5 ft (2.3 m) of sediment are characterized by olive-gray to medium-dark-gray muddy sand and sand with shell fragments concentrated in layers and disseminated throughout the sediment. Sand exposed above the water table is oxidized and contrasts sharply with underlying sediments that are darker and reduced. Horizontal stratification is faintly visible throughout the core except where burrow mottling is predominant.

Bed forms of incipient flood deltas include ripples, dunes, and transverse bars. These small- and large-scale features give rise to ripple laminations, trough cross-stratification, low-angle foresets, and uniform horizontal laminations.

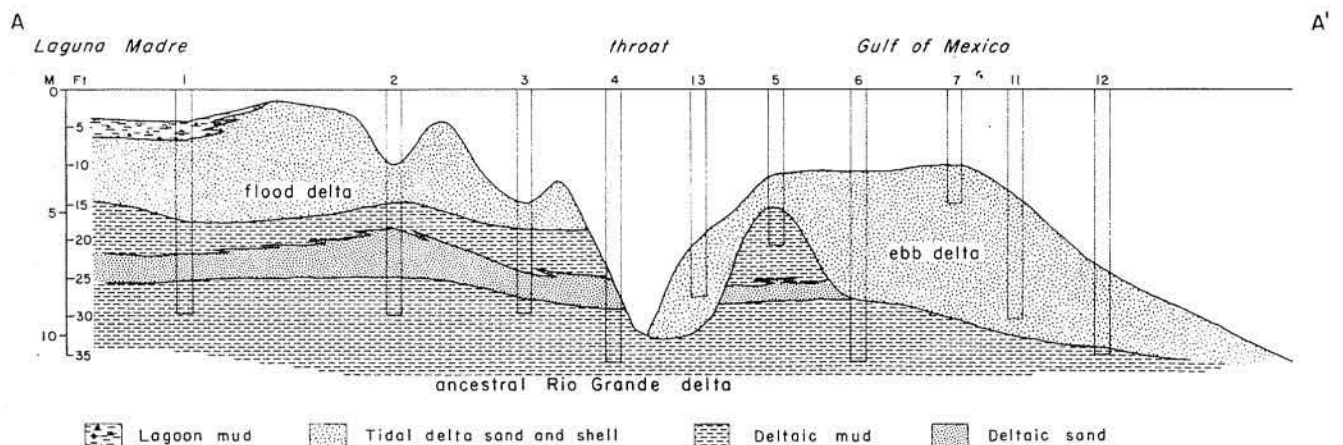
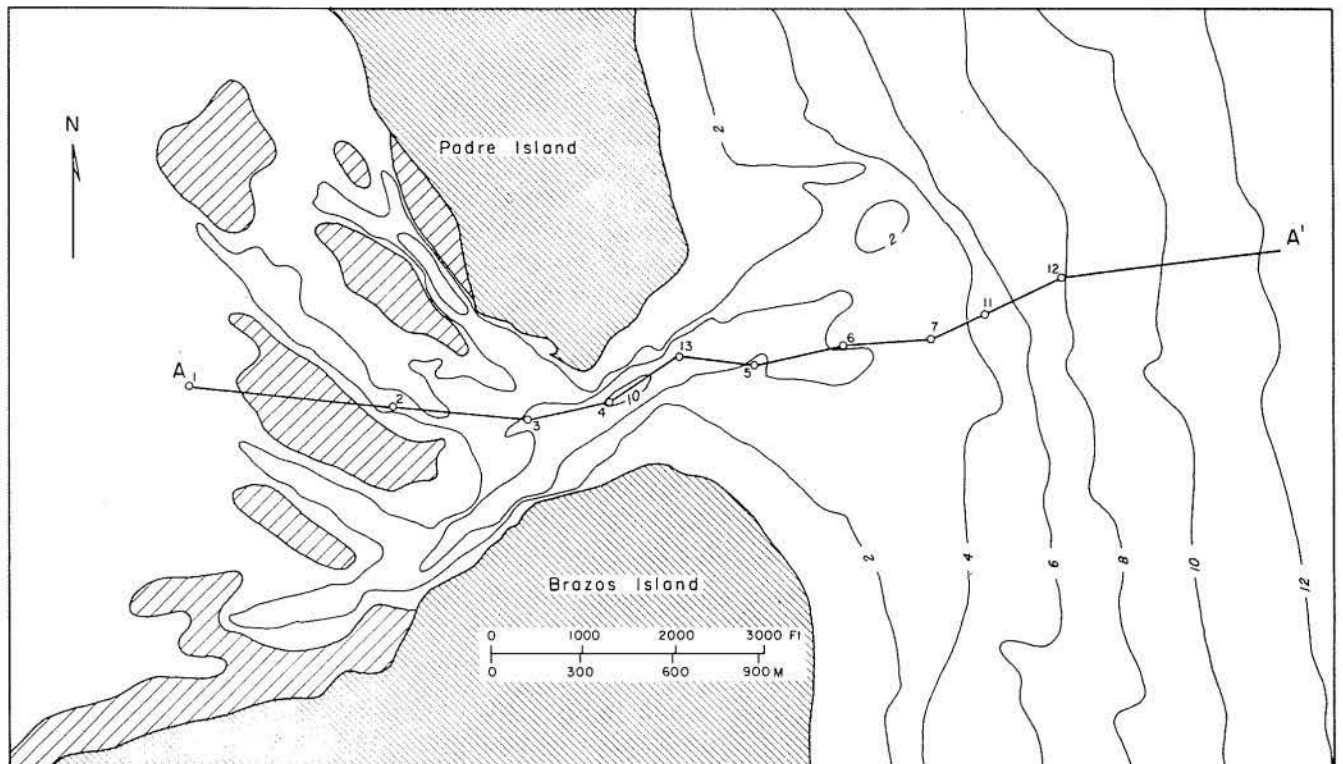


Figure 86. Tidal-delta bathymetry (in meters), channels, and shoals at Brazos-Santiago Pass, a microtidal inlet. Dip section of ebb-delta and flood-delta deposits and underlying fluvial-deltaic sediments interpreted from U.S. Army Corps of Engineers (1919). Port Isabel Quadrangle.

BARRIER ISLANDS AND PENINSULAS

Introduction

About 80 percent of the Texas Gulf Coast is composed of barrier islands and peninsulas. Morphologies of these two landforms vary systematically coastwide, and they are transitional with deltaic headlands (fig. 87), the third major physiographic unit (McGowen and others, 1977). Barriers have either high or low profiles (fig. 88), depending on dune height and continuity, size and spacing of hurricane washover channels, barrier-flat morphology, barrier width, and other factors that reflect shoreline evolution and development since sea-level stillstand.

Along the Texas coast, erosional (transgressive) and accretionary (regressive) landforms occupy orderly positions and are nearly equally represented (Morton, 1979b). Low-profile barriers are relatively young transgressive landforms when compared with adjacent high-profile barriers that are accretionary or stable landforms. These spatial relationships are best explained in a regional context whereby erosional deltaic headlands are flanked by transgressive barriers that, in turn, grade laterally into regressive barriers formed in interdeltatic bights (Morton, 1977a).

Morphologies and geometries of barriers also differ. Most low-profile barriers (fig. 88) are characterized by (1) narrow widths; (2) low, sparsely vegetated discontin-

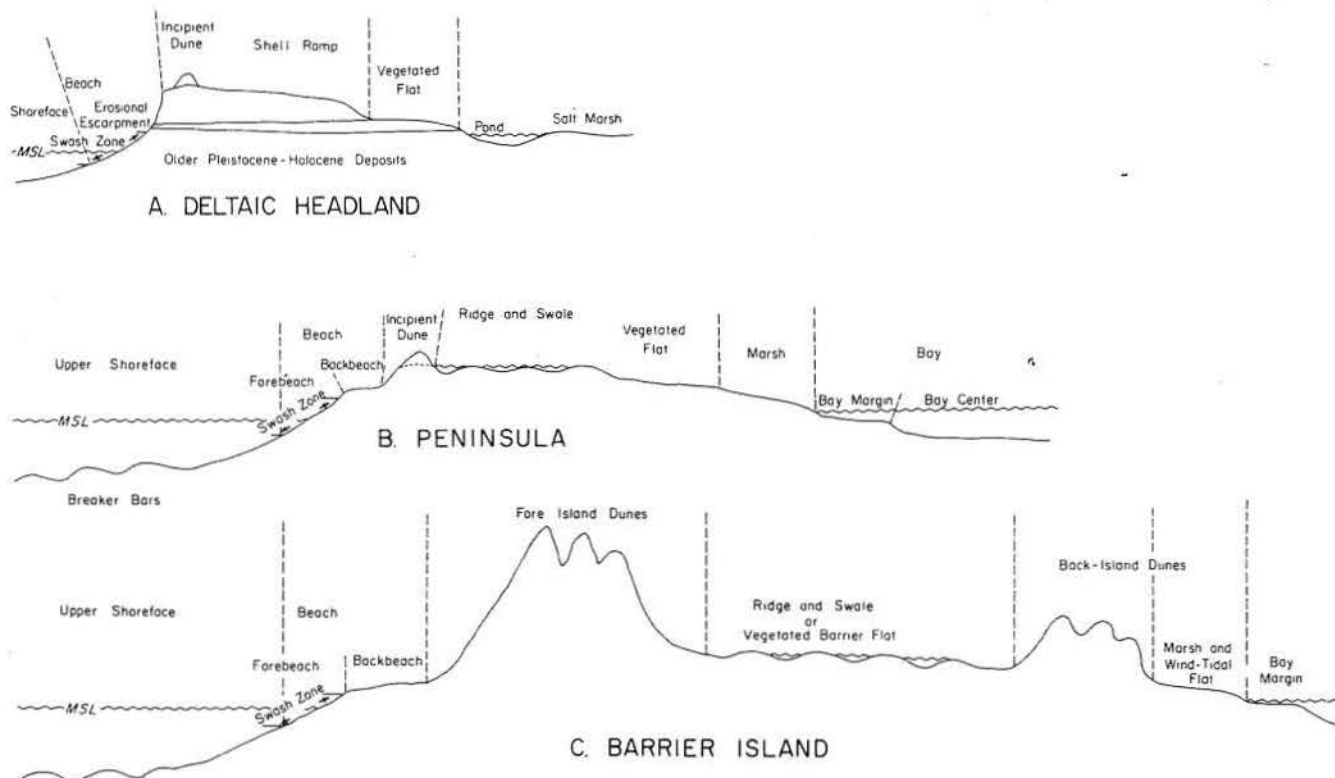
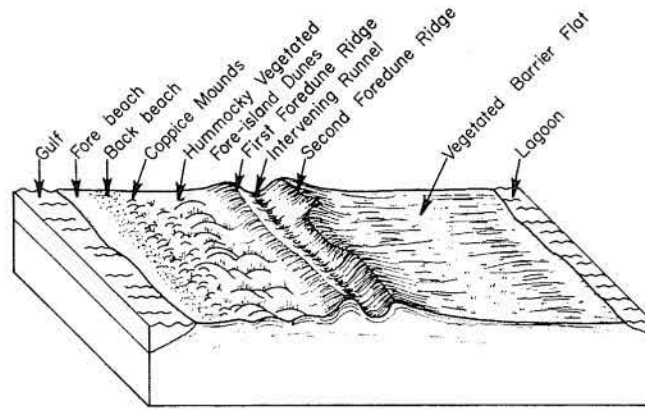


Figure 87. Generalized profiles across shoreline features associated with (A) erosional deltaic headlands, (B) peninsulas, and (C) barrier islands (after McGowen, Garner, and Wilkinson, 1977).

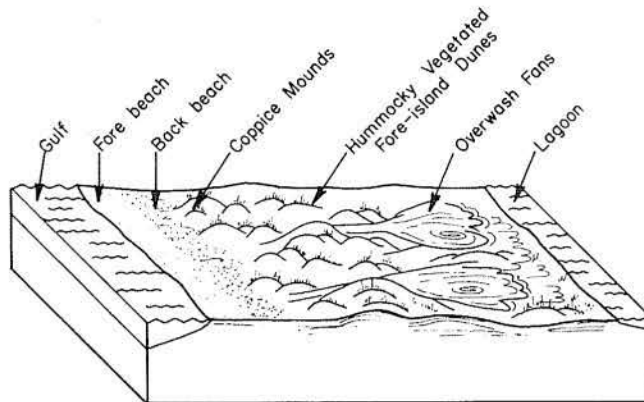
uous dunes; (3) numerous, closely spaced active washover channels; and (4) thin sand cores overlying stiff deltaic muds. In contrast, most high-profile barriers (fig. 88) are characterized by (1) broad widths; (2) high, continuous, well-vegetated fore-island dunes; (3) few, if any, active washover channels; (4) parallel accretion ridges; and (5) relatively thick sand cores (fig. 89) usually directly overlying or only a few feet above Pleistocene strandplain deposits. The latter were primary sources of sand that supplied vertical and seaward accretion of the barriers (McGowen and others, 1977).

Barrier-Island Facies

Subenvironments and equivalent facies of barrier islands are largely controlled by the interdependency of elevation, location, and attendant physical processes. As shown in figure 90, barrier subenvironments are arranged in a predictable pattern.



High-Profile Barrier Island



Low-Profile Barrier Island

transgressional

Figure 88. Generalized diagram of high- and low-profile barrier-island environments (after White and others, 1978).

Shoreface

The shoreface extends from submarine depths of about 30 to 40 ft (9 to 12 m), to the intertidal zone. Landward increases in physical energy across the shoreface are reflected in slope, morphology, and sediment textures. Lower shoreface muds and sandy muds are smooth and merge seaward with featureless muddy slopes of the inner continental shelf. The upper shoreface, however, is a dynamic area where bars are constructed and destroyed or driven landward by wave processes in conjunction with tidal and wind-driven currents. Upper shoreface sediments are typically fine to very fine sand with local concentrations of shell. If preserved, the sedimentary structures are low-angle, parallel-inclined laminations, irregular scour and fill, and stratification types formed by vertical accretion and migration of breaker bars and troughs. These include horizontal parallel laminations of the bar crest as well as ripple cross-laminations and foresets. On high-energy coasts that experience seasonal changes, physical structures are commonly preserved; however, on low-energy coasts, such as the Gulf Coast, abundant nearshore infauna effectively rework the sediments and destroy much of the stratification.

Beach

Slopes also serve to distinguish the forebeach and backbeach, which are separated by the berm. Forebeach slopes are 1° to 2° seaward and transitional with the upper shoreface, whereas backbeach slopes are nearly flat, except following storms; along Big Shell Beach where the setting is unusual, backbeach slopes are landward.

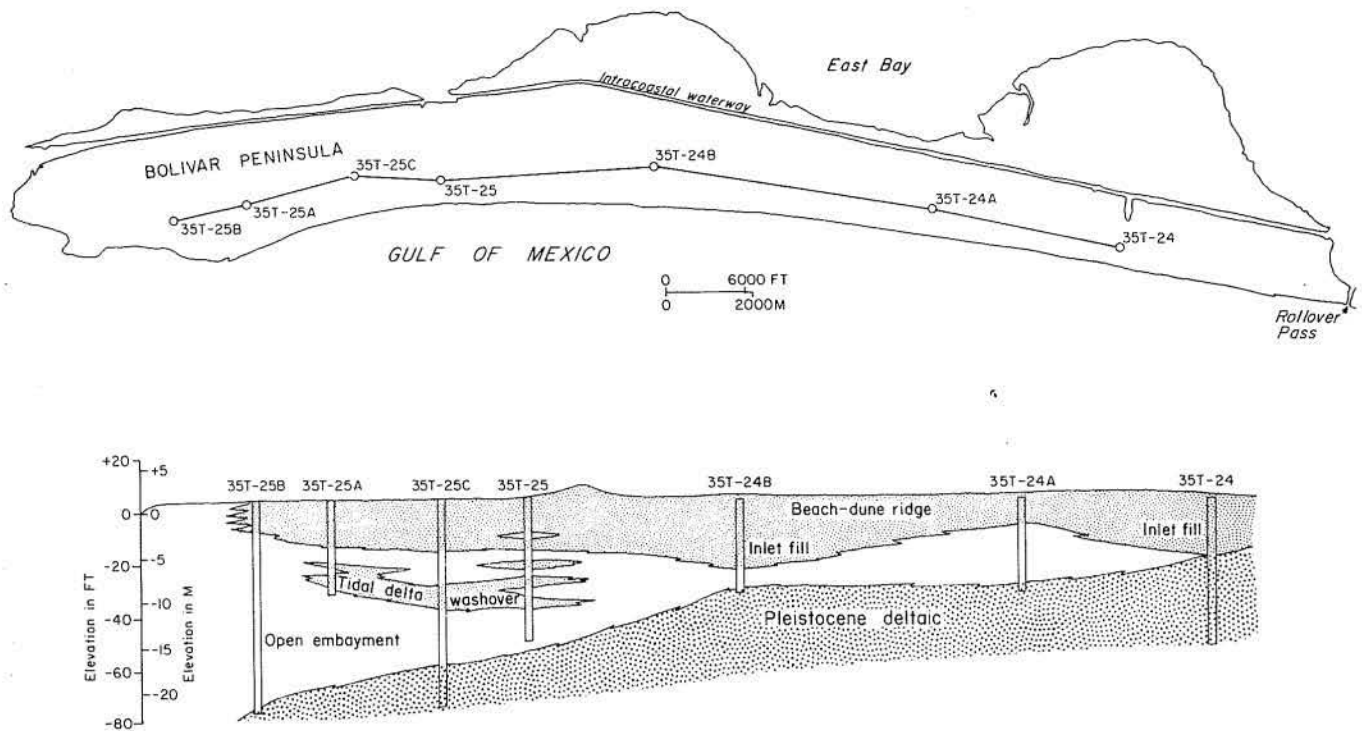


Figure 89. Strike section showing late Pleistocene and Holocene sediments beneath Bolivar Peninsula. Data interpreted from U.S. Army Corps of Engineers (1972). Flake Quadrangle.

Sedimentary structures and textural variations of forebeaches are produced by wave upwash and backwash. Sediments are mostly fine to very fine sand with some shell. Shell is locally concentrated (1) along berm crests, generally the limit of wave runup, (2) on horns of beach cusps, and (3) at the forebeach toe where opposing wave forces meet. Forebeach bed forms are mainly two-dimensional and ephemeral. Shallow flow depths and steep slopes contribute to formation of transition and upper flow regime antidunes and rhomboid ripples; occasionally straight crested ripples are formed. Extremely low bed-form amplitudes typically produce gently inclined parallel laminations often made visible by concentrations of heavy minerals or shell fragments. Burrowing by surf clams (*Donax* sp.) and ghost shrimp (*Calianassa major*), however, may disrupt the stratification.

Backbeach sediments are deposited by higher than normal waves and tides, excessive rainfall, and aeolian processes. The latter modify backbeach surfaces but contribute little to vertical accretion. Except for low wind-shadow dunes, backbeach surfaces are smooth, and internal stratification is faint. Rills formed by flood runoff may produce scour and fill structures.

Fore-Island Dunes

Foredunes and dune ridges form landward of the backbeach above the level of highest spring tides. These dunes are stabilized by salt-tolerant vegetation that thrives on water contained within the dunes; moisture is maintained by dew and rainfall. Under conditions of persistent winds and low rainfall, dunes can grow rapidly. Both vertical and lateral accretion is aided by flourishing grasses. If vegetation is weakened or destroyed, blowouts or active dunes may be initiated.

Foredunes provide the highest topographic elevations on barriers. Dune ridges are consistently 15 to 20 ft (4.5 to 6 m) high, although isolated peaks may be as high as 50 ft (15 m). Dune sediments are well-sorted fine to very fine sand with minor amounts of fine shell fragments.

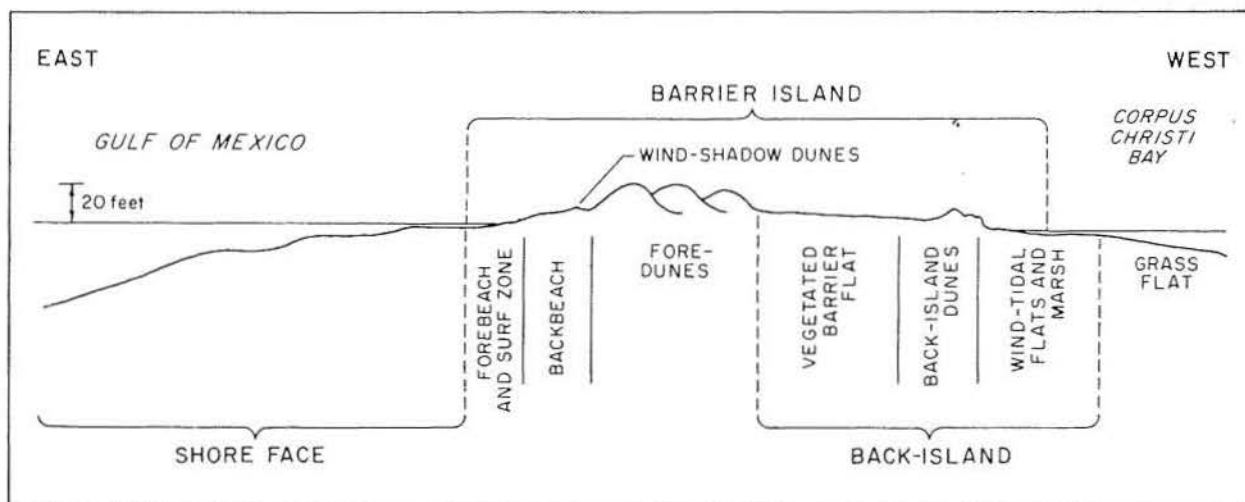


Figure 90. Generalized barrier-island (Mustang Island) profile (after Scott and others, 1964).

Wedge-shaped foresets with minor trough-fill cross-strata exhibit bimodal dip direction in response to dune morphology (McBride and Hayes, 1962) and dominant southeasterly winds (Hayes, 1967).

Vegetated Barrier Flats

Vegetated flats are a principal barrier subenvironment. Surface morphology is ramplike with elevations increasing toward the foredunes and decreasing toward the lagoon. Dense stands of grasses and other fresh-water biota are supported by a shallow aquifer. Accretion ridges and intervening swales formed by beach and dune sands (Beal and Shepard, 1956) characterize vegetated flats of upper and central coast barriers. In contrast, hummocky topography prevails over most barrier flats from Mustang to central Padre Island. Hummocks and concentric patterns of vegetated low ridges and barren sand attest to dune migration and subsequent deflation as the water table periodically fluctuates (Hunter and Dickinson, 1970). Trenches in vegetated barrier flats show structureless fine sand with root traces and rodent burrows.

Active Dunes

Extensive fields of barren mobile sand migrate across some barriers under the influence of dominant southeasterly winds. Dune forms are mostly longitudinal in back-island areas, but transverse and barchan dunes are also present. These active back-island dunes are supplied by sand blown from beaches and foredunes. After separation from foredune areas, dune migration is accomplished by downwind advancement accompanied by upwind erosion and deflation that maintain the sand supply.

Prolonged droughts in the 1890's and 1930's (Lowry, 1959; Price and Gunter, 1943) and more recent human activities have promoted dune activation. Vast dune fields that were active on Matagorda and Mustang Islands in the 1930's are now stable; however, active dunes are still common along much of Padre Island. Reported rates of migration range from 30 to 85 ft (9 to 26 m) per year (Price, 1971; Hunter and Dickinson, 1970). Active dunes are 5 to 15 ft (1.5 to 4.5 m) high and composed of well-sorted fine to very fine sand. Stratification formed by dune migration consists principally of horizontal to inclined plane parallel laminae, climbing ripple laminae, and ripple laminae (Hunter, 1977). Resultant vectors from predominant wind directions cause cross-strata to dip northwest.

Washover Fans

Although washover channels and fans may traverse the entire barrier width (fig. 88), these features are chiefly related to and gradational with beach and wind-tidal flat deposits. Washover fans vary considerably in size. The largest fans, which are presently inactive, formed when accretionary barriers (Matagorda Island, San José Island) were in transgressive phases prior to stabilization of sea level. Feeder channels for most of these fans were sealed during barrier outbuilding. The large fan studied by Andrews (1970) is essentially inactive but receives minor amounts of sand and is reworked during extreme hurricanes. At the other extreme are small washover fans, such as those on south Padre Island, that occupy interdune areas. A third type of active washover complex is the narrow, slightly curved, deeply incised channels and flame-shaped fans that respectively scoured through Matagorda Peninsula and prograded into Matagorda Bay during Hurricane Carla (Morton, 1979a).

Despite different morphologies, washover channels and fans display similar stratification types and grain-size changes from proximal channels through distal-fan sequences. Channels are distinguished by sand and shelly sand with lag concentrates of shell, reactivation surfaces, and pond deposits that represent quiescent periods when channels are submerged but slowly filled by suspended sediment from receding floodwaters, slopewash, and wind-blown sand. Sedimentary structures associated with small fans constructed by confined flow are horizontal parallel, ripple, and ripple-drift laminations and foresets. Well-sorted fine sands of distal fans are interbedded with wind-tidal flat deposits. Horizontal stratification, occasional graded bedding, and minor shell debris serve to distinguish storm deposits from other barrier-margin sediments.

Large-scale transverse bars and rhomboid bed forms are common products of storm surge (Scott and others, 1969; Morton, 1978). Surfaces of these washover deposits are greatly modified by wind, however, when subaerially exposed and un-stabilized by vegetation.

Wind-Tidal Flats

Broad barren sand flats that are low lying and alternately flooded by ponded rainwater and inundated by wind-driven bay water are termed wind-tidal flats (Fisk, 1959) because the latter process is associated with cyclic sedimentation somewhat analogous to intertidal deposits. Frequent salinity fluctuations and prolonged periods of exposure preclude establishment of most types of vegetation in these areas. Wind-tidal flats are often covered by mats of filamentous blue-green algae that thrive when wet but die and crack and peel when dry. Heaving from biogenic gases and air trapped beneath algal mats coupled with desiccation produces chaotic and contorted bedding. Process alternations collectively contribute to the uniqueness of wind-tidal flat deposits. For example, sand and shelly sand are introduced chiefly by washover and aeolian processes, whereas muds are mostly derived from adjacent lagoons. Bio-chemical precipitates of calcium carbonate are near-surface deposits that are interlaminated with algal mats.

Alternating layers of sand overlain by thin mud laminae or algal-bound sand are typical deposits. Rip-up clasts of mud drapes, gas-bubble structures, and contorted bedding are also common at sequence boundaries. The storm deposits are horizontal parallel laminae of well-sorted sand with some shell debris.

Accretionary Barriers

Galveston Island

Morphology and history

Surficial features that typify high-profile accretionary barrier islands (figs. 88 and 90) are present on Galveston Island (fig. 1). Gulf beaches are composed of sand and minor amounts of shell. East of the seawall, beaches are extremely flat and wide because of shoreline accretion of over 6,000 ft (1.8 km) attendant with jetty construction (Morton, 1974). In contrast, western beaches are approximately 200 ft (60 m) wide and slope gently seaward. Dunes are low (generally less than 5 ft [1.5 m])

Subsurface facies

Dip sections through Galveston Island (Bernard and others, 1970) show distinctly different vertical sequences for eastern and western barrier segments. A classical offlap sequence is preserved on east Galveston Island (fig. 91) where accretion ridges are predominant. Barrier-island models based on this sequence exhibit textural changes that coarsen upward. Lower shoreface and shelf deposits of interbedded sand and clay with shells grade laterally and upward into barrier and upper shoreface sand with thin shell beds (Bernard and others, 1970). On west Galveston Island near San Luis Pass, the Pleistocene-Holocene unconformity is overlain by Brazos River prodelta mud (fig. 91) which, in turn, is overlain by barrier-island and shoreface sands and muds similar to those previously described (Bernard and others, 1970). Facies relationships and carbon-14 dates for these two sections suggest that Galveston is a compound barrier with accretionary and transgressive segments (Morton, 1979b). Westward convergence of accretion ridges and their alignment with an arcuate offshore trend of coarse sediment (Morton and Winker, 1979) support the interpretation and mark the boundary at which Galveston Island was realigned. Shorelines east of the pivotal point built seaward while western shorelines retreated. As west Galveston Island transgressed the Holocene Brazos-Colorado delta, shoreface erosion and wave refraction combined to supply littoral drift for accretion of east Galveston Island. Basal barrier sands are stratigraphically higher and thin westward toward the Brazos delta plain. These relationships suggest that Galveston Island and adjacent Follets Island are progressively younger from east to west. This interpretation contradicts commonly held opinions that Galveston grew westward by spit accretion (Bernard and others, 1959).

Matagorda Island

Morphology and history

Matagorda Island (fig. 1) exhibits accretionary topography and generally conforms to the idealized high-profile barrier (fig. 92). Beaches are 200 to 350 ft (60 to 100 m) wide, and well-developed berms separate forebeach and backbeach environments. Backbeaches are nearly horizontal, whereas forebeaches slope gently (1° to 2°) seaward.

Except in washover and blowout areas, dunes on Matagorda Island are high and relatively continuous. Dune heights range up to 50 ft (15 m), but most fore-island dunes are only 15 to 20 ft (5 to 6 m) high. Along some segments, primary fore-island dunes are separated from the beach by secondary dunes (Wilkinson, 1974). Areas between primary and secondary dunes are vegetated and about 2.5 ft (0.75 m) higher than the backbeach. Primary dunes originated prior to 1857 when the shoreline essentially occupied the interdune area. Between 1857 and 1937, the Gulf shoreline advanced seaward, and low, sparsely vegetated secondary dunes formed in a position of equilibrium on the new backbeach.

A broad, densely vegetated area of accretion ridges and intervening swales lies landward of the foredunes. As elevations decrease bayward, fresh-water biota give way to salt marshes with tidal creeks and circular ponds. Unlike back-barrier environments on Galveston Island, large, inactive flood-tidal deltas are present on Matagorda Island. These flood deltas and associated inlets originated during late stages of the island's transgressive phase. Tidal exchange diminished, and inlets subsequently closed as the barrier built seaward.

Cedar Bayou is a minor tidal inlet that separates San José and Matagorda Islands. It remains open most of the time; however, it closed on several occasions during the past 40 years. Droughts in the 1930's and 1950's caused inlet shoaling that required considerable dredging to reestablish tidal flow.

Subsurface facies

Pleistocene and Holocene sediments beneath Matagorda Island (fig. 92) are similar to late Quaternary sequences underlying most central Texas barriers. Facies in ascending order are late Pleistocene deltaic mud and strandplain sand disconformably overlain by Holocene fluvial-deltaic sand and muddy sand, bay-estuarine mud, and barrier-island sand (Wilkinson, 1974). Holocene fluvial-deltaic sediments are principally confined to former stream valleys that filled as sea level rose. Overlying bay deposits form a nearly continuous blanket that averages 10 to 20 ft (3 to 6 m) thick. The strike-oriented sand body associated with Matagorda Island is relatively uniform in thickness. Barrier sediments, including subaerial back-island sediments, are 30 to 40 ft (10 to 13 m) thick along strike but pinch out or interfinger with bay and shelf deposits in landward and seaward directions (Wilkinson, 1974).

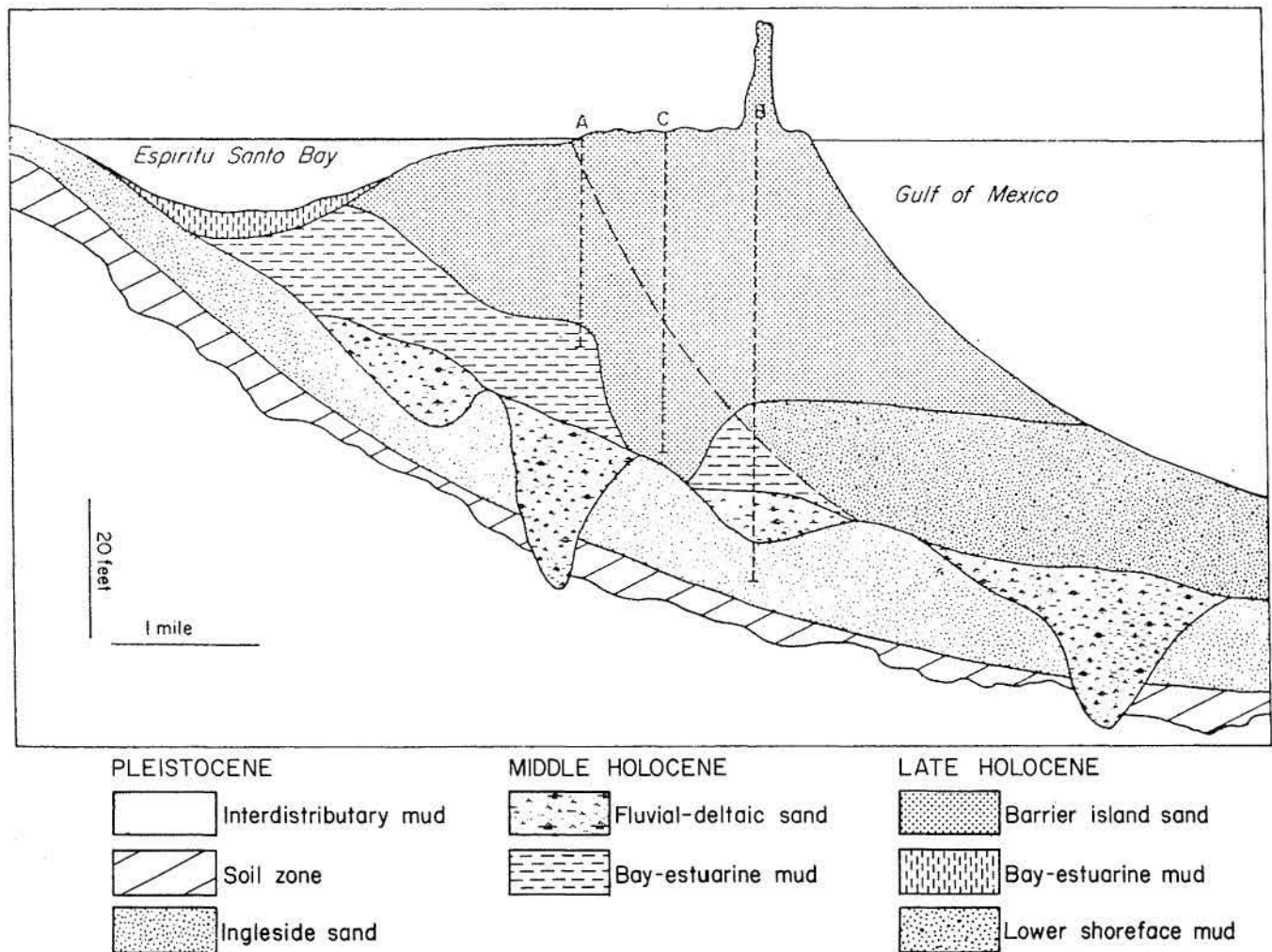


Figure 92. Dip section from northern part of Matagorda Island (after Wilkinson, 1974). Long Island Quadrangle.

Padre Island

Padre Island is the southernmost island within the Texas barrier-island chain and extends a distance of about 110 mi (176 km) from Corpus Christi Bay almost to the mouth of the Rio Grande. Padre Island is the longest of the barrier islands and during historic times has had only one natural tidal inlet (Brazos Santiago Pass). Two man-made passes have been cut through Padre Island. The first, Yarborough Pass, was dredged from the vicinity of Baffin Bay across Laguna Madre and Padre Island to the Gulf of Mexico; this pass was closed immediately by sands moving in the longshore drift system along the shoreface and beach. A second pass, Port Mansfield Ship Channel, was dredged from Port Mansfield across Laguna Madre and south Padre Island to the Gulf of Mexico; this pass was jettied and remains open today.

In plan Padre Island looks very much the same from its northern to southern limits. This similarity is superficial. A traverse of the island from north to south reveals that the beaches and fore-island dunes undergo some changes. The back side of the island also changes; the wind-tidal flats become wider from north to south. In the area south of Baffin Bay the wind-tidal flats merge with the mainland dividing Laguna Madre into a northern and southern segment (fig. 1). The wind-tidal flats constitute a large part of south Padre Island with the exception of the last, or southernmost, 13 mi (21 km) of the island.

Padre Island beaches grade southward from terrigenous sand to a mixture of sand and shell in the vicinity of Baffin Bay; this beach segment is known as "Little Shell" because of the high percentage of the surf clam *Donax*. Little Shell beaches extend laterally some 10 mi (16 km) where they grade into coarser shell beaches known as "Big Shell." As the composition of beach materials changes there is an accompanying change in beach morphology (fig. 93). Fore-island dune height and continuity decrease from north to south. Dune crests are generally 15 to 20 ft (4.5 to 6 m) above m.s.l., and a few exceptionally large dunes attain heights of 50 ft (15 m) along north Padre Island. About 30 mi (48 km) north of the Port Mansfield jetties, continuity of the fore-island dunes is broken by numerous storm channels; in this area back-island dunes coalesce to form a continuous, active dune field that is migrating northwestward into Laguna Madre.

North and Central Padre Island

Some of the surficial similarities of north and south Padre Island were stated in the introductory remarks. Similarities are restricted mostly to surface features. Histories of development, geometry, and facies are somewhat different for north and south Padre Island. North and central Padre Island can be considered as a unit.

History of development of north and central Padre Island

Fisk (1959) and Brown and others (1977) have shown that central Padre Island, Baffin Bay, and the Land-Cut Area are underlain by Pleistocene valleys that were scoured to depths of 80 to 150 ft (25 to 45 m). These valleys could have begun to be affected by the Holocene sea-level rise some 10,000 to 7,000 years B.P. (fig. 60).

According to Fisk (1959) Padre Island began to form around 5,000 years B.P. when sea level was some 20 to 30 ft (6 to 9 m) below present m.s.l. At that time the

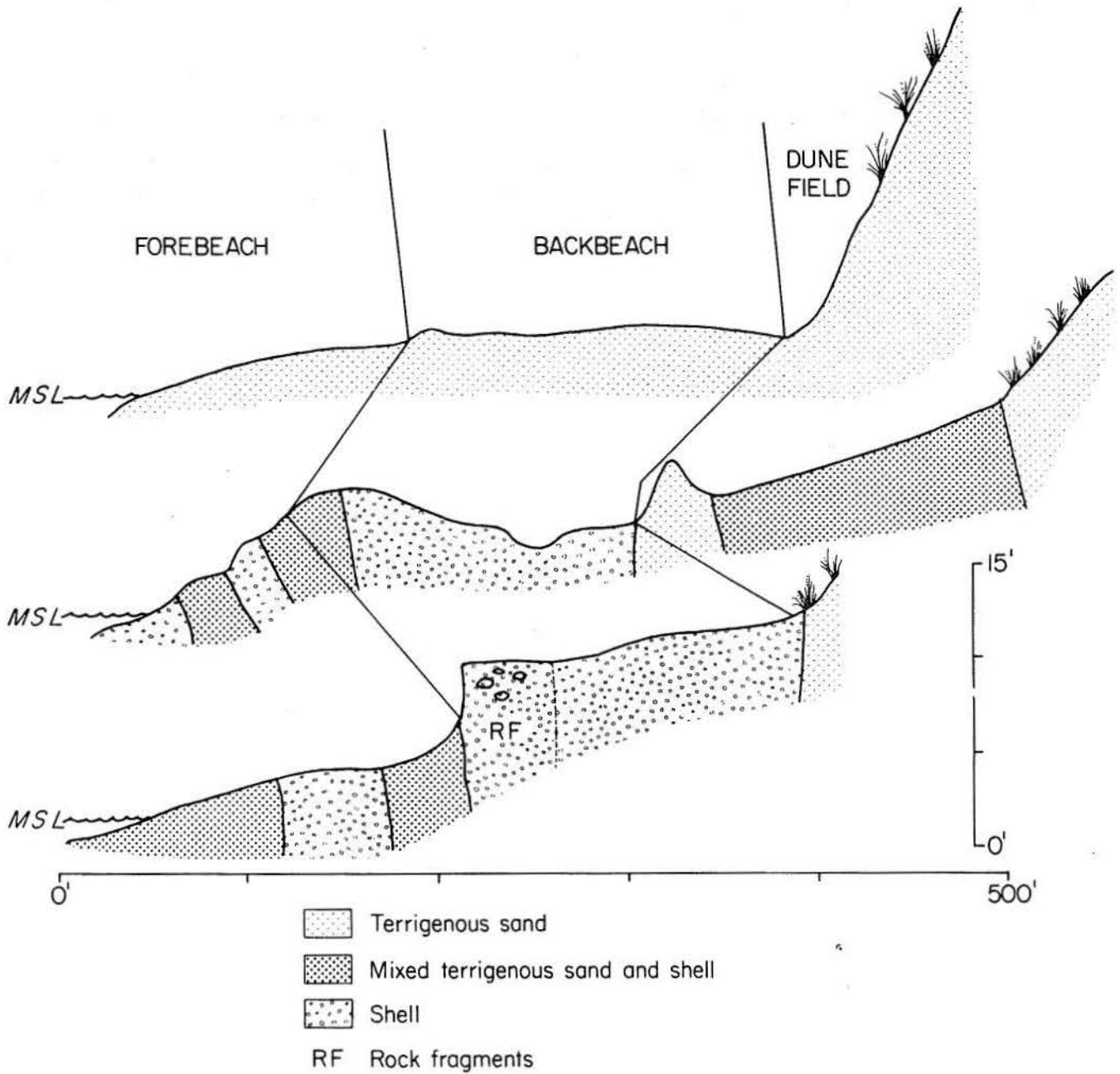


Figure 93. Padre Island beach profiles (January 1972). From top to bottom the profiles are (1) about 8 mi (13 km) south of the junction between Padre Island and Mustang Island, (2) midway between the junction of Padre and Mustang Islands and the Port Mansfield jetties, and (3) 0.25 mi (0.4 km) north of the Port Mansfield jetties. These profiles show only the surface distribution of sediment texture and composition. Beaches become narrow and steep; height of the backbeach above mean sea level increases as shell content increases (after McGowen, Garner, and Wilkinson, 1977).

Gulf shoreline was just slightly inland of its present position. Fisk (1959) states that the final rise in sea level was rapid and that Padre Island began, at that time, as a series of offshore islands. These were integrated about 4,000 years B.P. to form a continuous barrier system; Laguna Madre is said to have originated then.

Padre Island has greatly enlarged since 4,000 years B.P., chiefly through wind and storms that have transported large volumes of sand west and northwest toward Laguna Madre. Padre Island has accreted landward at the expense of Laguna Madre.

Like the wide barrier islands to the north (for example, Matagorda and San José Islands), Padre Island was initiated on Pleistocene drainage divides. Here, the similarities cease, as Padre Island did not experience rapid seaward accretion. Instead, Padre Island grew upward and lagoonward (fig. 94).

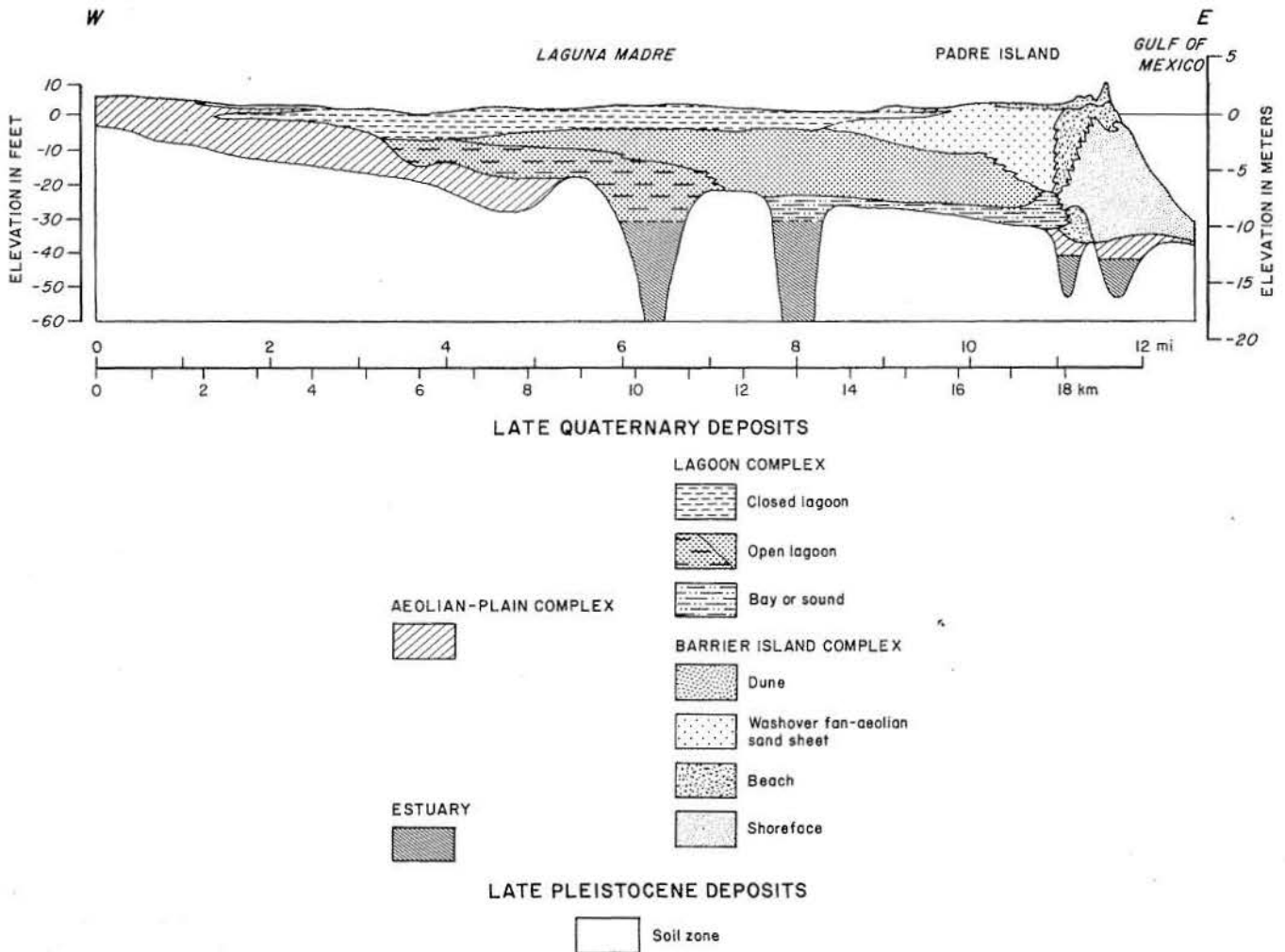


Figure 94. Modern barrier-island system, central Padre Island, near Land-Cut Area. Cross section after Fisk (1959). South of Potrero Lopeno Quadrangle.

Two-dimensional geometry of north and central Padre Island

Padre Island (fig. 94) accumulated on a Pleistocene erosional surface and on a Pleistocene soil. The sequence of late Quaternary deposits that overlies the erosional surface accumulated during rising sea level, and after sea level became relatively stable (Fisk, 1959). These deposits accumulated upon the aeolian plain, within the lagoon, within the numerous barrier-island environments, and in estuaries prior to development of Padre Island.

Estuary fill consists of greenish-gray sandy clay; it contains locally abundant shallow-water mollusks.

Aeolian plain comprises four depositional environments. These are (1) dunes, consisting of massive light-brown fine sand; (2) interdune swamps (terminology of Fisk, 1959) containing greenish-gray sandy clay with root casts; (3) ponds containing calcareous mud with land snails and crab fragments, and (4) clay dunes made up of sand-sized clay clasts and terrigenous fine sand. Deposits are thinly bedded and incorporate traces of pulmonate gastropods and rodent bones.

In cross section (fig. 94), lagoonal deposits are about 8 mi (14 km) wide and a maximum of about 35 ft (55 km) thick. Three facies compose the lagoonal fill. The uppermost, closed-lagoon deposits are made up of interbedded light-brown fine sand and gray clay. Gypsum occurs locally. Large numbers of dwarfed mollusks are present in some facies. Open lagoon (which existed prior to closure of tidal inlets along central Padre Island) is characterized by gray clean fine sand with an abundant marine fauna at the base; a restricted fauna comprising dwarfed mollusks occupies the upper part of the facies. The lower bay or sound facies (which records fresh-water influence) is made up of gray sandy clay with abundant oysters.

The barrier-island proper is between 45 and 47 ft (13.5 and 14.1 m) thick, and from lower shoreface to the western limit of the washover fan facies, the island is almost 5 mi (8 km) wide. Fisk (1959) recognized four barrier-island environments. These are (1) shoreface, consisting of gray fine sand containing abundant shell and burrowing organisms, and some wood fragments; (2) beach (no distinction was made between forebeach and backbeach), which is made up of light-brown fine sand with abundant shell and some wood fragments; (3) washover fan - aeolian flat (this is the facies that makes Padre Island wide between the lagoon margin and the fore-island dunes) is made up of light-brown fine sand with rare to abundant shell debris; and (4) fore-island and vegetated barrier flat consist of light-brown fine sand with scattered shell debris. (Fisk did not separate these two facies, but grouped them together as dune).

Characteristics of Surface Environments: North Padre Island

Relatively undisturbed physiographic elements of north Padre Island occur within the Padre Island National Seashore. From the Gulf of Mexico to Laguna Madre these elements are shoreface, beach, fore-island dunes, vegetated barrier flat, back-island dunes, and wind-tidal flat (Hunter and others, 1972; Shideler and others, 1978).

The shoreface (fig. 95) is the seaward extension of the barrier island and lies between the inner continental shelf and the toe of the forebeach. The shoreface is commonly divided into lower and upper shoreface segments (fig. 95). Lower shoreface (or offshore segment) is characterized by a smooth, concave-upward surface that

represents an equilibrium profile optimally adjusted to local wave conditions. Texturally, it is a size-graded sector, exhibiting a seaward transition from sand to mud. Wave surge and nearshore wind-driven currents are important sediment-transport agents. Intense bioturbation tends to destroy primary sedimentary structures, resulting in mottled to structureless deposits. The most common infauna groups are echinoderms and polychaete worms. The shallow upper shoreface (or nearshore segment) is characterized by a migrating bar-and-trough system. Upper shoreface is a high-energy environment encompassing the breaker and surf zones and is composed of clean fine-grained sand. Strong waves and littoral currents produce a variety of bed forms and stratification types that include (1) small-scale wave ripples parallel to wave crests (random lenticular ripple cross-laminae are dominant), (2) plane beds and parallel laminae on bar crests, (3) dunes in troughs oriented in direction of longshore currents (trough crossbedding), and (4) linguoid ripples in troughs (ripple cross-laminae). The infauna consists of ghost shrimp (Callianassa), sand dollars (Mellita quinquisperforata), mollusks, and polychaetes.

North Padre Island beach is made up of a forebeach (foreshore) segment (bathed by continuous swash and backwash) that dips gulfward at about 4° , and a backbeach (backshore) segment that is broad (up to 150 to 200 ft [39 to 60 m]) that generally slopes seaward at an angle less than 2° . Forebeach and backbeach are commonly separated by a berm crest. Both beach segments are mostly made up of fine sand; shell may be locally abundant on the berm and at the toe of the forebeach. Forebeach is hydraulically under the influence of the swash/backwash flow system. The decelerating swash is basically a depositional current, whereas the accelerating backwash can be either a depositional or an erosional current. The dominant stratification type is seaward-dipping (4° to 6°), parallel inclined laminae that are commonly accentuated by dark, heavy minerals. Other forebeach features that could be preserved in the geologic record include antidunes, rhomboid and straight-crested ripples, cusps, and heavy-mineral concentrations. The most common forebeach infauna include ghost shrimp (Callianassa), mollusks (especially Donax), and polychaetes. The backbeach comprises the relatively flat segment extending from forebeach to foredunes. The backbeach is formed during spring and storm tides, and has subsequently been reworked by aeolian processes. Ponding commonly accompanies high water, and the water subsequently returns to the Gulf through channels scoured across the forebeach. The backbeach has a wedge-shaped cross section, stratification being nearly horizontal or gently dipping toward or away from the Gulf. Other structures include ripple cross-lamination, cut-and-fill, and deflation shell concentrations. The dominant burrowing organisms are ghost crabs (Ocypode).

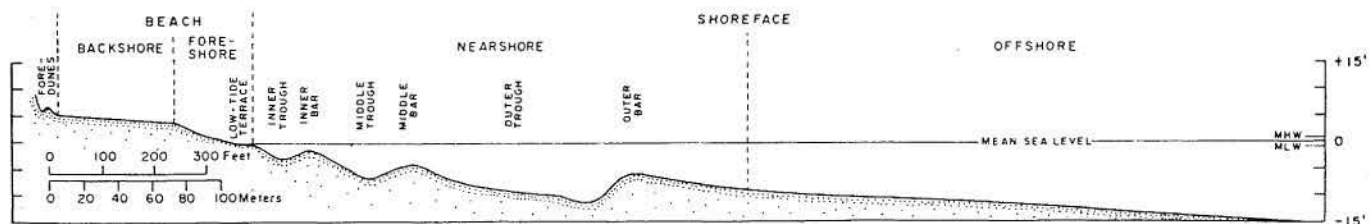


Figure 95. Profile of beach and shoreface. The morphology is typical of northern Padre Island during summer conditions. An ephemeral bar and runnel commonly replace the low-tide terrace. The part of the profile beyond wading depth was measured by fathometer (after Hunter and others, 1972).

Fore-island dunes lie immediately shoreward of the beach. Sand transported by onshore winds accumulates as dunes that are stabilized by vegetation. The dune complex consists of small vegetated aeolian mounds (coppice or wind-shadow dunes), and larger (15 to 50 ft [4.5 to 15 m] high) vegetated dunes. Continuity of the dunes is commonly disrupted by blowouts resulting from localized wind erosion. Downwind from blowouts there are unvegetated active dunes. Dunes are made up of very well sorted fine-grained sand. Stratification of dunes are trough-fill cross-strata and wedges of parallel inclined laminae that are oriented predominantly to the northwest in response to the southeasterly onshore winds (McBride and Hayes, 1962). Vegetation and burrowing animals tend to destroy the primary stratification.

The vegetated barrier flat (deflation flats of Hunter and others, 1972) is the relatively flat, vegetated area that extends between the fore-island dunes and the active back-island dunes. It is generally less than 5 ft (1.5 m) above mean sea level, and is an aeolian depositional-erosional surface whose deflation base is controlled by the water table. The flat actually consists of small-scale ridge-and-trough topography that formed by dune migration during alternating wet and dry periods. The fine sand composing the flats is nearly structureless as a result of intensive bioturbation.

Back-island dunes are common physiographic elements of the Texas barrier islands that lie between Aransas Pass and Brazos Santiago Pass. These dunes are well developed on southern Mustang Island and throughout most of the Padre Island system. These dunes date back to the late 1800's when overgrazing (by sheep and cattle) together with drought conditions liberated the sand stored in fore-island dunes of Padre Island (Price and Gunter, 1943). Once devegetated, the fore-island dune sands migrated northwestward across Padre Island toward Laguna Madre. Droughts in the 1930's and from 1948 to 1957 further enhanced movement and growth of back-island dune fields. These dunes will continue migrating toward Laguna Madre unless stabilized by vegetation, which is unlikely; sands of the back-island dunes will most likely come to rest in Laguna Madre. The back-island area of north Padre Island contains some active back-island dune fields (Hunter, 1977). The active fields contain transverse, barchan, and longitudinal dunes that are oriented by the southeasterly winds during the summer. Dune orientation is modified by strong northerly winds during winter months. Some persistent oblique dunes oriented east-west are also present. Characteristic back-island dune stratifications are listed in table 2. Wind-tidal flats, a featureless sand plain that is frequently inundated by lagoonal waters driven upon the back side of Padre Island by persistent strong winds or by a decrease in barometric pressure, generally occupy the same position on the island as the back-island dunes; wind-tidal flats are best developed where there are no back-island dunes. Wind-tidal deposits are made up predominantly of beach and dune sand transported by wind across the island. Interbedded with sand are thin mud units that are commonly stabilized by blue-green algae that form a tough leathery protective cover for the flat. Mud is derived from Laguna Madre. Thin micrite laminae are common associates of the algal mats. Gypsum crystals are rare to common; these are formed in the same manner as gypsum in sabkhas (Butler, 1969; Kinsman, 1966, 1969).

Table 2. Characteristics of Basic Types of Aeolian Stratification (after Hunter, 1977).

| Depositional process | Character of depositional surface | Type of stratification | Dip angle | Thickness of strata Sharpness of contacts | Segregation of grain types Size grading | Packing | Form of strata |
|------------------------------|-----------------------------------|---|--|---|--|--------------|--|
| Tractional deposition | Rippled | Subcritically climbing translent stratification | Stratification: low (typically 0-20°, maximum ~30°) Depositional surface: similarly low | Thin (typically 1-10 mm, maximum ~5 cm) Sharp, erosional | Distinct Inverse | Close | Tabular, planar |
| | | Supercritically climbing translent stratification | Stratification: variable (0-90°) Depositional surface: intermed. (10-25°) | Intermediate (typically 5-15 mm) Gradational | Distinct Inverse except in contact zones | Close | Tabular, commonly curved |
| | | Ripple-foreset cross-lamination | Relative to translent stratification: intermed. (5-20°) | Individual laminae: Thin (typically 1-3 mm) Sharp or gradational, non-erosional | Individual laminae and sets of laminae: Indistinct Normal and inverse, neither greatly predominating | Close | Tabular, concave-up or sigmoidal |
| | | Rippleform lamination | Generalized: intermediate (typically 10-25°) | Sets of laminae: Intermediate (typically 1-10 cm) Sharp or gradational, nonerosional | | Close | Very tabular, wavy |
| Largely grainfall deposition | Smooth | Planebed lamination | Low (typically 0-15°, max.?) | | | Close | Very tabular, planar |
| | | Grainfall lamination | Intermediate (typically 20-30°, min. 0° max. ~40°) | | | Intermediate | Very tabular, follows pre-existent topography |
| Grainflow deposition | Marked by avalanches | Sandflow cross-stratification | High (angle of repose) (typically 28-34°) | Thick (typically 2-5 cm) Sharp, erosional or nonerosional | Distinct to indistinct Inverse except near toe | Open | Cone-shaped, tongue-shaped, or roughly tabular |

Transgressive Barriers

Matagorda Peninsula

Morphology and history

On the western flank of the Brazos-Colorado delta is Matagorda Peninsula (fig. 1), a transgressive barrier whose surficial features and morphology are controlled primarily by storm washover and shoreline erosion (McGowen and Brewton, 1975; Morton and others, 1976). These same processes also cause landward migration of the peninsula. Beach profiles reflect shoreline erosion as well as sediment size, which is closely related to composition. Beaches are composed of terrigenous sand with varying amounts of shell and rock fragments. Concentrations of the coarse fraction (shell) are easily explained by their proximity to shelf sediments with similar characteristics.

Some beach segments east of the Colorado River are devoid of foredunes and have stepped profiles with one or more backbeach terraces. Highest terraces may either occur below the storm ramp, a broad vegetated plain that slopes gently bayward, or grade into it. Other beaches have vertical, wave-cut faces eroded into the storm ramp. These faces expose broad, low-relief scour-and-fill structures and alternating horizontal beds of sand and shell that accreted vertically during storm washover. Closely spaced and slightly curved washover channels with intervening marshes, tidal creeks, and ponds lie bayward of the storm ramp.

West of the Colorado River, foredunes are progressively better developed, and storm ramps are less pronounced. Here vegetated flats grade into marshes, some of which protrude noticeably into Matagorda Bay. These fans, originally flame-shaped, were deposited in a few hours by Hurricane Carla (1961). Bay-margin morphology is also influenced, but to a lesser degree, by shoreline erosion that occurs at average rates of 2 to 3 ft (60 to 90 cm) per year (McGowen and Brewton, 1975).

Matagorda Peninsula is segmented not only by the Colorado River, but also by Brown Cedar Cut (an ephemeral inlet) and Matagorda Ship Channel (a man-made channel). Dredging of the Colorado channel across Matagorda Peninsula has not significantly affected the Gulf shoreline, which continues to retreat despite additional sediment supplied by the river (Morton and others, 1976). Significant shoreline changes occurred, however, after Matagorda Ship Channel was opened. Updrift shoreline accretion and downdrift shoreline erosion followed jetty construction, but even more noticeable was lateral spit accretion at Decros Point that accounted for the extension of Matagorda Peninsula more than 2,800 ft (850 m) southwestward into Pass Cavallo (Morton and others, 1976).

Subsurface facies

Sediments beneath Matagorda Peninsula (fig. 96) record transgression of a barrier-lagoon complex attendant with Holocene sea-level rise. The transgressive sequence was interrupted by periods of delta progradation that gave way to landward migration of a barrier-lagoon complex that was subsequently modified by inlet migration (Wilkinson and Basse, 1978).

Late Pleistocene deltaic muds underlie an oxidized erosional surface with considerable relief. Overlying Holocene sediments are chiefly gray and red-brown bay-estuarine mud and sandy mud. Entrenched valleys other than the Brazos valley are filled with gray mud that lies below highest elevations of drainage divides (Wilkinson and Basse, 1978). Red-brown mud deposited by the ancestral Brazos-Colorado Rivers blankets the divides and climbs stratigraphically higher toward the northeast indicating time-transgressive deposition that persisted near the Brazos-Colorado delta. Red-brown deltaic mud is overlain by bay-estuarine mud that also occurs stratigraphically higher and thins northeastward (fig. 96). Uppermost sands of barrier-island tidal-inlet origin also thin northeastward even when greater sand thickness, attributed to inlet migration at Pass Cavallo (Wilkinson and McGowen, 1977), is taken into account. These stratigraphic relationships suggest that Matagorda Peninsula and underlying bay and deltaic muds become progressively younger toward the Brazos-Colorado deltaic plain (Wilkinson and Basse, 1978, fig. 2, p. 1594).

South Padre Island

The history of development of south Padre Island is related to the construction, abandonment, and subsidence of the northern lobe of the Holocene Rio Grande delta. Several depositional events preceded development of south Padre Island and its associated lagoon.

Holocene depositional history

Holocene barrier-strandplain sands began to accumulate in the Pleistocene Rio Grande valley when sea level had risen to a position about 70 ft (21 m) below present sea level (fig. 97). Barrier island - strandplain sediments continued to accumulate until the sea level had risen to about 30 ft (9 m) below mean sea level (m.s.l.). At that time the Rio Grande began to construct a delta (Brown and others, 1980).

Radiocarbon ages (McKinley, personal communication, 1977) indicate the following age relationships: (1) the lower 10 to 15 ft (3 to 4.5 m) of deltaic sediment, which lies 25 ft (7.5 m) below m.s.l., probably accumulated more than 4,000 years B.P.; (2) the distributary channel sand (approximately 2,600 years B.P.) may be younger than adjacent interdistributary bay - prodelta mud; and (3) lagoonal and tidal-flat environments developed (approximately 2,500 years B.P.) concurrently with the youngest deltaic deposits.

The Rio Grande subdelta became inactive and began to founder approximately 2,000 years B.P. South Padre Island, Laguna Madre, and wind-tidal flats began to develop at this time.

After delta abandonment and subsidence, south Padre Island migrated toward the lagoon. The processes of compactional subsidence, shoreline erosion, and northward sand transport continue today. Wind-tidal flat deposits are thickest near the present Gulf shoreline, and they thin progressively toward Laguna Madre. Laguna Madre grassflat deposits are thin, indicating a relatively young age for these deposits. Grassflat deposits, like wind-tidal flat deposits, thin in a westerly direction (fig. 97).

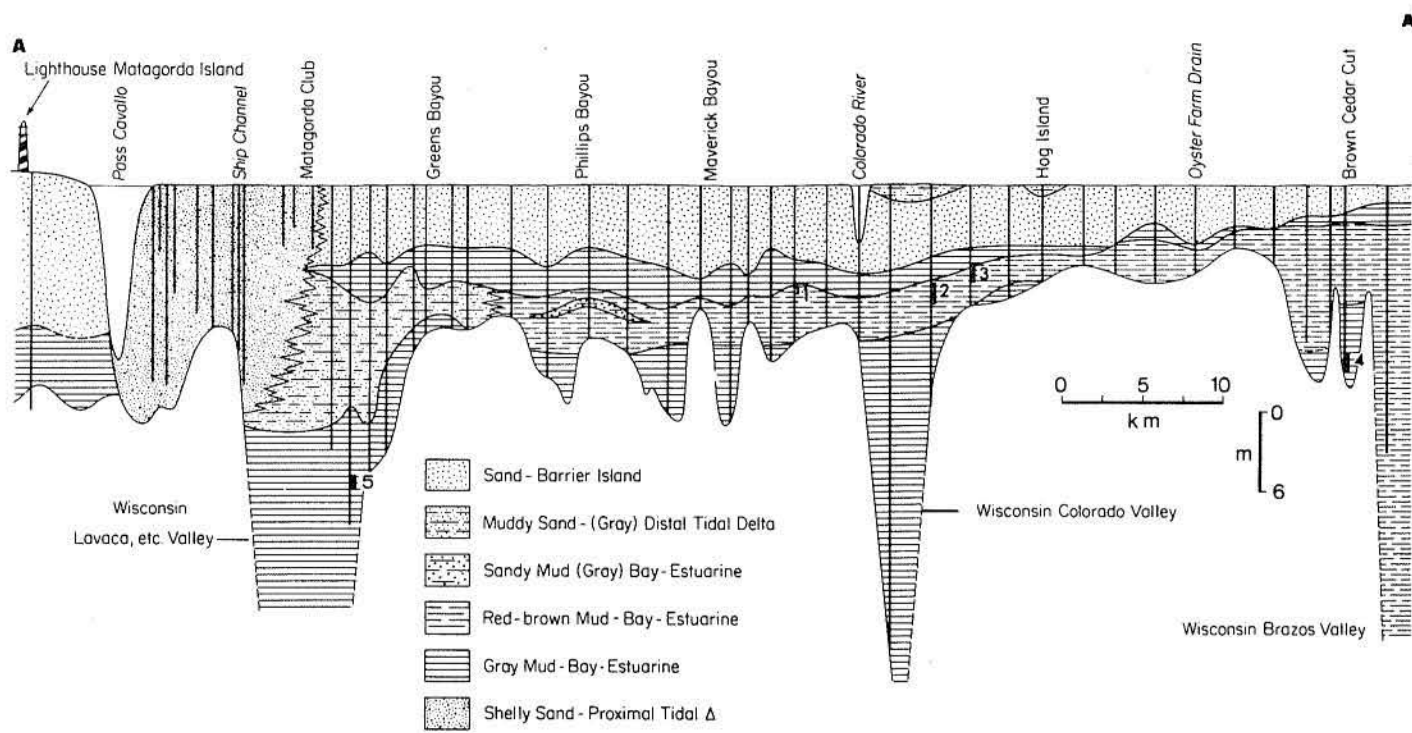


Figure 96. Strike section of late Pleistocene and Holocene sediments beneath Matagorda Peninsula (after Wilkinson and Basse, 1978). Decros Point Quadrangle.

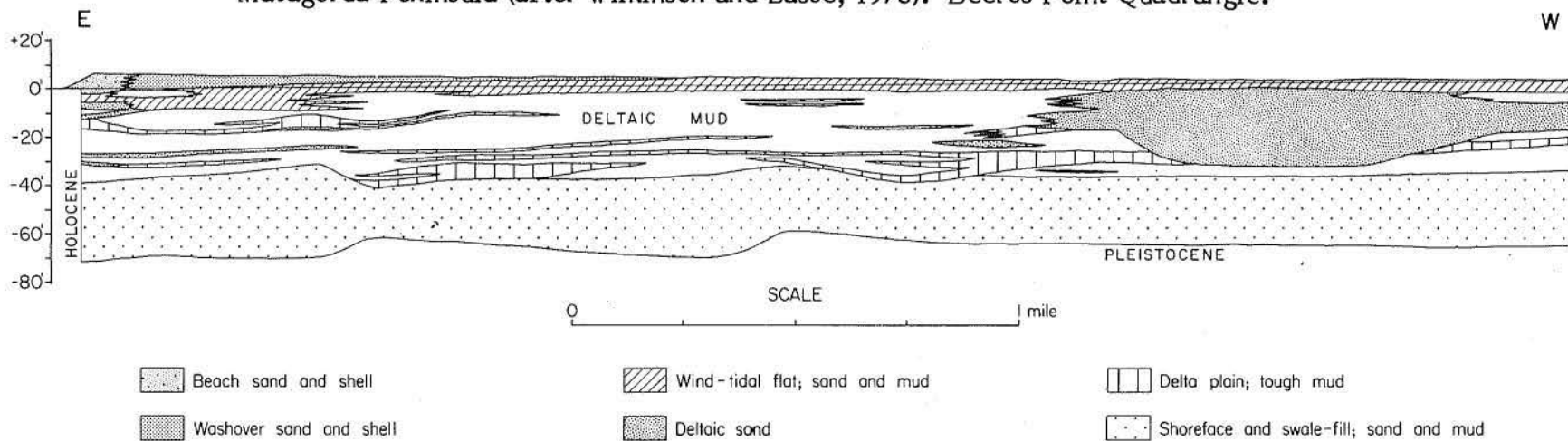


Figure 97. Cross section south Padre Island area, Texas. South Padre Island is less than 10 ft (3.0 m) of sand overlying wind-tidal flat and Holocene Rio Grande bay deltaic sediment (Brown and others, 1980). (Location on fig. 74). North of Port Isabel SW Quadrangle.

Two-dimensional geometry of south Padre Island and underlying Holocene Rio Grande delta

An east-west cross section (figs. 74 and 97) depicts the depositional facies of south Padre Island and underlying older Holocene deltaic units.

Holocene deposits that underlie south Padre Island from the Rio Grande to the vicinity of Port Mansfield Ship Channel accumulated in a valley cut by the Rio Grande when sea level was lowered between 390 and 450 ft (119 and 137 m) during the Wisconsin glacial stage (Curry, 1960; Bernard and Le Blanc, 1965; Brown and others, 1980).

Depositional facies

Subsurface depositional facies are shown in figure 97. Two broad genetic units constitute the subsurface facies: barrier island - strandplain facies and deltaic facies.

Barrier island - strandplain facies. The basal Holocene sand accumulated when sea level was some 30 to 70 ft (9 to 21 m) below present level. This sand is a transgressive unit that accumulated in a barrier island - strandplain depositional system. Sand that makes up most of this system was derived directly from the Rio Grande and was reworked almost immediately by marine processes. The process of formation is believed to have been analogous to that described by Curry, Emmel, and Crampton (1969) for the development of the strandplain of Nayarit, Mexico.

Sand accumulated in shoreface, beach, and barrier-flat environments. The relatively coarse grain size of some sand, presence of wood debris, and high biotite content indicate a fluvial source. Foraminifers and fragments of Gulf molluscan species record the marine influence. Sand with thin, soft, mud layers containing plant debris and shell fragments has been interpreted as a shoreface deposit.

Interpretation of mud as swale fill is based upon degree of induration of mud, high plant debris content, and its association with other facies.

Deltaic facies. The Rio Grande constructed a delta characterized by distributary channels, delta-front sands, interdistributary bays, and a sparsely vegetated delta plain. This delta began its growth when sea-level rise diminished, or stopped briefly, some 30 ft (9 m) below its present position. Sea level resumed its rise after the temporary stillstand, but more slowly because the Rio Grande delta was able to prograde the shoreline. Temporary halts or reduced rates in sea-level rise are recorded by tough delta-plain muds.

Distributary channel sands up to 30 ft (9.0 m) thick and 1.25 mi (2.0 km) wide are plano-convex in cross section. Sands are mostly brown, biotite and plant debris bearing, and fine grained. Distributary channel facies grade laterally into delta-plain and interdistributary muds. Crevasses are commonly associated with distributary channel deposits.

Vertical accretion and emergence of the delta plain is recorded by a series of tough, predominantly red and brown muds. These muds were emergent for a time sufficient for (1) dewatering, (2) establishment of a dense vegetation cover, and (3) development of large populations of fiddler crabs. Delta-plain muds were derived by overbanking from distributaries.

Interdistributary bay and prodelta muds are laterally equivalent to all the other deltaic facies. On the basis of the thickness of interdistributary bay-prodelta muds between zones of tough delta-plain muds, it is suggested that water was about 5 to 15 ft (1.5 to 4.5 m) deep during development of the Rio Grande delta. Interdistributary bay-prodelta muds are predominantly grayish brown with some greenish-gray mud. Muds characteristically contain plant debris.

Characteristics of surface facies

Five surface sediment facies are recognizable on south Padre Island. From east to west these are beach, fore-island dunes, washover fan, wind-tidal flat, and grassflat.

Beaches on south Padre Island are made up of a seaward-sloping forebeach and a gently lagoonward- or seaward-sloping backbeach. Forebeach slopes toward the Gulf at about 5°. Sediment composing the forebeach is pale-yellowish-brown, well-sorted, fine sand with common to abundant whole and fragmented shell material, and local heavy mineral placers. Shell material is derived from species that live in the nearshore Gulf of Mexico and from bay and lagoon species derived from erosion of older deposits that are exposed on the inner shelf and shoreface. Stratification of the forebeach is parallel inclined laminae or low-angle, wedge-shaped sedimentation units. Backbeach deposits are texturally similar to the forebeach; however, the backbeach may be locally covered with a shell pavement representing a lag, or wind-deflation deposit. Stratification of backbeach deposits consists of (1) parallel laminated sand and shell, (2) trough-fill cross-strata, (3) ripple cross-laminae, and (4) local channel-fill deposits.

Fore-island dunes are discontinuous and low, 10 to 15 ft (3 to 4.5 m) above m.s.l. They have the same general characteristics as dunes on north Padre Island. Wide breaks occur between fore-island dunes. During tropical storms and hurricanes south Padre Island is readily washed over (and commonly deeply eroded) in these low-lying areas (Brown and others, 1974; Morton and Pieper, 1975a). Within these areas the backbeach grades westward into washover deposits.

Washover deposits are gradational with backbeach deposits on the Gulf side and wind-tidal flat deposits toward Laguna Madre. These deposits are pale yellowish brown above the water table and medium dark gray below the water table, and consist of sand and shell with a few rock fragments. Washover deposits range from poorly sorted, shelly, fine sand to well-sorted, fine sand. Stratification includes (1) horizontally laminated and foreset crossbedded shelly sand, (2) parallel laminated and ripple cross-laminated sand, and (3) massive sand with worm burrows, mud drapes, and mud clasts.

Wind-tidal flat deposits are predominantly sand. The surface of the wind-tidal flat is generally covered with a filamentous blue-green algal mat. Depending upon how recently the flat has been inundated, the algal mat may persist unbroken almost continuously across the flat, or it may be severely desiccated with areas of the flat laid bare when the wind removes patches of desiccated algae. Wind-tidal flat sand exhibits several colors largely dependent upon the relative position of the water table. Above the water table well-sorted, fine-grained sands are yellowish gray, whereas below the water table sands are grayish green and medium bluish gray. Wind-tidal flat muds are mostly greenish gray but commonly contain thin (1 mm or less) white carbonate lamina. Muds are mostly sandy and commonly contain gypsum crystals. The

ratio of sand to mud varies over short distances, chiefly as a function of small differences in elevation across the flat. Mud units are thickest in local ponds, scour features, and toward Laguna Madre. Sedimentation units in sands are approximately 1 to 4 inches (2.4 to 10 cm) thick. Mud units range from less than 0.5 inch (1.2 cm) to about 2.0 inches (5 cm) thick. Stratification in sands are parallel laminae, ripple cross-laminae, parallel but wavy laminae, and gas-filled cavities commonly referred to as "sponge cake" texture. Stratification is locally accentuated by opaque heavy minerals. Root mottling, shell material, and "U-shaped" burrows are common in some horizons. In some areas mud content increases with depth. Thicker mud units appear to have accumulated in ponds or depressions; these units are massive and commonly contain plant debris. Thinner mud units occur as mud drapes over ripple cross-laminated sand, interlaminated with blue-green algae and sand. Mud units are commonly contorted and desiccated.

The floor of south Laguna Madre that is adjacent to wind-tidal flats slopes gently westward. Grassflats occur in this area; their deposits are light-olive-gray to greenish-gray shelly, muddy, fine sand. Vertical roots of Halodule wrightii, with plant material intact, occur throughout the thickness of grassflat deposits. Whole and fragmented shell, present throughout the entire thickness of the grassflat, generally increases upward.

INNER SHELF

Introduction

Rapid sea-level rise and attendant shoreline retreat significantly influenced surface sediment distribution on the inner shelf. Curray (1960) and van Andel (1960) recognized that relict sediments overlain by a thin veneer of Modern sediments (figs. 98 and 99) were typical over much of the northwest Gulf of Mexico. This is in accord with general findings of Emery (1968) and specific conclusions of McGowen and Morton (1979).

Currents generated by wind forcing are primarily responsible for present-day transport of sediments. Currents not associated with wind forcing are generally weak and attributed to density gradients (temperature and salinity) and tidal processes. Strong bottom currents generated by storms most likely cause small-scale cyclic sedimentation (graded beds) preserved in shelf cores (fig. 99). Hayes (1967) first recognized that graded shelf deposits were products of sediment transport associated with storm-surge ebb; however, Hayes may have overstated the importance of flood runoff through washover channels. Strongest shelf currents occur near or within the bottom boundary layer just prior to storm landfall and are directed parallel to shore or obliquely offshore. Such large-scale flows are necessary to conserve large volumes of water transported onshore as storm surges. Velocities associated with bottom-return flows of nearly 6 fps (2 m/s) have been recorded by Forristall and others (1977) on the Texas shelf during tropical storm Delia and by Murray (1970) off the Florida Panhandle during Hurricane Camille.

Sediment Textures

Inner shelf sediments are generally fine grained; coarse clasts (> 0.5 mm) are uncommon (< 1 percent) over much of the area. Gravel fractions are predominantly whole shells and shell fragments with subordinate amounts of lithic clasts. Indigenous shelf fauna and relict brackish-water mollusks (*Rangia* sp. and *Crassostrea virginica*) make up most of the skeletal debris. Multicyclic sands and muds are widespread and parallel the coast south of the Brazos delta; elsewhere, mud is substantially greater than sand (figs. 100 through 103).

The inner shelf can be divided into four areas according to (1) coarse fraction percent, (2) distribution of anomalous mollusks; and (3) occurrence of rock fragments (fig. 104). Three of these areas delineate ancestral deltas of the Rio Grande, Brazos-Colorado, and Trinity Rivers (Morton and Winker, 1979). The fourth trend, between Pass Cavallo and Aransas Pass (fig. 102), is enigmatic.

Coarse material (fig. 104) may be concentrated because of high productivity, low rates of sedimentation, selective sorting and deposition, and reworking of relict sediments with local concentrations of shell. None of these processes entirely explains the major trends, although low rates of sedimentation and delta-plain destruction during Holocene transgression are common to all areas (Morton and Winker, 1979).

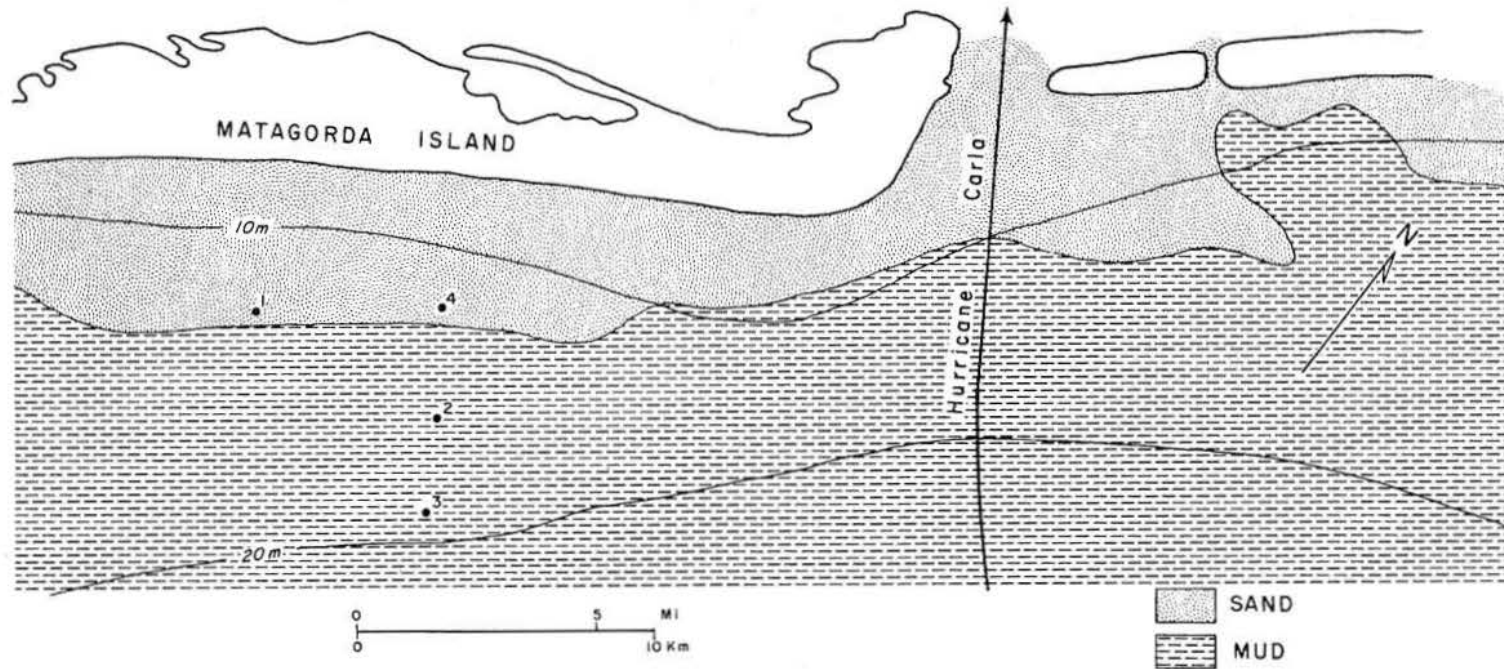


Figure 98. Generalized distribution of surface sediment, track of Hurricane Carla at landfall, and location of inner shelf cores. Surface sediment map modified from McGowen and Morton (1979). Pass Cavallo Quadrangle.

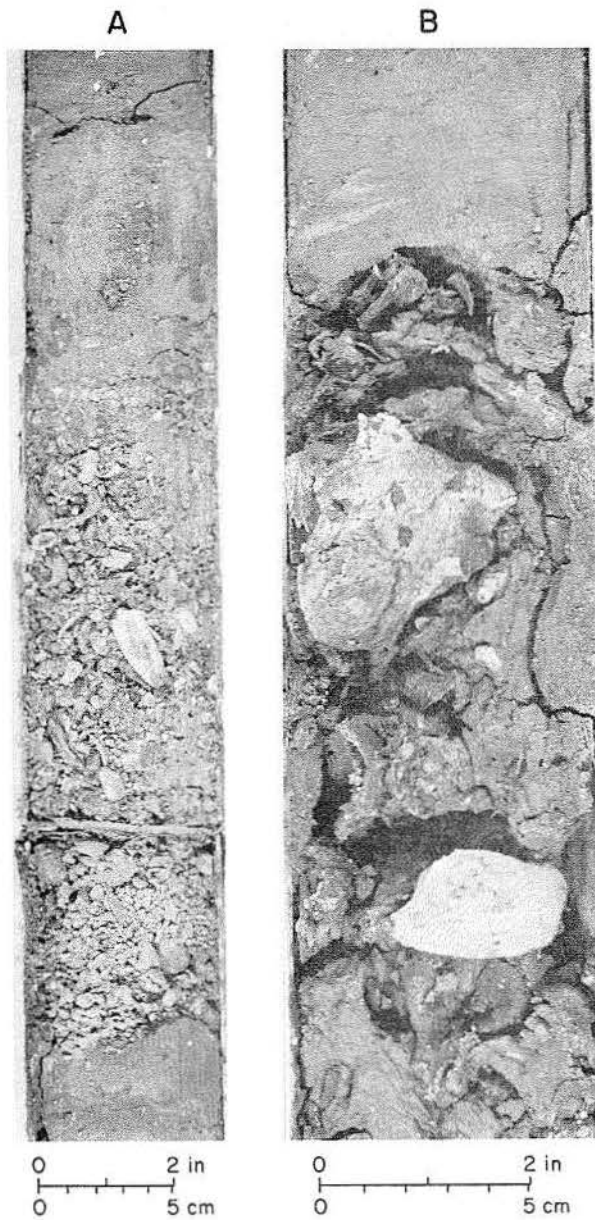


Figure 99. Segments of cores 4 and 2 from the Matagorda - San José trend showing (A) graded bedding interpreted as a storm deposit and (B) shelf deposits overlying relict estuarine sediments with abundant oystershells. Core locations shown in figure 98. Section A (core 4) taken from a depth of 1.1 m, section B (core 2) taken from a depth of 3.6 m.

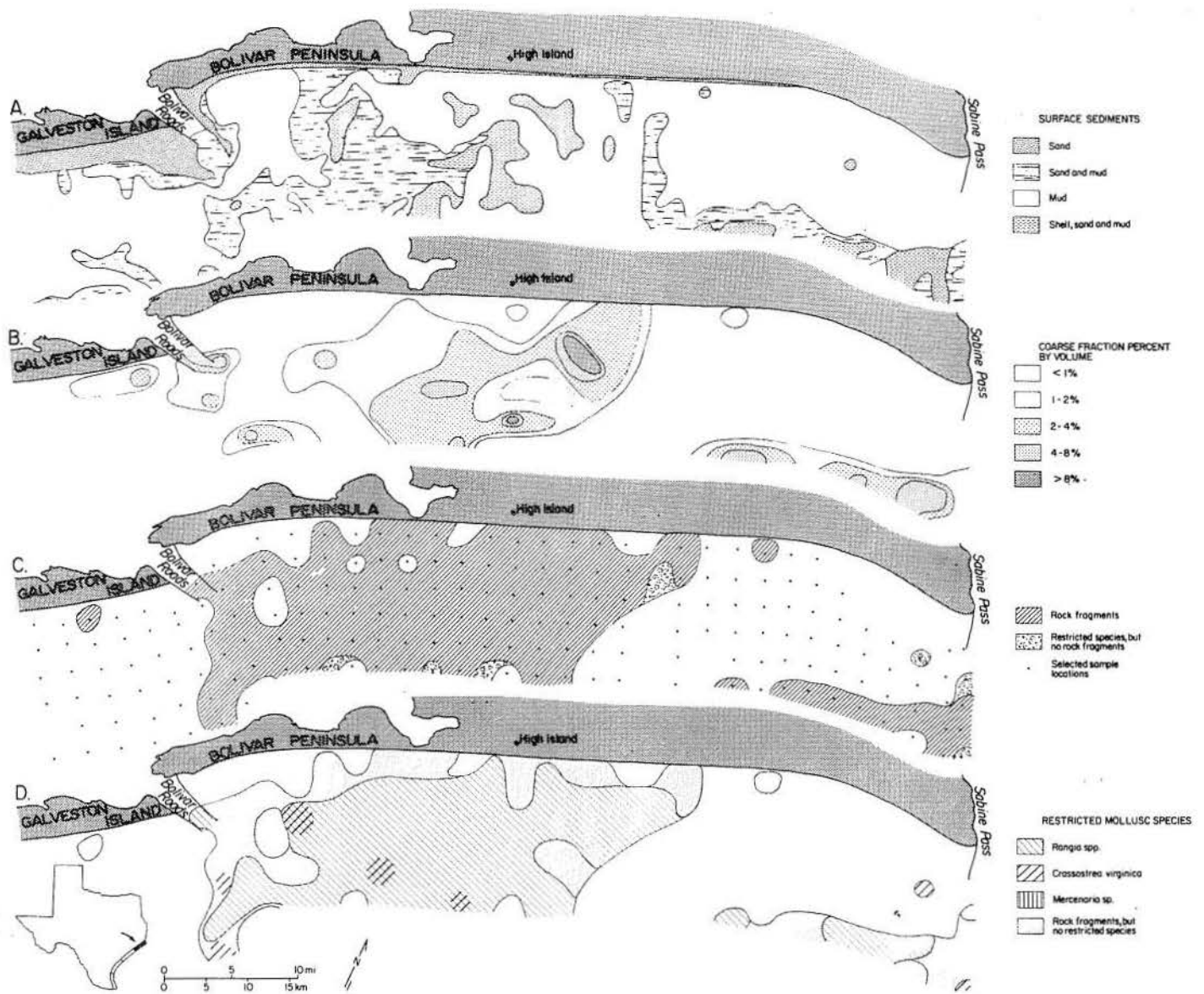


Figure 100. Maps of the Sabine - Bolivar area showing (A) surface sediment distribution, (B) coarse fraction percent by volume, (C) rock fragments, and (D) restricted mollusk species (after Morton and Winker, 1979).

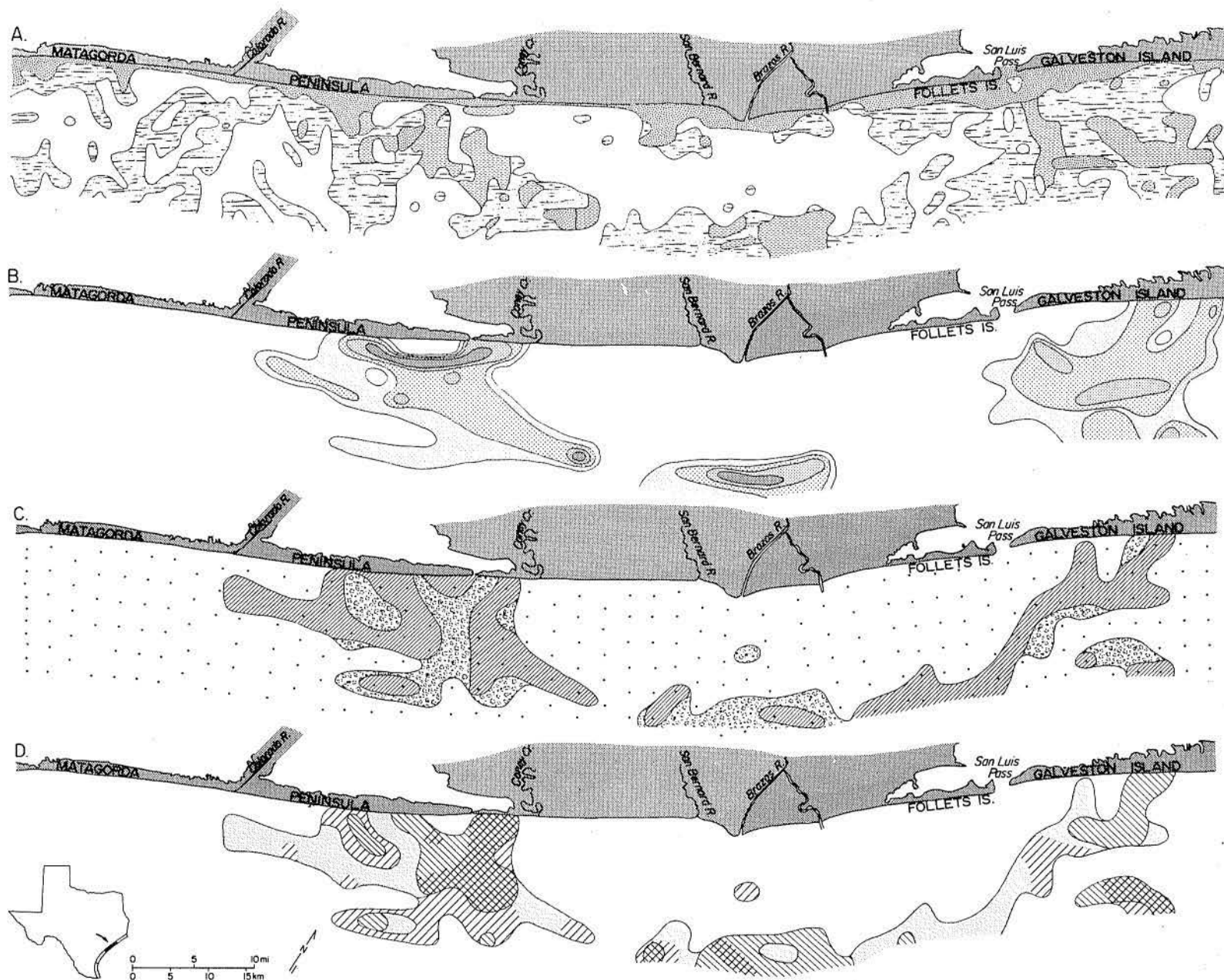


Figure 101. Maps of the Brazos - Colorado area showing (A) surface sediment distribution, (B) coarse fraction percent by volume, (C) rock fragments, and (D) restricted mollusk species. Symbols explained in figure 100 (after Morton and Winkler, 1979).

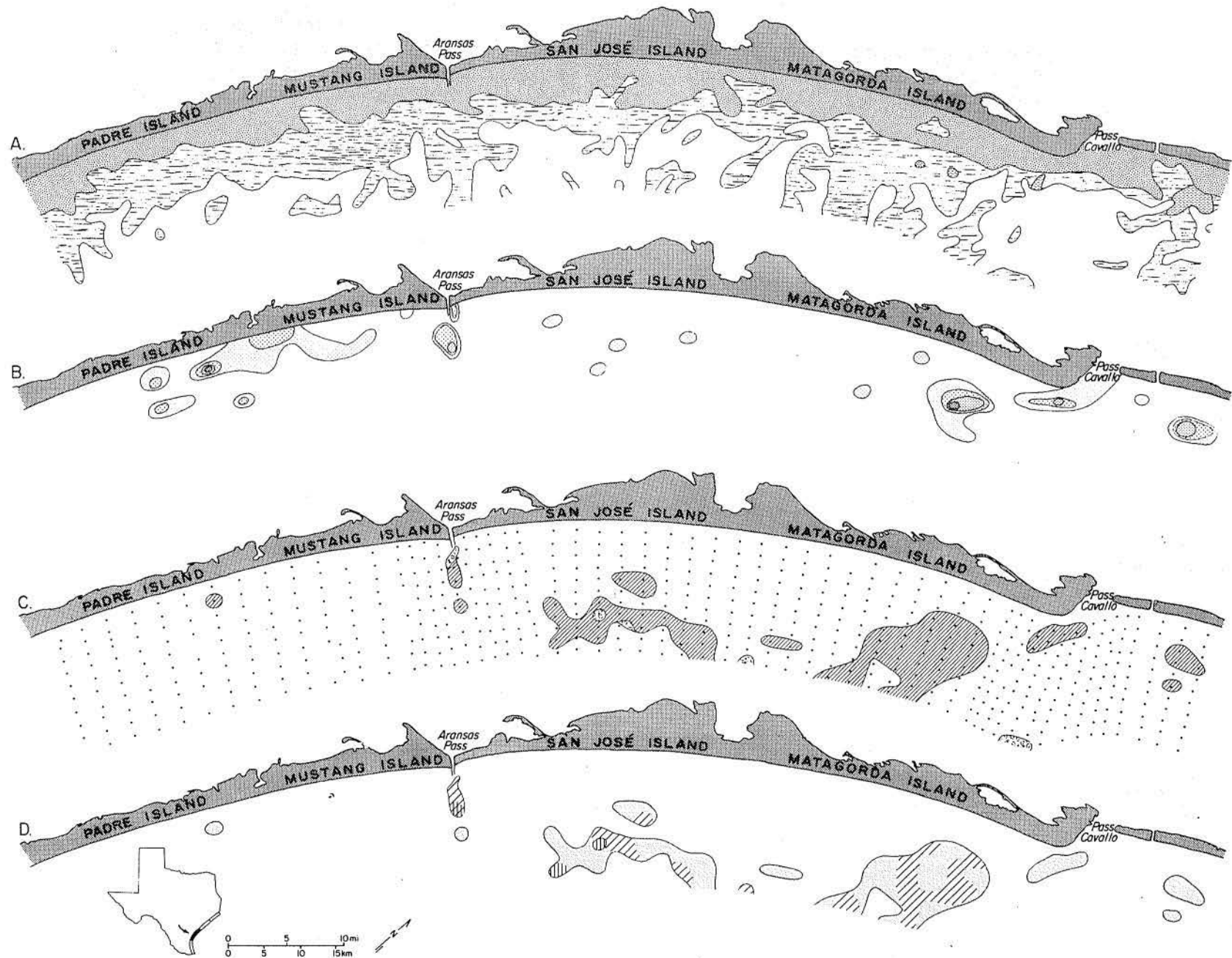


Figure 102. Maps of the Matagorda - San José area showing (A) surface sediment distribution, (B) coarse fraction percent by volume, (C) rock fragments, and (D) restricted mollusk species. Symbols explained in figure 100 (after Morton and Winker, 1979).

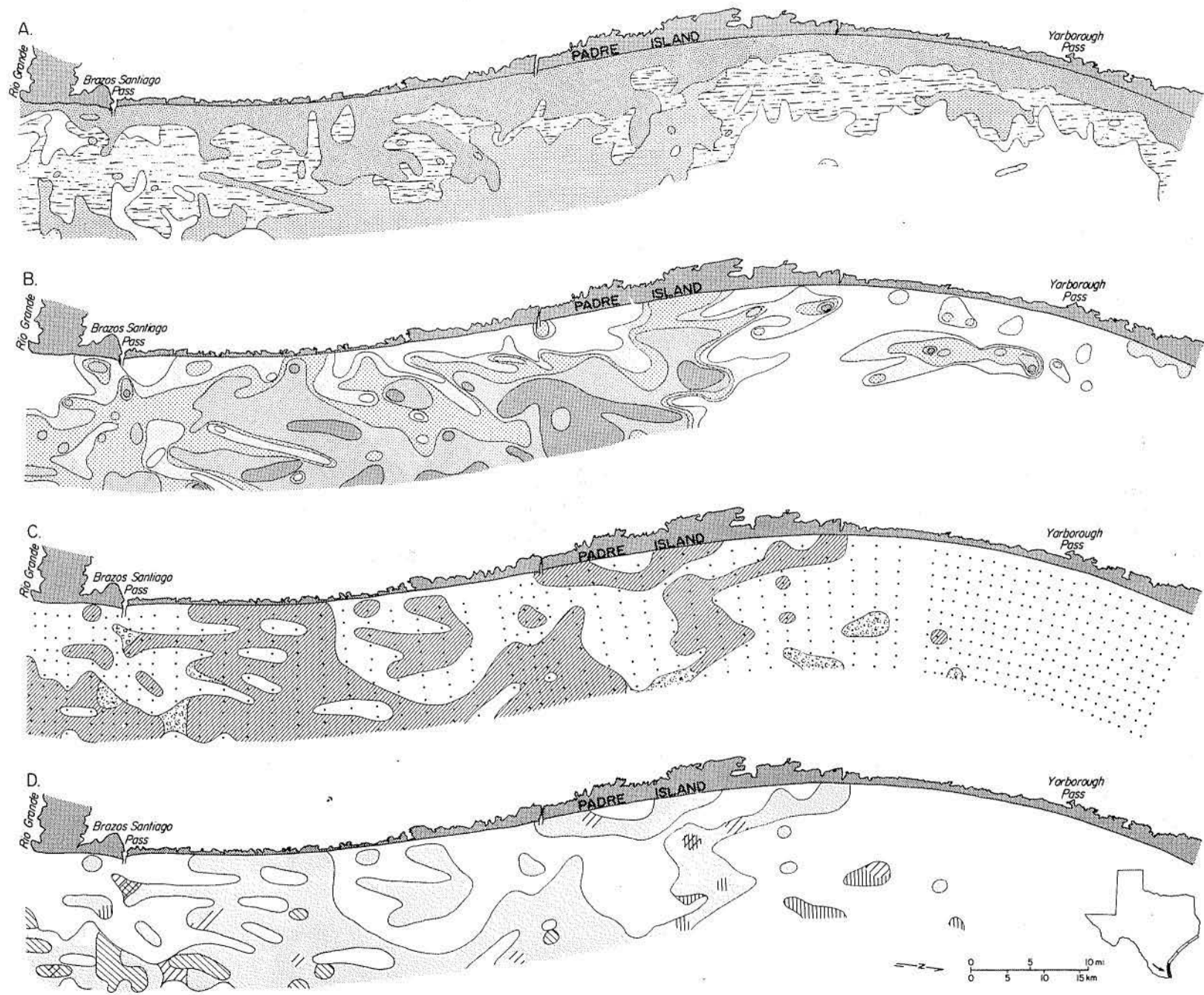


Figure 103. Maps of the Rio Grande area showing (A) surface sediment distribution, (B) coarse fraction percent by volume, (C) rock fragments, and (D) restricted mollusk species. Symbols explained in figure 100 (after Morton and Winker, 1979).

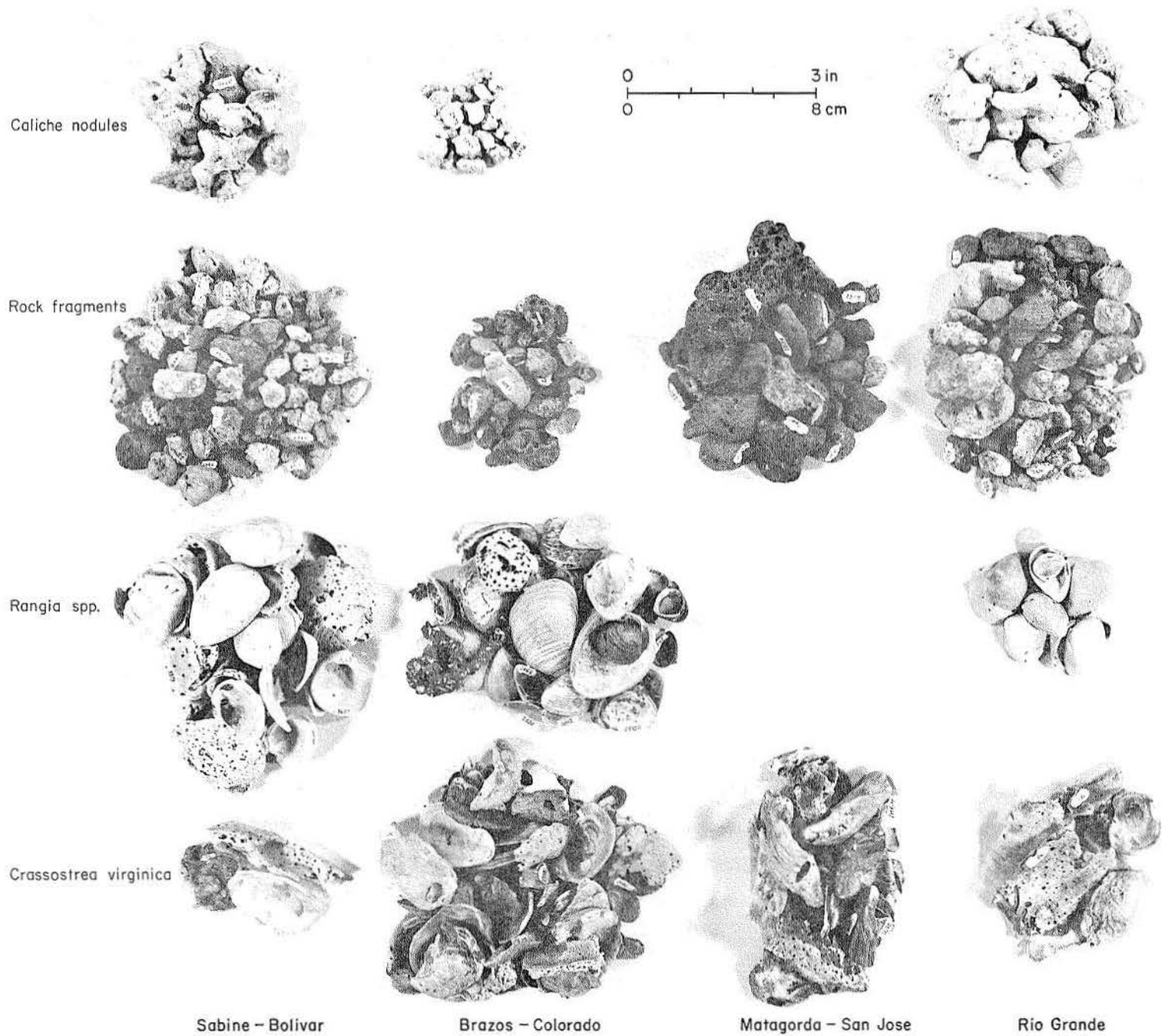


Figure 104. Surficial features, relative abundance, and distribution of restricted mollusk species, rock fragments, and caliche nodules in each of the four trends (after Morton and Winker, 1979).

High concentrations of shell in marine sediments are significant precursors of fossil shell assemblages. Modern shell deposits are analogous to basal transgressive sequences with abundant nearshore fauna that overlie or rest slightly above fluvial-deltaic sediments. Thus, their areal distribution may be useful for interpreting patchy occurrences of shell in subsurface samples or outcrops.

Relict Sediments

By definition, relict sediments are not in equilibrium with extant physical processes, but are sediments deposited under conditions different from those characterizing present-day environments (Emery, 1968). Reworking and mixing of relict and modern sediments, however, creates a transitional group of sediments (palimpsest) that cannot be distinguished from some relict sediments. Those relict sediments most easily identified are generally firm oxidized muds and sandy muds with root casts. Exceptions are clean, well-sorted, gravel-sized deposits composed of shell, caliche nodules, and rock fragments. These clean gravels are interpreted as relict beach deposits because of their similarity to present-day beaches east of High Island, at Sargent Beach, and west of the Colorado River on Matagorda Peninsula (McGowen and Morton, 1979).

Encrusted or thinly veneered outcrops of calcite-cemented sand, mud, and shell are also common in areas where highly irregular bathymetry has been charted. The pinnacles, knolls, and ridges represent erosional remnants of relict sediments that have been preferentially cemented. Some linear trends of rocks are clearly related to potentially active faults, whereas others are not. The most thoroughly studied indurated outcrops on the inner shelf are Freeport Rocks (Curry, 1960; Winchester, 1971) and the 7.5-fathom reef (Thayer and others, 1974) north of Port Mansfield Ship Channel. Despite the lack of confirming data, similar rocks probably crop out over much of the inner shelf southward from the vicinity of Port Mansfield Ship Channel, as suggested by irregular bathymetry and occurrence of rock fragments among backbeach sediments on south Padre Island.

Depth to relict sediments on the inner shelf varies from area to area. Offshore from deltaic headlands, relict sediments are exposed on the seafloor or covered by a thin veneer (< 3 ft) of mud. Modern shelf sediments are thickest between the Brazos-Colorado and Rio Grande deltas; however, thicknesses are generally less than 20 ft (6m) (fig. 99).

Stratification

Homogeneous mud, sand, and shelly sand, graded beds, interbedded sand and mud, and bioturbated sand and mud are typical shelf sediments (fig. 99). Primary bedding may be partly or completely destroyed by burrowing organisms that impart a mottled appearance. Seaward of the shoreface, mud and sandy mud predominate (fig. 98) in surface samples (McGowen and Morton, 1979) as well as long cores. Alternating parallel laminations and beds of sand and mud are the most conspicuous stratification types. Some beds are normally graded and show distinct fining-upward sequences from 0.7 to 1.5 ft thick (20 to 40 cm); a few beds are reverse graded.

Erosional bases of graded beds are commonly overlain by comminuted shell debris with rare rock fragments (fig. 99). Coarser sediments grade upward to fine and very fine sand that, in turn, is overlain by homogeneous mud. Flaser-lenticular bedding, present in some mud intervals, is subordinate to other primary structures. Graded beds and alternating beds of sand and mud are the most common stratification types. Although present in a few cores, alternating sand and mud laminae are rare.

Muddy intervals contain numerous sand-filled burrows from 0.25 to 0.5 inch (0.5 to 1 cm) in diameter. These burrows were formed by polychaete worms that are abundant in bottom sediments. High rates of sedimentation, disruption of feeding patterns, and recolonization are shown by gradual increases in burrow density above some graded units.

REFERENCES

- Adey, E. A., and Cook, H. M., 1964, Suspended-sediment load of Texas streams, compilation report, October 1959-September 1961: Texas Water Commission Bulletin 6410, 49 p.
- Andrews, P. B., 1964, Serpulid reefs, Baffin Bay, southeast Texas, *in* Field trip guidebook: Depositional environments, south-central Texas Coast: Gulf Coast Association of Geological Societies, Annual Meeting, October 28-31, 1964, p. 102-120.
- _____ 1970, Facies and genesis of a hurricane-washover fan, St. Joseph Island, central Texas coast: The University of Texas at Austin, Bureau of Economic Geology Report of Investigations 67, 147 p.
- Arbingast, S. A., Kennamer, L. G., and Bonine, M. E., 1967, Atlas of Texas: University of Texas, Austin, Bureau of Business Research, 131 p.
- Beal, M. A., and Shepard, F. P., 1956, A use of roundness to determine depositional environments: *Journal of Sedimentary Petrology*, v. 26, p. 49-60.
- Behrens, E. W., 1969, Hurricane effects on a hypersaline bay, *in* Castañares, Agustin Ayala, and Phleger, F. B., eds., *Lagunas costeras, un simposio* [Coastal lagoons, a symposium]: México, D. F., Universidad Nacional Autónoma de México, Instituto Biológica, UNAM-UNESCO International Symposium, p. 301-310.
- Bernard, H. A., and Le Blanc, R. J., 1965, Resume of the Quaternary geology of the northwestern Gulf of Mexico, *in* Wright, H. E., and Frey, D. G., eds., *The Quaternary of the United States*: Princeton, N. J., Princeton University Press, p. 137-185.
- Bernard, H. A., and Major, C. F., Jr., 1963, Recent meander belt deposits of the Brazos River: an alluvial sand model: *American Association of Petroleum Geologists Bulletin*, v. 47, no. 2, p. 350.
- Bernard, H. A., Major, C. F., Jr., and Parrott, B. S., 1959, The Galveston barrier island and environs: a model for predicting reservoir occurrence and trend: *Gulf Coast Association of Geological Societies Transactions*, v. 9, p. 221-224.
- Bernard, H. A., Major, C. F., Jr., Parrott, B. S., and Le Blanc, R. J., Sr., 1970, Recent sediments of southeast Texas, a field guide to the Brazos alluvial and deltaic plains and the Galveston barrier island complex: The University of Texas at Austin, Bureau of Economic Geology Guidebook 11, 132 p.
- Bluck, B. J., 1971, Sedimentation in the meandering River Endrick: *Scottish Journal of Geology*, v. 7, p. 93-138.
- Boothroyd, J. C., 1972, Coarse-grained sedimentation on a braided outwash fan, northeast Gulf of Alaska: University of South Carolina, Coastal Research Division, Technical Report No. 6-CRD, 127 p.

- Bouma, A. H., and Bryant, W. R., 1969, Rapid delta growth in Matagorda Bay, Texas, in Castañares, Agustín Ayala, and Phleger, F. B., eds., *Lagunas costeras, un simposio [Coastal lagoons, a symposium]*: México, D. F., Universidad Nacional Autónoma de México, Instituto Biológica, UNAM-UNESCO International Symposium, p. 171-190
- Breuer, J. P., 1962, An ecological survey of the lower Laguna Madre of Texas, 1953-1959: The University of Texas, Port Aransas, Institute of Marine Science Publications, v. 8, p. 153-183.
- Brown, L. F., Jr., Brewton, J. L., McGowen, J. H., Evans, T. J., Fisher, W. L., and Groat, C. G., 1976, Environmental geologic atlas of the Texas Coastal Zone -- Corpus Christi area: The University of Texas at Austin, Bureau of Economic Geology, 123 p.
- Brown, L. F., Jr., Cleaves, A. W., II, and Erxleben, A. W., 1973, Pennsylvanian depositional systems in North-Central Texas: The University of Texas at Austin, Bureau of Economic Geology Guidebook 14, 121 p.
- Brown, L. F., Jr., McGowen, J. H., Evans, T. J., Groat, C. G., and Fisher, W. L., 1977, Environmental geologic atlas of the Texas Coastal Zone--Kingsville area: The University of Texas at Austin, Bureau of Economic Geology, 131 p.
- Brown, L. F., Jr., Morton, R. A., McGowen, J. H., Kreidler, C. W., and Fisher, W. L., 1974, Natural hazards of the Texas Coastal Zone: The University of Texas at Austin, Bureau of Economic Geology, 13 p.
- Brown, L. F., Jr., Brewton, J. L., Evans, T. J., McGowen, J. H., White, W. A., Groat, C. G., and Fisher, W. L., 1980, Environmental geologic atlas of the Texas Coastal Zone -- Brownsville-Harlingen area: The University of Texas at Austin, Bureau of Economic Geology, 140 p.
- Bull, W. B., 1972, Recognition of alluvial-fan deposits in the stratigraphic record, in Rigby, J. K., and Hamblin, W. K., eds., *Recognition of ancient sedimentary environments*: Society of Economic Paleontologists and Mineralogists Special Publication 16, p. 63-83.
- Butler, G. P., 1969, Modern evaporite deposition and geochemistry of coexisting brines, the sabkhas, Trucial Coast, Arabian Gulf: *Journal of Sedimentary Petrology*, v. 39, p. 70-89.
- Byrne, J. R., 1975, Holocene depositional history of Lavaca Bay, central Texas coast: The University of Texas at Austin, Ph.D. dissertation, 149 p.
- Carr, J. T., Jr., 1967, The climate and physiography of Texas: Texas Water Development Board Report 53, 27 p.
- Cook, H. M., 1967, Suspended-sediment load of Texas streams, compilation report October 1961-September 1963: Texas Water Development Board Report 45, 61 p.
- _____ 1970, Suspended-sediment load of Texas streams, compilation report October 1963-September 1965: Texas Water Development Board Report 106, 61 p.
- Cook, M. F., 1968, Statistical summaries of stream-gaging station records, Louisiana 1938-1964: U.S. Geological Survey - State of Louisiana, Department of Public Works, Basic Records Report No. 1, 286 p.

- Curray, J. R., 1960, Sediments and history of Holocene transgression, continental shelf, northwest Gulf of Mexico, *in* Recent sediments, northwest Gulf of Mexico: American Association of Petroleum Geologists, p. 221-266.
- Curray, J. R., Emmel, F. J., and Crampton, P. J. S., 1969, Holocene history of a strandplain, lagoonal coast, Nayarit, Mexico, *in* Castañares, Augustin Ayala, and Phleger, F. B., eds., *Lagunas costeras, un simposio* [Coastal lagoons, a symposium]: México, D. F., Universidad Nacional Autónoma de México, Instituto Biológica, UNAM-UNESCO International Symposium, p. 63-100.
- Dalrymple, T., 1937, Major Texas floods of 1936: U.S. Geological Survey Water-Supply Paper 816, 146 p.
- Doeglas, D. J., 1962, The structure of sedimentary deposits of braided rivers: *Sedimentology*, v. 1, no. 3, p. 167-190.
- Donaldson, A. C., Martin, R. H., and Kanen, W. H., 1970, Holocene Guadalupe delta of Texas Gulf Coast, *in* Morgan, J. P., ed., *Deltaic sedimentation, modern and ancient*: Society of Economic Paleontologists and Mineralogists Special Publication 15, p. 107-137.
- Dowell, C. L., and Petty, R. G., 1971, Engineering data on dams and reservoirs in Texas, part III: Texas Water Development Board Report 126.
- _____ 1973, Engineering data on dams and reservoirs in Texas, part II: Texas Water Development Board Report 126.
- Emery, K. O., 1968, Relict sediments on continental shelves of the world: American Association of Petroleum Geologists Bulletin, v. 52, p. 445-464.
- Ethridge, F. G., 1978, River system I--processes and depositional models, Chapter II, *in* Lecture notes for short course on the fluvial system, March 20-25, 1978: Fort Collins, Colorado, Colorado State University, p. 28-65.
- Fagg, D. B., 1957, The recent marine sediments and Pleistocene surface of Matagorda Bay, Texas: Gulf Coast Association of Geological Societies Transactions, v. 7, p. 119-133.
- Fisher, W. L., 1969, Facies characterization of Gulf Coast Basin delta systems, with some Holocene analogues: Gulf Coast Association of Geological Societies Transactions, v. 19, p. 239-261.
- Fisher, W. L., and Brown, L. F., Jr., 1972, Clastic depositional systems--a genetic approach to facies analysis: The University of Texas at Austin, Bureau of Economic Geology, 211 p.
- Fisher, W. L., and McGowen, J. H., 1969, Lower Eocene lagoonal systems in the Texas Gulf Coast Basin, *in* Castañares, Augustin Ayala, and Phleger, F. B., eds., *Lagunas costeras, un simposio* [Coastal lagoons, a symposium]: México, D. F., Universidad Nacional Autónoma de México, Instituto Biológica, UNAM-UNESCO International Symposium, p. 263-274.
- Fisk, H. N., 1944, Geological investigation of the alluvial valley of the lower Mississippi River: Vicksburg, Mississippi, U.S. Army Corps of Engineers, Mississippi River Commission, 78 p.

- _____. 1959, Padre Island and the Laguna Madre flats, coastal south Texas: Louisiana State University, 2d Coastal Geography Conference, p. 103-151.
- _____. 1961, Bar-finger sands of Mississippi delta, *in* Geometry of sandstone bodies: American Association of Petroleum Geologists, p. 29-52.
- Forristall, G. Z., Hamilton, R. C., and Cardone, V. J., 1977, Continental shelf currents in tropical storm Delia: observations and theory: *Journal of Physical Oceanography*, v. 7, p. 532-546.
- Frazier, D. E., 1974, Depositional episodes: their relationship to the Quaternary stratigraphic framework in the northwestern portion of the Gulf basin: The University of Texas at Austin, Bureau of Economic Geology Geological Circular 74-1, 28 p.
- Fulton, K. J., 1975, Subsurface stratigraphy, depositional environments, and aspects of reservoir continuity -- Rio Grande delta, Texas: University of Cincinnati, Ph.D. dissertation, 314 p.
- Galloway, W. E., 1977, Catahoula Formation of the Texas Coastal Plain: depositional systems, composition, structural development, ground-water flow history, and uranium distribution: The University of Texas at Austin, Bureau of Economic Geology Report of Investigations 87, 59 p.
- _____. 1979, Fluvial depositional systems, *in* Depositional and ground-water flow systems in the exploration for uranium, a research colloquium: The University of Texas at Austin, Bureau of Economic Geology, p. 13-42.
- Harms, J. C., and Fahnestock, R. K., 1965, Stratification, bed forms, and flow phenomena (with an example from the Rio Grande), *in* Primary sedimentary structures and their hydrodynamic interpretation: Society of Economic Paleontologists and Mineralogists Special Publication 12, p. 84-115.
- Hayes, M. O., 1965, Sedimentation on a semiarid wave-dominated coast (South Texas) with emphasis on hurricane effects: University of Texas, Ph.D. dissertation, 350 p.
- _____. 1967, Hurricanes as geological agents: case studies of Hurricanes Carla, 1961, and Cindy, 1963: The University of Texas at Austin, Bureau of Economic Geology Report of Investigations 61, 56 p.
- _____. 1975, Morphology of sand accumulation in estuaries: an introduction to the symposium, *in* Cronin, L. E., ed., *Estuarine Research*, v. II: New York, Academic Press, p. 3-22.
- Hayes, M. O., and Kana, T. W., 1976, Terrigenous clastic depositional environments: University of South Carolina, Department of Geology, Coastal Research Division, Technical Report No. 11-CRD, 302 p.
- Herber, J. P., in progress, Holocene sediments under Laguna Madre, Cameron County, Texas: The University of Texas at Austin, Master's thesis.
- Hicks, S. D., 1972, On the classification and trends of long period sea-level series: *Shore and Beach*, v. 40, p. 20-23.

- Holmes, A., 1965, Principles of physical geology (2d ed.): New York, The Roland Press Co., 288 p.
- Hoover, R. A., 1968, Physiography and surface sediment facies of a recent tidal delta, Harbor Island, Central Texas Coast: The University of Texas at Austin, Ph.D. dissertation, 184 p.
- Hunter, R. E., 1977, Basic types of stratification in small eolian dunes: *Sedimentology*, v. 24, p. 361-387.
- Hunter, R. E., and Dickinson, K. A., 1970, Map showing land forms and sedimentary deposits of the Padre Island portion of the South Bird Island 7.5-minute Quadrangle, Texas: U.S. Geological Survey Miscellaneous Geologic Investigations Map I-659, scale 1:24,000.
- Hunter, R. E., Watson, R. L., Hill, G. W., and Dickinson, K. A., 1972, Modern depositional environments and processes, northern and central Padre Island, Texas, in Padre Island National Seashore Field Guide: Gulf Coast Association of Geological Societies, p. 1-27.
- Jackson, R. G., II, 1975, Velocity - bedform - texture patterns of meander bends in the lower Wabash River of Illinois and Indiana: *Geological Society of America Bulletin*, v. 86, p. 1511-1522.
- Kanes, W. H., 1970, Facies and development of the Colorado River delta in Texas, in Morgan, J. P., ed., Deltaic sedimentation, modern and ancient: Society of Economic Paleontologists and Mineralogists Special Publication 15, p. 78-106.
- Kendall, C. G. St. C., Kinsman, D. J. J., Shearman, D. J., and Skipwith, P. A. d'E., 1964, Recent anhydrite from the Trucial Coast of the Arabian Gulf: *Geological Society of London Circular* 120, 3 p.
- Kessler, L. G., II, 1971, Characteristics of braided streams depositional environment with examples from the South Canadian River, Texas: *Earth Science Bulletin*, v. 4, no. 1, p. 25-35.
- Kinsman, D. J. J., 1966, Gypsum and anhydrite of Recent age, Trucial Coast, Persian Gulf, in Second symposium on salt: Northern Ohio Geological Society, v. 1, p. 302-326.
- _____ 1969, Modes of formation, sedimentary associations, and diagnostic features of shallow-water and supratidal evaporites: *American Association of Petroleum Geologists Bulletin*, v. 53, p. 830-840.
- Kreitler, C. W., 1976, Lineations and faults in the Texas Coastal Zone: The University of Texas at Austin, Bureau of Economic Geology Report of Investigations 85, 32 p.
- Le Blanc, R. J., and Hodgson, W. D., 1959, Origin and development of the Texas shoreline: Louisiana State University, Coastal Studies Institute, 2d Coastal Geography Conference, p. 57-101.
- Leopold, L. B., Wolman, M. G., and Miller, J. P., 1964, Fluvial processes in geomorphology: San Francisco, W. H. Freeman, 522 p.

- Levey, R. A., 1978, Bed-form distribution and internal stratification of coarse-grained point bars, Upper Congaree River, S.C., *in* Miall, A. D., ed., *Fluvial sedimentology: Canadian Society of Petroleum Geologists Memoir 5*, p. 105-127.
- Lohse, E. A., 1955, Dynamic geology of the modern coastal region, northwest Gulf of Mexico, *in* *Finding ancient shorelines: Society of Economic Paleontologists and Mineralogists Special Publication 3*, p. 99-103.
- Lohse, E. A., and Cook, T. D., 1958, Development of the recent Rio Grande deltaic plain, *in* *Sedimentology of South Texas, field trip guidebook: Gulf Coast Association of Geological Societies*, p. 55-60.
- Lowry, R. L., Jr., 1959, A study of droughts in Texas: Texas Board of Water Engineers Bulletin 5914, 76 p.
- Manka, L. L., and Steinmetz, R., 1971, Sediments and depositional history of the southeast lobe of the Colorado River delta, Texas: *Gulf Coast Association of Geological Societies Transactions*, v. 21, p. 309-323.
- Mason, C., and Sorensen, R. M., 1971, Properties and stability of a Texas barrier beach inlet: Texas A&M University, Sea Grant Publication TAMU-SG-71-217, 166 p.
- McBride, E. F., and Hayes, M. O., 1962, Dune cross-bedding on Mustang Island, Texas: *American Association of Petroleum Geologists Bulletin*, v. 46, p. 546-551.
- McEwen, M. C., 1969, Sedimentary facies of the Modern Trinity delta, *in* Lankford, R. R., and Rogers, J. J. W., eds., *Holocene geology of the Galveston Bay area: Houston Geological Society*, p. 53-77.
- McGowen, J. H., 1970, Gum Hollow fan delta, Nueces Bay, Texas: The University of Texas at Austin, Bureau of Economic Geology Report of Investigations 69, 91 p.
- _____ 1979, Coastal plain systems, *in* *Depositional and ground-water flow systems in the exploration for uranium, a research colloquium: The University of Texas at Austin, Bureau of Economic Geology*, p. 80-117.
- McGowen, J. H., and Brewton, J. L., 1975, Historical changes and related coastal processes, Gulf and mainland shorelines, Matagorda Bay area, Texas: The University of Texas at Austin, Bureau of Economic Geology, Special Publication, 72 p.
- McGowen, J. H., Brown, L. F., Jr., Evans, T. J., Fisher, W. L., and Groat, C. G., 1976, Environmental geologic atlas of the Texas Coastal Zone -- Bay City - Freeport area: The University of Texas at Austin, Bureau of Economic Geology, 98 p.
- McGowen, J. H., and Garner, L. E., 1970, Physiographic features and stratification types of coarse-grained point bars: Modern and ancient examples: *Sedimentology*, v. 14, no. 1/2, p. 77-111.
- _____ 1972, Relation between Texas barrier islands and late Pleistocene depositional history [abs.]: *American Association of Petroleum Geologists Bulletin*, v. 56, no. 3, p. 638-639.
- McGowen, J. H., Garner, L. E., and Wilkinson, B. H., 1977, The Gulf shoreline of Texas: processes, characteristics, and factors in use: The University of Texas at Austin, Bureau of Economic Geology Geological Circular 77-3, 27 p.

- McGowen, J. H., Groat, C. G., Brown, L. F., Jr., Fisher, W. L., and Scott, A. J., 1970, Effects of Hurricane Celia--a focus on environmental geologic problems of the Texas Coastal Zone: The University of Texas at Austin, Bureau of Economic Geology Geological Circular 70-3, 35 p.
- McGowen, J. H., and Morton, R. A., 1979, Sediment distribution, bathymetry, faults, and salt diapirs, submerged lands of Texas: The University of Texas at Austin, Bureau of Economic Geology, 31 p.
- McGowen, J. H., and Scott, A. J., 1975, Hurricanes as geologic agents on the Texas coast, in Cronin, L. E., ed., Estuarine research, v. II, Geology and engineering: New York, Academic Press, p. 23-46
- Miall, A. D., 1977, A review of the braided river depositional environment: Earth Science Reviews, v. 13, p. 1-62.
- Mirabal, J., 1974, Suspended-sediment load of Texas streams, compilation report, October 1965 - September 1971: Texas Water Development Board Report 184, 119 p.
- Morton, R. A., 1974, Shoreline changes on Galveston Island (Bolivar Roads to San Luis Pass): The University of Texas at Austin, Bureau of Economic Geology Geological Circular 74-2, 34 p.
- _____ 1977a, Historical shoreline changes and their causes, Texas Gulf Coast: Gulf Coast Association of Geological Societies Transactions, v. 27, p. 352-364.
- _____ 1977b, Nearshore changes at jettied inlets, Texas coast: Coastal Sediments '77 Symposium, American Society of Civil Engineers, p. 267-286.
- _____ 1978, Large-scale rhomboid bed forms and sedimentary structures associated with hurricane washover: Sedimentology, v. 25, p. 183-204.
- _____ 1979a, Subaerial storm deposits on barrier flats formed by wind-driven currents: Sedimentary Geology, v. 24, p. 105-122.
- _____ 1979b, Temporal and spatial variations in shoreline changes and their implications, examples from the Texas Gulf Coast: Journal of Sedimentary Petrology, v. 49, p. 1101-1111.
- Morton, R. A., and Donaldson, A. C., 1973, Sediment distribution and evolution of tidal deltas along a tide-dominated shoreline, Wachapreague, Virginia: Sedimentary Geology, v. 10, p. 285-299.
- _____ 1978a, Hydrology, morphology, and sedimentology of the Guadalupe fluvial-deltaic system: Geological Society of America Bulletin, v. 89, p. 1030-1036.
- _____ 1978b, The Guadalupe River and delta of Texas--a modern analogue for some ancient fluvial - deltaic systems, in Miall, A. D., ed., Fluvial sedimentology: Canadian Society of Petroleum Geologists, Memoir 5, p. 773-787.

- Morton, R. A., and Pieper, M. J., 1975a, Shoreline changes on Brazos Island and South Padre Island (Mansfield Channel to mouth of the Rio Grande): The University of Texas at Austin, Bureau of Economic Geology Geological Circular 75-2, 39 p.
- _____ 1975b, Shoreline changes in the vicinity of the Brazos River delta (San Luis Pass to Brown Cedar Cut): The University of Texas at Austin, Bureau of Economic Geology Geological Circular 75-4, 47 p.
- _____ 1976, Shoreline changes on Matagorda Island and San José Island (Pass Cavallo to Aransas Pass): The University of Texas at Austin, Bureau of Economic Geology Geological Circular 76-4, 42 p.
- Morton, R. A., Pieper, M. J., and McGowen, J. H., 1976, Shoreline changes on Matagorda Peninsula (Brown Cedar Cut to Pass Cavallo): The University of Texas at Austin, Bureau of Economic Geology Geological Circular 76-6, 37 p.
- Morton, R. A., and Winker, C. D., 1979, Distribution and significance of coarse biogenic and clastic deposits on the Texas inner shelf: Gulf Coast Association of Geological Societies Transactions, v. 29, p. 136-146.
- Munson, M. G., 1975, Tidal delta facies relationships, Harbor Island, Texas: The University of Texas at Austin, Master's thesis, 126 p.
- Murray, S. P., 1970, Bottom currents near the coast during Hurricane Camille: Journal of Geophysical Research, v. 75, p. 4579-4582.
- Nelson, H. F., and Bray, E. E., 1970, Stratigraphy and history of the Holocene sediments in the Sabine-High Island area, Gulf of Mexico, in Morgan, J. P., and Shaver, R. H., eds., Deltaic sedimentation, modern and ancient: Society of Economic Paleontologists and Mineralogists Special Publication 15, p. 48-77.
- Nienaber, J. H., 1963, Shallow marine sediments offshore from the Brazos River, Texas: University of Texas, Port Aransas, Institute of Marine Science Publications, v. 9, p. 311-372.
- Nijman, W., and Puigdefabregas, C., 1978, Coarse-grained point bar structure in a molasse-type fluvial system, Eocene Castisents sandstone formation, South Pyrenean Basin, in Miall, A. D., ed., Fluvial sedimentology: Canadian Society of Petroleum Geologists, Memoir 5, p. 487-510.
- Ore, H. T., 1963, The braided stream depositional environment: University of Wyoming, Ph.D. dissertation, 205 p.
- _____ 1964, Some criteria for recognition of braided stream deposits: University of Wyoming Contributions in Geology, v. 3., no. 1, p. 1-14.
- _____ 1965, Characteristic deposits of rapidly aggrading streams: Wyoming Geological Association, 19th Field conference guidebook, p. 195-201.
- Parker, R. H., 1959, Macro-invertebrate assemblages of Central Texas coastal bays and Laguna Madre: American Association of Petroleum Geologists Bulletin, v. 43, p. 2100-2166.
- Piety, W. D., 1972, Surface sediment facies and physiography of a Recent tidal delta, Brown Cedar Cut: University of Houston, Master's thesis, 208 p.

- Price, W. A., 1933, Role of diastrophism in topography of Corpus Christi area, South Texas: American Association of Petroleum Geologists Bulletin, v. 17, p. 907-962.
- _____ 1952, Reduction of maintenance by proper orientation of ship channels through tidal inlets: Proceedings, 2d Coastal Engineering Conference, p. 243-255.
- _____ 1958, Sedimentology and Quaternary geomorphology of South Texas: Gulf Coast Association of Geological Societies Transactions, v. 8, p. 41-75.
- _____ 1971, Environmental impact of Padre Isles development: Shore and Beach, v. 39, p. 4-10.
- Price, W. A., and Gunter, G., 1943, Certain recent geological and biological changes in South Texas with consideration of probable causes: Texas Academy of Science Proceedings, v. 26, p. 138-156.
- Pritchard, D. W., 1967, What is an estuary: physical viewpoint, in Lauff, G. H., ed., Estuaries: American Association for the Advancement of Science, Publication No. 83, p. 3-5.
- Pryor, W. A., Fulton, K., and Harrison, L., 1975, Stratigraphy, petrology, and paleontology of several Holocene Rio Grande delta distributary systems in Cameron County, Texas [abs.]: American Association of Petroleum Geologists Bulletin, v. 2, p. 61.
- Schubel, J. R., Hayes, M. O., and Pritchard, D. W., 1971, The estuarine environment: estuaries and estuarine sedimentation: Short Course Lecture Notes, October 30-31, 1971, Falls Church, Va., Wye Institute, American Geological Institute.
- Schumm, S. A., 1968, Speculations concerning paleohydrologic controls of terrestrial sedimentation: Geological Society of America Bulletin, v. 79, p. 1573-1588.
- _____ 1972, Fluvial paleochannels, in Rigby, J. K., and Hamblin, W. K., eds., Recognition of ancient sedimentary environments: Society of Economic Paleontologists and Mineralogists, Special Publication No. 16, p. 98-107.
- Scott, A. J., Hayes, M. O., Andrews, P. B., Behrens, E. W., and Siler, W. L., 1964, Depositional environments, south-central Texas coast: Field trip guidebook for 1964 meeting of Gulf Coast Association of Geological Societies, 170 p.
- Scott, A. J., and Fisher, W. L., 1969, Delta systems and deltaic deposition, in Fisher, W. L., and others, Delta systems in the exploration for oil and gas: A research colloquium: The University of Texas at Austin, Bureau of Economic Geology, p. 10-29.
- Scott, A. J., Hoover, R. A., and McGowen, J. H., 1969, Effect of Hurricane Beulah, 1967, on Texas coastal lagoons and barriers, in Castañares, Agustin Ayala, and Phleger, F. B., eds., Lagunas costeras, un simposio [Coastal lagoons, a symposium]: México, D. F., Universidad Nacional Autónoma de México, Instituto Biológica, UNAM-UNESCO International Symposium, p. 221-236.
- Seelig, W. N., and Sorensen, R. M., 1973, Investigation of shoreline changes at Sargent Beach, Texas: Texas A&M University, Sea Grant Publication No. TAMU-SG-73-212, 153 p.

- Shepard, F. P., 1960, Rise of sea level along northwest Gulf of Mexico, in Shepard, F. P., Phleger, F. B., and van Andel, T. H., eds., Recent sediments, northwest Gulf of Mexico: American Association of Petroleum Geologists, p. 338-344.
- Shepard, F. P., and Moore, D. G., 1960, Bays of central Texas coast, in Shepard, F. P., Phleger, F. B., and van Andel, T. H., Recent sediments, northwest Gulf of Mexico: American Association of Petroleum Geologists, p. 117-152.
- Shideler, G. L., McGowen, J. H., and Price, W. A., 1978, U.S.G.S. Office of Energy Resources field conference on clastic sedimentary environments, modern and ancient field notes for Corpus Christi Area: U.S. Geological Survey, Office of Marine Geology, Corpus Christi, 42 p.
- Smith, N. D., 1970, The braided stream depositional environment: Comparison of the Platte River with some Silurian clastic rocks, north-central Appalachians: Geological Society of America Bulletin, v. 81, p. 2993-3014.
- Stout, I. M., Bentz, L. C., and Ingram, H. W., 1961, Silt load of Texas streams, a compilation report June 1889-September 1959: Texas Board Water Engineers Bulletin, 6108, 236 p.
- Swanson, R. L., and Thurlow, C. I., 1973, Recent subsidence rates along the Texas and Louisiana coast as determined from tide measurements: Journal of Geophysical Research, v. 78, p. 2665-2671.
- Thayer, P. A., La Rocque, A., and Tunnell, J. W., Jr., 1974, Relict lacustrine sediments on the inner continental shelf, southeast Texas: Gulf Coast Association of Geological Societies Transactions, v. 24, p. 337-347.
- Thornthwaite, C. W., 1948, An approach toward a rational classification of climate: Geographical Review, v. 38, p. 55-94.
- U.S. Army Corps of Engineers, 1919, Brazos Island Harbor, Texas: House Document 1710, 65th Congress, 3d session, 30 p.
- _____ 1920, Galveston Island and Galveston Channel, Texas: House Document 693, 66th Congress, 2d session, 66 p.
- _____ 1972, Texas coast hurricane study: Galveston District, Corps of Engineers.
- U.S. Geological Survey, 1968, Water resources data for Texas, Part I: Surface Water Records: Austin, Water Resources Division, 591 p.
- van Andel, T. H., 1960, Sources and dispersion of Holocene sediments, northern Gulf of Mexico, in Recent sediments, northwest Gulf of Mexico: American Association of Petroleum Geologists, p. 34-55.
- Wadsworth, A. H., Jr., 1941, The lower Colorado River, Texas: University of Texas, Master's thesis, 61 p.
- _____ 1966, Historical delatation of the Colorado River, Texas, in Shirley, M. L., and Rogedale, J. A., eds., Deltas in their geological framework: Houston Geological Society, p. 99-105.

- Waechter, N. B., 1972, Hydrology, morphology, and sedimentology of an ephemeral stream: Prairie Dog Town Fork of the Red River, Texas Panhandle: The University of Texas at Austin, Master's thesis, 58 p.
- Watson, R. L., 1968, Origin of shell beaches, Padre Island, Texas: The University of Texas at Austin, Master's thesis, 121 p.
- Wenzel, R. A., 1975, Effect of floods on selected sand bars, San Bernard and Brazos rivers, Austin County, Texas: The University of Texas at Austin, Master's thesis, 81 p.
- White, W. A., Morton, R. A., Kerr, R. S., Kuenzi, W. D., and Brogden, W. B., 1978, Land and water resources, historical changes, and dune criticality, Mustang and North Padre Islands, Texas: The University of Texas at Austin, Bureau of Economic Geology, Report of Investigations 92, 46 p.
- Wilkinson, B. H., 1974, Matagorda Island -- The evolution of a Gulf Coast barrier complex: The University of Texas at Austin, Ph.D. dissertation, 178 p.
- _____, 1975, Matagorda Island, Texas: the evolution of a Gulf Coast barrier complex: Geological Society of America Bulletin, v. 86, no. 7, p. 959-967.
- Wilkinson, B. H., and Basse, R. A., 1978, Late Holocene history of the Central Texas coast from Galveston Island to Pass Cavallo: Geological Society of America Bulletin, v. 89, p. 1592-1600.
- Wilkinson, B. H., and McGowen, J. H., 1977, Geologic approaches to the determination of long-term coastal recession rates, Matagorda Peninsula, Texas: Environmental Geology, v. 1, p. 359-365.
- Wilkinson, B. H., and Byrne, J. R., 1977, Lavaca Bay--transgressive deltaic sedimentation in central Texas estuary: American Association of Petroleum Geologists Bulletin, v. 61, no. 4, p. 527-545.
- Winchester, P. D., 1971, Geology of the Freeport rocks, offshore Texas: Gulf Coast Association of Geological Societies Transactions, v. 21, p. 211-222.
- Winker, C. D., 1979, Late Pleistocene fluvial-deltaic deposition, Texas coastal plain and shelf: The University of Texas at Austin, Master's thesis, 187 p.

